THE MINOR PLANET BULLETIN

BULLETIN OF THE MINOR PLANETS SECTION OF THE ASSOCIATION OF LUNAR AND PLANETARY OBSERVERS

VOLUME 49, NUMBER 4, A.D. 2022 OCTOBER-DECEMBER

ROTATIONAL PERIOD DETERMINATION FOR ASTEROIDS 5237 YOSHIKAWA

Massimiliano Mannucci, Nico Montigiani
Associazione Astrofili Fiorentini
Osservatorio Astronomico Margherita Hack (A57)
Florence, ITALY
info@astrofilifiorentini.it

(Received: 2022 July 3)

CCD photometric observations of main-belt asteroid 5237 Yoshikawa were obtained in order to measure its rotation period. These measures were performed during two different nights on 2022/04/05 and 2022/04/10, using the instrumentation available at the Osservatorio Astronomico Margherita Hack located on the hills near Florence (Italy).

CCD photometric observations of one main-belt asteroid were carried out in 2022 April at the Osservatorio Astronomico Margherita Hack (A57). We used a 0.35-m f/8,25 Smith-Cassegrain telescope, a SBIG ST10 XME CCD camera, and clear filter. The pixel scale was 1 arcsec when binned at 2×2 pixels and the exposures were 300 sec long. Data processing and analysis were done with *MPO Canopus* (Warner, 2019). All the images were calibrated with dark and flat field frames using *Astroart 6.0* (Warner, 2006). Table I shows the observing circumstances and results.

5237 Yoshikawa was discovered on 1990 Oct 26 by Urata, T. at Oohira and it was chosen from the asteroid light curve database (LCDB; Warner et al., 2009). It is a main-belt asteroid with a semi-major axis of 2.240 AU, eccentricity 0.096, inclination 5.138 deg, and an orbital period of 3.35 years. Its absolute magnitude is H = 13.52 (JPL, 2022; MPC, 2022). Our observations were conducted in the night across 2022/04/05 and 2022/04/10 and provided 98 data points. The period analysis shows a bimodal solution for the rotational period with P = 3.4693 ± 0.0002 h and an amplitude A = 0.31 ± 0.03 mag (Figure 1). The split-halves plot (Figure 2) doesn't let us solve the potential ambiguity between monomodal and bimodal solution by showing that the two halves of the 3.4693 h solution are almost superimposable. On the other hand, the monomodal solution would involve a rotation period of 1.7347 hours, thus suggesting that this asteroid may belong to the fast rotator class. Further observations are desirable to better resolve the remaining doubts.

Moreover, we consulted the asteroid lightcurve database (LCDB, 2022; Warner et al., 2009) and we found one previous calculated period: P = 3.47 +/- 0.0004 h (Waszczak, 2015). The period we found seems to be in good agreement with the previous mentioned period.

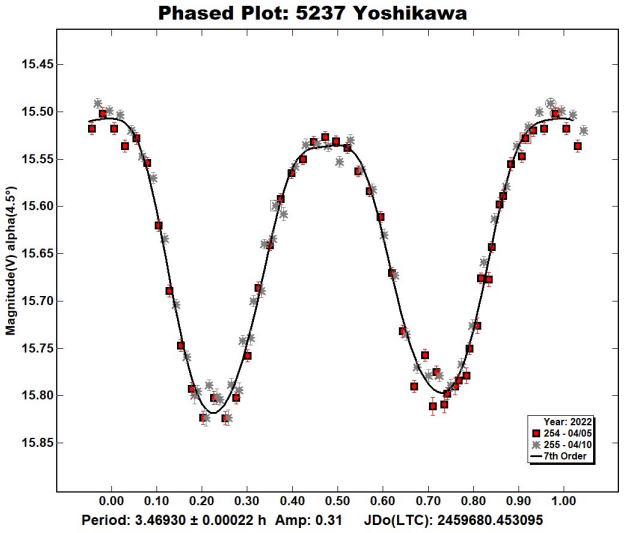

Figure 1. Phased lightcurve of 5237 Yoshikawa.

Number	Name	2022 mm/dd	Pts	Phase	L_{PAB}	B_{PAB}	Period(h)	P.E.	Amp	A.E.	Grp
5237	Yoshikawa	04/05 - 04/10	98	4.5 - 1.8	202.4	2.2	3.4693	±0.0002	0.31	0.03	MBA

Table I. Observing circumstances and results. Pts is the number of data points. The phase angle is given for the first and last date. L_{PAB} and B_{PAB} are the approximate phase angle bisector longitude and latitude at mid-date range (see Harris *et al.*, 1984). Grp is the asteroid family/group (Warner *et al.*, 2009).

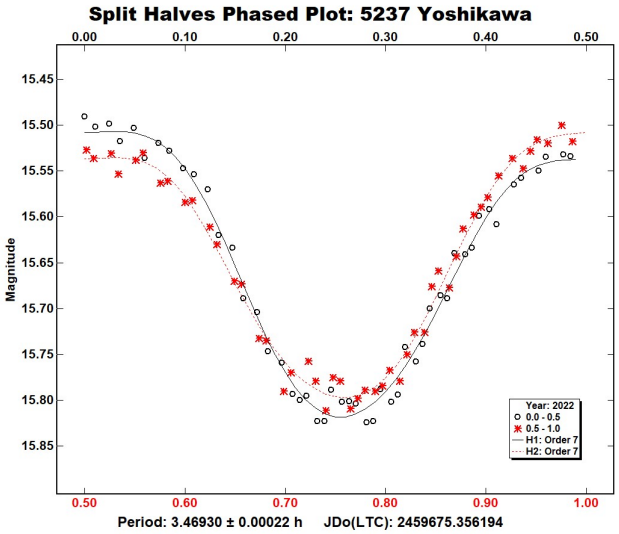

Figure 2. Split halves lightcurve of 5237 Yoshikawa.

References

Harris, A.W.; Young, J.W.; Scaltriti, F.; Zappala, V. (1984). "Lightcurves and phase relations of the asteroids 82 Alkmene and 444 Gyptis." *Icarus* **57**, 251-258.

JPL (2022). Small-Body Database Browser. *http://ssd.jpl.nasa.gov/sbdb.cgi#top*

LCDB (2022). The Asteroid Lightcurve Database. *http://www.minorplanet.info/php/lcdb.php*

MPC (2022). MPC Database. *http://www.minorplanetcenter.net/db_search/*

Warner, B.D. (2006). A Practical Guide to Lightcurve Photometry and Analysis (2nd edition). *Springer*, New York.

Warner, B.D.; Harris, A.W.; Pravec, P. (2009). "The Asteroid Lightcurve Database." *Icarus* 202, 134-146. Updated 2018 June 23.

Warner, B.D. (2019). MPO Software, MPO Canopus v10.8.1.1. Bdw Publishing. *http://minorplanetobserver.com*

Waszczak, A.; Chang, C.-K.; Ofek, E.O.; Laher, R.; Masci, F.; Levitan, D.; Surace, J.; Cheng, Y.-C.; Ip, W.-H.; Kinoshita, D.; Helou, G.; Prince, T.A.; Kulkarni, S. (2015). "Asteroid Light Curves from the Palomar Transient Factory Survey: Rotation Periods and Phase Functions from Sparse Photometry." *Astron. J.* **150**, A75.

LIGHTCURVE PHOTOMETRY OF ASTEROID 8693 MATSUKI

Idris Abubakar Sani
NASRDA-Centre for Basic Space Science Nsukka, Enugu State, NIGERIA
idrisabu4me@yahoo.com

Matthew C. Nowinski
George Mason University
mnowinsk@gmu.edu

Umahi A. E., Okike O.
Ebonyi State University
Abakaliki, NIGERIA

Oyibo M, Umeh C. N., Okolo O. E., Bonaventure Okere
NASRDA-Centre for Basic Space Science

(Received: 2022 Jun 9)

Lightcurve photometry of the main-belt asteroid 8693 Matsuki yielded an estimated period of 6.10550 ± 0.00225 h and an amplitude of 0.53 ± 0.01 mag.

CCD photometric observations of the main-belt asteroid 8693 Matsuki were carried out in 2017 April and May at the Cerro Tololo Inter-American Observatory, La Serena, Chile (807). Data were obtained with a 0.41-m *f*/17.3 Ritchey-Chretien telescope and an Andor Aspen CG230 camera using an open filter. The pixel size was 0.874 arcseconds with binning set to 2×2. All exposures were 120 seconds.

Data processing and analysis were done with *MPO Canopus* (Warner, 2019). All images were calibrated with bias, dark, and flat field frames, and the instrumental magnitudes converted to R magnitudes using solar-colored field stars from the CMC-15 catalogue. Table I shows the observing circumstances and results.

8693 Matsuki was discovered on 1992 November 16 by K. Endate and K. Watanabe at Kitami in Japan. It is a main-belt asteroid with an orbital period of 3.73 years, semi-major axis of 2.41 au, eccentricity of 0.1581, and inclination of 6.927°. It has an absolute magnitude of 13.03. The WISE/NEOWISE survey (Masiero et al., 2011) reported a diameter of 5.944 ± 0.191 km and a visible albedo of 0.379 ± 0.083. Carvano et al. (2010) assigned an S-type taxonomic class. The asteroid's dynamical family is reported as 4 Vesta (Nesvorny, 2015). While asteroids in the Vesta dynamical family are commonly associated with the V-type taxonomic class, several studies have demonstrated that a wide range of taxonomic classes are also represented (Erasmus et al., 2019; Erasmus et al., 2020).

Observations for 8693 Matsuki were conducted over two nights and collected 233 data points. The lightcurve analysis showed a solution for the rotational period of P = 6.10550 ± 0.00225 h and with an amplitude A = 0.53 ± 0.01 mag, suggested by the strongest peak in the period spectrum.

Number	Name	yyyy mm/dd	Phase	L_{PAB}	B_{PAB}	Period(h)	P.E.	Amp	A.E.
8693	Matsuki	2017 04/30-05/01	8.8	8	-4	6.10550	0.00225	0.53	0.01

Table I. Observing circumstances and results. The phase angle is given for the first and last date. If preceded by an asterisk, the phase angle reached an extrema during the period. L_{PAB} and B_{PAB} are the approximate phase angle bisector longitude/latitude at mid-date range (see Harris et al., 1984).

A search through the asteroid lightcurve database (LCDB); Warner et al., 2009) and ADS indicated a period of 6.09724 ± 0.00005 h (Pal et al., 2020) for this asteroid based on photometry obtained using the Transiting Exoplanet Survey Satellite (TESS). Our result agreed with that published by Pal et al. (2020).

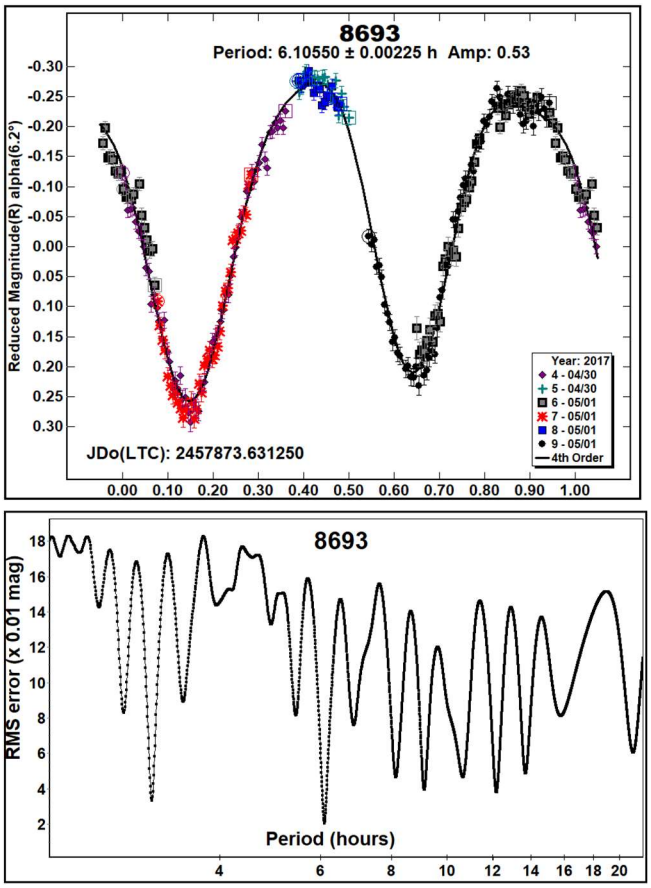

Acknowledgements

The authors would like to acknowledge the IAU ROAD offices, including NA-ROAD, WA-ROAD, and SA-ROAD; and Geneva Lake Astrophysics and STEAM (GLAS) Education, in Lake Geneva, Wisconsin. We would also like to thank the staff of the CTIO Skynet Robotic Telescope Network, including Daniel Reichart, Joshua Haislip, Vladimir Kouprianov, and Justin Moore. We would like to specially thank Kate Meredith, Amanda Pagul, Adam McCulloch, and Katya Gozman.

References

Carvano, J.M.; Hasselmann, P.H.; Lazzaro, D.; Mothe-Diniz, T. (2010). "SDSS-based taxonomic classification and orbital distribution of main belt asteroids." *Astronomy and Astrophysics* **510**, 1-12.

Erasmus, N. and 5 colleagues (2019). "A Taxonomic Study of Asteroid Families from KMTNET-SAAO Multiband Photometry." *Astrophysical Journal Supplement Series* **242:15**, 1-12.

Erasmus, N. and 8 colleagues (2020). "Investigating Taxonomic Diversity within Asteroid Families through ATLAS Dual-band Photometry." *Astrophysical Journal Supplement Series* **2472:13**, 1-7.

Harris, A.W.; Young, J.W.; Scaltriti, F.; Zappala, V. (1984). "Lightcurves and phase relations of the asteroids 82 Alkmene and 444 Gyptis." *Icarus* **57**, 251-258.

Masiero, J. and 17 colleagues (2011). "Main Belt Asteroids with WISE/NEOWISE. I. Preliminary Albedos and Diameters." *Astrophys. J.* **741**, 68.

Nesvorny, D. (2015). "Nesvorny HCM Asteroid Families V3.0." EAR-A-VARGBDET-5-NESVORNYFAM-V3.0. NASA Planetary Data System.

Pal, A.; Szakats, R., Kiss, C.; Bodi, A.; Bognar, Z.; Kalup, C.; Kiss, L.; Marton, G.; Molnar, L.; Plachy, E.; Sarneczky, K.; Szabo, G.M.; Szabo R. (2020). "Solar system objects observed with TESS - first data release; bright main-belt and trojan asteroids from the southern survey" *Astrophysical Journal Supplement Series* **247**, id. 26.

Warner, B.D.; Harris, A.W.; Pravec, P. (2009). "The Asteroid Lightcurve Database." *Icarus* **202**, 134-146. Updated 2021 Dec. *http://www.minorplanet.info/lightcurvedatabase.html*

Warner, B.D. (2019). *MPO Canopus Software*, version 10.8.1.1. BDW Publishing. *http://www.bdwpublishing.com*

ASTEROID 471109 VLADOBAHYL (2010 CO12): OBSERVATIONS OF THE LIGHTCURVE

Vladimír Bahýl
Observatory "Júlia"
962 01 Zvolenská, Slatina
Slovakia
basoft@zv.psg.sk

Jaromír Volný,
(private astronomical observatory)
Stupava, Slovakia

(Received: 2022 June 16)

We present CCD photometry results for the asteroid 471109 Vladobahyl (2010 CO12). From 507 images we have constructed the lightcurve of this asteroid and estimate its rotational period to be 4.9217 ± 0.1746 h.

The asteroid 471109 Vladobahyl was discovered by Stefan Kürti in 2010. Since discovery, there have been very few observations of it. We attempted to observe it at its opposition in 2022 since it was accessible to our telescopes at the time.

We used the Newton AG 14 telescope equipped with the Atik 460EXm camera with the pixel dimensions 4.54 μm × 4.54 μm at the J. Volny observatory in Stupava, Slovak Republic, during two nights. On 2022 January 6 we observed from the evening (19^h 04^{min} 06^{sec} UT) till the early morning of 2022 January 7 (03^h 42^{min} 12^{sec} UT). The next night on 2022 January 7 we have observed from the evening (18^h 03^{min} 38^{sec} UT) till the early morning of 2022 January 8 (02^h 26^{min} 24^{sec} UT). The exposure time was 120 s with no filters used. The sets of 'fits' files were stacked in *Astrometrica* (Raab, 2012) and the resultant fits images were measured using the *AstroImageJ* (Collins et al., 2017) software.

For the analysis of our measurements, we used the *Astrometrica* and *AstroImageJ* packages mentioned above. With *Astrometrica*, we first correctly detected the asteroid and then we measured it with *AstroImageJ*. We would like to emphasize that the measurements were done only if the object was clearly visible in the image. We used *AstroImageJ* for magnitude measurements since we found that *AstroImageJ* was more precise in our case. The comparison stars were selected individually from the Tycho-2 catalogue and were used for measurements on both nights.

Despite careful measurements, the dispersion of the observed magnitudes was quite high. Therefore, we decided to smooth the data using the *Mathematica* (Wolfram Research, 2021) package with a 7-point running average. The smoothed data were treated in the *Peranso* (Paunzen and Vanmunster, 2016) package to find the lightcurve of the asteroid using the CLEANest (Foster) and Lomb-Scrangle methods. Both methods gave us the same results within the limits of errors. We applied the *Peranso* package three times, i.e., for the data from both nights separately, and for the combined data from both nights with very similar results. The results were used to determine the rotation period of the asteroid to be 4.927 ± 0.1746 h (Table I).

While we acknowledge the fact that the dispersion of the observed data is high, we had two full nights of continuous observations with consistent results of the observed rotation period of the asteroid.

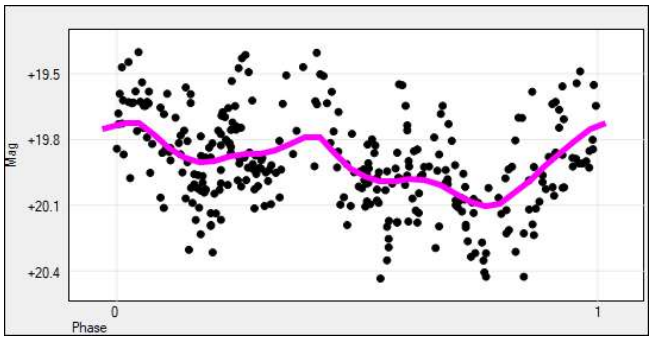

Figure 1. The lightcurve of the asteroid 471109 Vladobahyl.

Acknowledgements

This research made use of the NASA Exoplanet Archive, which is maintained by the California Institute of Technology, under contract with the National Aeronautics and Space Administration and the Exoplanet Exploration Program.

References

Collins, K.A.; Kielkopf, J.F.; Stasson, K.G.; Hessman, F.V. (2017). "*ASTROIMAGEJ*: Image processing and photometric extraction for ultra-precise astronomical light curves." *Astron. J.* **152:77**, 13pp. *http://www.astro.louisville.edu/software/astroimagej/*

Paunzen, E.; Vanmunster, T. (2016). *Peranso* - Light Curve and Period Analysis Software.

Raab, H. (2012). *Astrometrica*: Astrometric data reduction of CCD images, Astrophysics Source Code Library, record ascl: 1203.012.

Wolfram Research, Inc. (2021). *Mathematica,* Version 13.0.0, Champaign, IL.

Number	Name	yyyy mm/dd	Phase	L_{PAB}	B_{PAB}	Period(h)	P.E.	Amp	A.E.	r
471109	Vladobahyl	2022 01/06-01/08	7.8,8.5	94	5.9	4.9217	0.1746	0.38	0.21	2.15

Table I. Observing circumstances and results.

LIGHTCURVE ANALYSIS OF ASTEROID 2999 DANTE

Caroline Odden, Claire Cahill, Nishani Clarke,
Isabella Clemmons, Ethan Gerakaris, Yihao Huang, Fred Javier,
Davin Jeong, Stewart Kristiansen, Lauren Lee, Jeremy Lin,
Mason McCormack, Emily Mae Murtha, Marah Quran,
Lexiana Tucci, Olha Yarynich, Ki Zhang
Phillips Academy Observatory (MPC I12)
180 Main Street
Andover, MA 01810 USA
ceodden@andover.edu

Jonathan Kemp
Middlebury College
Mittelman Observatory
Middlebury, VT 05753 USA

(Received: 2022 July 14)

Photometric measurements were conducted on asteroid 2999 Dante from the Phillips Academy Observatory (PAO), the Mittelman Observatory, and the iTelescope T18 Observatory from 2022 February 06 to March 04. The rotational period and amplitude were determined to be 49.714 ± 0.001 h and 0.55 ± 0.05 mag.

Asteroid 2999 Dante was chosen from the CALL website. Observations were mostly made from the Phillips Academy Observatory (PAO), located in Andover, Massachusetts. Observations from PAO were made with a 0.50-m f/6.8 Corrected Dall-Kirkham (CDK) Astrograph telescope manufactured by PlaneWave Instruments and an FLI ProLine 4240 Camera with a 2048×2048 array of 13.5-micron pixels cooled to a temperature of -40°C. The resulting image scale was 0.81 arcseconds per pixel. 300 second exposures were taken through a luminance filter. Exposures were unbinned and unguided. All images were corrected using dark frames, flat-fields, and bias frames using *AstroImageJ* Software v.3.2.21 (Collins et. al., 2017). Observations from the Phillips Academy Observatory were supplemented with a data set from the iTelescope T18 telescope in Nerpio, Spain as well as a data set from the Mittelman Observatory at New Mexico Skies. Detailed information about the additional observatory sites used are listed in the table below.

Site	Telescope	Camera	Sessions
Mittelman Observatory	PlaneWave CDK20 0.50-m f/6.8	SBIG STX (KAF-16803)	2022 February 9 (session 260)
iTelescope T18 Astrocamp	PlaneWave CDK12 0.32-m f/8.0	SBIG STL-6303E	2022 February 9 (sessions 264,265)

MPO Canopus (Warner, 2018) was used to make photometric measurements of the images using differential photometry as well as to generate the final lightcurves. Comparison stars were chosen to have near solar-color, a B-V value close to 0.8, and a V-R value close to 0.45 (Warner, 2012). Data merging and period analysis were done with *MPO Canopus* using the Fourier Analysis for Lightcurves (FALC) algorithm developed by Alan Harris (Harris et al., 1989) and modified by Petr Pravec (Warner, 2012). The research was conducted for the Astronomy Research course at Phillips Academy, a high school in Andover, Massachusetts.

2999 Dante was discovered on 1981 February 6 by Norman G. Thomas at Lowell Observatory in Flagstaff, Arizona (JPL, 2022). The Asteroid Lightcurve Database (LCDB; Warner et al., 2009) did not have any recorded rotational period. Over the course of 11 nights between 2022 Febrary 06 and 2022 March 04, 979 data points were collected. These data points fit a rotational period of 49.714 ± 0.01 h with amplitude 0.55 ± 0.05 mag. Since Dante is a very slow rotator with a period close to twice the rotational period of the Earth, multiple sessions of images across different nights were required to obtain full coverage of the lightcurve. Images were taken from different observatory sites to further increase the coverage of the lightcurve. In spite of a dedicated campaign involving three different observatories, complete coverage could not be achieved due to moon placement and weather. Regardless, a bimodal solution with a period of P = 49.714 ± 0.001 h is favored. The period spectrum is included along with the phased plot.

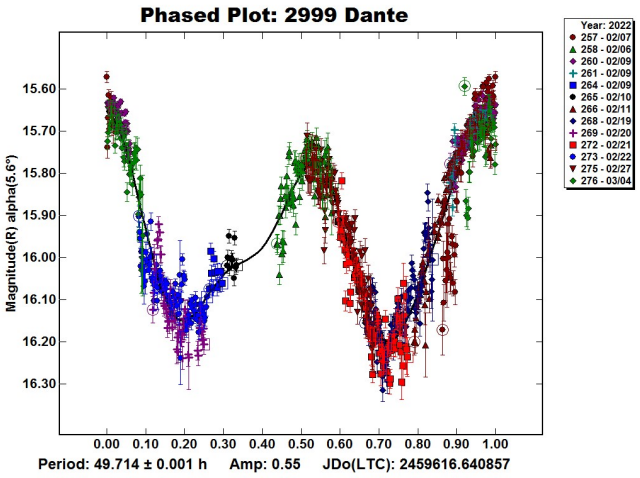

Number	Name	yyyy mm/dd	Phase	L_{PAB}	B_{PAB}	Period(h)	P.E.	Amp	A.E.	Grp
2999	Dante	2022 02/06-03/04	5.5, 15.3	137.9	9	49.714	0.001	0.55	0.05	MB-M

Table I. Observing circumstances and results. The phase angle is given for the first and last date. If preceded by an asterisk, the phase angle reached an extrema during the period. L_{PAB} and B_{PAB} are the approximate phase angle bisector longitude/latitude at mid-date range (see Harris et al., 1984). Grp is the asteroid family/group (Warner et al., 2009).

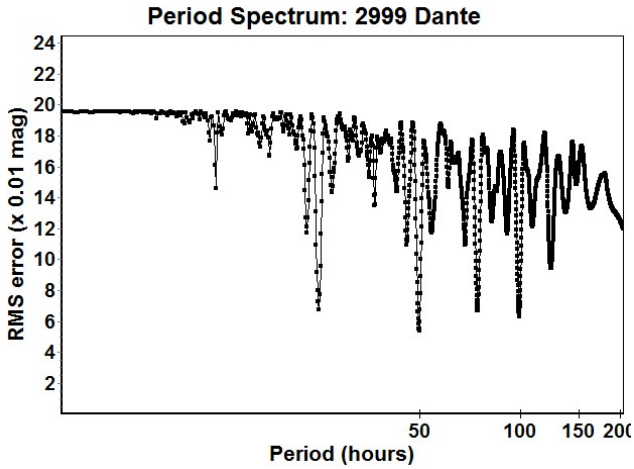

Acknowledgements

Research at the Phillips Academy Observatory is supported by the Israel Family Foundation. Funding for the FLI camera and PlaneWave telescope at Phillips Academy was provided by the Abbot Academy Association and the Donald T. Ganem Fund. This work includes observations obtained with the Mittelman Observatories 0.5-m telescope at New Mexico Skies in Mayhill, New Mexico.

References

CALL: Potential Lightcurve Targets (with LCDB data) Query. *http://www.minorplanet.info/PHP/call_OppLCDBQuery.php*

Collins, K.A.; Kielkopf, J.F.; Stasson, K.G.; Hessman, F.V. (2017). "*ASTROIMAGEJ*: Image processing and photometric extraction for ultra-precise astronomical light curves." *Astron. J.* **152:77**, 13pp. AstroImageJ, v.3.2.21. *http://www.astro.louisville.edu/software/astroimagej/*

Harris, A.W.; Young, J.W.; Scaltriti, F.; Zappala, V. (1984). "Lightcurves and phase relations of the asteroids 82 Alkmene and 444 Gyptis." *Icarus* **57**, 251-258.

Harris, A.W.; Young, J.W.; Bowell, E.; Martin, L.J.; Millis, R.L.; Poutanen, M.; Scaltriti, F.; Zappala, V.; Schober, H.J.; Debehogne, H.; Zeigler, K. (1989). "Photoelectric Observations of Asteroids 3, 24, 60, 261, and 863." *Icarus* **77**, 171-186.

JPL (2022). Small Body Database Browser. *http://ssd.jpl.nasa.gov/sbdb.cgi*

Warner, B.D.; Harris, A.W.; Pravec, P. (2009). "The Asteroid Lightcurve Database." *Icarus* **202**, 134-146. Updated 2021 Dec. *http://www.minorplanet.info/lightcurvedatabase.html*

Warner, B.D. (2012). The MPO Users Guide: A Companion Guide to the MPO Canopus/PhotoRed Reference Manuals. BDW Publishing, Colorado Springs, CO.

Warner, B.D. (2018). MPO Software, *MPO Canopus* v10.7.12.2. Bdw Publishing. *http://bdwpublishing.com*

LIGHTCURVE ANALYSIS OF ASTEROID 5889 MICKIEWICZ

Caroline Odden, Claire Cahill, Victoria Darling, Anna Du, Nicholas von Eckartsberg, Ethan Gerakaris, Jessica He, Yifei Jin, Jeremy Lin, Mason McCormack, Brooklyn Reagan, Xinkai Shen
Phillips Academy Observatory (MPC I12)
180 Main Street
Andover, MA 01810 USA
ceodden@andover.edu

(Received: 2022 July 14)

Photometric observations of asteroid 5889 Mickiewicz were performed at the Phillips Academy Observatory (PAO) from 2022 April 30 to May 26. The rotational period and amplitude were determined to be: P = 6.141 ± 0.001h, A = 0.51 ± 0.05 mag.

CCD photometric observations of the asteroids were made from the Phillips Academy Observatory. The asteroids were chosen from the CALL website. All observations were made with a 0.50-m *f*/6.8 Corrected Dall-Kirkham (CDK) Astrograph telescope manufactured by PlaneWave Instruments and an Andor Tech iKon DW436 CCD camera with a 2048×2048 array of 13.5-micron pixels. The resulting image scale was 0.81 arcseconds per pixel. All images were corrected using dark frames, flat-fields, and bias frames using *AstroImageJ* software (Collins et. al., 2017). All exposures were taken through a luminance filter at -50°C and were unbinned. Exposures were 300 s in length and unguided.

MPO Canopus (Warner, 2018) was used to make photometric measurements of the images using differential photometry as well as to generate the final lightcurves. Comparison stars were chosen to have near solar-color, a B-V value close to 0.8, and a V-R value close to 0.45 (Warner, 2012). In addition, brighter comparison stars were favored. Data merging and period analysis were done with *MPO Canopus* using the Fourier Analysis for Lightcurves (FALC) algorithm developed by Alan Harris (Harris et al., 1989) and modified by Petr Pravec (Warner, 2012). The research was conducted for the Astronomy Research course at Phillips Academy, a high school in Andover, Massachusetts.

5889 Mickiewicz was discovered by N. S. Chernykh at Nauchnyj on 1979 March 31. In the Asteroid Lightcurve Database (LCBD; Warner et al., 2009), there are two observed periods: P = 6.14148 ± 0.00002 (Ďurech et al., 2019) with no lightcurve and quality code U, and P = 6.1412 ± 0.0543, A=0.37 (Ergashev et al., 2019) with quality code value 3-.

Data were collected from 2022 April 20 to 2022 May 26, with a total of 295 data points included in the plot. Double coverage for the entire period is presented. Note that a portion of the session from 10 March 2022 appears to deviate from the typical behavior. Inspection of the original images did not reveal any abnormality. Finding no justification for removing this data, the authors have left it in. The period spectrum shows several favorable solutions, but the bimodal solution P = 6.141 h is most likely given the amplitude (Harris et. al, 2014). This result corresponds with the previously reported periods.

Number	Name	yyyy mm/dd	Phase	L_{PAB}	B_{PAB}	Period(h)	P.E.	Amp	A.E.	Grp
5889	Mickiewicz	2022 4/30-05/26	12.7,10.3	240	20.9	6.141	0.001	0.51	0.05	MB-M

Table I. Observing circumstances and results. The phase angle is given for the first and last date. If preceded by an asterisk, the phase angle reached an extrema during the period. L_{PAB} and B_{PAB} are the approximate phase angle bisector longitude/latitude at mid-date range (see Harris et al., 1984). Grp is the asteroid family/group (Warner et al., 2009).

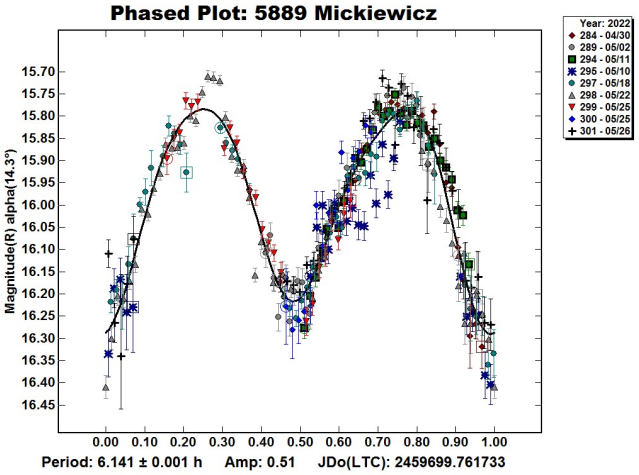

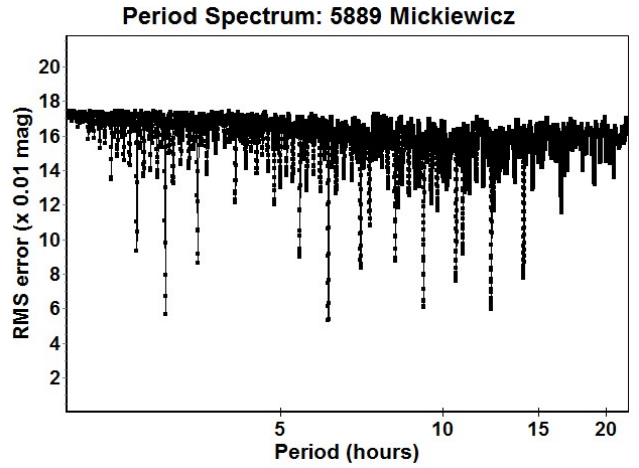

Acknowledgements

Research at the Phillips Academy Observatory is supported by the Israel Family Foundation. Funding for the Andor Tech camera and PlaneWave telescope at Phillips Academy was provided by the Abbot Academy Association, the Donald T. Ganem Fund, and the Taylor Family.

References

CALL: Potential Lightcurve Targets (with LCDB data) Query. *http://www.minorplanet.info/PHP/call_OppLCDBQuery.php*

Collins, K.A.; Kielkopf, J.F.; Stasson, K.G.; Hessman, F.V. (2017). "*ASTROIMAGEJ*: Image processing and photometric extraction for ultra-precise astronomical light curves." *Astron. J.* **152:77**, 13pp. AstroImageJ, v.3.2.21. *http://www.astro.louisville.edu/software/astroimagej/*

Ďurech, J.; Hanuš, J.; Vančo, R. (2019). "Inversion of asteroid photometry from Gaia DR2 and the Lowell Observatory photometric database." *Astronomy & Astrophysics* **631**, id. A2, 4. doi: 10.1051/0004-6361/201936341.

Ergashev, K.E.; Ehgamberdiyev, Sh.A.; Burkhonov, O.A.; Turayev, Y.Sh.; Yoshida, F. (2019). "Rotation Period Determination of 5889 Mickiewicz and 13063 Purifoy." *Bulletin of the Minor Planets Section of the Association of Lunar and Planetary Observers* **46**, 229-230. *https://ui.adsabs.harvard.edu/abs/2019MPBu...46..229E*

Harris, A.W.; Young, J.W.; Scaltriti, F.; Zappala, V. (1984). "Lightcurves and phase relations of the asteroids 82 Alkmene and 444 Gyptis." *Icarus* **57**, 251-258.

Harris, A.W.; Young, J.W.; Bowell, E.; Martin, L.J.; Millis, R.L.; Poutanen, M.; Scaltriti, F.; Zappala, V.; Schober, H.J.; Debehogne, H.; Zeigler, K. (1989). "Photoelectric Observations of Asteroids 3, 24, 60, 261, and 863." *Icarus* **77**, 171-186.

Harris, A.W.; Pravec, P.; Galad, A.; Skiff, B.A.; Warner, B.D.; Vilagi, J.; Gajdos, S.; Carbognani, A.; Hornoch, K.; Kusnirak, P.; Cooney, W.R.; Gross, J.; Terrell, D.; Higgins, D.; Bowell, E.; Koehn, B.W. (2014). "On the maximum amplitude of harmonics on an asteroid lightcurve." *Icarus* **235**, 55-59.

Warner, B.D.; Harris, A.W.; Pravec, P. (2009). "The Asteroid Lightcurve Database." *Icarus* **202**, 134-146. Updated 2021 Dec. *http://www.minorplanet.info/lightcurvedatabase.html*

Warner, B.D. (2012). The MPO Users Guide: A Companion Guide to the MPO Canopus/PhotoRed Reference Manuals. BDW Publishing, Colorado Springs, CO.

Warner, B.D. (2018). MPO Software, *MPO Canopus* v10.7.12.2. Bdw Publishing. *http://bdwpublishing.com*

LIGHTCURVE ANALYSIS AND ROTATION PERIOD DETERMINATION OF ASTEROID 1466 MUNDLERIA

Melissa Hayes-Gehrke, Tochukwu Ibe-Ekeocha,
Aravind Ganeshan, Jaelah Jupiter, Ryan Leeson,
Catherine Ondrusek, Nana Owusu, Dhvani Patel,
Jay Rajpara, Carly Redett, Gabriela Rodriguez-Velez,
Roma Sheth, Anthony Vo
Department of Astronomy
University of Maryland, College Park, MD 20742 USA
mhayesge@umd.edu

Martin Mifsud
Manikata Observatory
Manikata, Malta

Charles Galdies
Znith Observatory
Naxxar, Malta

Alessandro Marchini, Riccardo Papini
Astronomical Observatory of the University Siena
Siena, Italy

(Received: 2022 June 22)

Photometric observations of asteroid 1466 Mundleria (e = 0.15, i = 13.15°, H = 12.23) were conducted using telescopes located in New Mexico, Italy, and Malta between 2022 Mar 24 and Apr 25. An analysis of these data yielded a rotation period of 89.280 ± 0.065 h.

1466 Mundleria (1938 KA) was discovered by Karl Reinmuth at the Heidelberg Observatory in 1938 and named in honor German astronomer Max Mundler. It orbits the inner part of the main belt with a semi-major axis of 2.38 AU. 1466 Mundleria has an absolute magnitude of 12.23, a diameter of 22.13 km, an eccentricity of 0.15, and an inclination of 13.15° (JPL, 2022).

The University of Maryland authors observed the asteroid with the T21 telescope located in Mayhill, New Mexico, using a 0.43-m reflector with an f/4.5 focal reducer and an FLI-PL6303E CCD camera. A luminance filter was used along with an exposure time of 300 seconds and binning of 1. Marchini at the University of Siena used a 0.30-m f/5.6 Maksutov-Cassegrain telescope, SBIG STL-6303E NABG CCD camera, and a Clear filter. The pixel scale was 2.30 arcsec when binned 2 × 2 pixels and all exposures were 300 seconds. Mifsud at the Manikata Observatory used an 8-in Meade LX90 telescope with a SBIG ST10xme CCD camera. Galdies at the Znith Observatory used a 203-mm SCT telescope with a G2-1600 CCD camera binned at 1×1 pixels.

MPO Canopus (Warner, 2018) was used to perform aperture and differential photometry. A series of phased lightcurves were constructed using telescope observations between the nights of 2022 Mar 24 and Apr 25. The observing schedule along with results from the lightcurve analysis are summarized in Table I.

Period analysis shows a rotation period of 89.280± 0.065 h with an amplitude of 0.24 ± 0.04 mag. We could not find any previous rotation periods reported for 1466 Mundleria in the Asteroid Lightcurve Database (LCDB; Warner et al., 2009).

The phased lightcurve shows a bimodal distribution typical for asteroids. The determined rotation period, however, is larger than for most asteroids, and further observations are needed for refinement.

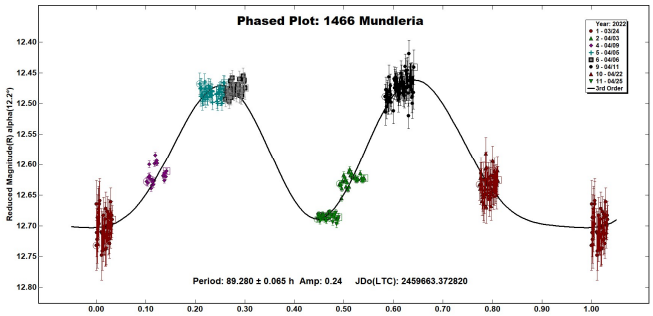

Acknowledgments

Use of the iTelescope online observing platform was made possible with funding provided by the University of Maryland Department of Astronomy. We would also like to credit the creators of the *MPO Canopus* and *DS9* platforms which were used for image-viewing and lightcurve analysis.

References

Harris, A.W.; Young, J.W.; Scaltriti, F.; Zappala, V. (1984). "Lightcurves and phase relations of the asteroids 82 Alkmene and 444 Gyptis." *Icarus* **57**, 251-258.

JPL. (2022). Small-Body Database Browser. *http://ssd.jpl.nasa.gov/sbdb.cgi*

Warner, B.D.; Harris, A.W.; Pravec, P. (2009). "The Asteroid Lightcurve Database." *Icarus* **202**, 134-146. Updated 2021 Dec. *http://www.minorplanet.info/lightcurvedatabase.html*

Warner, B.D. (2018). MPO Software, *MPO Canopus* version 10.12.9.0. *http://minorplanetobserver.com*

Number	Name	yyyy mm/dd	Phase	L_{PAB}	B_{PAB}	Period(h)	P.E.	Amp	A.E.	Grp
1466	Mundleria	2022 3/24-4/25	8.9	200.5	13.7	89.280	0.065	0.24	0.04	MB-I

Table I. Observing circumstances and results. The phase angle is given for the first and last date. If preceded by an asterisk, the phase angle reached an extrema during the period. L_{PAB} and B_{PAB} are the approximate phase angle bisector longitude/latitude at mid-date range (see Harris et al., 1984). Grp is the asteroid family/group (Warner et al., 2009).

ROTATION PERIOD DETERMINATION AND LIGHTCURVE ANALYSIS OF ASTEROID 3736 ROKOSKE

Melissa Hayes-Gehrke, Colin Bragger, Jason Dang, Jennifer Houston, Asia Mackay, Khunoot Mansoor, Ryan Lienemann, Steven O'Ferrall, Alexander Smelson, Aaron Epstein, Jeet Patel, Nathan Gallagher, Shamira Miles
UMD Astronomy Department
1113 PSC Bldg 415, College Park, MD 20742 USA
mhayesge@umd.edu

Charles Galdies
Znith Observatory
Naxxar, Malta

Alessandro Marchini, Riccardo Papini
Astronomical Observatory of the University of Siena
Siena, Italy

(Received: 2022 June 22)

Observations of the main-belt asteroid 3736 Rokoske were conducted over 8 nights between 2022 March 25 and 2022 April 23. Images were collected using three telescopes in the USA, Malta, and Italy. 3736 Rokoske has a diameter of 19.5 km and an absolute magnitude of 11.15. *MPO Canopus* was used for calibration and lightcurve analysis. The phased lightcurve resulted in a rotation period of 17.411 ± 0.004 h and 0.10 ± 0.02 mag amplitude.

3736 Rokoske was first discovered in 1987 by Edward Bowell in Flagstaff, AZ (LCDB; Warner et al., 2009). It is a main-belt asteroid with a semi-major axis of 3.02 AU, eccentricity of 0.08, inclination of 11.30°, orbital period of 5.3 years, a diameter of 19.5 km, and an absolute magnitude of 11.15. Following a search through the Asteroid Lightcurve Database, we discovered the rotation period is currently unknown. The present lightcurve analysis can provide insight into a possible rotation period for the asteroid.

Images were collected during 8 nights between 2022 Mar 25 and Apr 23. The University of Maryland observers used the iTelescope 21 located in Mayhill, New Mexico (MPC Code: H06) on Apr 1, Apr 4, Apr 7, Apr 9, and Apr 23. The Planewave 17" CDK telescope has a focal length of 1940 mm, and an aperture of 431 mm. The FLI-PL6303E CCD camera used has a pixel size of 9 µm square, array of 3072 × 2048 pixels, and a resolution of 0.96 arcsec/pix. The luminance filter was used for all observations.

Galdies observed from the Znith Observatory in Malta on Mar 25 and Apr 23 using a 203-mm SCT telescope with a Moravian G2-1600 CCD camera at 1 × 1 binning and a luminance filter.

Marchini and Papini observed from the Astronomical Observatory of the University of Siena (MPC Code: K54). Observations were made on Apr 10, Apr 11, and Apr 12 with a 0.30-m f/5.6 Maksutov-Cassegrain telescope, SBIG STL-6303 NABG CCD camera, and Clear filter at 2 × 2 binning.

Lightcurve analysis was done with *MPO Canopus* (version 10.7.12.0; Warner 2019). Raw lightcurves were made for each night and, in the case of a meridian flip of the telescope, independent lightcurves were created for before and after the flip. Raw lightcurves were phased to numerous test periods with data from all three telescopes. Analysis of the resulting phased lightcurve shows that asteroid 3736 Rokoske has a typical lightcurve with two peaks and two troughs. The derived rotation period is 17.411 ± 0.004 h with an amplitude of 0.10 ± 0.02 mag.

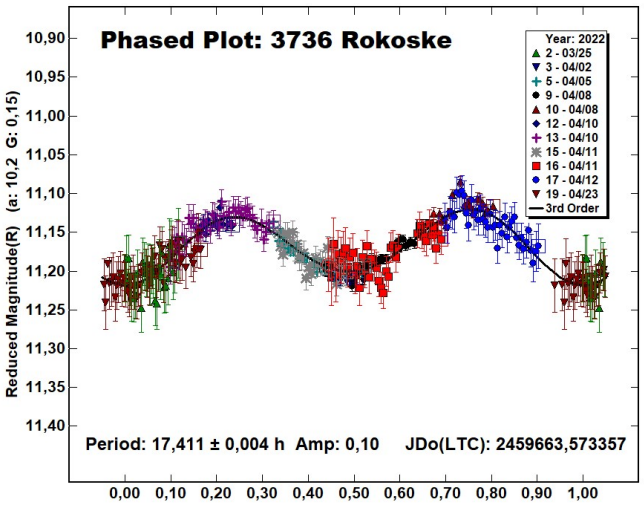

Acknowledgments

The University of Maryland authors would like to gratefully acknowledge funding from the Department of Astronomy of the University of Maryland, College Park. Additionally, they would like to thank iTelescope, which made our observations of 3736 Rokoske possible.

References

Harris, A.W.; Young, J.W.; Scaltriti, F.; Zappala, V. (1984). "Lightcurves and phase relations of the asteroids 82 Alkmene and 444 Gyptis." *Icarus* **57**, 251-258.

JPL (2020). Small Body Database Browser. *https://ssd.jpl.nasa.gov*

Warner, B.D.; Harris, A.W.; Pravec, P. (2009). "The Asteroid Lightcurve Database." *Icarus* **202**, 134-146. Updated 2016 Sep. *http://www.minorplanet.info/lightcurvedatabase.html*

Warner, B.D. (2019). MPO Software, *MPL Canopus* v10.7.12.9 Bdw Publishing. *http://minorplanetobserver.com*

Number	Name	yyyy mm/dd	Phase	L_{PAB}	B_{PAB}	Period(h)	P.E.	Amp	A.E.	Grp
3736	Rokoske	2022 3/25-4/23	10.2,5.3	208.7	12.3	17.411	0.004	0.10	0.02	MB

Table I. Observing circumstances and results. The phase angle is given for the first and last date. If preceded by an asterisk, the phase angle reached an extrema during the period. L_{PAB} and B_{PAB} are the approximate phase angle bisector longitude/latitude at mid-date range (see Harris et al., 1984). Grp is the asteroid family/group (Warner et al., 2009).

A REEXAMINATION OF THE ROTATION PERIOD OF 1541 ESTONIA

Frederick Pilcher
Organ Mesa Observatory (G50)
4438 Organ Mesa Loop
Las Cruces, NM 88011 USA
fpilcher35@gmail.com

Eric V. Dose
3167 San Mateo Blvd NE #329
Albuquerque, NM 87110 USA

(Received: 2022 July 14)

A previously published period ambiguity for 1541 Estonia of 6.444 or 12.890 hours has been reexamined. We prefer a 12.889 ± 0.001-hour period with amplitude 0.16 ± 0.01 magnitudes.

The two authors of this paper made independent photometric investigations of the rotational properties of 1541 Estonia in the interval 2022/02 to 2022/04. Dose (2022) found a period of 6.444 hours and Pilcher (2022) found a period twice as great, 12.890 hours. After learning of our respective results, we have merged our data in an attempt to resolve the ambiguity. Our equipment and observational procedures have been previously described in our papers referenced above. To reduce the number of data points on the lightcurves and make them easier to read, data points have been binned in sets of 3 with maximum time difference 5 minutes. Earlier published rotation periods are by Behrend (2015web), 10.1 hours; and by Polakis (2021), 12.84 hours.

Sessions 1732-1757, 2022 Feb. 25 to Apr. 3, are by Pilcher, originally obtained in CMC15 R band, where R=r'-0.22. Sessions 1818-1823, 2022 Feb. 9 - Apr. 4, are by Dose, originally obtained with the exoplanet/blue-blocker filter and transformed to the Sloan r' band. During the merger of the two data sets the zero points of one set had to be adjusted by about 0.17 magnitudes to obtain best fit to the other set. Lightcurve construction and period solution was done with *MPO Canopus* software.

MPO Canopus software uses the FALC algorithm written by Alan Harris to find the rotation period that best fits the data within the range specified by the user. This algorithm finds the coefficients of each order of the Fourier series up to a user specified maximum number, 10 in the calculations performed here, for a specified range of periods, and computes for each period within that range the rms residual, in units of 0.01 magnitudes, of all the individual data points from the graph specified by the Fourier components. It then plots the lightcurve for that period within the specified range for which the rms is a minimum and writes the both the period and rms residual of the individual data points. The saved lightcurves do not state the rms residual, but the first author has written them onto each lightcurve.

For all twelve sessions, range of phase angles 12.9º to a minimum of 1.6º to 10.6º, lightcurves were to drawn to 6.445 hours (Fig. 1) with a mean residual of 1.3932 × 0.01 magnitudes and to 12.889 hours (Fig. 2) with a mean residual of 1.1622 × 0.01 magnitudes. The data scatter by eyeball scanning is notably smaller for the 12.889-hour lightcurve. The split halves plot for the 12.889-hour lightcurve (Fig. 3) also shows a small systematic difference between the two halves for some segments of the lightcurve. By all three criteria a period of 12.889 hours is preferred to one of 6.445 hours. The minimum near phase 0.5 of the 12.889-hour lightcurve is deeper for the larger phase angles than for the smaller ones. This is a commonly occurring effect found in lightcurves sampled over a large range of phase angles for many asteroids. The change of depth with phase angle is not seen in the minimum near phase zero. If the period really were 6.445 hours, the depths of the minima should change in step. The different behaviors of the two minima constitute a fourth criterion for which the longer period 12.889 hours is preferred.

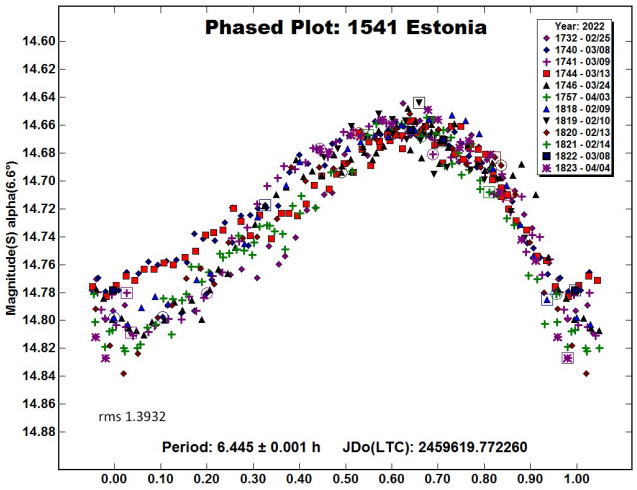

Figure 1. Lightcurve of 1541 Estonia, 2022/02/09 to 2022/04/04 phased to 6.445 hours.

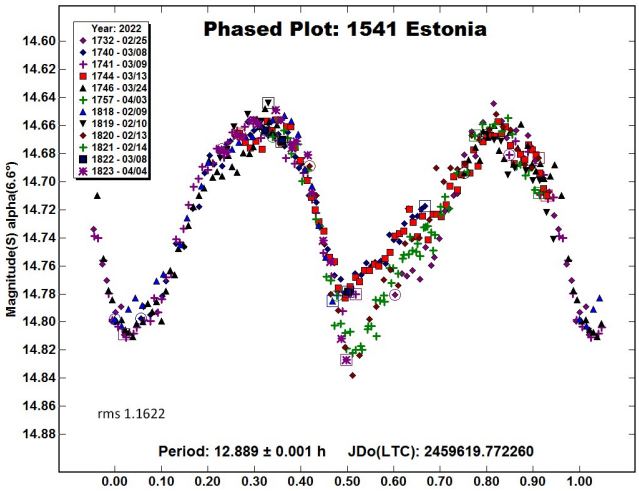

Figure 2. Lightcurve of 1541 Estonia, 2022/02/09 to 2022/04/04 phased to 12.889 hours.

Number	Name	yyyy/mm/dd	Phase	L_{PAB}	B_{PAB}	Period(h)	P.E	Amp	A.E.
1541	Estonia	2022/02/09-2022/04/04	*12.9, 10.6	170	1	12.889	0.001	0.16	0.01

Table I. Observing circumstances and results. Pts is the number of data points. The phase angle is given for the first and last date, unless a minimum (second value) was reached. L_{PAB} and B_{PAB} are the approximate phase angle bisector longitude and latitude at mid-date range (see Harris *et al.*, 1984).

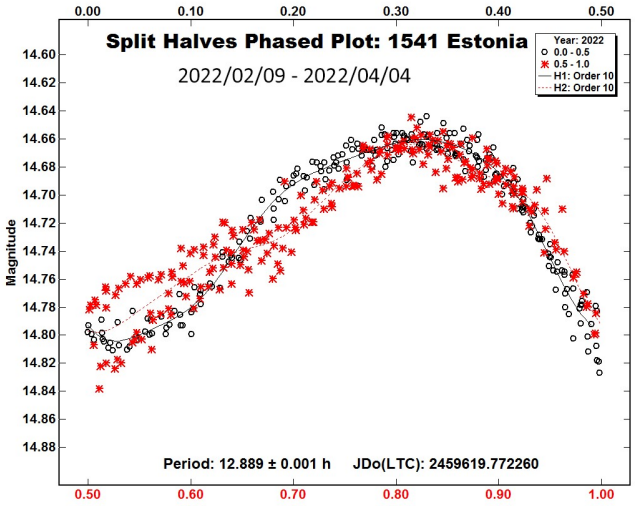

Figure 3. Split halves lightcurve of 1541 Estonia for the interval 2022/02/09 to 2022/04/04.

A long interval of observations, nearly two months for the study in this paper, covers a larger number of rotational cycles and provides a more accurate period. There is a trade-off, in that the shape of the lightcurve changes with phase angle and reduces any shape differences in any bimodal lightcurve. A subset of five sessions from 03/08 at phase angle 1.6º through 03/24 at phase angle 6.0º does not include a large enough change of phase angle for this effect to be apparent. A lightcurve drawn to a period of 6.449 hours (Fig. 4) shows a rms residual of 1.2382 × 0.01 magnitudes and a bifurcation of data points near the single minimum. A lightcurve drawn to a period of 12.894 hours (Fig. 5) shows a clearly asymmetric lightcurve with rms residual only 0.7010 × 0.1 magnitudes. The split halves lightcurve for the interval March 08 to March 24 (Fig. 6) also shows a distinct separation of many corresponding segments of the two halves. The evidence at a small range of phase angles favoring the longer period is now very strong.

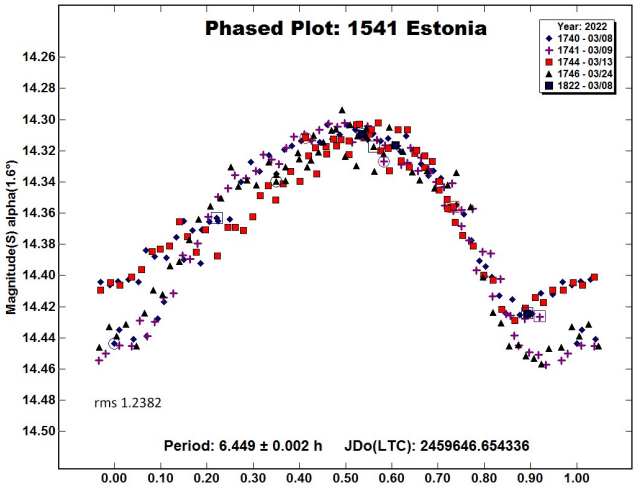

Figure 4. Lightcurve of 1541 Estonia, 2022/03/08 to 2022/03/24 phased to 6.449 hours.

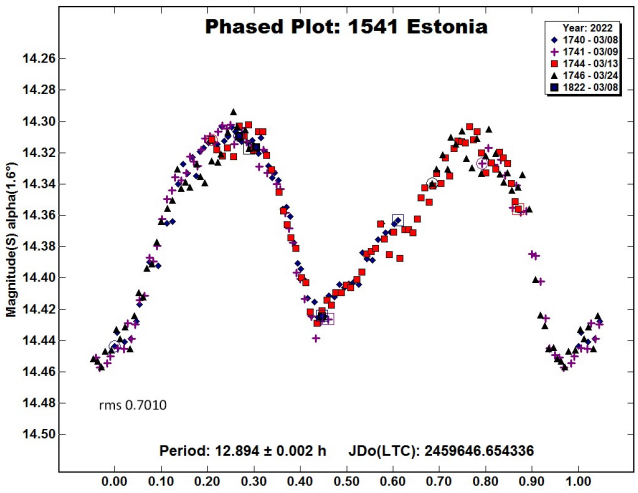

Figure 5. Lightcurve of 1541 Estonia, 2022/03/08 to 2022/03/24 phased to 12.894 hours.

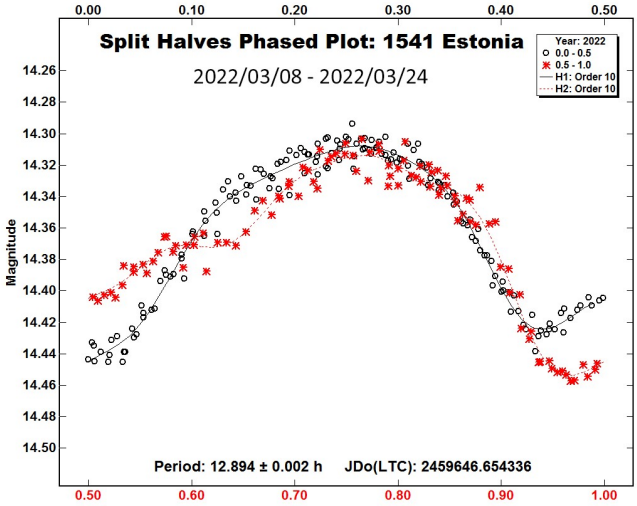

Figure 6. Split halves lightcurve of 1541 Estonia for the interval 2022/03/08 to 2022/03/24.

We conclude that the synodic rotation period of 1541 Estonia is 12.889 ± 0.001 hours and the amplitude is 0.16 ± 0.01 magnitudes. The new observations are consistent with Polakis (2021) and rule out the 10.1-hour period reported by Behrend (2015web).

References

Behrend, R. (2015web). Observatoire de Geneve web site. *http://*obswww.unige.ch/*~behrend/page_cou.html*

Dose, E.V. (2022). "Lightcurves of eight asteroids." *Minor Planet Bull.* **49**, 218-222.

Harris, A.W.; Young, J.W.; Scaltriti, F.; Zappala, V. (1984). "Lightcurves and phase relations of the asteroids 82 Alkmene and 444 Gyptis." *Icarus* **57**, 251-258.

Pilcher, F. (2022). "Lightcurves and rotation periods of 49 Pales, 424 Gratia, 705 Erminia, 736 Harvard, 1261 Legia, 1541 Estonia, and 6371 Heinlein." *Minor Planet Bull.* **49**, 185-188.

Polakis, T. (2021). "Period determination for seventeen minor planets." *Minor Planet Bull.* **48**, 158-163.

ROTATION PERIOD DETERMINATION FOR ASTEROID 3616 GLAZUNOV

Alessandro Marchini, Riccardo Papini
Astronomical Observatory, DSFTA - University of Siena (K54)
Via Roma 56, 53100 - Siena, ITALY
marchini@unisi.it

(Received: 2022 July 14)

Photometric observations of the main-belt asteroid 3616 Glazunov were conducted in order to determine its synodic rotation period. We found P = 18.932 ± 0.004 h, A = 0.14 ± 0.03 mag.

CCD photometric observations of the main-belt asteroid 3616 Glazunov were carried out in 2022 May-July at the Astronomical Observatory of the University of Siena (K54), a facility inside the Department of Physical Sciences, Earth and Environment (DSFTA, 2022). We used a 0.30-m *f*/5.6 Maksutov-Cassegrain telescope, SBIG STL-6303E NABG CCD camera, and clear filter; the pixel scale was 2.30 arcsec when binned at 2×2 pixels and all exposures were 300 seconds.

Data processing and analysis were done with *MPO Canopus* (Warner, 2018). All images were calibrated with dark and flat-field frames and the instrumental magnitudes converted to R magnitudes using solar-colored field stars from a version of the CMC-15 catalogue distributed with *MPO Canopus*. Table I shows the observing circumstances and results.

A search through the asteroid lightcurve database (LCDB; Warner et al., 2009) indicates that our result may be the first reported lightcurve observations and results for this asteroid.

3616 Glazunov (1984 JJ2) was discovered on 1984 May 3 at Nauchnyj by L. V. Zhuravleva and named in honor of Il'ya Sergeevich Glazunov, a well-known Russian painter who died in 2017. It is a main-belt asteroid with a semi-major axis of 2.600 au, eccentricity 0.123, inclination 12.769°, and an orbital period of 4.19 years. Its absolute magnitude is H = 12.40 (JPL, 2022). The WISE/NEOWISE satellite infrared radiometry survey (Masiero et al., 2014) found a diameter D = 9.811 ± 0.145 km using an absolute magnitude H = 12.2.

Observations were conducted over nine nights and collected 275 data points. The period analysis shows a possible solution for the rotational period at P = 18.932 ± 0.004 h with an amplitude A = 0.14 ± 0.03 mag as the most likely bimodal solution for this asteroid. Because of the low amplitude and the precision of the photometry due to the not optimal sky conditions, further observations are highly recommended in future apparitions to verify the result.

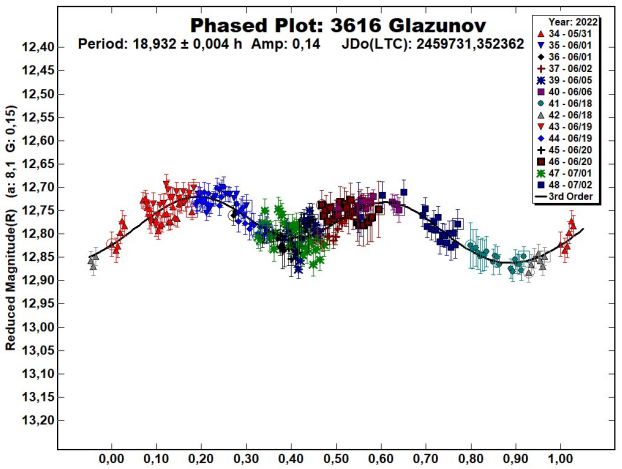

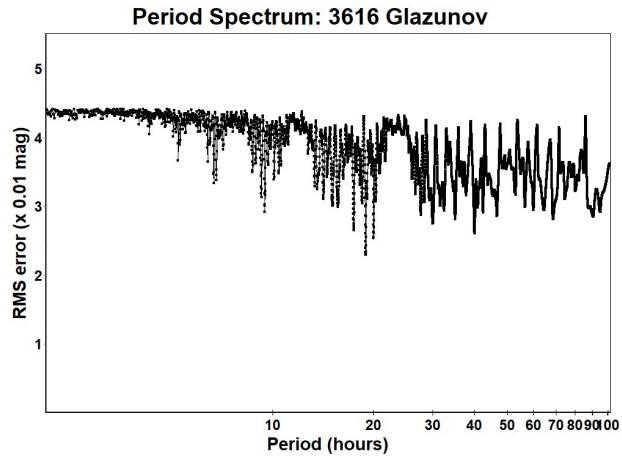

References

DSFTA (2022). Dipartimento di Scienze Fisiche, della Terra e dell'Ambiente – Astronomical Observatory. *https://www.dsfta.unisi.it/en/research/labs/astronomical-observatory*

Harris, A.W.; Young, J.W.; Scaltriti, F.; Zappala, V. (1984). "Lightcurves and phase relations of the asteroids 82 Alkmene and 444 Gyptis." *Icarus* **57**, 251-258.

JPL (2022). Small Body Database Search Engine. *https://ssd.jpl.nasa.gov*

Masiero, J.R.; Grav, T.; Mainzer, A.K.; Nugent, C.R.; Bauer, J.M.; Stevenson, R.; Sonnett, S. (2014). "Main-belt Asteroids with WISE/NEOWISE: Near-infrared Albedos." *Astrophys. J.* **791**, 121.

Warner, B.D.; Harris, A.W.; Pravec, P. (2009). "The Asteroid Lightcurve Database." *Icarus* **202**, 134-146. Updated 2022 July. *http://www.minorplanet.info/lightcurvedatabase.html*

Warner, B.D. (2018). MPO Software, *MPO Canopus* v10.7.7.0. Bdw Publishing. *http://minorplanetobserver.com*

Number	Name	2022/mm/dd	Phase	L_{PAB}	B_{PAB}	Period(h)	P.E.	Amp	A.E.	Grp
3616	Glazunov	05/31-07/03	*8.1,12.3	259	11	18.932	0.004	0.14	0.03	EUN

Table I. Observing circumstances and results. The phase angle is given for the first and last date. If preceded by an asterisk, the phase angle reached an extrema during the period. L_{PAB} and B_{PAB} are the approximate phase angle bisector longitude/latitude at mid-date range (see Harris et al., 1984). Grp is the asteroid family/group (Warner et al., 2009).

LIGHTCURVE FOR KORONIS FAMILY MEMBER (1363) HERBERTA

Francis P. Wilkin, Jayson Bromberg, Zuhair AlMassri,
Louis Beauchaine, Minh Nguyen
Union College
Department of Physics and Astronomy
807 Union St
Schenectady, NY 12308
wilkinf@union.edu

(Received: 2022 June 28 Revised: 2022 August 8)

We present our composite lightcurve for Koronis family asteroid (1363) Herberta. Based upon six nights in 2022 we obtained an improved rotation period of 3.016 ± 0.002 h with amplitude 0.13 ± 0.02 mag.

We have begun a program to observe members of the Koronis asteroid family in order to determine improved periods for use in obtaining spin solutions and shape models (Kaasalainen et al., 2001; Slivan et al., 2003).

Observation planning used the Koronisfamily.com web tool (Slivan, 2003), and images were obtained using four telescopes including the Union College Observatory and remote access through the networks iTelescope.net (T21) and Telescope.Live (Spa-2 and Chi-3; see Table 1). Exposure times were generally 240 s and binning 2×2 except on Chi-3 where they were 180 s and 1×1 respectively. All observations used a red filter but specific filters varied by observatory due to availability.

A total of six observing nights spanning approximately 40 days was obtained. The specific nights are indicated by the legend of the lightcurve figure, and parameter values for phase and phase angle bisector appearing in Table II were found using the NASA Horizons ephemeris tool. Images were processed for bias, dark, and flat field corrections. We used *AstroImageJ* software (Collins et al., 2017) to process the Union College images and to perform photometry on all images. Light-time corrections were applied using NASA Horizons ephemerides.

Because the individual nights were not calibrated to a common brightness zero-point, constant brightness offsets were used to shift each night's data to arrive at a self-consistent lightcurve. We obtained a best fit synodic period P = 3.016 ± 0.002 h, in agreement with the previous value of 3.015 ± 0.005 (Black et al., 2016). The amplitude (from trough to peak) is 0.13 ± 0.02 mag.

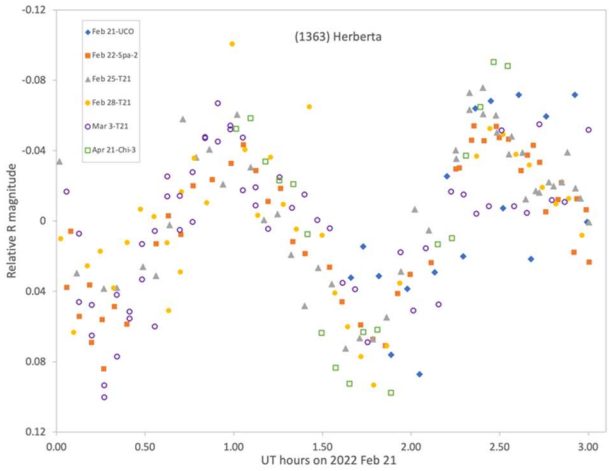

Acknowledgements

FPW received funding from the Union College Faculty Research Fund. We are grateful to S. Slivan for helpful suggestions. Student researchers were funded by the Union College Research Assistant work-study program. We thank A. Quirk and D. Zuckerman of the Scholars Program for making this opportunity available.

References

Black, S.; Linville, D.; Michalik, D.; Wolf, M.; Ditteon, R. (2016). "Lightcurve Analysis of Asteroids Observed at the Oakley Southern Sky Observatory: 2015 December - 2016 April." *Minor Planet Bull.* **43**, 287-289.

Collins, K.A.; Kielkopf, J.F.; Stassun, K.G.; Hessman, F.V. (2017). "AstroImageJ: Image Processing and Photometric Extraction for Ultra-precise Astronomical Light Curves." *Astron. J.* **153**, 77-89.

Kaasalainen, M.; Torppa, J.; Muinonen, K. (2001). "Optimization methods for asteroid lightcurve inversion. II. The complete inverse problem." *Icarus* **153**, 37-51.

NASA Horizons. *https://ssd.jpl.nasa.gov/horizons/app.html#/*

Slivan, S.M. (2003). "A Web-based tool to calculate observability of Koronis program asteroids." *Minor Planet Bull.* **30**, 71-72.

Slivan, S.M.; Binzel, R.P.; Crespo de Silva, L.D.; Kaasalainen, M; Lyndaker, M.M.; Krčo, M (2003) "Spin vectors in the Koronis family: comprehensive results from two independent analyses of 213 rotation lightcurves." *Icarus* **162**, 285-307.

Name	Site	Telescope	Camera	Array	Filter	FOV(')	Scale ("/pix)
UCO	Schenectady, NY	0.50-m RC f/8.1	SBIG STXL-11002	2004×1336x9µm	R	30×20	0.93
T21	Mayhill, NM	0.43-m CDK f/6.8	FLI-PL6303	3072×2048x9µm	R	33×49	1.92
Spa-2	Oria, Spain	0.70-m RC f/8	FLI-PL16803	2048×2048x9µm	r'	29×29	0.86
Chi-3	Rio Hurtado, Chile	1.0-m RC f/6.8	FLI-PL16803	4096×4096x9µm	Red	19×19	0.27

Table I. Telescopes and Cameras: RC=Ritchey-Chrétien. CDK = Planewave with f/4.5 focal reducer. UCO = Union College Observatory.

Number	Name	yyyy mm/dd	Phase	L_{PAB}	B_{PAB}	Period(h)	P.E.	Amp	A.E.	Grp
1363	Herberta	2022 02/21-04/21	0.5,17.3	151	-1	3.016	0.002	0.13	0.02	Kor

Table II. Observing circumstances and results. The phase angle is given for the first and last dates. L_{PAB} and B_{PAB} are the approximate phase angle bisector longitude/latitude at mid-date range.

THE ROTATION PERIOD AND VARIABILITY AMPLITUDE OF 1664 FELIX

Misty C. Bentz, Megan Birch, Zo Chapman, Varun Chaturmutha, Sakib Hossain, Jarvious Jones, Anthony Koutroulakis, Vanders Lewis, Ningxin Li, Luke Wohlbach
Department of Physics and Astronomy
Georgia State University
25 Park Place, Suite 605
Atlanta, GA 30303 USA
bentz@astro.gsu.edu

(Received: 2022 May 26 Revised: 2022 July 24)

Photometric monitoring of 1664 Felix was carried out in 2022 February through a Johnson V filter. Based on 90 images collected over two nights, we find a best-fit rotation period of 3.345±0.001 hours, in good agreement with previous results, and a V-band variability amplitude of 0.45±0.02 mag that is slightly larger than previously reported from observations through a clear filter.

Asteroid 1664 Felix was discovered on 1929 February 04 by Belgian astronomer Eugène Delporte at the Royal Observatory of Belgium in Uccle (JPL, 2022). 1664 Felix is an inner main belt asteroid (family 9104; Warner et al., 2009) with orbital semi-major axis a = 2.34 AU. Observations of 1664 Felix in 2008 March by Higgins et al. (2008) constrained its rotation period to be 3.3454±0.0002 h, with a variability amplitude of 0.38±0.01 mag through a clear filter. A similar rotation period of 3.344855±0.000010 hours was determined by Ďurech et al. (2020) from observations collected by the Asteroid Terrestrial-impact Last Alert System (ATLAS) program.

As part of the course work for the Georgia State University class *Astronomical Techniques and Instrumentation,* observations of 1664 Felix were obtained at GSU's Hard Labor Creek Observatory in 2022 February. Monitoring through the Johnson *V* filter was carried out with the 24-inch Miller Telescope, an *f*/6.5 Planewave Corrected Dall-Kirkham Astrograph, equipped with an Apogee Alta CCD with 2048×2048 pixels, giving a field of view of 26.3 arcmin × 26.3 arcmin and a pixel scale of 0.77 arcsec. A total of 36 images were collected on UT date Feb 12 with exposure times of 4 min, and an additional 54 images were collected on UT date Feb 20 with exposure times of 5 min.

All images were reduced in *IRAF* following standard procedures, which included bias and overscan subtraction, dark subtraction, and flat fielding. Aperture photometry of the asteroid and 7 field stars was carried out in IRAF with an aperture radius of 7 pix for the Feb 12 images and a radius of 9 pix for the images collected on Feb 20. APASS *V*-band photometry of the field stars (Henden et al., 2009) was used to convert instrumental magnitudes to calibrated magnitudes.

The rotation period of 1664 Felix was determined from the calibrated magnitudes with *MPO Canopus*, which implements the Fourier Analysis of Light Curves (FALC) algorithm of Harris et al. (1989). The best-fit period was found to be 3.345±0.001 hours with a *V*-band variability amplitude of 0.45±0.02 mag. This rotation period is in excellent agreement with that determined by Higgins et al. (2008) and Ďurech et al. (2020). The *V*-band variability amplitude we find is somewhat larger than that reported for observations through a clear filter by Higgins et al. (2008).

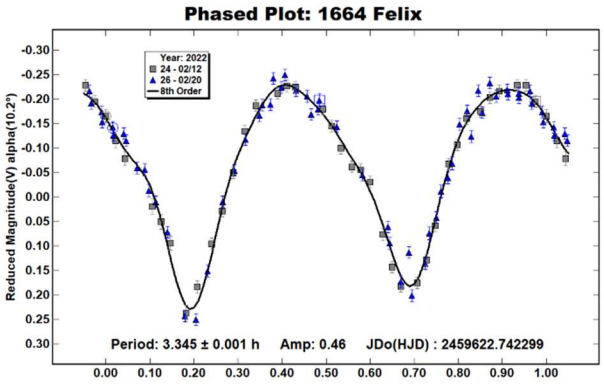

Acknowledgements

IRAF is distributed by the National Optical Astronomy Observatory, which is operated by the Association of Universities for Research in Astronomy (AURA) under a cooperative agreement with the National Science Foundation. This research was made possible in part based on data from the AAVSO Photometric All-Sky Survey (APASS), funded by the Robert Martin Ayers Sciences Fund and NSF AST-1412587.

References

Ďurech, J.; Tonry, J.; Erasmus, N.; Denneau, L.; Heinze, A.N.; Flewelling, H.; Vančo, R. (2020). "Asteroid models reconstructed from ATLAS photometry." *Astron. Astrophys.* **643**, A59.

Harris, A.W.; Young, J.W.; Scaltriti, F.; Zappala, V. (1984). "Lightcurves and phase relations of the asteroids 82 Alkmene and 444 Gyptis." *Icarus* **57**, 251-258.

Harris, A.W.; Young, J.W.; Bowell, E.; Martin, L.J.; Millis, R.L.; Poutanen, M.; Scaltriti, F.; Zappala, V.; Schober, H.J.; Debehogne, H.; Zeigler, K.W. (1989). "Photoelectric Observations of Asteroids 3, 24, 60, 261, and 863." *Icarus* **77**, 171-186.

Henden, A.A.; Terrell, D.; Levine, S.E.; Templeton, M.; Smith, T.C.; Welch, D.L. (2009). "APASS: The AAVSO Photometric All-Sky Survey." *http://www.aavso.org/apass*

Higgins, D.; Pravec, P.; Kusnirak, P.; Hornoch, K.; Brinsfield, J.W..; Allen, B.; Warner, B.D. (2008). "Asteroid Lightcurve Analysis at Hunters Hill Observatory and Collaborating Stations: November 2007 - March 2008." *Minor Planet Bull*. **35**, 123-126.

JPL (2022). "Small-Body Database Browser." *https://ssd.jpl.nasa.gov/tools/sbdb_lookup.html*

Warner, B.D.; Harris, A.W.; Pravec, P. (2009). "The Asteroid Lightcurve Database." *Icarus* **202**, 134-146. Updated 2021 Dec. *http://www.minorplanet.info/lightcurvedatabase.html*

Number	Name	yyyy mm/dd	Phase	L_{PAB}	B_{PAB}	Period(h)	P.E.	Amp	A.E.	Grp
1664	Felix	2022 02/12-02/20	10.15,7.24	154	9	3.345	0.001	0.45	0.02	9104

Table I. Observing circumstances and results. The phase angle is given for the first and last date. If preceded by an asterisk, the phase angle reached an extrema during the period. L_{PAB} and B_{PAB} are the approximate phase angle bisector longitude/latitude at mid-date range (see Harris et al., 1984). Grp is the asteroid family/group (Warner et al., 2009).

BROAD-BAND PHOTOMETRIC MONITORING OF 1226 GOLIA AND 6349 ACAPULCO

Misty C. Bentz, Michael Duffee, Dorsa Erfani, Julia Falcone, Emma Galligan, Nathan Holden, Dan Johns, Jarvious Jones, Aman Kar, Fallon P. Konow, Lynn Orr, Ryan Parkhill, Garrett Polack, Jacob Tutterow
Department of Physics and Astronomy
Georgia State University
25 Park Place, Suite 605
Atlanta, GA 30303 USA
bentz@astro.gsu.edu

(Received: 2022 May 26 Revised:2022 Jul 24)

Broad-band photometric monitoring of 1226 Golia and 6349 Acapulco was carried out in 2021 February-March. For 1226 Golia, we report a rotation period of 4.46 ± 0.05 h and a V-band variability amplitude of 0.41 ± 0.02 mag, which are in agreement with the range of previously reported measurements. For 6349 Acapulco, we find typical colors for a C-type asteroid of B-V = 0.7 ± 0.1 mag and V-R = 0.3 ± 0.1 mag and little evidence for color changes as a function of time. We report a rotation period of 4.48 ± 0.05 h that is in good agreement with a previous measurement, and a variability amplitude of 0.55 ± 0.02 mag that is three times larger than previously reported.

Asteroids 1226 Golia and 6349 Acapulco were monitored through broad-band filters over the course of a few nights in 2021 February and March. Observations were obtained as part of the course work for the Georgia State University class *Astronomical Techniques and Instrumentation* at GSU's Hard Labor Creek Observatory. Monitoring was carried out with the 24-inch Miller Telescope, an *f*/6.5 Planewave Corrected Dall-Kirkham Astrograph, equipped with an Apogee Alta CCD with 2048×2048 pixels, giving a field of view of 26.3 arcmin × 26.3 arcmin and a pixel scale of 0.77 arcsec.

All images were reduced in *IRAF* following standard procedures, which included bias and overscan subtraction, dark subtraction, and flat fielding. Aperture photometry of the asteroids and field stars was carried out in *IRAF*. APASS *B*- and *V*-band photometry of field stars (Henden et al., 2009) was used to convert instrumental magnitudes to calibrated magnitudes, while the transformation equations of Jordi et al. (2006) for Population I stars were used to determine the effective *R* magnitudes for field stars using the Sloan *r*′ magnitudes and the *g*′-*r*′ colors from APASS.

Rotation periods and variability amplitudes of the asteroids were determined using *MPO Canopus*, which implements the Fourier Analysis of Light Curves (FALC) algorithm of Harris et al. (1989). Below, we discuss our analysis and findings for each asteroid separately.

1226 Golia was discovered on 1930 April 22 by Dutch astronomer Hendrik Van Gent at Leiden Southern Station, Johannesburg (JPL, 2022). 1226 Golia is an S-type (stony) asteroid in the inner main belt (family 9104; Warner et al., 2009). Observations were collected through the Johnson *V* filter on UT dates Feb 8 and Feb 21. A total of 74 images with exposure time 90 s were collected on Feb 8, while wind and cloud conditions on Feb 21 only allowed for 23 images with exposure times of 210 s to be collected. The amplitude of variability in *V* was found to be 0.41 ± 0.02 mag, while the final determination of the rotation period is sensitive to the choice of order in *MPO Canopus*: the adoption of order = 5,7,8 all give a best-fit period of 4.409 ± 0.001 h while order = 6 gives a best-fit period of 4.472 ± 0.001 h. If the period finder is restricted to the observations collected on Feb 8, then periods of 4.48-4.52 h are found. We therefore adopt a best-fit period of 4.46 ± 0.05 h. Previous determinations of the rotation period have found values that range between 4.10 h (di Martino et al., 1994; Waszczak et al., 2015) and 4.47 h (Behrend, 2021web; Ďurech et al., 2018) and include variability amplitudes of 0.24-0.40 mag. Our measurements agree well with the upper ends of these ranges.

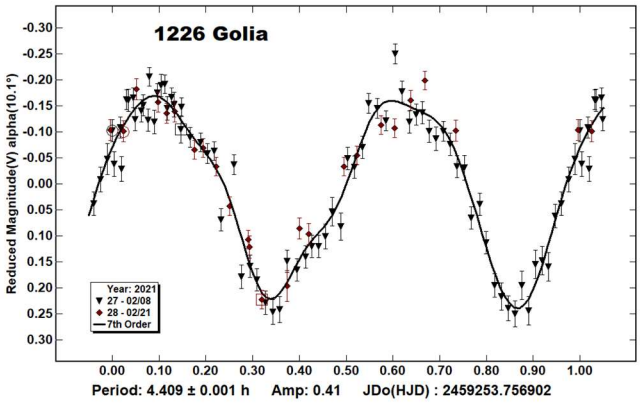

6349 Acapulco was discovered on 1995 February 8 by Japanese astronomer Masahiro Koishikawa at the Ayashi Station of the Sendai Astronomical Observatory (JPL, 2022). It is a member of the Adeona family of carbonaceous (C-type) main-belt asteroids, which are believed to have formed when the parent body, 145 Adeona, underwent a massive collision about 600 million years ago (Carruba et al., 2003). Observations through the Johnson-Cousins *B*, *V*, and *R* filters were collected on UT date 2021 March 5 with typical exposure times of 240 s for each of the 63 good frames. Exploration of the asteroid color shows little evidence for color changes as a function of time, with B-V = 0.7 ± 0.1 mag and V-R = 0.3 ± 0.1 mag. These colors are typical for other C-type asteroids (Dandy et al., 2003). A rotation period of 4.48 ± 0.05 h and variability amplitude of 0.55 ± 0.02 mag was determined by adjusting the *B*- and *R*-band light curves to match the *V* band and then fitting all three bands simultaneously. Given the low signal-to-noise of the *B*-band measurements (blue boxes in the figure below), we also fit each band separately:

Number	Name	2021 mm/dd	Phase	L_{PAB}	B_{PAB}	Period(h)	P.E.	Amp	A.E.	Grp
1226	Golia	02/08-02/21	10.12,5.42	156	9	4.46	0.05	0.41	0.02	9104
6349	Acapulco	03/05	12.62	138	1	4.48	0.05	0.55	0.02	505

Table I. Observing circumstances and results. The phase angle is given for the first and last date. If preceded by an asterisk, the phase angle reached an extrema during the period. L_{PAB} and B_{PAB} are the approximate phase angle bisector longitude/latitude at mid-date range (see Harris et al., 1984). Grp is the asteroid family/group (Warner et al., 2009).

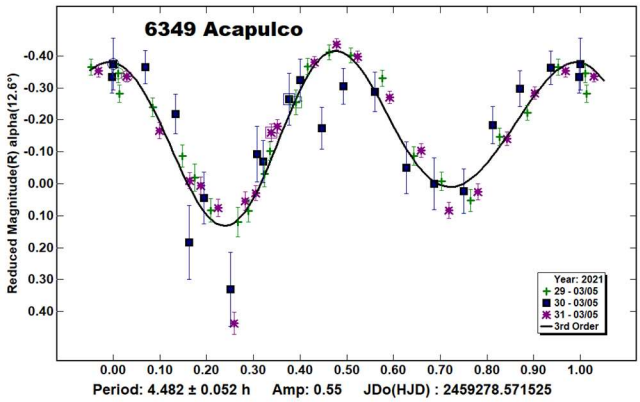

B: rotation period = 4.50 ± 0.06 h, amplitude = 0.57 ± 0.02 mag
V: rotation period = 4.49 ± 0.04 h, amplitude = 0.54 ± 0.02 mag
R: rotation period = 4.38 ± 0.09 h, amplitude = 0.62 ± 0.02 mag

The results of analyzing each band separately agree with the results derived from fitting all bands simultaneously, although the scatter in variability amplitude is a bit larger than the formal uncertainties and appears to be driven by the low sampling rate in each band and a few discrepant measurements. The only previously reported period is 4.376 ± 0.002 h with a variability amplitude of 0.18 mag, determined from 64 observations collected over 51 days through the Mould *R* filter as part of the Palomar Transient Factory survey (Waszczak et al., 2015). The rotation period we find from observations collected in a single night is just slightly longer than this previous measurement, but we find a variability amplitude that is three times larger and does not seem to be strongly dependent on the filter choice.

Acknowledgements

IRAF is distributed by the National Optical Astronomy Observatory, which is operated by the Association of Universities for Research in Astronomy (AURA) under a cooperative agreement with the National Science Foundation. This research was made possible in part based on data from the AAVSO Photometric All-Sky Survey (APASS), funded by the Robert Martin Ayers Sciences Fund and NSF AST-1412587.

References

Behrend, R. (2021web). "Courbes de rotation d'astéroïdes et de comètes." *http://obswww.unige.ch/~behrend/page_cou.html*

Carruba, V.; Burns, J.A.; Bottke, W.; Nesvorný, D. (2003). "Orbital evolution of the Gefion and Adeona asteroid families: close encounters with massive asteroids and the Yarkovsky effect." *Icarus* **162**, 308-327.

Dandy, C.L.; Fitzsimmons, A.; Collander-Brown, S.J. (2003). "Optical colors of 56 near-Earth objects: trends with size and orbit." *Icarus* **163**, 363-373.

di Martino, M.; Dotto, E.; Barucci, M.A.; Fulchignoni, M.; Rotundi, A. (1994). "Photoelectric Photometry of Ten Small and Fast Spinning Asteroids." *Icarus* **109**, 210-218.

Ďurech, J.; Hanuš, J.; Alí-Lagoa, V. (2018). "Asteroid models reconstructed from the Lowell Photometric Database and WISE data." *Astron. Astrophys.* **617***,* A57.

Harris, A.W.; Young, J.W.; Scaltriti, F.; Zappala, V. (1984). "Lightcurves and phase relations of the asteroids 82 Alkmene and 444 Gyptis." *Icarus* **57**, 251-258.

Harris, A.W.; Young, J.W.; Bowell, E.; Martin, L.J.; Millis, R.L.; Poutanen, M.; Scaltriti, F.; Zappala, V.; Schober, H.J.; Debehogne, H.; Zeigler, K.W. (1989). "Photoelectric Observations of Asteroids 3, 24, 60, 261, and 863." *Icarus* **77**, 171-186.

Henden, A.A.; Terrell, D.; Levine, S.E.; Templeton, M.; Smith, T.C.; Welch, D.L. (2009). "APASS: The AAVSO Photometric All-Sky Survey." *http://www.aavso.org/apass*

Jordi, K.; Grebel, E.K.; Ammon, K. (2006). "Empirical color transformations between SDSS photometry and other photometric systems." *Astron. Astrophys*. **460**, 339-347.

JPL (2022). "Small-Body Database Browser." *https://ssd.jpl.nasa.gov/tools/sbdb_lookup.html*

Warner, B.D.; Harris, A.W.; Pravec, P. (2009). "The Asteroid Lightcurve Database." *Icarus* **202**, 134-146. Updated 2021 Dec. *http://www.minorplanet.info/lightcurvedatabase.html*

Waszczak, A.; Chang, C-K.; Ofek, E.O.; Laher, R.; Masci, F.; Levitan, D.; Surace, J.; Cheng, Y-C.; Ip, W-H.; Kinoshita, D.; Helou, G.; Prince, T.A.; Kulkarni, S. (2015). "Asteroid Light Curves from the Palomar Transient Factory Survey: Rotation Periods and Phase Functions from Sparse Photometry." *Astron. J.* **150**, A75.

V-BAND PHOTOMETRIC MONITORING OF 782 MONTEFIORE

Misty C. Bentz, Kristin Baker, KhaDeem Coumarbatch, Nicholas Davis, Becky E. Flores, Elizabeth Lincoln, Gillian Millard, Christopher Powell, Patrick Tarrant, Anderson Thrasher
Department of Physics and Astronomy
Georgia State University
25 Park Place, Suite 605
Atlanta, GA 30303 USA
bentz@astro.gsu.edu

(Received: 2022 May 26 Revised: 2022 Jul 24)

Photometric monitoring of 782 Montefiore was carried out in 2020 February through a Johnson V filter. Based on 247 images collected over three nights, we find a best-fit rotation period of 4.073±0.001 h and a V-band variability amplitude of 0.50±0.02 mag, in good agreement with previous results.

Asteroid 782 Montefiore was discovered on 1914 March 18 by Austrian astronomer Johann Palisa at Vienna Observatory (JPL, 2022). A member of the inner main belt (family 9104; Warner et al., 2009), 782 Montefiore is an S-type (stony) asteroid.

As part of the course work for the Georgia State University class *Astronomical Techniques and Instrumentation,* observations of 782 Montefiore were obtained at GSU's Hard Labor Creek Observatory near Rutledge, GA in 2020 February. Monitoring through the Johnson *V* filter was carried out with the 24-inch Miller Telescope, an *f*/6.5 Planewave Corrected Dall-Kirkham Astrograph, equipped with an Apogee Alta CCD with 2048×2048 pixels, giving a field of view of 26.3 arcmin × 26.3 arcmin and a pixel scale of 0.77 arcsec. A total of 247 individual images with exposure times of 4-5 min were obtained over the course of three separate nights: UT dates Feb 08, Feb 23, and Feb 28.

All images were reduced in *IRAF* following standard procedures, which included bias and overscan subtraction, dark subtraction, and flat fielding. Aperture photometry of the asteroid and several field stars was carried out in *IRAF* with an aperture radius of 11 pixels (Feb 08) or 9 pixels (Feb 23 and Feb 28). APASS *V*-band photometry of the field stars (Henden et al., 2009) was used to convert instrumental magnitudes to calibrated magnitudes.

The asteroid rotation period was determined from the calibrated magnitudes with *MPO Canopus*, which implements the Fourier Analysis of Light Curves (FALC) algorithm of Harris et al. (1989). The best-fit period was found to be 4.073±0.001 h with a *V*-band variability amplitude of 0.50±0.02 mag. Several high-quality measurements of the rotation period already exist, with values ranging from 4.069-4.08 h (Wisniewski et al., 1997; Behrend, 2007web; Galad, 2008; Han et al., 2013; Schmidt, 2015; Benishek, 2016; Ďurech et al., 2020; Franco et al., 2020; Pál et al., 2020). While previous measurements of the rotation period have agreed quite well, the variability amplitude has been reported as ranging from 0.31-0.54 mag. The higher end of this range is generally from filtered photometry (Bessel *R*), while unfiltered, near-infrared, or very wide-band photometry has led to smaller values of the variability amplitude. Our measurements appear to be the first reported for the Johnson *V* filter, and agree well with the upper end of previous amplitude measurements.

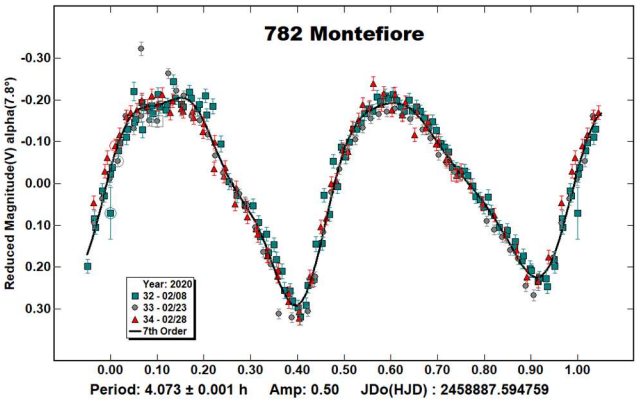

Acknowledgements

IRAF is distributed by the National Optical Astronomy Observatory, which is operated by the Association of Universities for Research in Astronomy (AURA) under a cooperative agreement with the National Science Foundation. This research was made possible in part based on data from the AAVSO Photometric All-Sky Survey (APASS), funded by the Robert Martin Ayers Sciences Fund and NSF AST-1412587.

References

Behrend, R. (2007web). "Courbes de rotation d'astéroïdes et de comètes." *http://obswww.unige.ch/~behrend/page_cou.html*

Benishek, V. (2016). "Photometric Observations and Lightcurve Analysis for Asteroids 782 Montefiore, (294739) 2008 CM, and (303142) 2004 DU24." *Minor Planet Bull.* **43**, 186-188.

Ďurech, J.; Tonry, J.; Erasmus, N.; Denneau, L.; Heinze, A.N.; Flewelling, H.; Vančo, R. (2020). "Asteroid models reconstructed from ATLAS photometry." *Astron. Astrophys.* **643**, A59.

Franco, L.; Marchini, A.; Saya, L.-P.; Galli, G.; Baj, G.; Ruocco, N.; Tinelli, L.; Scarfi, G.; Aceti, P.; Banfi, M.; Bacci, P.; Maestripieri, M.; Papini, R.; Salvaggio, F.; Mortari, F.; Mauro, B.; Giovanni Battista, C.; Benedetto, C. (2020). "Collaborative Asteroid Photometry from UAI: 2020 January-March." *Minor Planet Bull.* **47**, 242-246.

Galad, A. (2008). "Several Byproduct Targets of Photometric Observations at Modra." *Minor Planet Bull.* **35**, 17-21.

Han, X.L.; Li, B.; Zhao, H.; Liu, W.; Sun, L.; Shi, J.; Gao, S.; Wang, S.; Pan, X.; Jiang, P.; Zhou, H. (2013). "Photometric Observations of 782 Montefiore, 3842 Harlansmith 5542 Moffatt, 6720 Gifu, and (19979) 1989 VJ." *Minor Planet Bull.* **40**, 99-100.

Number	Name	yyyy mm/dd	Phase	L_{PAB}	B_{PAB}	Period(h)	P.E.	Amp	A.E.	Grp
782	Montefiore	2020 02/08-02/28	*7.8,6.8	150	7	4.073	0.001	0.50	0.02	9104

Table I. Observing circumstances and results. The phase angle is given for the first and last date. If preceded by an asterisk, the phase angle reached an extrema during the period. L_{PAB} and B_{PAB} are the approximate phase angle bisector longitude/latitude at mid-date range (see Harris et al., 1984). Grp is the asteroid family/group (Warner et al., 2009).

Harris, A.W.; Young, J.W.; Scaltriti, F.; Zappala, V. (1984). "Lightcurves and phase relations of the asteroids 82 Alkmene and 444 Gyptis." *Icarus* **57**, 251-258.

Harris, A.W.; Young, J.W.; Bowell, E.; Martin, L.J.; Millis, R.L.; Poutanen, M.; Scaltriti, F.; Zappala, V.; Schober, H.J.; Debehogne, H.; Zeigler, K.W. (1989). "Photoelectric Observations of Asteroids 3, 24, 60, 261, and 863." *Icarus* **77**, 171-186.

Henden, A.A.; Terrell, D.; Levine, S.E.; Templeton, M.; Smith, T.C.; Welch, D.L. (2009). "APASS: The AAVSO Photometric All-Sky Survey." *http://www.aavso.org/apass*

JPL (2022). "Small-Body Database Browser." *https://ssd.jpl.nasa.gov/tools/sbdb_lookup.html*

Pál, A.; Szakáts, R.; Kiss, C.; Bódi, A.; Bognár, Z.; Kalup, C.; Kiss, L.L.; Marton, G.; Molnár, L.; Plachy, E.; Sárneczky, K.; Szabó, G.M.; Szabó, R. (2020). "Solar System Objects Observed with TESS-First Data Release: Bright Main-belt and Trojan Asteroids from the Southern Survey." *Ap. J. Supl. Ser.* **247**, A26.

Schmidt, R.E. (2015). "NIR Minor Planet Photometry from Burleith Observatory: 2014 February - June." *Minor Planet Bull.* **42**, 1-3.

Warner, B.D.; Harris, A.W.; Pravec, P. (2009). "The Asteroid Lightcurve Database." *Icarus* **202**, 134-146. Updated 2021 Dec. *http://www.minorplanet.info/lightcurvedatabase.html*

Wisniewski, W.Z.; Michałowski, T.M.; Harris, A.W.; McMillan, R.S. (1997). "Photometric Observations of 125 Asteroids." *Icarus* **126**, 395-449.

ROTATIONAL PERIOD OF SMALL NEA 2022 KK5

Adrian Bruno Sonka
Astronomical Institute of the Romanian Academy,
5 Cuţitul de Argint, 040557 Bucharest, ROMANIA
sonka@astro.ro

Alin Nedelcu, Mirel Birlan
Astronomical Institute of the Romanian Academy,
Bucharest, Romania, and IMCCE,
Observatoire de Paris, CNRS UMR8028, Paris, France

(Received: 2022 June 20 Revised: 2022 August 8)

We have observed minor planet 2022 KK5 during a close approach on 30th of May 2022 and determined that it is a fast rotator, having a rotational period of 0.0830±0.0002 h, with uneven minima and maxima.

Minor planet 2022 KK5, discovered on May 27th, 2022, is small (H = 25.1) Apollo type NEA. It passed at a nominal distance of 0.00893 UA from the Earth two days after the discovery. This is part of the "observations on alert" program started using the telescope facilities owned by the Astronomical Institute of the Romanian Academy whose results were already published in the past (Gornea et al., 2018; Sonka et al., 2018, 2019, 2021).

Usually, small NEAs can be observed for a short period of time (Birlan et al., 2015), at their closest approach, at their maximum apparent brightness, but with a large sky motion. This object in particular will not become brighter than 24th magnitude in the foreseeable future. We observed the asteroid one night after the closest approach, during a 2-hour observing run.

Observations were made from Bucharest Observatory (IAU MPC 073 code), branch of The Astronomical Institute of the Romanian Academy. We used Riccardi Dall-Kirkham telescope, with a 0.5-m primary mirror and 3,500 mm focal length, a FLI CCD camera PL16803 with a 4096×4096 array, 9 μm size pixels and 60% maximum Quantum Efficiency. The combination gives a visual field of 36'×36', with 1.07"/pixel at binning of 2×2 (Birlan et al., 2019).

We started to observe the asteroid on May 30th, 2022, in order to secure astrometry, with exposure time of 30 seconds, and no filter. During our observing run we noticed large brightness variations from one image to another and continued to observe the asteroid for 2.2 hours.

Our data was properly reduced (dark, bias, flat) and analyzed with *Tycho-Tracker* software (*https://www.tycho-tracker.com)*. Comparison stars V magnitudes were automatically chosen from The ATLAS All-Sky Stellar Reference Catalog (Tonry et al., 2018).

The raw (unphased photometric data) lightcurve shows a large amplitude brightness variation and uneven minima and maxima, together with a very short rotational period.

Number	Name	yyyy mm/dd	Phase	L_{PAB}	B_{PAB}	Period(h)	P.E.	Amp	A.E.	Grp
	2022 KK5	2022 05/30	44.4,44.1	242	22	0.0830	0.0002	0.81	0.30	NEA

Table I. Observing circumstances and results. The phase angle is given for the first and last date. If preceded by an asterisk, the phase angle reached an extrema during the period. L_{PAB} and B_{PAB} are the approximate phase angle bisector longitude/latitude at mid-date range (see Harris et al., 1984). Grp is the asteroid family/group (Warner et al., 2009).

Using the period search module in *Tycho-Tracker* we were able to fit our data with a 2nd degree order Fourier fit. The rotational period was computed for a value of 0.0830±0.0002 h. The amplitude of the Fourier fit is 0.81 magnitudes although we could observe deeper minima (visible as data points well below the Fourier fit).

Of great concern was the possibility of rotational smearing as identified by Pravec et al. (2000). For exposure times longer than 0.187 times the rotation period, an accurate rotational period cannot be found from data. In our case the limit of exposure time is 55 seconds, while our exposure is only 30 seconds. In this way the rotational period determined can be regarded as a solid result.

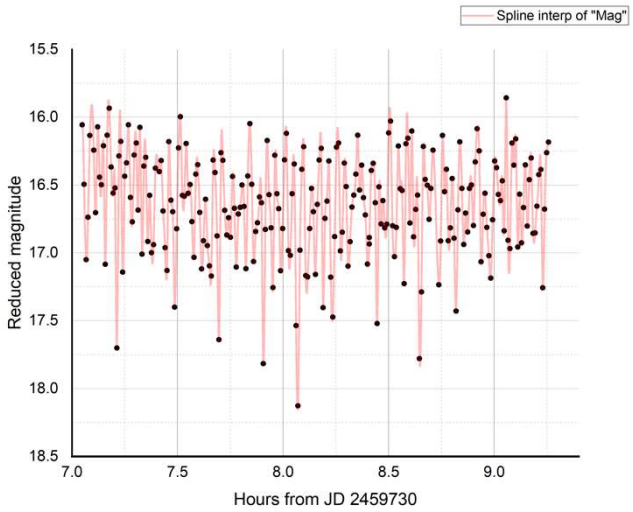

Figure 1. Raw lightcurve for 2022 KK5, with data points and a spline interpolation between them.

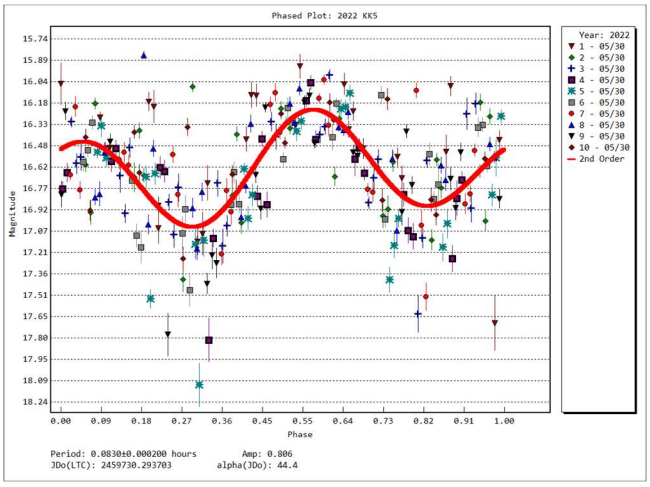

Figure 2: Phased lightcurve of 2022 KK5. Color code corresponding to each field of star used to fold the date for the computed period.

References

Birlan, M.; Popescu, M.; Nedelcu, D.A.; Turcu, V.; Pop, A.; Dumitru, B.; Stevance, F.; Vaduvescu, O.; Moldovan, D.; Rocher, P.; Sonka, A.; Mircela, L. (2015). "Characterization of (357439) 2004 BL86 on its close approach to Earth in 2015." *Astronomy & Astrophysics* **581**, id A3.

Birlan, M.; Sonka, A.; Nedelcu, D.A.; Balan, M.; Anghel, S.; Pandele, C.; Trusculescu, M.; Dragasanu, C.; Plesca, V.; Gandescu, C. H.; Banica, C.; Georgescu, T. (2019). "Telescope calibration for mobile platforms: first results." *Romanian Astronomical Journal* **29(1)**, 23-32.

Gornea, A.I.; Sonka, A.B.; Birlan, M.; Anghel, S. (2018). "Photometric Observations of Near-Earth Asteroid 2018 GE3." *Minor Planet Bulletin* **45(4)**, 315-316.

Harris, A.W.; Young, J.W.; Scaltriti, F.; Zappala, V. (1984). "Lightcurves and phase relations of the asteroids 82 Alkmene and 444 Gyptis." *Icarus* **57**, 251-258.

Pravec, P.; Hergenrother, C.; Whiteley, R.; Šarounová, L.; Kušnirák, P.; Wolf, M. (2000). "Fast rotating asteroids 1999 TY2, 1999 SF10, and 1998 WB2." *Icarus* **147(2)**, 477-486.

Sonka, A.B.; Gornea, A.I.; Birlan, M. (2018). "Photometric monitoring of PHA (3122) Florence." *Romanian Astronomical Journal* **28(1)**, 81-88.

Sonka, A.B.; Birlan, M.; Anghel, S.; Vachier, F.; Berthier, J.; Klotz, A.; Theirry, P.; Peyrot, A.; Teng, J.-P. (2019). "The (155140) 2005 UD lightcurve and rotational period from simultaneous observations." *Romanian Astronomical Journal* **29(3)**, 191-200.

Sonka, A.B.; Turcu, V.; Nedelcu, A.; Birlan, M.; Moldovan, D. (2021). "Fast Rotator Minor Planet 2020 UA From Cluj and Berthelot Observatory." *Minor Planet Bulletin* **48(2)**, 100-101.

Tonry, J.L.; Denneau, L.; Flewelling, H.; Heinze, A.N.; Onken, C.A.; Smartt, S.J.; Stalder, B.; Weiland, H.J.; Wolf, C. (2018). "The ATLAS All-Sky Stellar Reference Catalog." *Ap. J.* **867**, A105.

Warner, B.D.; Harris, A.W.; Pravec, P. (2009). "The Asteroid Lightcurve Database." *Icarus* **202**, 134-146. Updated 2016 Sep. *http://www.minorplanet.info/lightcurvedatabase.html*

(29606) 1998 QN94: A BINARY ASTEROID IN A SELF-SYNCHRONOUS ORBIT

Robert D. Stephens
Center for Solar System Studies
11355 Mount Johnson Court
Rancho Cucamonga, CA 91737 USA
rstephens@foxandstephens.com

Daniel R. Coley
Center for Solar System Studies
Corona, CA USA

Brian D. Warner
Center for Solar System Studies
Eaton, CO USA
brian@MinorPlanetObserver.com

(Received: 2022 July 5 Revised: 2022 August 5)

We report that asteroid (29606) 1998 QN94 is a binary asteroid. The primary lightcurve has a period of 2.8965 ± 0.0001 h and an amplitude 0.17 mag. The orbital period of the secondary matches what we deduce as its own rotation period: 19.666 ± 0.004 h.

Observations of this member of the Phocaea dynamical family (Nesvorny, 2015; Nesvorny et al., 2015) were made at the Center for Solar System Studies in 2022 May. Either a 0.35-m *f*/10 Schmidt-Cassegrain and FLI Microline CCD camera or a 0.4-m *f*/10 Ritchey-Chretien and FLI Proline CCD camera was used to acquire images. Both cameras use a KAF-1001E chip, which has a 1024×1024×24m array of pixels.

All lightcurve observations were unfiltered since a clear filter can cause a 0.1-0.3 mag loss. The exposure duration ranged from 180 to 360 seconds, depending on the asteroid's brightness and sky motion.

Measurements were made using *MPO Canopus*. The Comp Star Selector utility in *MPO Canopus* found up to five comparison stars of near solar-color for differential photometry. To reduce the number of adjusted nightly zero points and their amounts, the analysis of the data used the ATLAS catalog r´ (SR) magnitudes (Tonry et al., 2018). The rare zero-point adjustments of ≥ ±0.03 mag may be related in part to using unfiltered observations, poor centroiding of the reference stars, not correcting for second-order extinction, or selecting a star that is an unresolved pair.

The Y-axis values are ATLAS SR "sky" (catalog) magnitudes. The two values in the parentheses are the phase angle (a) and the value of *G* used to normalize the data to the comparison stars used in the earliest session. This, in effect, corrected all the observations to seem to have been made at a single fixed date/time and phase angle, leaving any variations due only to the asteroid's rotation and/or albedo changes. The X-axis shows rotational phase from -0.05 to 1.05. If the plot includes the amplitude, e.g., "Amp: 0.65", this is the amplitude of the Fourier model curve and *not necessarily the adopted amplitude for the lightcurve*.

No previous periods were found in the asteroid lightcurve database (Warner et al., 2009). Quickly it became apparent that there were deviations from the Fourier curve suggestive of a binary asteroid. Because of interference from high winds and a near Full Moon, the error bars for several sessions were larger than desired. The plot labeled "NoSub" shows the raw plot with suggestions of a secondary frequency in several sessions.

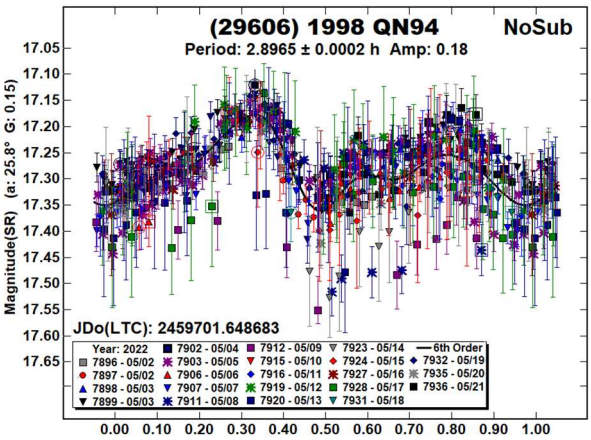

A search for a secondary frequency was done using the dual-period search feature in *MPO Canopus*. A primary period of 2.8965 ± 0.0001 h (Plot "P1") and a secondary period of 19.666 ± 0.004 h (Plot "P2") were found.

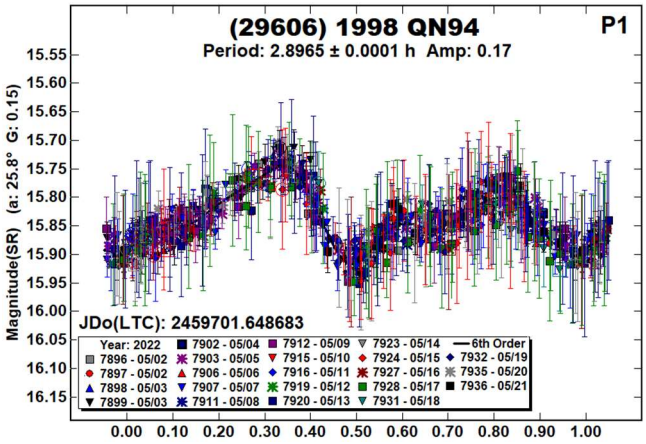

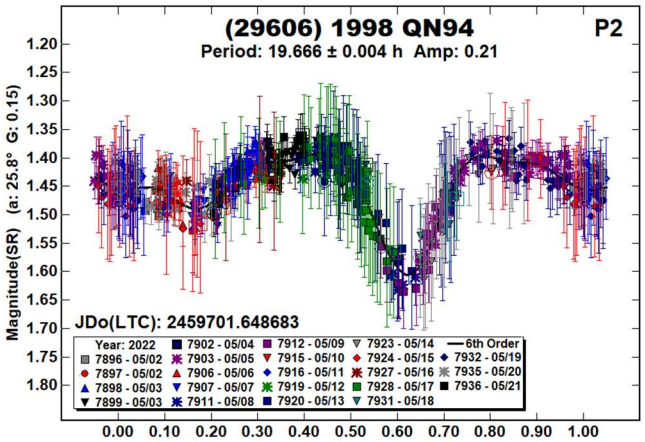

Number	Name	2022 mm/dd	Phase	L_{PAB}	B_{PAB}	Period(h)	P.E.	Amp	A.E.	Grp/DsDp
29606	1998 QN94	05/02-05/21	25.9,30.1	192	26	2.8965	0.0001	0.17	0.01	PHO
						19.666	0.004	0.21	0.02	≥0.29

Table II. Observing circumstances. The first line gives the primary or dominant period for the system. The additional line gives the secondary period(s). The phase angle (α) is given at the start and end of each date range. L_{PAB} and B_{PAB} are, respectively the average phase angle bisector longitude and latitude (see Harris et al.,1984).

After 21 May, the lightcurve started to evolve as, over the course of observations, the phase angle increased from 26° to 30°. On the last night of observations, the mutual event (deep minimum) at phase 0.65 disappeared, leaving just the secondary lightcurve from the elongation of the satellite.

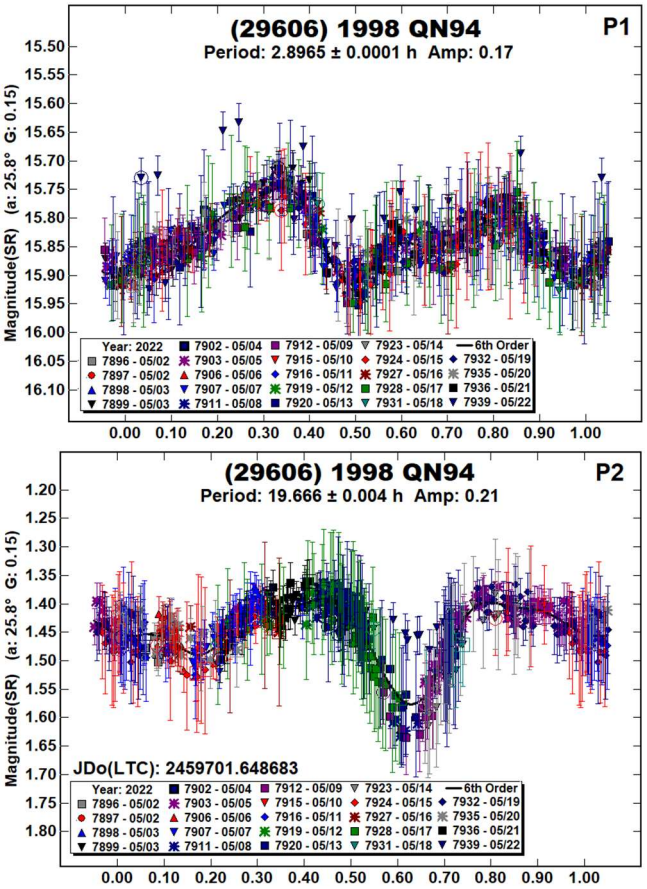

This lightcurve evolution, producing both mutual events, which eventually vanished, and what we deduce as the secondary's own rotation, allows us to determine both the secondary's orbital period and the secondary's rotational period. These values appear to be synchronous, i.e., the satellite's orbital period matches its 19.666 ± 0.004 h rotation. The satellite-to-primary effective diameter ratio is Ds/Dp ≥ 0.29 ± 0.03.

Looking ahead, the 2026 July (16.9, +22°) is the next good chance for observations. However, the asteroid will be embedded in the galactic bulge at that time.

Acknowledgements

The authors gratefully acknowledge Shoemaker NEO Grants from the Planetary Society (2007, 2013). These were used to purchase some of the telescopes and CCD cameras used in this research. This work includes data from the Asteroid Terrestrial-impact Last Alert System (ATLAS) project. ATLAS is primarily funded to search for near earth asteroids through NASA grants NN12AR55G, 80NSSC18K0284, and 80NSSC18K1575; byproducts of the NEO search include images and catalogs from the survey area. The ATLAS science products have been made possible through the contributions of the University of Hawaii Institute for Astronomy, the Queen's University Belfast, the Space Telescope Science Institute, and the South African Astronomical Observatory.

References

Harris, A.W.; Young, J.W.; Scaltriti, F.; Zappala, V. (1984). "Lightcurves and phase relations of the asteroids 82 Alkmene and 444 Gyptis." *Icarus* **57**, 251-258.

Nesvorny, D. (2015). "Nesvorny HCM Asteroids Families V3.0." NASA Planetary Data Systems, id. EAR-A-VARGBET-5-NESVORNYFAM-V3.0.

Nesvorny, D.; Broz, M.; Carruba, V. (2015). "Identification and Dynamical Properties of Asteroid Families." In *Asteroids IV* (P. Michel, F. DeMeo, W.F. Bottke, R. Binzel, Eds.). Univ. of Arizona Press, Tucson, also available on astro-ph.

Tonry, J.L.; Denneau, L.; Flewelling, H.; Heinze, A.N.; Onken, C.A.; Smartt, S.J.; Stalder, B.; Weiland, H.J.; Wolf, C. (2018). "The ATLAS All-Sky Stellar Reference Catalog." *Ap. J.* **867**, A105.

Warner, B.D.; Harris, A.W.; Pravec, P. (2009). "The Asteroid Lightcurve Database." *Icarus* **202**, 134-146. Updated 2022 June. *http://www.minorplanet.info/lightcurvedatabase.html*

ON CONFIRMED AND SUSPECTED BINARY ASTEROIDS OBSERVED AT THE CENTER FOR SOLAR SYSTEM STUDIES: 2022 MARCH-JUNE

Brian D. Warner (CS3)
Center for Solar System Studies
446 Sycamore Ave.
Eaton, CO 80615 USA
brian@MinorPlanetObserver.com

Robert D. Stephens
Center for Solar System Studies (CS3)
Rancho Cucamonga, CA 91730

Daniel R. Coley (CS3)
Center for Solar System Studies
Corona, CA

(Received: 2022 July 3)

Analysis of CCD photometric observations of seven asteroids from 2022 March to June at the Center for Solar System Studies indicate that, by virtue of a suspected or distinct second period, they are either suspected or confirmed binary asteroids.

CCD photometric observations of five near-Earth and two inner main-belt asteroids were made at the Center for Solar System Studies from 2022 March to June. Each one is considered to be a suspected or confirmed binary asteroid. This is based on there being a sufficiently distinct secondary period, even if it might be a simple harmonic of the primary period.

The observations were made with a 0.35-m Schmidt-Cassegrain and either an FLI Proline or Microline CCD camera as well as a 0.40-m Schmidt-Cassegrain with FLI Proline CCD camera. All cameras use a KAF-1001E chip, which has a pixel array of 1024×1024×24µ. The field-of-view and image scale were about 26×26 arcminutes and 1.5 arcsec/pixel, respectively, for the 0.35-m telescopes. The 0.4-m values were 20×20 arcminutes and 1.2 arcsec/pixel.

All lightcurve observations were unfiltered or with a clear filter, even though the clear filter can cause a 0.1-0.3 mag loss. The exposures varied depending on the asteroid's brightness and sky motion. Whether guiding on a field star or not, sometimes the asteroid was trailed on the image.

Measurements were made using *MPO Canopus*. The Comp Star Selector utility in *MPO Canopus* found up to five comparison stars of near solar-color for differential photometry. To reduce the number of adjusted nightly zero points and their amounts, the analysis of the data used the ATLAS catalog r´ (SR) magnitudes (Tonry et al., 2018). The rare zero-point adjustments of ≥ ±0.03 mag may be related to using unfiltered/clear observations, poor centroiding of the reference stars, not correcting for second-order extinction, or selecting a comp star that is an unresolved pair.

The Y-axis values are ATLAS SR "sky" (catalog) magnitudes. The two values in the parentheses are the phase angle (a) and the value of *G* used to normalize the data to the comparison stars used in the earliest session. This, in effect, corrected all the observations to appear that they were made at a single fixed date/time and phase angle, presumably leaving any variations due only to the asteroid's rotation and/or albedo changes. The X-axis shows rotational phase from -0.05 to 1.05. If the plot includes the amplitude, e.g., "Amp: 0.65", this is the amplitude of the Fourier model curve and *not necessarily the adopted amplitude for the lightcurve*.

References to previous works were taken from the asteroid lightcurve database (Warner et al., 2009), known as "LCDB" from here on. Since most listed rotation periods for the primary were very similar, only a few of the LCDB references have been used.

2778 Tangshan. We observed this inner main-belt asteroid twice before (Warner, 2004; Stephens and Warner, 2019). Behrend (2018web) found a period of 3.457 h, which is in good agreement with our earlier results of 3.461 h and 3.468 h, respectively.

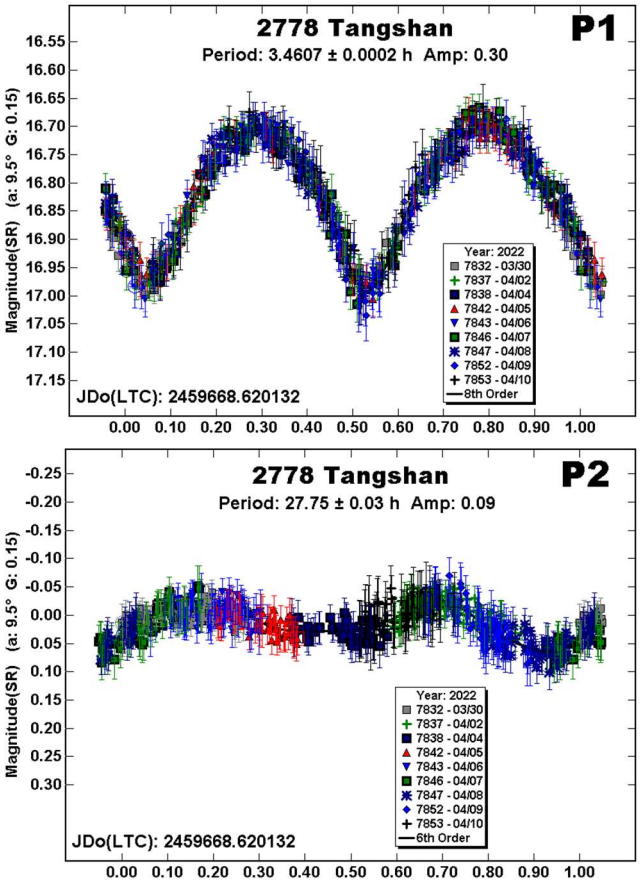

The 2020 observations led to a dominant period of 3.4607 h, in keeping with the previous results. However, unlike previous years, they also appeared to include a secondary period. This was extracted using the dual-period search of *MPO Canopus* and found to be a bimodal lightcurve with a period 27.75 h and amplitude of 0.09 mag. This is within the typical range of for the orbital period of the satellite in small asteroid binaries (Pravec et al., 2018).

There were no mutual events (occultation/eclipses) so it was not possible to determine the ratio of the effective diameters of the satellite versus the primary (Ds/Dp). However, the 0.09 mag amplitude indicates a nearly spheroidal object (a/c = 1.09) with its rotation period tidally-locked to the orbital period.

(6455) 1992 HE. The estimated diameter of this NEA is 4.6 km (Mainzer et al., 2019). Based on observations in 2002, Pravec et al. (2002web) found several synodic periods as the viewing aspect changed. The average period was about 5.48 h with amplitudes $A \leq 0.13$ mag. Observations made by Gaftonyuk and

Krugly (2004), led to period of 2.736 h, or half that of the Pravec et al. (2002web) period. Wolters et al. (2005) also observed in 2002 (late September) and found a similar half-period: 2.736 h. The amplitude of their lightcurve was 0.21 mag. Many other reports in the LCDB also indicate a period near 2.7 h, including ours from observations in 2019 (Warner and Stephens, 2020).

When low lightcurve amplitudes are involved, $A < 0.2$ mag and especially $A < 0.10$ mag, it should not be assumed that a lightcurve will be bimodal, i.e., two min/max pairs per rotation (Harris et al., 2014). Even with the larger amplitude from Wolters et al. (2005), the true period of the asteroid was at least somewhat ambiguous.

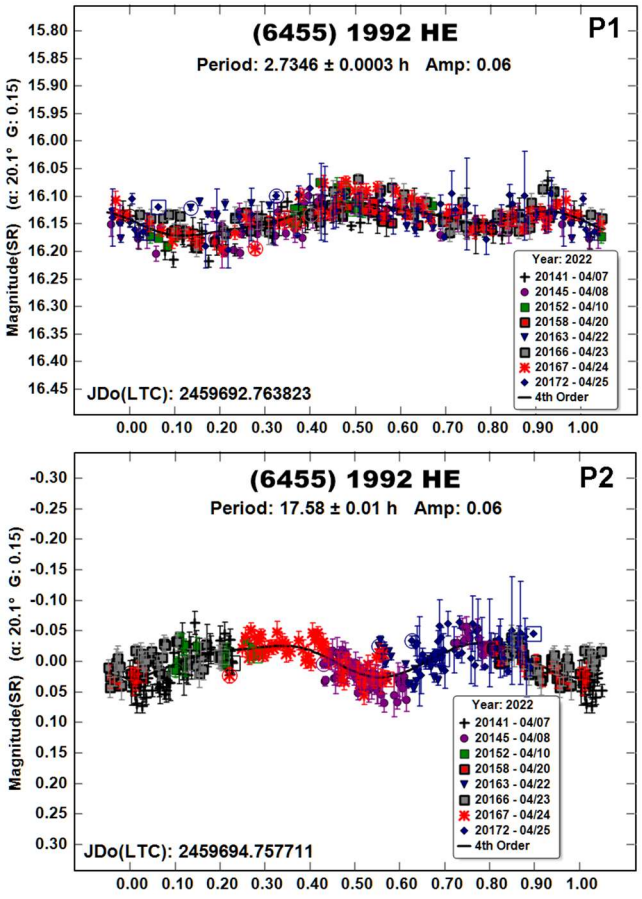

Our 2022 observations also produced a low amplitude primary lightcurve (0.06 mag). Using a liberal interpretation, our lightcurve is bimodal that is asymmetrical (minimums at about 0.1 and 0.8 rotation phase). Even so, we found that looking for and finding a secondary period produced a much "cleaner" primary lightcurve.

The secondary lightcurve is noticeably asymmetrical, which casts some doubt about the solution since one explanation would be an unusually eccentric orbit for a satellite. However, the assumed orbital period is in keeping with those of other small binary asteroids (Pravec et al., 2018). As with 2778 Tangshan above, the low amplitude of the secondary lightcurve could imply a nearly spheroidal satellite and, as with all other asteroids included here, we highly recommend follow-up observations in the future.

(7889) 1994 LX. The synodic rotation period for the primary of this NEA is well-established at about 2.74 h, e.g., Warner (2015).

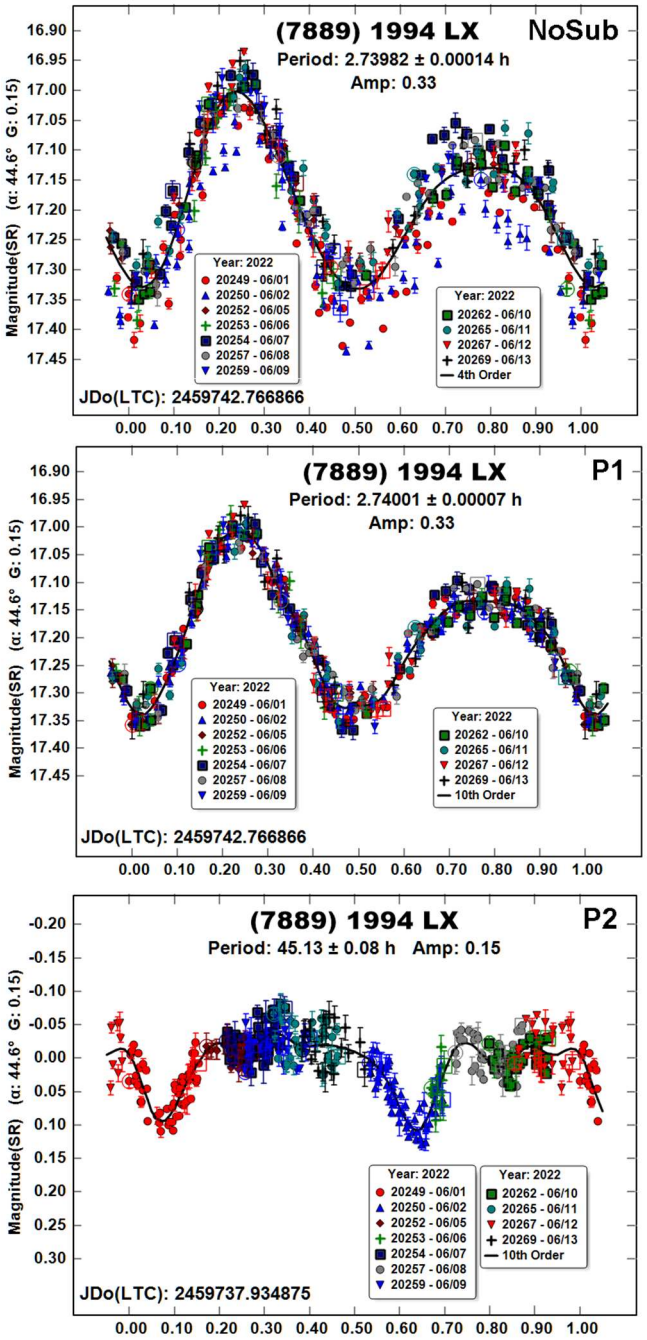

Our 2022 observations clearly indicated a secondary period in the data ("NoSub" plot). No listing in the LCDB indicated that the asteroid is binary and a check with the Johnston binaries web site (Johnston, 2022web) seemed to confirm that ours are the first observations to confirm that the asteroid is binary.

It took almost a fortnight to obtain the necessary data to establish that the asteroid is binary with an orbital period of 45.13 h. It seems to be comprised of two nearly equal-sized bodies, as indicated by the two mutual events differing by only 0.01 mag amplitude. The lesser amplitude of 0.11 mag gives an effective secondary-primary diameter ratio of Ds/Dp ≥ 0.33 ± 0.02.

9509 Amfortas. The only previous period listed in the LCDB was ours (Stephens and Warner, 2020), which was 3.996 h with a lightcurve amplitude of 0.07 mag. Our 2022 observations were of similar quality: error bars near the amplitude of the lightcurve. Our analysis found a dominant period of 3.849 h, significantly different from the previous result, as well as a secondary period.

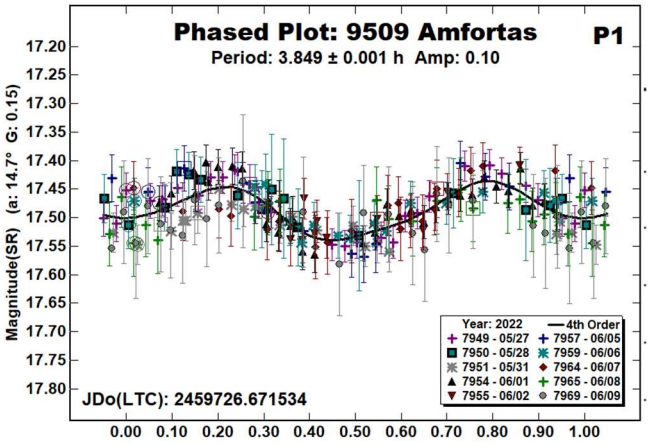

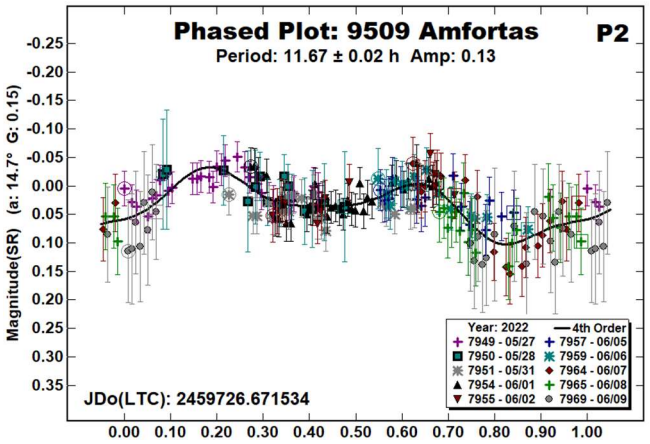

The signal for the secondary period is somewhat weak. The greatest concern is that *P2:P1* = 3.03, or nearly an integral ratio. This is followed by the distinct asymmetry of the primary lightcurve. The true nature of this asteroid may be found only with additional observations at future apparitions at usefully different phase angle bisector longitudes and/or phase angles.

(85628) 1998 KV2. This is a known binary discovered at CS3 in 2020 (Warner et al., 2020a, 2020b; Pravec et al., 2020web).

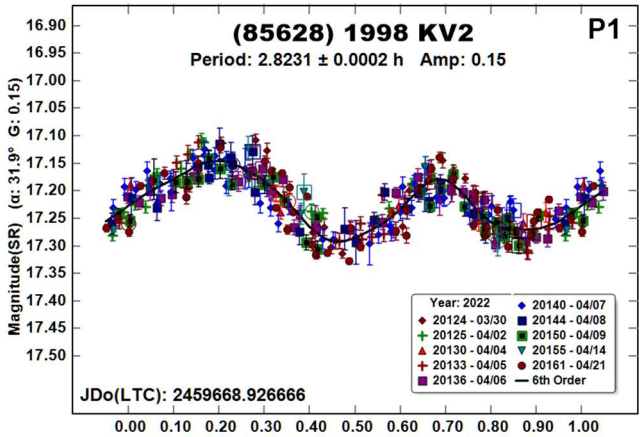

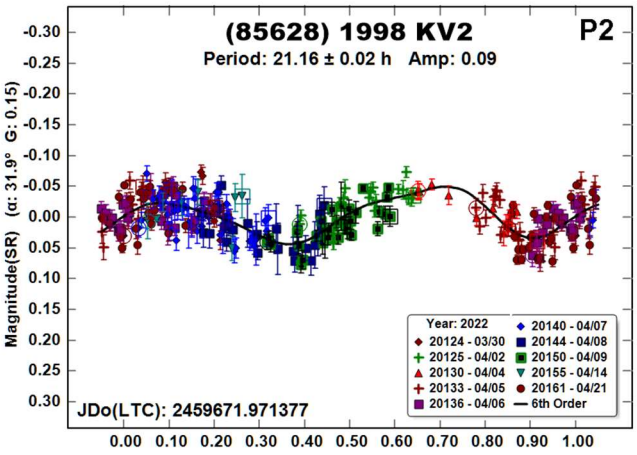

Our 2020 observations indicated Ds/Dp ≥ 0.28 ± 0.02 based on event amplitudes of 0.08 and 0.13 mag. In 2022, they were 0.05 and 0.06 mag, giving Ds/Dp ≥ 0.22 ± 0.02 and indicating a significantly different viewing aspect of the binary orbit. The orbital periods derived from data analysis in 2020 and 2022 are statistically the same. The changes in the events should prove useful for modeling the system at some point.

(377732) 2005 XJ8. Vaduvescu et al. (2017) reported a very short period of 0.132 h (7.92 min). Keeping this mind, our initial exposures were kept short to avoid what can be called "rotational smearing," as explained by Pravec et al. (2000). In short, exposures must be no longer than 0.185 * *P* (the rotational period). Otherwise, lightcurve features will blend into one another and so make it hard, if not impossible, to find the true period.

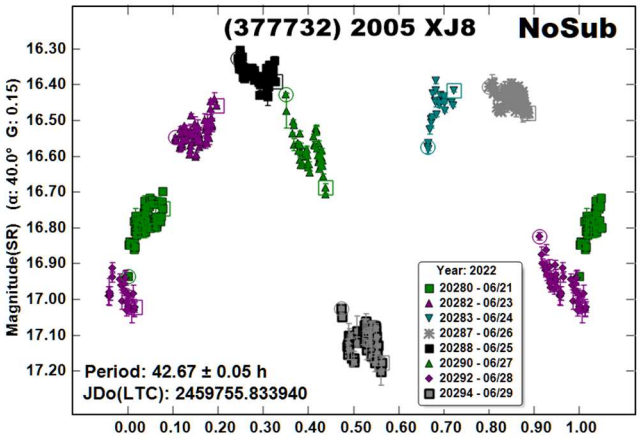

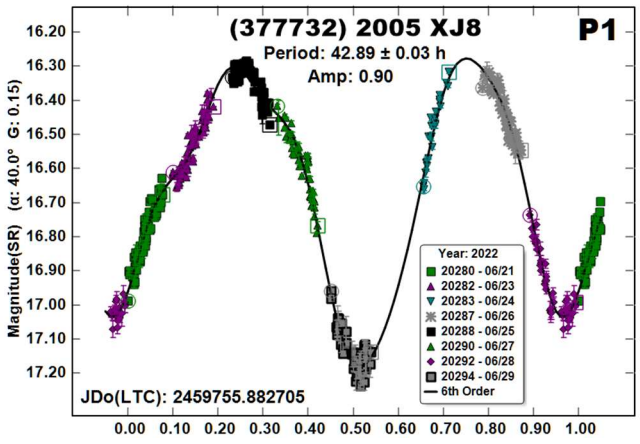

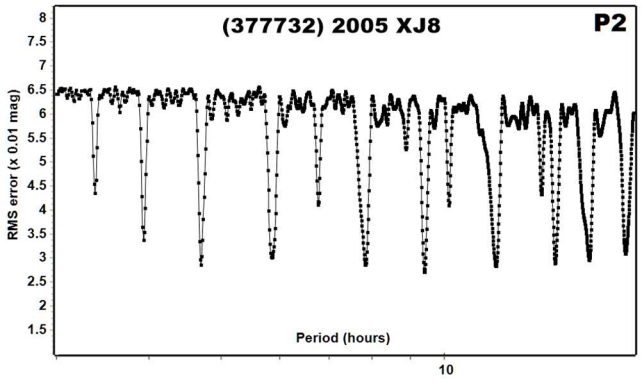

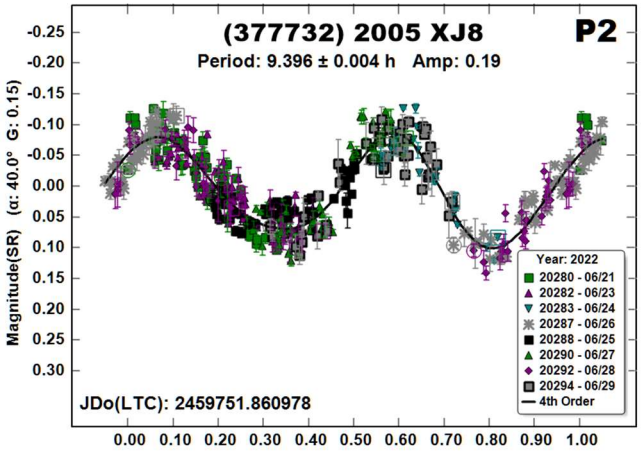

It became clear after the first session that a very short period was unlikely and so exposure times were increased. As more data were obtained, it was apparent that the period was tens of hours. Furthermore, the growing lightcurve showed distinct signs of a second period ("NoSub" plot).

Our final data set covered nine out of ten nights from 2022 June 21 to 29. Dual-period analysis of the data with *MPO Canopus* found a primary period of P_1 = 42.89 h and a strong, but ambiguous, secondary period ("P2 period spectrum"). We have adopted P_2 = 9.396 h because 1) it is likely, but not certain, that the lightcurve should be bimodal (Harris et al., 2014) and 2) a split-halves plot (Harris et al., 2014) shows a distinct asymmetry of the halves at the adopted period and too much symmetry for the doubled period.

As to the physical cause of the second period, one possibility is that the asteroid is a *very wide binary* (Warner and Stephens, 2019; and references therein). This is a system where the primary has spun down to a long period as the secondary "stole" rotational angular momentum, converting it to orbital angular momentum to migrate outward. (Angular momentum is conserved.) Usually, the secondary period is in the range of 2-4 hours, but it can be much longer. The two periods here are within the ranges seen so far in very wide binary candidates.

(475665) 2006 VY13. Our previous observations in 2017 (Warner, 2017) were split into two sets: one centered on early April and the other on early June. The first set gave a synodic period P = 17.507 h and amplitude 1.39 mag at phase a phase angle of 32°. The second set, at phase angle 14°, had a longer sideral period (17.544 h) and smaller amplitude (0.89 mag). There were no signs of a satellite. Monteiro et al. (2018) found 17.545 h based on observations in 2012.

The decrease in amplitude in 2017 as the phase angle decreased is expected behavior (Zappala et al., 1990). In the meantime, the phase angle bisector longitude (Harris et al., 1984) in 2017 was *decreasing* as the asteroid approached opposition (minimum phase angle); this implies a retrograde rotation for the asteroid (Alan Harris, *private communications*).

The *P1* lightcurve was made considerably better (lower RMS) by finding and subtracting a second period. As with 9509 Amfortas, if the secondary lightcurve was more certain (and longer in this case), it would look similar to one of a satellite displaying mutual events. However, also as with 9509 Amfortas, the secondary period is very close to a 3:1 ratio with the primary period. Observations at future apparitions are needed to define the true nature of the asteroid.

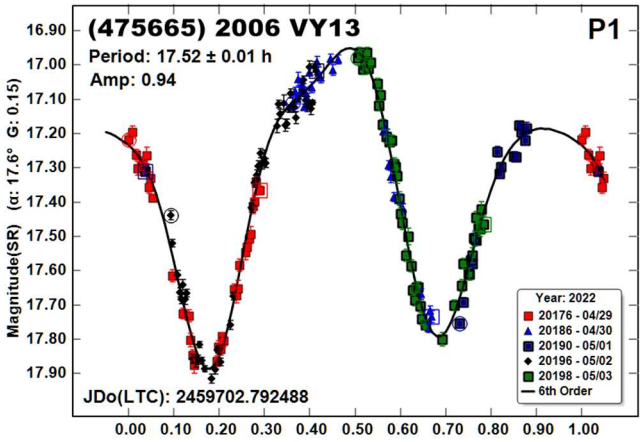

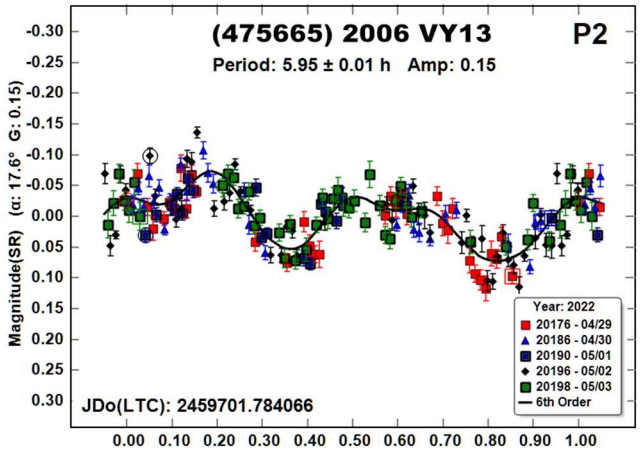

Acknowledgements

The authors gratefully acknowledge Shoemaker NEO Grants from the Planetary Society (2007, 2013). These were used to purchase some of the telescopes and CCD cameras used in this research. This work includes data from the Asteroid Terrestrial-impact Last Alert System (ATLAS) project. ATLAS is primarily funded to search for near earth asteroids through NASA grants NN12AR55G, 80NSSC18K0284, and 80NSSC18K1575; byproducts of the NEO search include images and catalogs from the survey area. The ATLAS science products have been made possible through the contributions of the University of Hawaii Institute for Astronomy, the Queen's University Belfast, the Space Telescope Science Institute, and the South African Astronomical Observatory.

Number	Name	2022 mm/dd	Phase	L_{PAB}	B_{PAB}	Period(h)	P.E.	Amp	A.E.	Grp/Dr
2778	Tangshan	03/30-04/09	9.5,13.4	176	5	3.4607	0.0002	0.30	0.01	MB-I
						27.75	0.03	0.09	0.01	*UD*
6455	1992 HE	04/06-04/25	19.8,28.6	178	21	2.7346	0.0003	0.06	0.01	NEA
						17.58	0.01	0.06	0.01	*UD*
7889	1994 LX	06/01-06/13	44.6,42.5	222	48	2.74001	0.00007	0.33	0.02	NEA
						45.13	0.08	0.15	0.01	0.33
9509	Amfortas	05/27-06/08	14.8,20.1	225	7	3.849	0.001	0.10	0.01	MB-I
						11.67	0.02	0.13	0.02	*UD*
85628	1998 KV2	03/30-04/21	31.9,16.4	211	19	2.8231	0.0002	0.15	0.02	NEA
						21.16	0.02	0.09	0.01	0.22
377732	2005 XJ8	06/24-06/29	34.3,16.3	301	8	42.89	0.03	0.90	0.03	NEA
						9.396	0.004	0.19	0.03	*UD*
475665	2006 VY13	04/29-05/02	17.6,15.3	234	9	17.52	0.01	0.94	0.03	NEA
						5.95	0.01	0.15	0.02	*UD*

Table II. Observing circumstances. The first line for an asteroid gives the primary or dominant period. The second line gives the secondary period. The phase angle (α) is given at the start and end of each date range. L_{PAB} and B_{PAB} are, respectively the average phase angle bisector longitude and latitude (see Harris et al.,1984). For the Grp/Dr column, the first line gives the group/family: MB-I: inner main-belt, PHO: Phocaea; NEA: near-Earth asteroid. The code "UD" on the second line in the Grp/Dr column means "undetermined," primarily because there were no mutual events. Otherwise, the value is the ratio of the secondary-to-primary effective diameters.

This paper made use of the services provided by the SAO/NASA Astrophysics Data System, which is operated by the Smithsonian Astrophysical Observatory under NASA Cooperative Agreement 80NSSC211M0056.

References

Behrend, R. (2018web). Observatoire de Geneve web site. *http://obswww.unige.ch/~behrend/page_cou.html*

Gaftonyuk, N.M.; Krugly, Yu.N. (2004). *Astronomical School Report* **5***, No. 1-2*, 122-125 (in Russian).

Harris, A.W.; Young, J.W.; Scaltriti, F.; Zappala, V. (1984). "Lightcurves and phase relations of the asteroids 82 Alkmene and 444 Gyptis." *Icarus* **57**, 251-258.

Harris, A.W.; Pravec, P.; Galad, A.; Skiff, B.A.; Warner, B.D.; Vilagi, J.; Gajdos, S.; Carbognani, A.; Hornoch, K.; Kusnirak, P.; Cooney, W.R.; Gross, J.; Terrell, D.; Higgins, D.; Bowell, E.; Koehn, B.W. (2014). "On the maximum amplitude of harmonics on an asteroid lightcurve." *Icarus* **235**, 55-59.

Johnston, W.R. (2022web). *Asteroids with Satellites*. *https://www.johnstonsarchive.net/astro/asteroidmoons.html*

Mainzer, A.; Bauer, J.; Cutri, R.; Grav, T.; Kramer, E.; Masiero, J.; Sonnett, S.; Wright, E., Eds. (2019). "NEOWISE Diameters and Albedos V2.0." NASA Planetary Data System. urn:nasa:pds:neowise_diameters_albedos::2.0. *https://doi.org/10.26033/18S3-2Z54*

Monteiro, F.; Silva, J.S.; Lazzaro, D.; Arcoverde, P.; Medeiros, H.; Rodrigues, T.; Souza, R. (2018). "Rotational properties of near-earth objects obtained by the IMPACTON project." *Plan. Space Sci.* **164**, 54-74.

Pravec, P.; Hergenrother, C.; Whiteley, R.; Sarounova, L.; Kusnirak, P. (2000). "Fast Rotating Asteroids 1999 TY2, 1999 SF10, and 1998 WB2." *Icarus* **147**, 477-486.

Pravec, P.; Wolf, M.; Sarounova, L. (2002web, 2020web). *http://www.asu.cas.cz/~ppravec/neo.htm*

Pravec, P.; Fatka, P.; Vokrouhlicky, D.; Scheeres, D.J.; Kusnirak, P.; Hornoch, K.; Galad, A.; Vrastil, J.; Pray, D.P.; Krugly, Yu.N.; Gaftonyuk, N.M.; Inasaridze, R.Ya.; Ayvazian, V.R.; Kvaratskhelia, O.I.; Zhuzhunadze, V.T.; Husarik, M.; Cooney, W.R.; Gross, J.; Terrell, D.; Világi, J. Kornos, L.; Gajdos, S.; Burkhonov, O.; Ehgamberdiev, Sh.A.; Donchev, Z.; Borisov, G.; Bonev, T.; Rumyantsev, V.V.; Molotov, I.E. (2018). "Asteroid clusters similar to asteroid pairs." *Icarus* **304**, 110-126.

Stephens, R.D.; Warner, B.D. (2019). "Main-belt Asteroids Observed from CS3: 2019 April to June." *Minor Planet Bull.* **46**, 449-456.

Stephens, R.D.; Warner, B.D. (2020). "Main-belt Asteroids Observed from CS3: 2019 July to September." *Minor Planet Bull.* **47**, 50-60.

Tonry, J.L.; Denneau, L.; Flewelling, H.; Heinze, A.N.; Onken, C.A.; Smartt, S.J.; Stalder, B.; Weiland, H.J.; Wolf, C. (2018). "The ATLAS All-Sky Stellar Reference Catalog." *Ap. J.* **867**, A105.

Vaduvescu, O.; Macias, A.A.; Tudor, V.; Predatu, M.; Galád, A.; Gajdoš, Š.; Világi, J.; Stevance, H.F.; Errmann, R.; Unda-Sanzana, E.; Char, F.; and 16 coauthors. (2017). "The EURONEAR Lightcurve Survey of Near Earth Asteroids." *Earth, Moon, and Planets* **120**, 41-100.

Warner, B.D. (2004). "Lightcurve analysis for numbered asteroids 1351, 1589, 2778, 5076, 5892, and 6386." *Minor Planet Bull*. **31**, 36-39.

Warner, B.D.; Harris, A.W.; Pravec, P. (2009). "The Asteroid Lightcurve Database." *Icarus* **202**, 134-146. Updated 2021 Dec. *https://www.minorplanet.info/php/lcdb.php*

Warner, B.D. (2015). "Near-Earth Asteroid Lightcurve Analysis at CS3-Palmer Divide Station: 2015 March - June." *Minor Planet Bull*. **42**, 256-266.

Warner, B.D. (2017). "Near-Earth Asteroid Lightcurve Analysis at CS3-Palmer Divide Station: 2017 April thru June." *Minor Planet Bull*. **44**, 335-344.

Warner, B.D.; Stephens, R.D. (2019). "Another Trio of Possible Very Wide Binaries." *Minor Planet Bull.* **46**, 153-157.

Warner, B.D.; Stephens, R.D. (2020). "Near-Earth Asteroid Lightcurve Analysis at the Center for Solar System Studies: 2019 September - 2020 January." *Minor Planet Bull*. **47**, 105-120.

Warner, B.D.; Stephens, R.D.; Harris, A.W. (2020a). *CBET* **4757**.

Warner, B.D.; Stephens, R.D.; Harris, A.W. (2020b). "Binary Asteroids at the Center for Solar System Studies." *Minor Planet Bull*. **47**, 305-308.

Wolters, S.D.; Green, S.F.; McBride, N.; Davies, J.K. (2005). "Optical and thermal infrared observations of six near-Earth asteroids in 2002." *Icarus* **175**, 92-110.

Zappala, V.; Cellini, A.; Barucci, A.M.; Fulchignoni, M.; Lupishko, D.E. (1990). "An anlaysis of the amplitude-phase relationship among asteroids." *Astron. Astrophys*. **231**, 548-560.

LIGHTCURVES FOR THREE KORONIS FAMILY ASTEROIDS FROM THE UNION COLLEGE OBSERVATORY

F.P. Wilkin, Z. AlMassri, P. Bowles, M. Pargiello, J. Sindoni
Department of Physics and Astronomy, Union College
807 Union St., Schenectady, NY 12308
wilkinf@union.edu

(Received: 2022 June 3)

We present lightcurves for Koronis family asteroids (243) Ida, (321) Florentina, and (2713) Luxembourg. All had periods consistent with previously reported values and showed classic doubly-periodic lightcurves.

At the Union College Observatory we have undertaken a program to observe rotation lightcurves of Koronis family asteroids in support of determining spin vectors and shape models (Kaasalainen et al., 2001; Slivan et al., 2003). Members of this family (named for its lowest numbered member (158) Koronis) are believed to share a common progenitor which was broken up in a collision long ago; thus, they share similar orbits in the outer asteroid belt and similar S-type spectral characteristics. Long-term interaction with solar radiation via the YORP effect has modified members' spin properties (Slivan, 2002; Vokrouhlicky et al., 2003), and determination of spin vectors for a sufficiently large sample of Koronis members may shed light on YORP-driven evolution in the solar system.

We have obtained lightcurves for three Koronis Family asteroids using observations at the Union College Observatory during 2018-2019. This represents the first published asteroid data from the Union College Observatory. Target selection and ephemerides were based upon the Koronis family asteroids web tool (Slivan, 2003). The three selected objects for our first study were chosen because they have well-established short periods and large enough amplitudes. All observations were conducted at the 0.51-m Optical Guidance Systems f/8.1 Ritchey-Chrétien telescope using an SBIG STXL 11002 CCD camera, cooled to -30°C, with an Astrodon Bessel R filter. The detector has 4008 × 2672 9μm square pixels. With 2×2 binning, the pixel scale is 0.93 "/pix and the field of view is 30'×20'.

Bias, dark, flat field corrections and subsequent photometry were performed in *AstroImageJ* software (Collins et al., 2017). We corrected for light travel time for all three targets using ephemerides from the NASA Horizons website.

(243) Ida has the distinction in that it is only the second asteroid to have been photographed at close range by a spacecraft. On 1993 Aug 28 NASA's Galileo flew by Ida at a distance of roughly 1,500 miles on its way to Jupiter. Its sidereal period was determined to be 4.633632 ± 0.000007 h (Binzel et al., 1993) using pre-Galileo observations. Because the pre-encounter analysis was based upon 9 years of observations and the flyby extended this by only three months, the Galileo spacecraft trajectory was not well-suited to

Number	Name	yyyy mm/dd	Phase	L_{PAB}	B_{PAB}	Period(h)	P.E.	Amp	A.E.	Grp
243	Ida	2019 9/18	6.9	338	0	4.67	0.04	0.76	0.04	KOR
321	Florentina	2019 10/24-11/4	19.1,17.0	86	2	2.8708	0.0003	0.35	0.03	KOR
2713	Luxembourg	2018 12/05-12/11	5.6,7.9	59	2	3.581	0.002	0.53	0.05	KOR

Table I. Observing circumstances and results. The phase angle is given for the first and last date. L_{PAB} and B_{PAB} are the approximate phase angle bisector longitude/latitude at mid-date range. Grp is the asteroid family/group.

refinement of that period (Davies et al., 1996). Given the years since the intense study of the 1990s, new observations of the object may prove useful for this purpose. The single-night lightcurve from Union College Observatory yields a rotation period of 4.67 ± 0.04 h, which is consistent with published periods. We obtain an amplitude of 0.76 ± 0.04 mag.

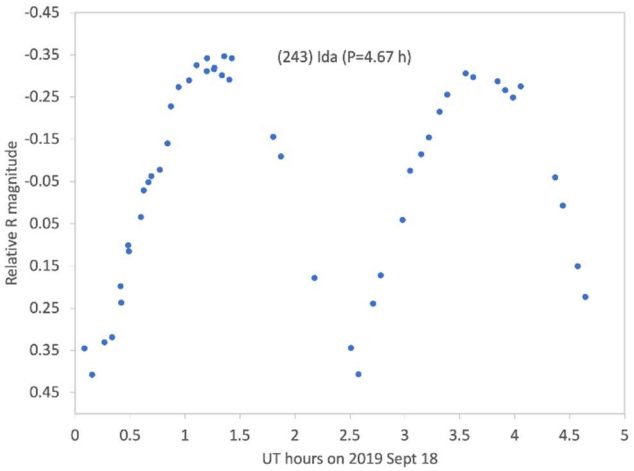

(321) Florentina has a sidereal rotation period of 2.87086579 ± 0.00000019 h determined by Slivan et al. (2003), who also reported a spin pole and shape model. We observed this object on 2019 Oct 23 and 2019 Nov 3. We determined a period of 2.8708 ± 0.0003 h, consistent with previously-reported values, and amplitude 0.35 ± 0.03 mag.

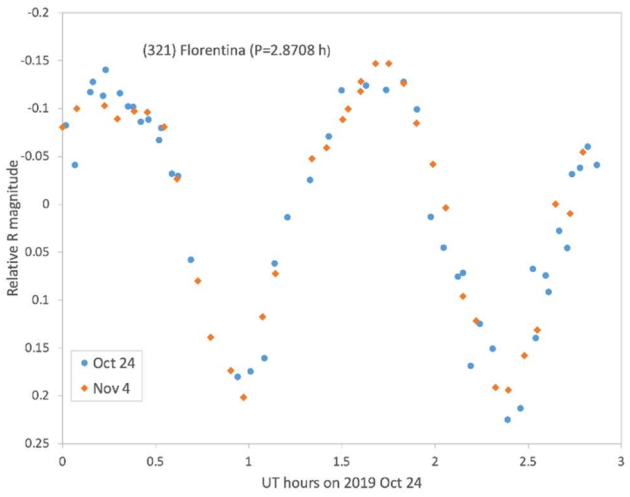

(2713) Luxembourg. A complete lightcurve and unambiguous period of P=3.579 ± 0.002 h were presented by Mailhot and Midkiff (2014). They remarked that the relative brightness of the minima changed noticeably over the range of solar phase angle observed. We observed Luxembourg two nights in 2018 Dec. The magnitude values of Dec 11 were shifted visually for a self-consistent composite by a constant offset relative to those of Dec 5. Our best-fit period of 3.581 ± 0.002 h is in agreement with that of Mailhot and Midkiff. Amplitude was 0.53 ± 0.05 mag for Luxembourg in Dec 2018.

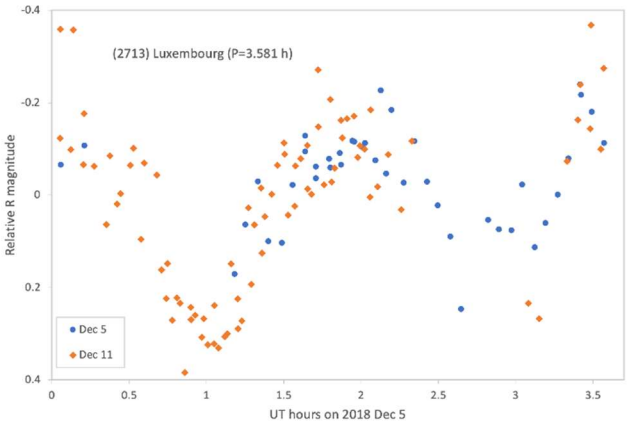

Acknowledgements

F.P.W. is grateful for encouragement from S. Slivan to initiate this observing program and for the use of the *koronisfamily.com* website.

References

Binzel, R.P; Slivan, S.M.; Magnusson, P.; Wisniewski; W.Z.; and 15 coauthors. (1993). "Asteroid 243 Ida: Groundbased Photometry and a Pre-Galileo Physical Model." *Icarus* **105**, 310-325.

Collins, K.A.; Kielkopf, J.F.; Stassun, K.G.; Hessman, F.V. (2017). "AstroImageJ: Image Processing and Photmetric Extraction for Ultra-precise Astronomical Light Curves." *Astronomical Journal* **153**, 77-89.

Davies, M.E.; Colvin, T.R.; Belton, M.J.S.; Veverka, J.; Thomas, P.C. (1996). "The Direction of the North Pole and the Control Network of Asteroid 243 Ida." *Icarus* **120**, 33-37.

Kaasalainen, M.; Torppa, J.; Muinonen, K. (2001). "Optimization methods for asteroid lightcurve inversion. II. The complete inverse problem." *Icarus* **153**, 37-51.

Mailhot, E.A.; Midkiff, A.H. (2014). "Lightcurve Analysis for 2713 Luxembourg." *Minor Planet Bull.* **41**, 157.

NASA Horizons. *https://ssd.jpl.nasa.gov/horizons/app.html#/*

Slivan, S.M. (2002). "Spin vector alignment of Koronis family asteroids." *Nature* **419**, 49-51.

Slivan, S.M. (2003). "A Web-based tool to calculate observability of Koronis program asteroids." *Minor Planet Bull.* **30**, 71-72.

Slivan, S.M.; Binzel, R.P.; Crespo de Silva, L.D.; Kaasalainen, M.; Lyndaker, M.M.; Krčo, M. (2003). "Spin vectors in the Koronis family: comprehensive results from two independent analyses of 213 rotation lightcurves." *Icarus* **162**, 285-307.

Vokrouhlicky, D.; Nesvorny, D.; Bottke, W.F. (2003). "The vector alignments of asteroid spins by thermal torques." *Nature* **425**, 147-151.

LIGHTCURVE ANALYSIS OF HILDA ASTEROIDS AT THE CENTER FOR SOLAR SYSTEM STUDIES: 2022 MARCH-MAY

Brian D. Warner
Center for Solar System Studies (CS3)
446 Sycamore Ave.
Eaton, CO 80615 USA
brian@MinorPlanetObserver.com

Robert D. Stephens
Center for Solar System Studies (CS3)
Rancho Cucamonga, CA

(Received: 2022 July 3)

CCD photometric observations of four Hilda asteroids were made at the Center for Solar System Studies between 2022 March and May. Of those, 3561 Devine and 8551 Daitarabochi had distinct secondary periods.

CCD photometric observations of four Hilda asteroid were carried out at the Center for Solar System Studies (CS3) from 2022 March-May as part of an ongoing study of the family/group that is located between the outer main-belt and Jupiter Trojans in a 3:2 orbital resonance with Jupiter. The goal is to determine the spin rate statistics of the Hildas and to find pole and shape models when possible. We also look to examine the degree of influence that the YORP (Yarkovsky-O'Keefe-Radzievskii-Paddack) effect (Rubincam, 2000) has on distant objects and to compare the spin rate distribution against the Jupiter Trojans, which can provide evidence that the Hildas are more "comet-like" than main-belt asteroids.

Telescopes	Cameras
0.30-m *f*/6.3 Schmidt-Cass	FLI Microline 1001E
0.35-m *f*/9.1 Schmidt-Cass	FLI Proline 1001E
0.35-m *f*/11 Schmidt-Cass	SBIG STL-1001E
0.40-m f/10 Schmidt-Cass	
0.50-m *f*/8.1 Ritchey-Chrétien	

Table I. List of available telescopes and CCD cameras at CS3. The exact combination for each telescope/camera pair can vary due to maintenance or specific needs.

Table I lists the telescopes and CCD cameras that are available to make observations. All the cameras use CCD chips from the KAF 1001 blue-enhanced family and so have essentially the same response. The pixel scales ranged from 1.24-1.60 arcsec/pixel. All lightcurve observations were unfiltered or with a clear filter, even though the latter can result in a 0.1-0.3 magnitude loss. The exposures varied depending on the asteroid's brightness.

To reduce the number of times and amounts of adjusting nightly zero-points, the ATLAS catalog r´ (SR) magnitudes (Tonry et al., 2018) are used. Those adjustments are usually ≤ ±0.03 mag. The rare greater corrections may have been related in part to using unfiltered observations, poor centroiding of the reference stars, and not correcting for second-order extinction. Another cause may be selecting what appears to be a single star but is actually an unresolved pair.

The Y-axis values are ATLAS SR "sky" (catalog) magnitudes. The two values in the parentheses are the phase angle (a) and the value of *G* used to normalize the data to the comparison stars used in the earliest session. This, in effect, made all the observations seem to be made at a single fixed date/time and phase angle, leaving any variations presumably due only to the asteroid's rotation and/or albedo variations. The X-axis shows rotational phase from -0.05 to 1.05. If the plot includes the amplitude, e.g., "Amp: 0.65", this is the amplitude of the Fourier model curve and *not necessarily the adopted amplitude for the lightcurve*.

For brevity, only some of the previous results are referenced. A more complete listing is in the asteroid lightcurve database (Warner et al, 2009; "LCDB" from here on).

2067 Aksnes. Dahlgren et al. (1998) reported a period of 17.75 h and amplitude of 0.24 mag. From observations in 2021, we (Warner and Stephens, 2021) found a similar period of 17.677 h and an identical amplitude. Our 2022 results are consistent with the previous results. We note the unusual shape of the lightcurve.

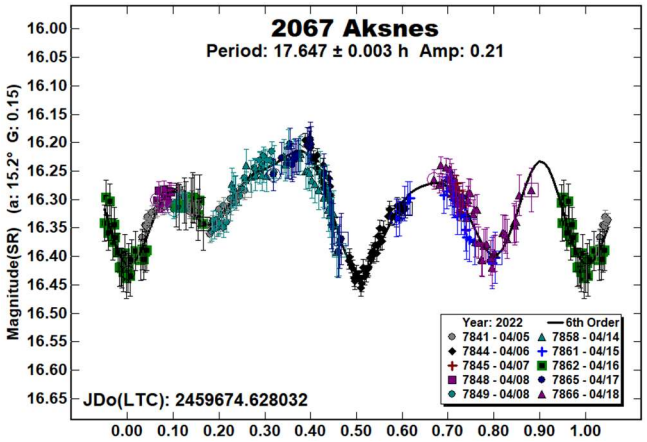

3561 Devine. Our previous results include Stephens (2016; 4.376 h), Warner et al. (2018; 9.61 h), and Warner et al. (2021; 4.7985 h). In very sharp contrast, Pál et al. (2020) reported a period of 108.068 h using data from TESS. Reviewing their frequency spectrum, there were much less prominent solutions at 3.077 h, 3.840 h, and 4.948 h, the last being somewhat close to our 2021 result.

Our 2022 observations unexpectedly showed a primary period of 39.16 h and a secondary period of 16.038 h that were found with the dual-period search in *MPO Canopus*. Those two periods do not have a simple integer ratio, which helps remove the possibility, but not completely, that they are harmonically related. On the other hand, the Pál et al. and our primary period have a close to 11:4 ratio (11.039). Allowing for uncertainties in one or both periods, it's possible that two are harmonically tied to one another.

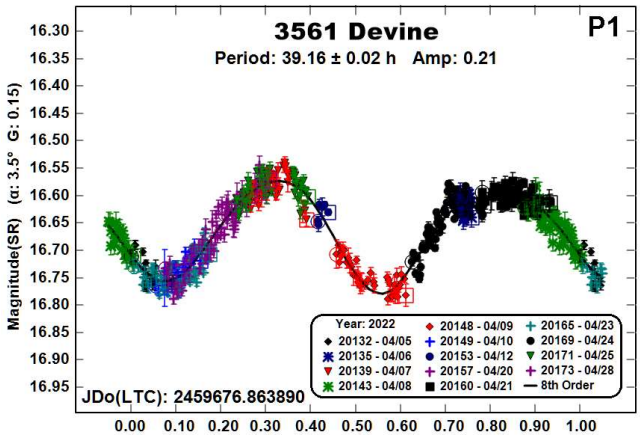

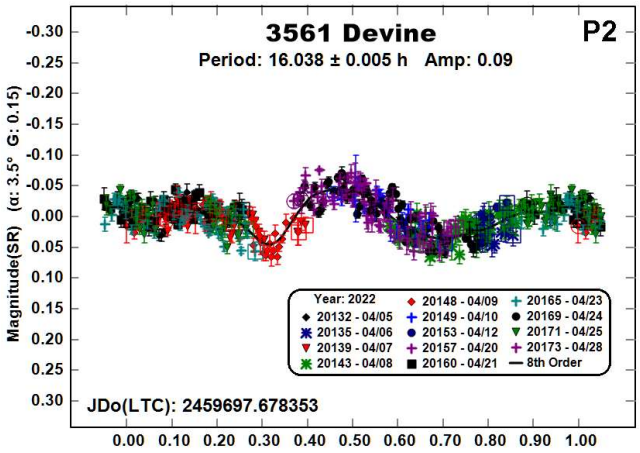

Given the shape of the P2 lightcurve, it seems unlikely that it is due to a satellite. Instead, it may be one of the byproducts of *MPO Canopus* doing what it *not* designed to do: find the periods of rotation and precession of a tumbling asteroid. The most optimistic estimate of the tumbling damping time for the asteroid (0.2 Gyr) requires a period of 101 h (Pravec et al., 2014; 2005), which is close to the period from Pál et al. (2020). Future observations are highly recommended.

8551 Daitarabochi. Our previous result of $P = 6.62$ h (Warner et al., 2018) was the only one listed in the LCDB. The results from the 2022 data are dramatically different, the most significant being a much longer dominate period and finding a secondary period.

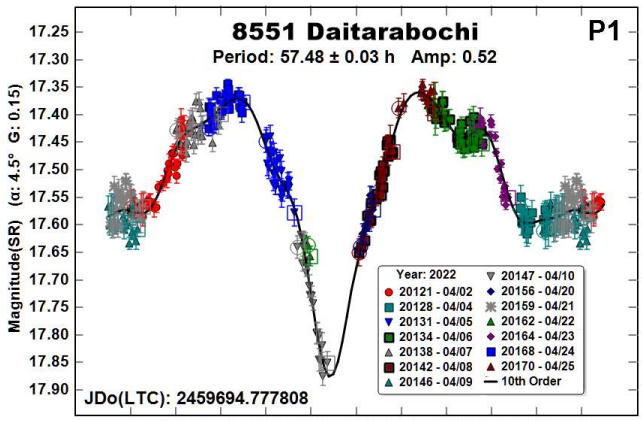

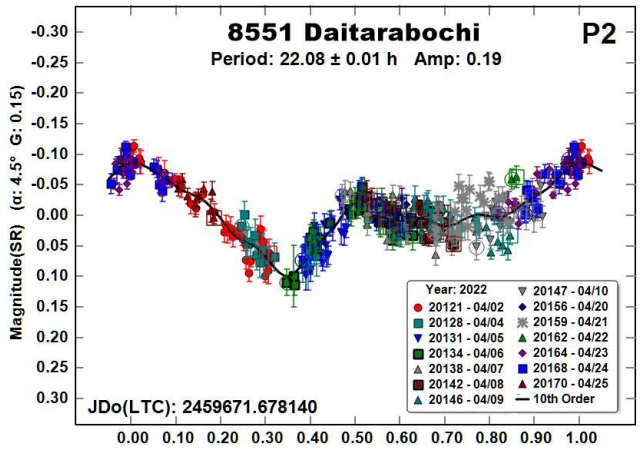

As with 3561 Devine, there were two distinct periods extracted from the data, the periods don't have a simple integral ratio, and the secondary period is unlikely due to a satellite. "More Data!"

A side note: the data from the first night, March 30, were inexplicably 0.7 mag too bright even after confirming that SR magnitudes were being used and the asteroid correctly identified. As a result, the data were not used in period analysis since they were an obvious outlier compared to the rest of the data set, even if considering the possibility of tumbling.

8743 Keneke. Pál et al. (2020) found a period of 99.3073 h. In our previous work (Warner and Stephens, 2021), we found a period of 46.74 h based on 2021 observations and, after remeasuring the original images from 2016, a revised period of 63.7 h. Instead of our 2022 data analysis removing ambiguities it only added to them.

The period spectrum indicates several possible solutions, including some close to those in Warner and Stephens (2021). None of the four periods given here has a simple integer period ratio with the other three.

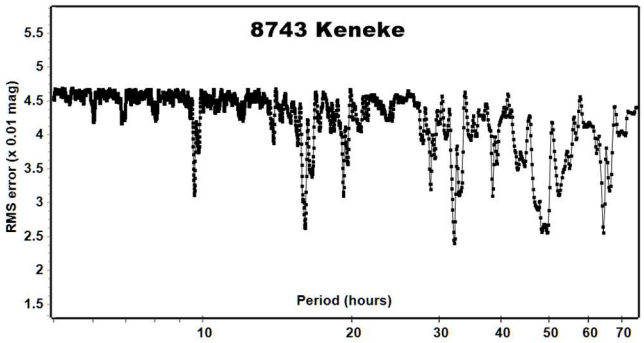

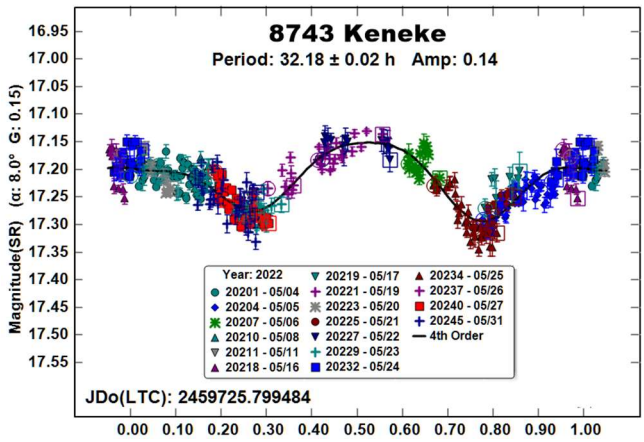

Acknowledgements

This work includes data from the Asteroid Terrestrial-impact Last Alert System (ATLAS) project. ATLAS is primarily funded to search for near earth asteroids through NASA grants NN12AR55G, 80NSSC18K0284, and 80NSSC18K1575; byproducts of the NEO search include images and catalogs from the survey area. The ATLAS science products have been made possible through the contributions of the University of Hawaii Institute for Astronomy, the Queen's University Belfast, the Space Telescope Science Institute, and the South African Astronomical Observatory. The authors gratefully acknowledge Shoemaker NEO Grants from the Planetary Society (2007, 2013). These were used to purchase some of the telescopes and CCD cameras used in this research.

Number	Name	2022/mm/dd	Phase	L_{PAB}	B_{PAB}	Period(h)	P.E.	Amp	A.E.
2067	Aksnes	04/05-04/18	15.2,16.3	137	0	17.647	0.003	0.21	0.02
3561	Devine	04/05-04/28	3.5,8.3	189	11	39.16	0.02	0.21	0.02
						16.038	0.005	0.09	0.01
8551	Daitarabochi	03/30-04/25	4.1,8.9	179	12	57.48	0.03	0.52	0.02
						22.08	0.01	0.19	0.02
8743	Keneke	05/04-05/31	8.1,13.3	201	16	32.18	0.02	0.14	0.02

Table II. Observing circumstances and results. The phase angle (α) is given at the start and end of each date range. The asterisk indicates that the phase angle reached an extremum over the span of the observations. L_{PAB} and B_{PAB} are the average phase angle bisector longitude and latitude (see Harris et al., 1984).

References

Dahlgren, M.; Lahulla, J.F.; Lagerkvist, C.-I.; Lagerros, J.; Mottola, S.; Erikson, A.; Gonano-Beurer, M.; Di Martino, M. (1998). "A Study of Hilda Asteroids. V. Lightcurves of 47 Hilda Asteroids." *Icarus* **133**, 247-285.

Harris, A.W.; Young, J.W.; Scaltriti, F.; Zappala, V. (1984). "Lightcurves and phase relations of the asteroids 82 Alkmene and 444 Gyptis." *Icarus* **57**, 251-258.

Pál, A.; Szakáts, R.; Kiss, C.; Bódi, A.; Bognár, Z.; Kalup, C.; Kiss, L.L.; Marton, G.; Molnár, L.; Plachy, E.; Sárneczky, K.; Szabó, G.M.; Szabó, R. (2020). "Solar System Objects Observed with TESS - First Data Release: Bright Main-belt and Trojan Asteroids from the Southern Survey." *Ap. J. Suppl Ser*. **247**, id. 26.

Pravec, P.; Harris, A.W.; Scheirich, P.; Kušnirák, P.; Šarounová, L.; Hergenrother, C.W.; Mottola, S.; Hicks, M.D.; Masi, G.; Krugly, Yu.N.; Shevchenko, V.G.; Nolan, M.C.; Howell, E.S.; Kaasalainen, M.; Galád, A.; Brown, P.; Degraff, D.R.; Lambert, J.V.; Cooney, W.R.; Foglia, S. (2005). "Tumbling asteroids." *Icarus* **173**, 108-131.

Pravec, P.; Scheirich, P.; Durech, J.; Pollock, J.; Kusnirak, P.; Hornoch, K.; Galad, A.; Vokrouhlicky, D.; Harris, A.W.; Jehin, E.; Manfroid, J.; Opitom, C.; Gillon, M.; Colas, F.; Oey, J.; Vrastil, J.; Reichart, D.; Ivarsen, K.; Haislip, J.; LaCluyze, A. (2014). "The tumbling state of (99942) Apophis." *Icarus* **233**, 48-60.

Rubincam, D.P. (2000). "Relative Spin-up and Spin-down of Small Asteroids." *Icarus* **148**, 2-11.

Stephens, R.D. (2016). "Asteroids Observed from CS3: 2015 July - September." *Minor Planet Bull.* **43**, 52-56.

Tonry, J.L.; Denneau, L.; Flewelling, H.; Heinze, A.N.; Onken, C.A.; Smartt, S.J.; Stalder, B.; Weiland, H.J.; Wolf, C. (2018). "The ATLAS All-Sky Stellar Reference Catalog." *Astrophys. J.* **867**, A105.

Warner, B.D.; Harris, A.W.; Pravec, P. (2009). "The Asteroid Lightcurve Database." *Icarus* **202**, 134-146. Updated 2021 Dec. *http://www.minorplanet.info/lightcurvedatabase.html*

Warner, B.D.; Stephens, R.D.; Coley, D.R. (2018). "Lightcurve Analysis of Hilda Asteroids at the Center for Solar System Studies: 2017 October - December." *Minor Planet Bull.* **45**, 147-161.

Warner, B.D.; Stephens, R.D. (2021). "Lightcurve Analysis of Hilda Asteroids at the Center for Solar System Studies: 2021 January - March." *Minor Planet Bull.* **48**, 303-308.

Warner, B.D.; Stephens, R.D.; Coley, D.R. (2021). "On Confirmed and Suspected Binary Asteroids at the Center for Solar System Studies." *Minor Planet Bull.* **48**, 274-280.

PHOTOMETRY AND LIGHTCURVE ANALYSIS OF FOUR MARS-CROSSING ASTEROIDS

Jonatan Michimani, Daniela Lazzaro, Eduardo Rondón,
Filipe Monteiro, Plícida Arcoverde, Marçal Evangelista-Santana,
Weslley Pereira, Wesley Mesquita, Roberto Souza,
Teresinha Rodrigues.
Observatório Nacional, COAA,
Rua Gal. José Cristino 77, 20921-400
Rio de Janeiro, Brazil
jonatangarcia@on.br

(Received: 2022 May 31)

Rotational periods of four Mars-crossing asteroids (MCs) were determined from lightcurves acquired at the Observatório Astronômico do Sertão de Itaparica (MPC Y28, OASI) between 2020 July to 2021 October.

CCD photometric observations of four Mars-crossers were made at the Observatório Astronômico do Sertão de Itaparica (MPC code Y28) between 2020 July and 2021 October. Images were obtained with the 1.0-m *f*/8 telescope of the IMPACTON project and an FLI PL424 CCD camera (2048×2048 pixels) set to 2×2 binning (Rondón et al., 2020) and Johnson-Cousins R filter. The raw images were calibrated with dark and flat frames. *MPO Canopus* (Warner, 2017) was used for magnitude measurement, Fourier analysis (Harris et al., 1989), and to produce the final lightcurve.

The observational circumstances for each observed object are given in Table I along with the results, which are discussed individually below. The phased rotational lightcurve and the periodogram are shown for each object.

(27995) 1997 WL2. The only previously reported rotational period in the LCDB (Warner et al. 2009) for this small Solar System body is from Behrend et al. (2021web), who reported a period of 9.229 ± 0.001 h with 0.49 mag amplitude. Our results used observations from 2021 May and June and showed a period of 9.235 ± 0.001 h with an amplitude of 0.50 mag. The resulting two-peaked lightcurve is consistent with the previously published value both in period and amplitude.

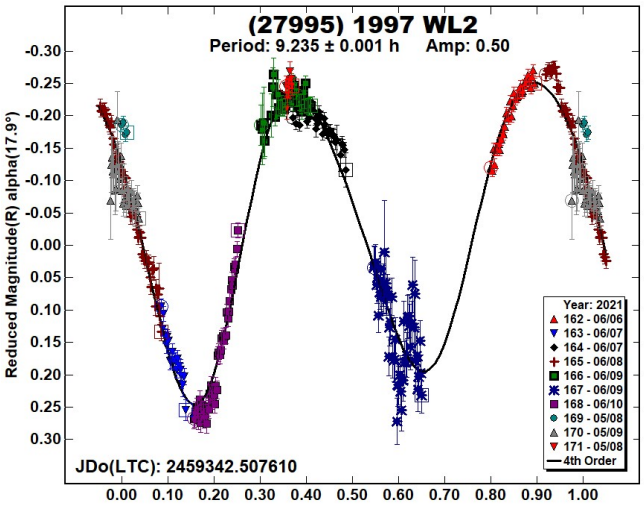

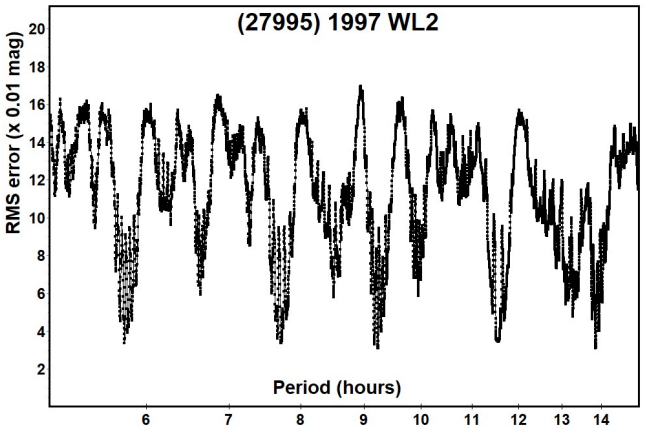

(46780) 1998 HH52. One previously reported period in the LCDB for this Mars-crosser (Pravec et al., 2021web) showed P = 3.6122 ± 0.0008 h and amplitude 0.09 mag. Our observations from 2021 November 12, 13, and 14 best fit a rotational period of 3.611 ± 0.002 h and an amplitude of 0.13 mag. Our result is in concordance with the one previously reported.

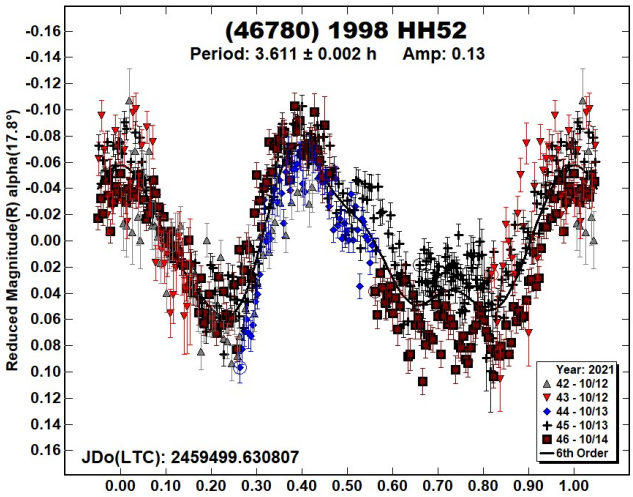

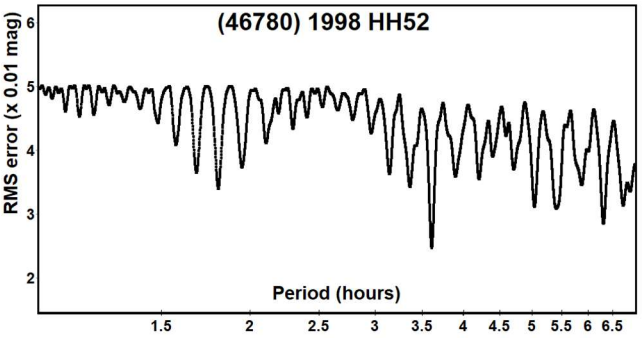

(61343) 2000 PC5. A search in the Asteroid Lightcurve Photometry Database did not find any previously reported result for this asteroid. It was possible to derive a rotational period of 2.828 ± 0.002 h from observations acquired on 2020 June 27 and 28. The lightcurve has an amplitude of 0.24 mag and displays two maxima and two minima per rotational cycle.

Number	Name	yyyy mm/dd	Phase	L_{PAB}	B_{PAB}	Period(h)	P.E.	Amp	A.E.
27995	1997 WL2	2021 05/08-06/10	*2.0,20.7	229	2	9.235	0.001	0.50	0.02
46780	1998 HH52	2021 10/12-10/14	17.0	40	0	3.611	0.002	0.13	0.01
61343	2000 PC5	2020 07/27-07/28	8.0	295	-1	2.828	0.002	0.24	0.01
351068	2003 TS13	2020 11/16-12/16	*3.0,15.0	58	-1	14.010	0.005	0.44	0.02

Table I. Observing circumstances and results. The phase angle is given for the first and last date. If preceded by an asterisk, the phase angle reached an extrema during the period. L_{PAB} and B_{PAB} are the approximate phase angle bisector longitude/latitude at mid-date range (see Harris et al., 1984).

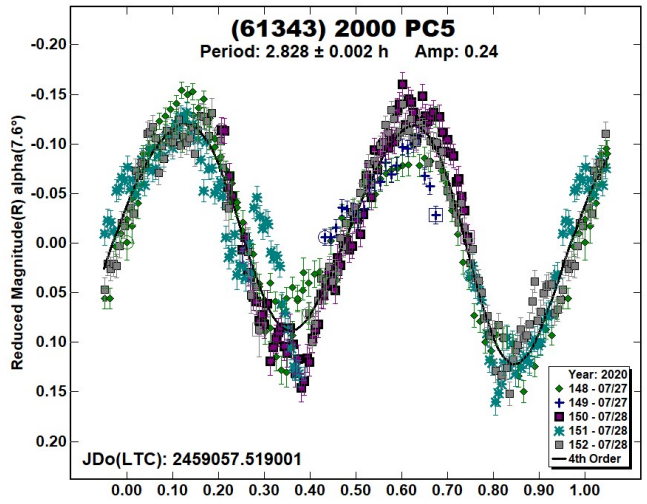

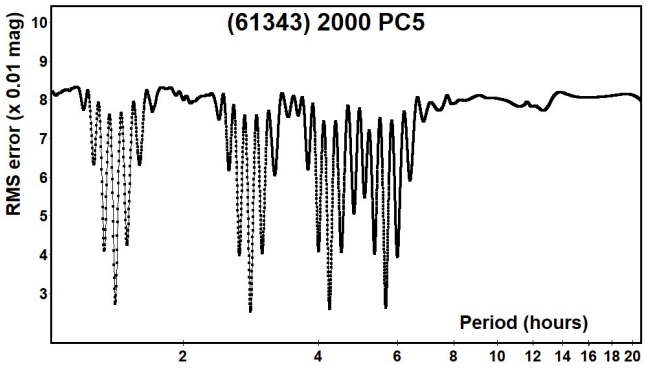

(351068) 2003 TS13. A search in the LCDB (Warner et al., 2009) did not find any previously reported period for this object. Our analysis using the photometric observations carried over several nights in 2020 November and December indicate a possible period of 14.010 ± 0.005 h with an amplitude of 0.44 h.

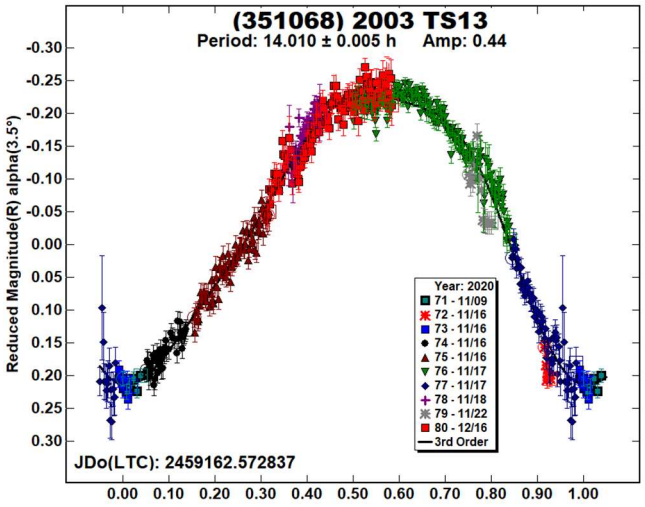

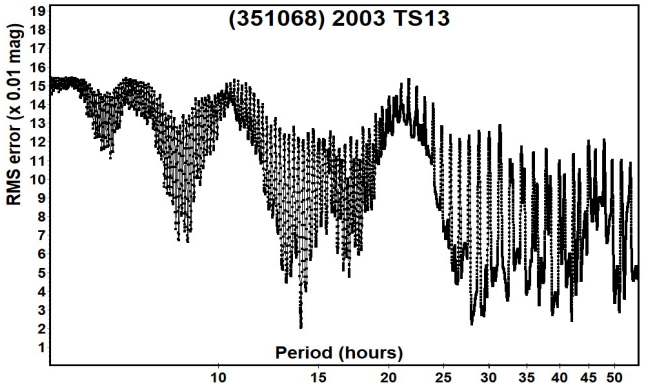

The true period might be about 28 h, or double our result; the periodogram shows a second RMS minima between 25 and 30 h. It was not possible to follow this Mars-crosser long enough to derive a "full" bimodal lightcurve, so our result is based on the best fit to a monomodal lightcurve.

Acknowledgements

The authors acknowledge CNPq, CAPES and FAPERJ for supporting this work through diverse fellowships and grants, and are grateful to the IMPACTON team, in particular, A. Santiago and J. dos Santos, for the technical support at OASI.

References

Behrend, R. et al. (2021 web). Observatoire de Genève web site. *http://obswww.unige.ch/~behrend/page_cou.html*

Harris, A.W.; Young, J.W.; Scaltriti, F.; Zappala, V. (1984). "Lightcurves and phase relations of the asteroids 82 Alkmene and 444 Gyptis." *Icarus* **57**, 251-258.

Harris, A.W.; Young, J.W.; Bowell, E.; Martin, L.J.; Millis, R.L.; Poutanen, M.; Scaltriti, F.; Zappala, V.; Schober, H.J.; Debehogne, H.; Zeigler, K.W. (1989). "Photoelectric Observations of Asteroids 3, 24, 60, 261, and 863." *Icarus* **77**, 171-186.

Pravec, P. et al. (2021 web). Photometric Survey for Asynchronous Binary Asteroids web site. *https://www.asu.cas.cz/~asteroid/binastphotsurvey.htm*

Rondón, E.; Lazzaro, D.; Rodrigues, T.; Carvano, J.M.; Roig, F.; Monteiro, F.; Arcoverde, P.; Medeiros, H.; Silva, J.; Jasmim, F.; de Prá, M.; Hasselmann, P.; Ribeiro, A.; Dávalos, J.; Souza, R. (2020). "OASI: A Brazilian Observatory Dedicated to the Study of Small Solar System Bodies-Some Results of NEOs Physical Properties." *PASP* **132**, 065001.

Warner, B.D.; Harris, A.W.; Pravec, P. (2009). "The Asteroid Lightcurve Database." *Icarus* **202**, 134-146. Updated 2021 Dec. *http://www.minorplanet.info/lightcurvedatabase.html*

Warner, B.D. (2017). *MPO Canopus* Software, version 10.7.11.1, BDW Publishing. *http://www.bdwpublishing.com*

NEAR-EARTH ASTEROID LIGHTCURVE ANALYSIS AT THE CENTER FOR SOLAR SYSTEM STUDIES: 2022 MARCH-JUNE

Brian D. Warner
Center for Solar System Studies (CS3)
446 Sycamore Ave.
Eaton, CO 80615 USA
brian@MinorPlanetObserver.com

Robert D. Stephens
Center for Solar System Studies (CS3)
Rancho Cucamonga, CA

(Received: 2022 July 3)

CCD photometry of 11 near-Earth asteroids (NEAs) obtained at the Center for Solar System Studies (CS3) in 2022 March to June were analyzed for rotation period, peak-to-peak amplitude, and signs of satellites or tumbling. While there were no signs of any of the asteroids being binary, seven of them are suspected tumblers: (10302) 1989 ML, (100756) 1998 FM5, (163692) 2003 CY18, (388945) 2008 TZ3, (464798) 2004 JX20, and 2018 XV5.

CCD photometric observations of 11 near-Earth asteroids (NEAs) were made at the Center for Solar System Studies (CS3) in 2022 March to June. Seven of the set were found to be tumbling, though the true periods of rotation and precession could not be determined.

Table I lists the telescopes and CCD cameras that were available to make observations. All the cameras use a KAF-1001E blue-enhanced CCD and so have essentially the same response. The pixel scales ranged from 1.24-1.60 arcsec/pixel.

Telescopes	Cameras
0.30-m *f*/10 Schmidt-Cass	FLI Microline 1001E
0.35-m *f*/9.1 Schmidt-Cass	FLI Proline 1001E
0.40-m *f*/10 Schmidt-Cass	SBIG STL-1001E
0.40-m *f*/10 Schmidt-Cass	
0.50-m *f*/8.1 Ritchey-Chrétien	

Table I. List of telescopes and CCD cameras at CS3 used for this paper. The exact combination for each telescope/camera pair is chosen to meet specific needs.

All lightcurve observations were unfiltered or with a clear filter, even though the latter can cause a 0.1-0.3 mag loss. The exposure duration varied depending on the asteroid's brightness and sky motion. Not all images were guided. Regardless, sometimes the asteroid was trailed on the image. In those cases, elliptical apertures were used to increase the target's SNR during measuring.

Measurements were made using *MPO Canopus*. The Comp Star Selector utility in *MPO Canopus* found up to five comparison stars of near solar-color for differential photometry. To reduce the number of times and amounts of adjusting nightly zero points, we use the ATLAS catalog r´ (SR) magnitudes (Tonry et al., 2018). Those adjustments are usually $|\Delta mag| \leq 0.03$. The rare larger corrections may have been due in part to using unfiltered observations, poor centroiding of the target and stars, not correcting for second-order extinction, and/or selecting what appears to be a single star but is actually an unresolved pair.

The Y-axis values are ATLAS SR "sky" (catalog) magnitudes. The two values in the parentheses are the phase angle (a) and the value of *G* used to normalize the data to the comparison stars used in the earliest session. This, in effect, corrects all the observations to seem to have been made at a single fixed date/time and phase angle, presumably leaving any variations due only to the asteroid's rotation and/or albedo changes. The X-axis shows rotational phase from -0.05 to 1.05. If the plot includes the amplitude, e.g., "Amp: 0.65", this is the amplitude of the Fourier model curve and *not necessarily the adopted amplitude for the lightcurve*.

"LCDB" substitutes for "Warner et al. (2009)" from here on.

4055 Magellan. Pravec et al. (2000web) first reported a period of 7.475 h based on observations made in 2000. Several other results were obtained over the years and listed in the LCDB, including two of our previous efforts (Warner, 2015b; 2017). All entries had periods close to 7.50 h, save Warner (2014), who reported 6.384 h.

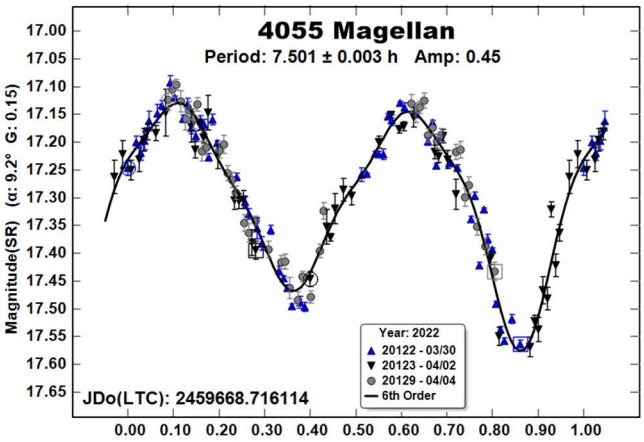

6569 Ondaatje. Pravec et al. (1996) found a period of 5.959 h and amplitude of 0.98 mag. We (Warner and Stephens, 2020b) faced a highly symmetrical lightcurve with 0.92 mag amplitude based on our 2020 observations that had one of two periods: 5.295 h or 5.956 h, which happened to be 0.5 rotations difference per 24 hours. We adopted the shorter period for its slightly lower RMS, but that now seems to be incorrect. Our latest results reinforce a period near 5.96 h with no ambiguity because of the asymmetrical lightcurve.

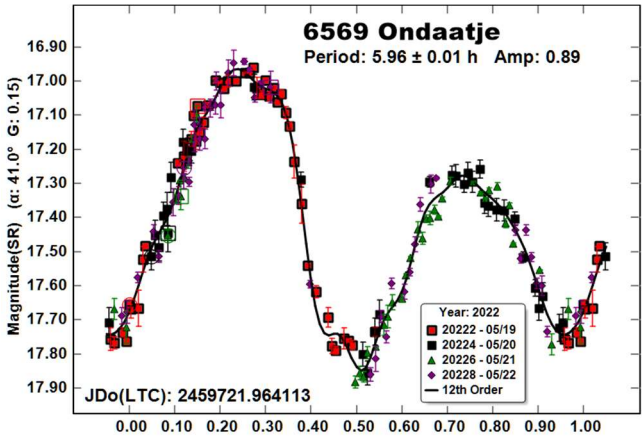

(8566) 1996 EN. The only previously reported period in the LCDB was ours of 4.849 h (Warner and Stephens, 2020a) based on data from 2020. The analysis of the 2022 data gave a similar value, P = 4.80 h. The slight difference is probably due to the lower amplitude (0.15 vs. 0.20 mag) and amount of available data.

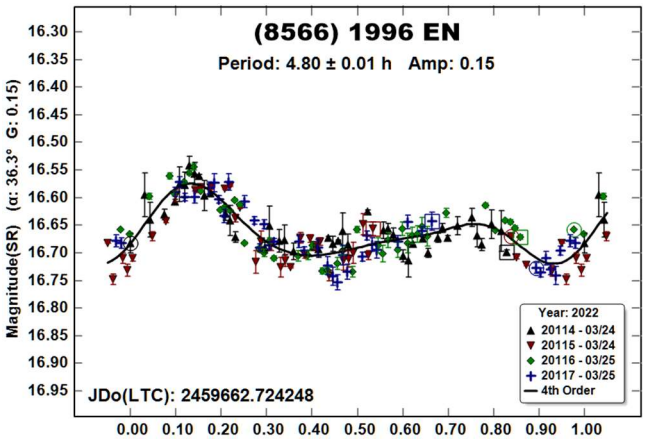

(10302) 1989 ML. Pravec et al. (2019web) found a period of 19.164 h and indications that the asteroid is tumbling. Our 2022 observations support both conclusions.

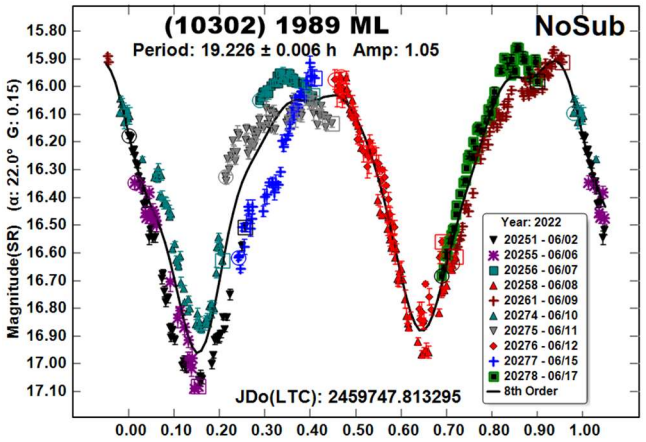

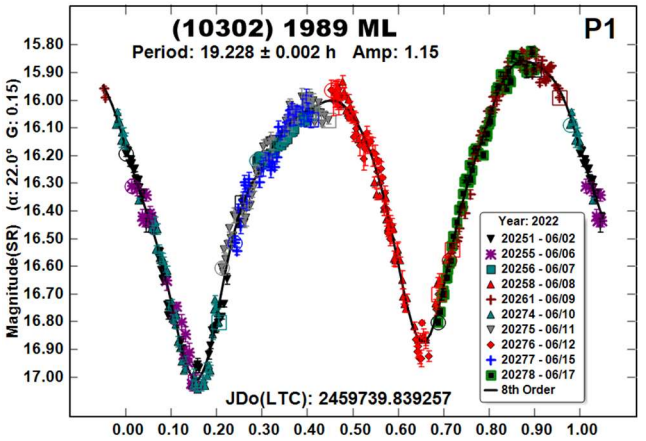

Pravec et al. (2019web) can analyze tumbling asteroids properly (Pravec et al., 2005; 2014). *MPO Canopus* cannot. Even so, we used it to extract the dominant period and two others that, when subtracted from the full data set, allowed a good fit to a bimodal lightcurve with P_1 = 19.228 h. The other periods, P_2 = 20.46 h and P_3 = 18.90 h, are unlikely to have a direct physical cause but are, instead, artifacts of holding two periods constant while searching for a third. Proper analysis would have two periods solved simultaneously.

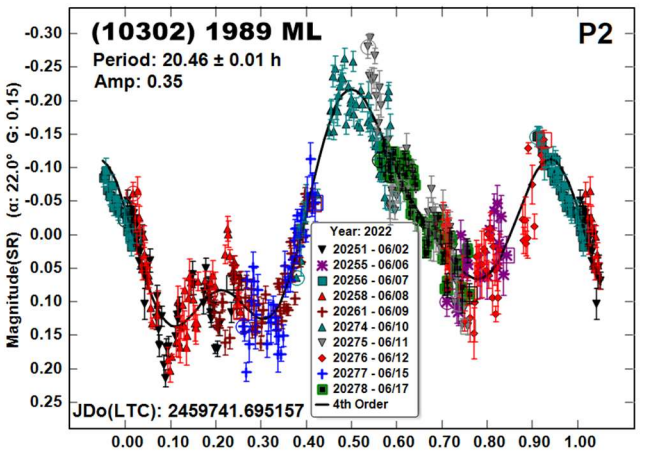

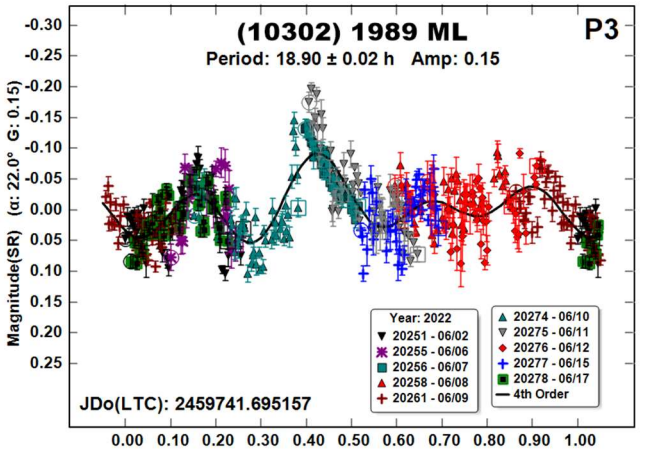

(25916) 2001 CP44. Rare within this work is found a simple lightcurve with easily determined period. This NEA was one of those rare occurrences. There are numerous entries in the LCDB with a period near 4.6 h. Our latest results are in good agreement.

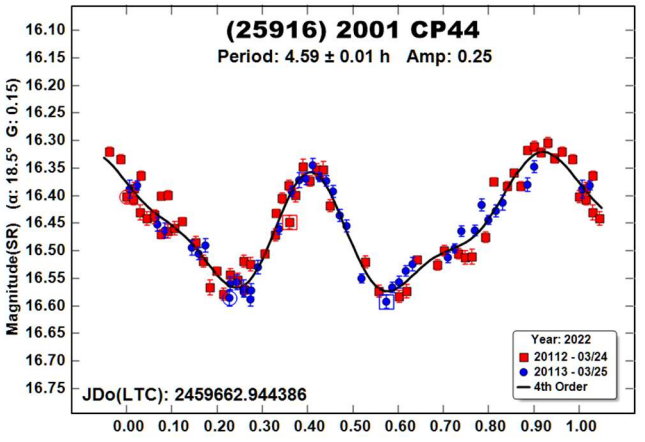

(66251) 1999 GJ2. Pravec et al. (2005web) first reported a period of 2.4621 h. Polishook (2012) found a somewhat reliable solution of 2.50 h. In 2020 (Warner and Stephens, 2020b) determined a period of 50.9 h, but this was based on a data set where the error bars were comparable to the amplitude (0.14 mag) of the lightcurve. Our result from 2022, P = 2.573 h, is in alignment with previous results, but not perfectly so since it's 0.07 to 0.11 h longer. What's more is that the doubled period (~5.14 h; bimodal lightcurve), cannot be formally excluded (Harris et al., 2014).

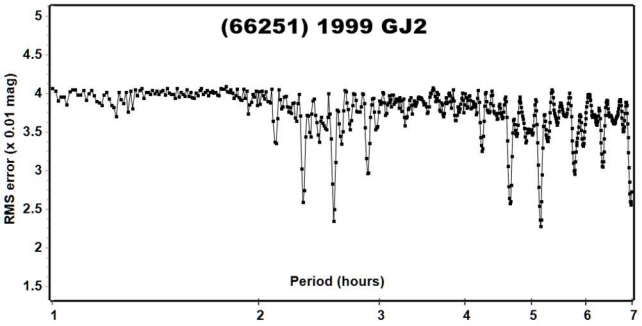

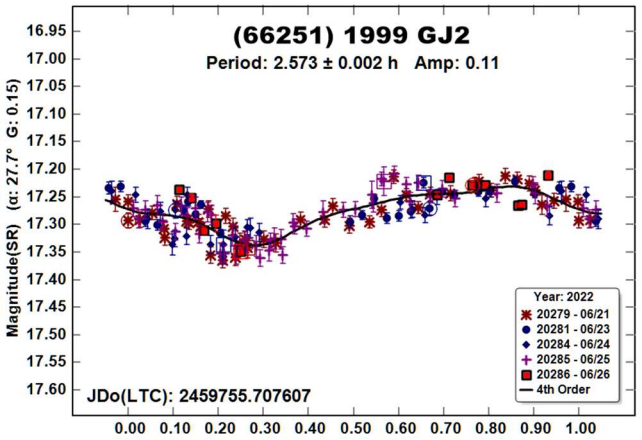

(100756) 1998 FM5. Pravec et al. (1998web) reported a period of 6.35 h based on data obtained in 1998.We observed the asteroid in 2014 (Warner, 2015a) and found a similar result of 6.369 h.

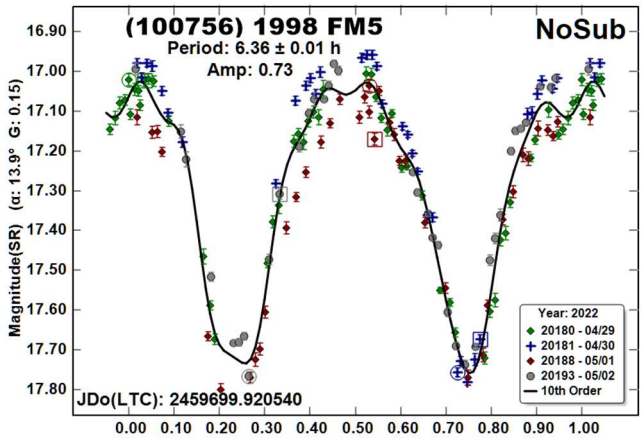

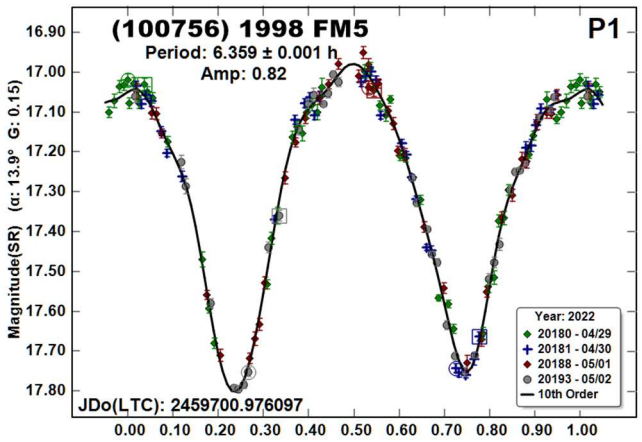

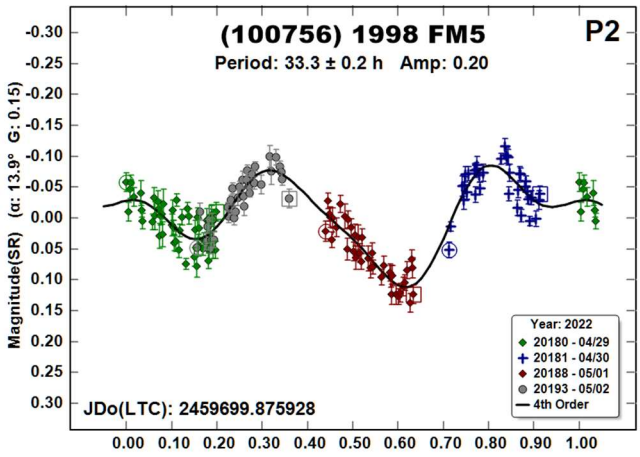

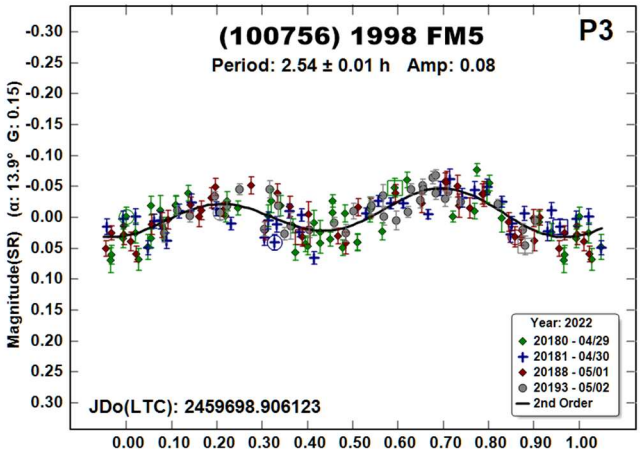

The 2022 data set led to a dominant period of about 6.36 h, but as with many others in this work, would not resolve to a single period. In the end, periods of P_2 = 33.6 h and P_3 = 2.54 h were required to get a clear dominant period of P_1 = 6.359 h. As mentioned before, these are probably the artifacts of an improperly executed dual-period search on a tumbling asteroid.

(163692) 2003 CY18. This appears to be the first reported rotation period for 2003 CY18. We were again faced with a data set that could not be properly analyzed because the asteroid appears to be tumbling. The "NoSub" plot clearly shows that a single-period solution does not work. After many trial solutions and iterations of holding two periods constant to find a third, we found a good fit to a dominant period of P_1 = 27.66 h.

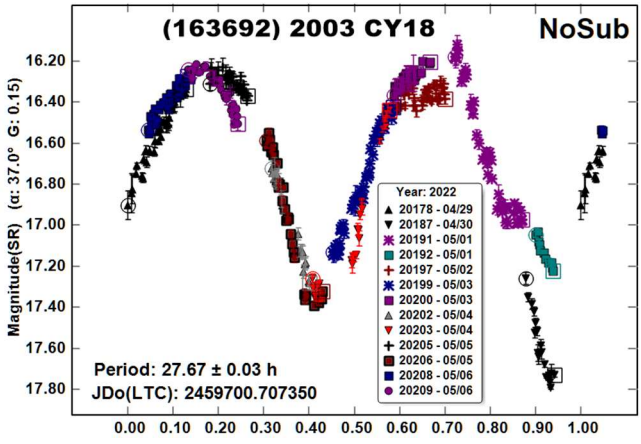

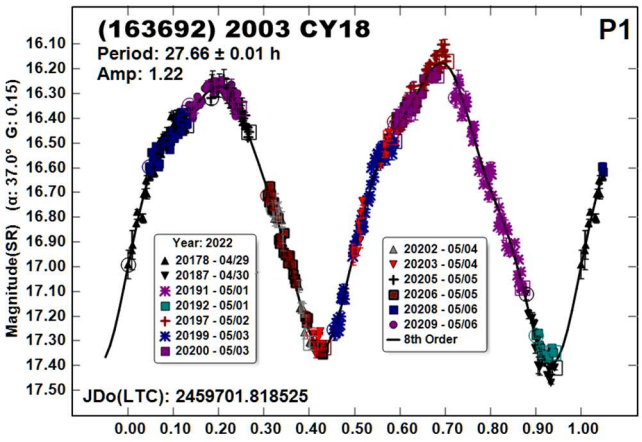

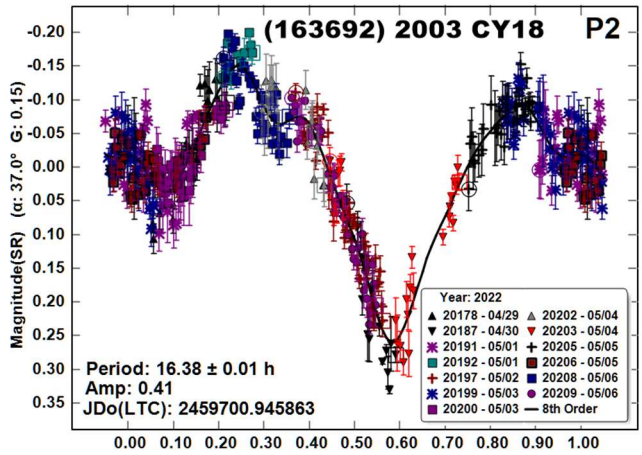

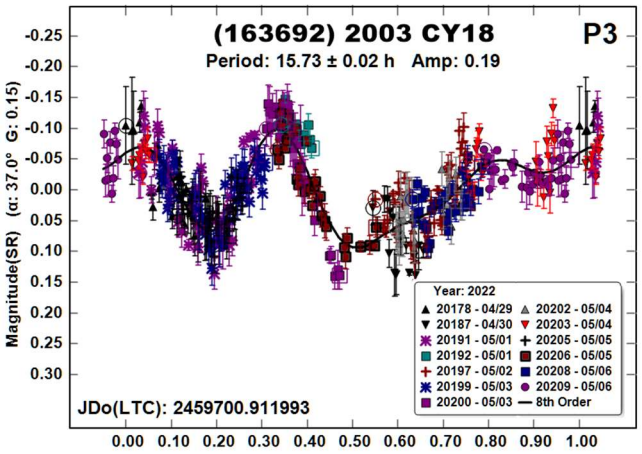

(388945) 2008 TZ3. Pravec et al. (2019web; 2020web) determined that this is a tumbling asteroid with a dominant period of 39.15 h in both cases and a second period of 34.11 h (2019) or 34.16 h (2020). It's rated -3 on the tumbling scale (Pravec et al., 2005), meaning that the solution is considered secure.

In 2016 (Warner, 2016), we suspected that the asteroid was tumbling when we found periods of 44.2 h and 52.4 h. These have no simple relation to the periods from Pravec et al. (2019web; 2020web). The results from our 2022 observations are even more divergent. The "NoSub" lightcurve shows some deviations from a single period solution, but not so much that the final result would be about half the second period found by Pravec et al. (2019web; 2020web). Our final periods, 17.04 h and 9.15 h, are the best we could find but they are far from being in agreement with earlier results.

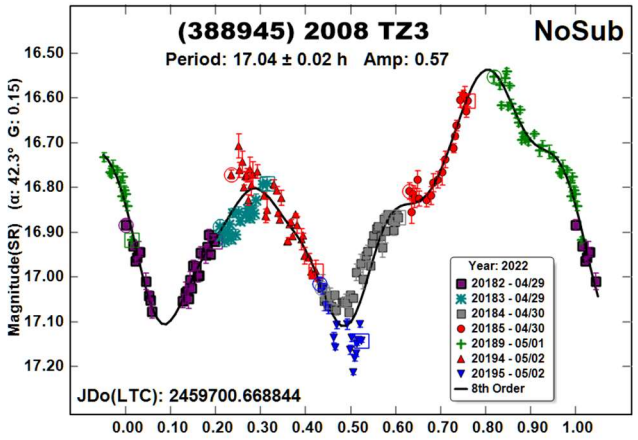

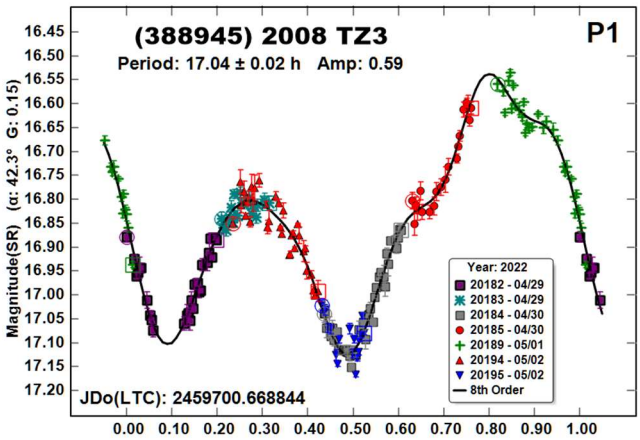

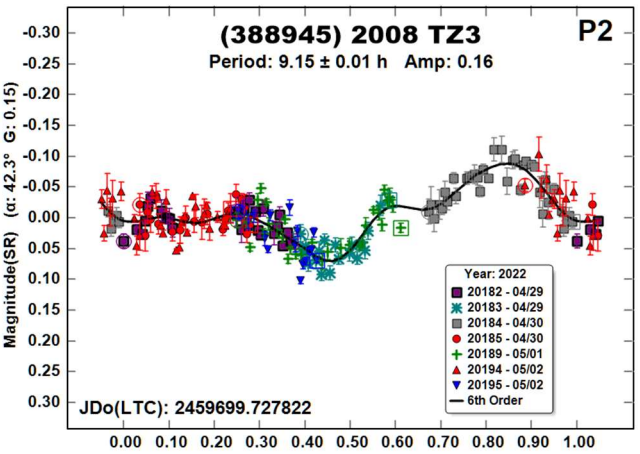

(464798) 2004 JX20. We observed this asteroid in 2016 (Warner, 2016) and found a single period of 36 ± 1 h. There was reasonable reason to believe that it was tumbling but a second period could not be found. Skiff (2019web) also had sufficient reason to suspect tumbling and reported periods of 10.758 h and 9.24 h. Then came our 2022 observations. These also indicate tumbling but with periods dissimilar to those reported before.

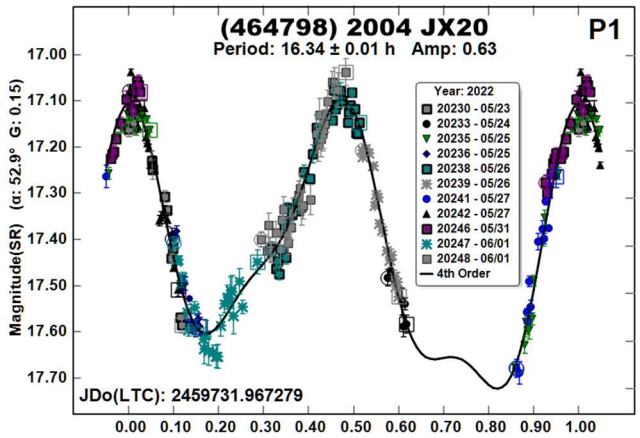

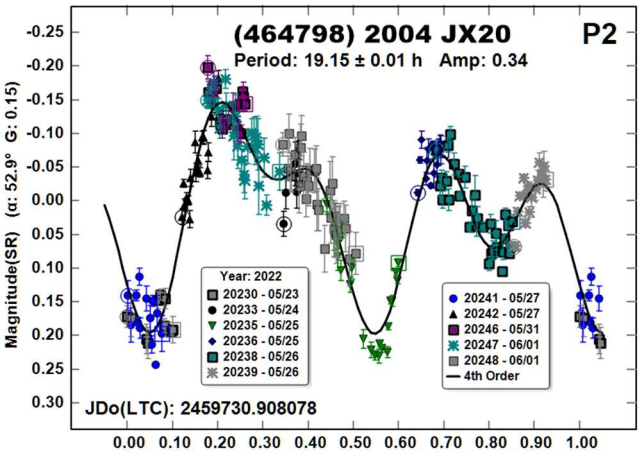

2018 XV5. There were no previously reported rotation periods for this NEA. We had a relatively sparse data set on which to do analysis, so our results have more than the usual uncertainty.

The "Single-Period" lightcurve clearly shows that trying to find one, even with more data, would probably be to no avail. As described previously, we attempted to extract one or two periods that, when subtracted from the data set, would at least give a good fit to a dominant period. We were able to do this. However, once again, the two additional periods are more likely due to the inability of *MPO Canopus* to properly handle a dual-period search on a tumbling asteroid. Regardless, it's intriguing that P_2 and P_3, are close to one another and that the P_3 lightcurve would be a welcome single-period solution under other circumstances.

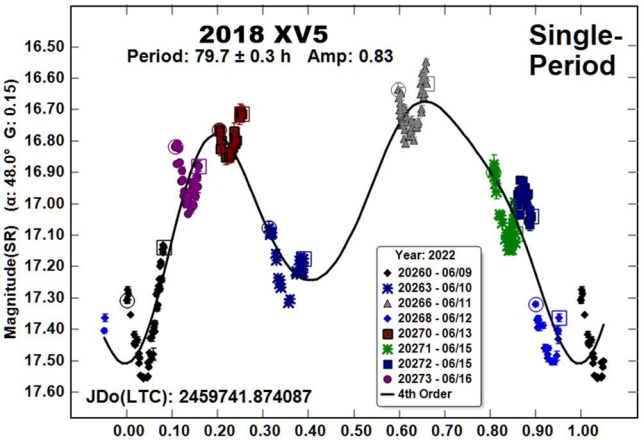

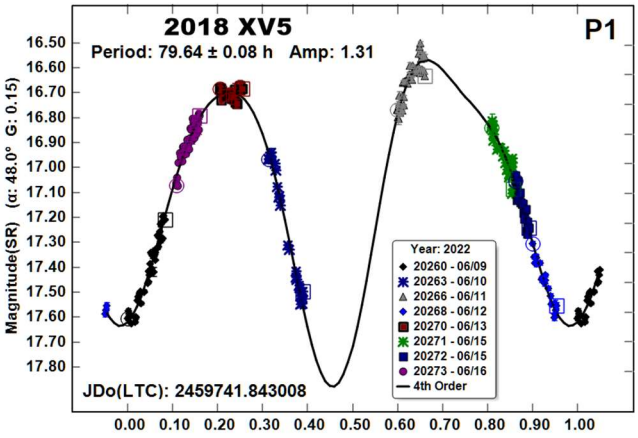

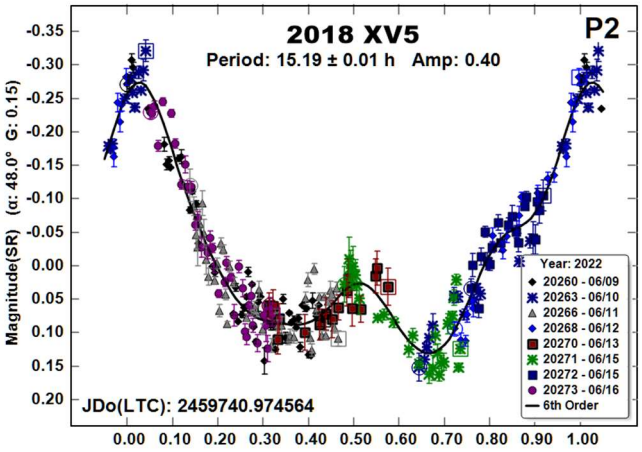

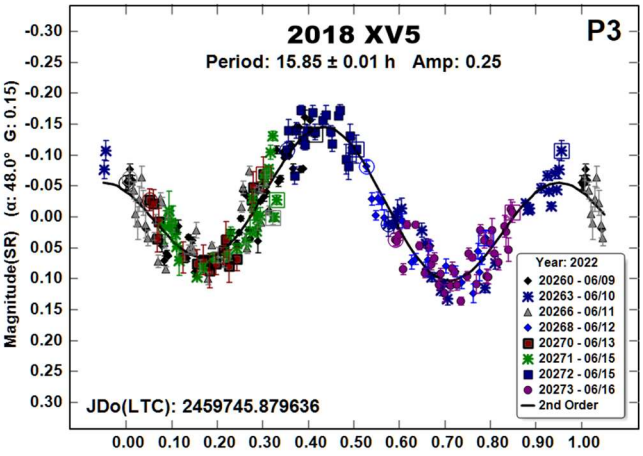

Acknowledgements

The authors gratefully acknowledge Shoemaker NEO Grants from the Planetary Society (2007, 2013). These were used to purchase some of the telescopes and CCD cameras used in this research. This work includes data from the Asteroid Terrestrial-impact Last Alert System (ATLAS) project. ATLAS is primarily funded to search for near earth asteroids through NASA grants NN12AR55G, 80NSSC18K0284, and 80NSSC18K1575; byproducts of the NEO search include images and catalogs from the survey area. The ATLAS science products have been made possible through the contributions of the University of Hawaii Institute for Astronomy, the Queen's University Belfast, the Space Telescope Science Institute, and the South African Astronomical Observatory.

This paper made use of the services provided by the SAO/NASA Astrophysics Data System, which is operated by the Smithsonian Astrophysical Observatory under NASA Cooperative Agreement 80NSSC211M0056.

References

References from web sites should be considered transitory, unless from an agency with a long lifetime expectancy. Sites run by private individuals, even if on an institutional web site, do not necessarily fall into this category.

Harris, A.W.; Young, J.W.; Scaltriti, F.; Zappala, V. (1984). "Lightcurves and phase relations of the asteroids 82 Alkmene and 444 Gyptis." *Icarus* **57**, 251-258.

Harris, A.W.; Pravec, P.; Galad, A.; Skiff, B.A.; Warner, B.D.; Vilagi, J.; Gajdos, S.; Carbognani, A.; Hornoch, K.; Kusnirak, P.; Cooney, W.R.; Gross, J.; Terrell, D.; Higgins, D.; Bowell, E.; Koehn, B.W. (2014). "On the maximum amplitude of harmonics on an asteroid lightcurve." *Icarus* **235**, 55-59.

Polishook, D. (2012). "Lightcurves and Spin Periods of Near-Earth Asteroids, The Wise Observatory." *Minor Planet Bull*. **39**, 187-192.

Pravec, P.; Sarounova, L.; Wolf, M. (1996). "Lightcurves of 7 Near-Earth Asteroids." *Icarus* **124**, 471-482.

Pravec, P.; Wolf, M.; Sarounova, L. (1998web; 2000web; 2005web; 2019web; 2020web). *http://www.asu.cas.cz/~ppravec/neo.htm*.

Pravec, P.; Harris, A.W.; Scheirich, P.; Kušnirák, P.; Šarounová, L.; Hergenrother, C.W.; Mottola, S.; Hicks, M.D.; Masi, G.; Krugly, Yu.N.; Shevchenko, V.G.; Nolan, M.C.; Howell, E.S.; Kaasalainen, M.; Galád, A.; Brown, P.; Degraff, D.R.; Lambert, J.V.; Cooney, W.R.; Foglia, S. (2005). "Tumbling asteroids." *Icarus* **173**, 108-131.

Pravec, P.; Scheirich, P.; Durech, J.; Pollock, J.; Kusnirak, P.; Hornoch, K.; Galad, A.; Vokrouhlicky, D.; Harris, A.W.; Jehin, E.; Manfroid, J.; Opitom, C.; Gillon, M.; Colas, F.; Oey, J.; Vrastil, J.; Reichart, D.; Ivarsen, K.; Haislip, J.; LaCluyze, A. (2014). "The tumbling state of (99942) Apophis." *Icarus* **233**, 48-60.

Skiff, B.A. (2019web). Posting on CALL web site: *https://minplanobs.org/MPInfo/php/call.php*

Tonry, J.L.; Denneau, L.; Flewelling, H.; Heinze, A.N.; Onken, C.A.; Smartt, S.J.; Stalder, B.; Weiland, H.J.; Wolf, C. (2018). "The ATLAS All-Sky Stellar Reference Catalog." *Ap. J.* **867**, A105.

Warner, B.D.; Harris, A.W.; Pravec, P. (2009). "The Asteroid Lightcurve Database." *Icarus* **202**, 134-146. Updated 2021 Dec. *http://www.minorplanet.info/lightcurvedatabase.html*

Warner, B.D. (2014). "Near-Earth Asteroid Lightcurve Analysis at CS3-Palmer Divide Station: 2014 January - March." *Minor Planet Bull.* **41**, 157-168.

Warner, B.D. (2015a). "Near-Earth Asteroid Lightcurve Analysis at CS3-Palmer Divide Station: 2014 October - December." *Minor Planet Bull*. **42**, 115-127.

Warner, B.D. (2015b). "Near-Earth Asteroid Lightcurve Analysis at CS3-Palmer Divide Station: 2015 March - June." *Minor Planet Bull.* **42**, 256-266.

Warner, B.D. (2016). "Near-Earth Asteroid Lightcurve Analysis at CS3-Palmer Divide Station: 2016 April - July." *Minor Planet Bull*. **43**, 311-319.

Warner, B.D. (2017). "Near-Earth Asteroid Lightcurve Analysis at CS3-Palmer Divide Station: 2016 December thru 2017 April." *Minor Planet Bull*. **44**, 223-237.

Warner, B.D.; Stephens, R.D. (2020a). "Near-Earth Asteroid Lightcurve Analysis at CS3-Palmer Divide Station: 2019 December - 2020 April." *Minor Planet Bull.* **47**, 200-213.

Warner, B.D.; Stephens, R.D. (2020b). "Near-Earth Asteroid Lightcurve Analysis at CS3-Palmer Divide Station: 2020 April - June." *Minor Planet Bull.* **47**, 290-304.

Number	Name	2022/mm/dd	Phase	L_{PAB}	B_{PAB}	Period(h)	P.E.	Amp	A.E.
4055	Magellan	03/30-04/04	9.3,12.0	177	10	7.501	0.003	0.45	0.03
6569	Ondaatje	05/19-05/22	41.0,41.3	230	39	5.96	0.01	0.89	0.03
8566	1996 EN	03/24-03/25	36.4,37.4	187	34	4.80	0.01	0.15	0.02
10302	1989 ML	06/02-06/15	22.0,24.6	250	11	T19.228	0.002	1.15	0.03
						20.46	0.01	0.35	0.04
						18.90	0.02	0.15	0.04
25916	2001 CP44	03/24-03/25	18.5,18.3	206	21	4.59	0.01	0.25	0.02
66251	1999 GJ2	06/21-06/26	27.8,30.5	267	21	2.573	0.002	0.11	0.02
100756	1998 FM5	04/29-05/02	13.8,13.0	225	15	T6.359	0.001	0.82	0.03
						33.3	0.2	0.20	0.03
						2.54	0.01	0.08	0.01
163692	2003 CY18	04/29-05/05	37.1,44.2	219	27	T27.66	0.01	1.22	0.05
						16.38	0.01	0.41	0.04
						15.73	0.02	0.19	0.03
388945	2008 TZ3	04/29-05/02	42.6,47.4	196	8	T17.04	0.02	0.59	0.03
						9.15	0.01	0.16	0.02
464798	2004 JX20	05/23-05/31	52.9,43.8	252	30	T16.34	0.01	0.63	0.03
						19.15	0.01	0.34	0.05
	2018 XV5	06/09-06/16	48.2,57.3	256	37	T79.64	0.08	1.25	0.10
						15.19	0.01	0.40	0.03
						15.85	0.01	0.25	0.03

Table II. Observing circumstances and results. The phase angle (α) is given at the start and end of each date range. L_{PAB} and B_{PAB} are the average phase angle bisector longitude and latitude (see Harris et al., 1984). If more than one line for an asteroid, the first line gives the dominant solution and has a ^{T} superscript. Subsequent lines are additional, not alternate, periods. See the text for more details.

LIGHTCURVE ANALYSIS FOR SEVEN NEAR-EARTH ASTEROIDS

Peter Birtwhistle
Great Shefford Observatory
Phlox Cottage, Wantage Road
Great Shefford, Berkshire, RG17 7DA
United Kingdom
peter@birtwhistle.org.uk

(Received: 2022 July 7)

Lightcurves and amplitudes for seven near-Earth asteroids observed from Great Shefford Observatory during close approaches between 2022 April and June are reported. Four are superfast rotators with periods P < 1 minute. The effects of lightcurve smoothing due to an inappropriately chosen exposure length are modelled for 2022 JL.

Photometric observations of near-Earth asteroids during close approaches to Earth between 2022 April and June were made at Great Shefford Observatory using a 0.40-m Schmidt-Cassegrain and Apogee Alta U47+ CCD camera. All observations were made unfiltered and with the telescope operating with a focal reducer at *f*/6. The 1K×1K, 13-micron CCD was binned 2×2 resulting in an image scale of 2.16 arc seconds/pixel. All the images were calibrated with dark and flat frames and *Astrometrica* (Raab, 2018) was used to measure photometry using APASS Johnson V band data from the UCAC4 catalogue (Zacharias et al., 2013). *MPO Canopus* (Warner, 2022), incorporating the Fourier algorithm developed by Harris (Harris et al., 1989) was used for lightcurve analysis.

No previously reported results for any of the objects reported here have been found in the Asteroid Lightcurve Database (LCDB) (Warner et al., 2009), from searches via the Astrophysics Data System (ADS, 2022), or from wider searches unless otherwise noted. All size estimates are calculated using *H* values from the Small-Body Database Lookup (JPL 2022b), using an assumed albedo for NEAs of 0.2 (LCDB readme.pdf file) and are therefore uncertain and offered for relative comparison only.

2022 GY2. With *H* = 21.7 and a Minimum Orbit Intersection Distance (MOID) from Earth of 0.0011 au = 0.4 Lunar Distances (LD), this Apollo is classified by the Minor Planet Center as a PHA, a potentially hazardous asteroid, with an estimated diameter of ~135 m. It was a mag 15 discovery from the ATLAS-HKO, Haleakala site on 2022 Apr 7 (Serrano et al., 2022) and was observed over the next three nights, fading from mag +16.2 to +18.0 during that time. Initial measurement of the 2549 usable images obtained showed variation over several hours. The images were then stacked using *Astrometrica* to produce 154 data points, with each measurement typically combining 16 images. A period spectrum from continuous observation of 5.9 h on Apr 7, 4.4 h on Apr 8 and 4.8 h on Apr 9 indicated the lightcurve is probably bimodal with a period of 9.26 h with the data points covering almost the entire lightcurve. A quadrimodal solution at 18.5 h also fits the data but with the limited coverage, is rejected in favour of the shorter period. The longest effective exposure (Δt), from start of the first to the end of the last exposure in any one stack was 10.4 minutes and so Δt /*P* = 0.019, indicating that lightcurve smoothing due to the stacking process is negligible (Pravec et al., 2000).

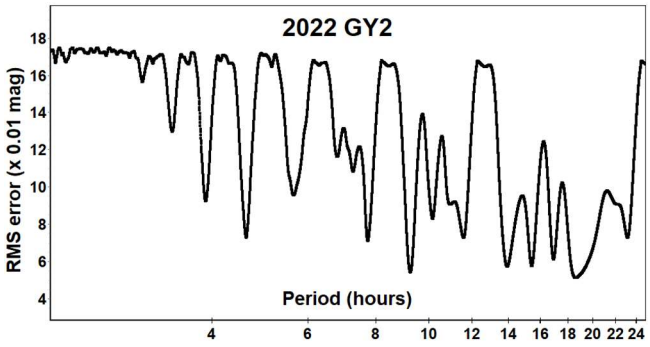

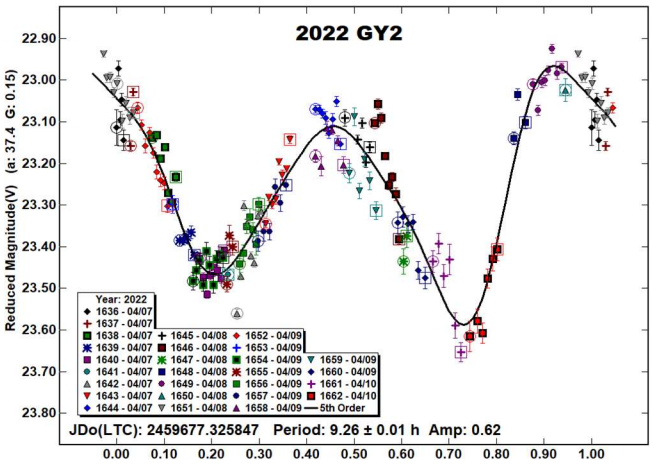

2022 HA. This Aten, with an estimated diameter of ~40 m, was discovered by the ZTF team at Palomar on 2022 Apr 18.37 UTC, just three hours before a close approach to within 7 LD of Earth (Bacci et al., 2022a). It was observed for 5.8 h starting at 2022 Apr 18.87 UTC and initial 4 s exposures did not show any significant variability between consecutive images. With the apparent motion of 50 arcsec/min, exposures were then lengthened to 10 s and 585 usable images obtained. Although relatively faint at mag +17, conditions were good and the resulting lightcurve reveals a large amplitude and rotation period of 19 minutes, meaning that 18 revolutions occurred during the observing session.

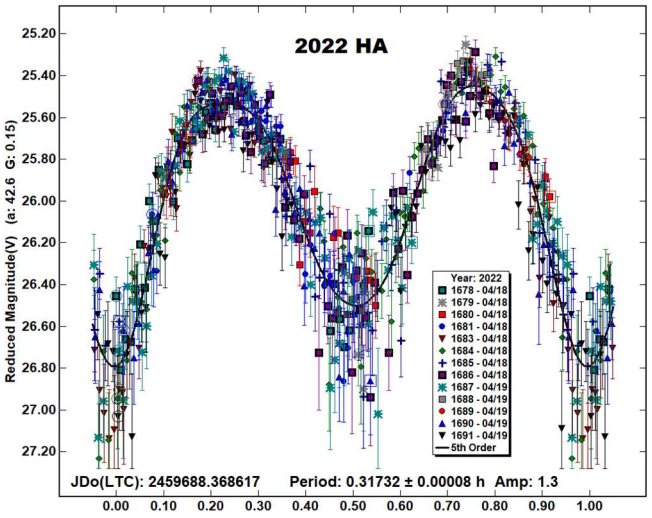

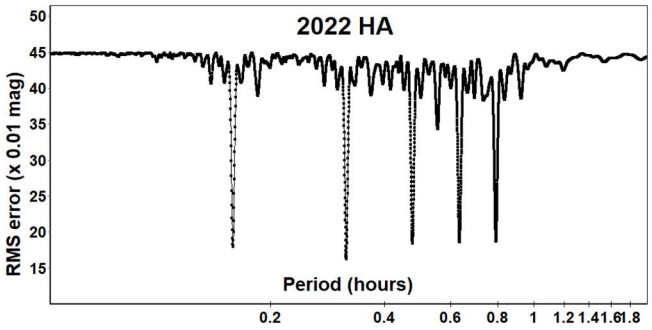

2022 HC. This was a discovery made on 2022 Apr 19.52 UTC by the 1.05-m Schmidt at the Tokyo-Kiso station, about eight hours after an approach to 3 LD of Earth (Bacci et al., 2022b). With $H = 25.1$, its estimated diameter is ~28 m. Observations were made on 2022 Apr 19.92 UTC for 78 min when its sky motion was 90 arcsec/min and again on Apr 21.05 UTC for 62 min when sky motion had decelerated to 30 arcsec/min. Although fading as it receded from Earth, the 1.2 mag decrease in brightness due to changing geometry was partially offset by the expected ~0.8 mag brightening due to the phase angle reducing from 34° to 10°. On both nights, it was relatively faint, with significant noise in the measurements, but, especially on the first date, very short-term magnitude variations were obvious. Exposures were limited to between 2-6 s on the first date and 8 s on the last. Independent period spectra from the two dates are given here, together with a solution combining data from both dates, showing that very similar periodicities are detected in the data from the two nights.

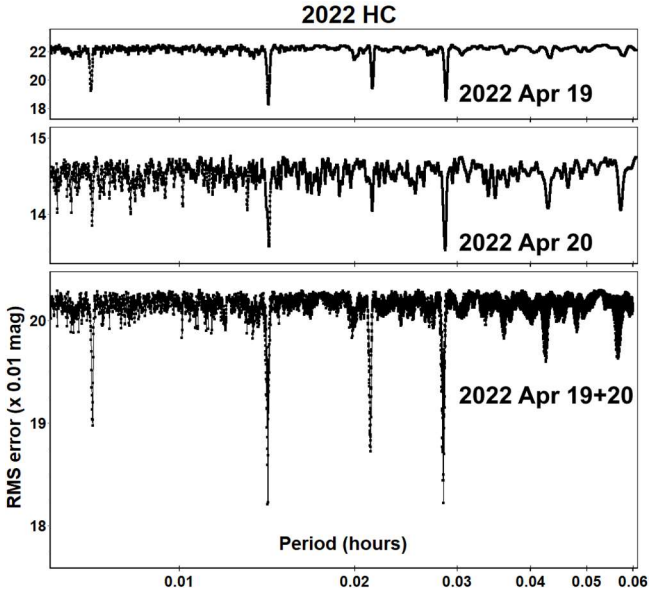

Although the lightcurves are very noisy, as expected the amplitude is seen to decrease as the phase angle reduced. The lightcurve from the combined nights indicates that the period is 51 seconds and that 91 and 72 revolutions, respectively, would have occurred during the periods of observation on the two nights.

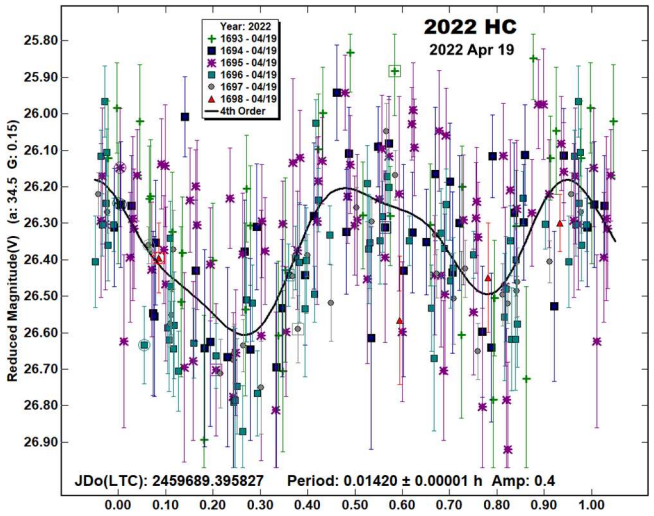

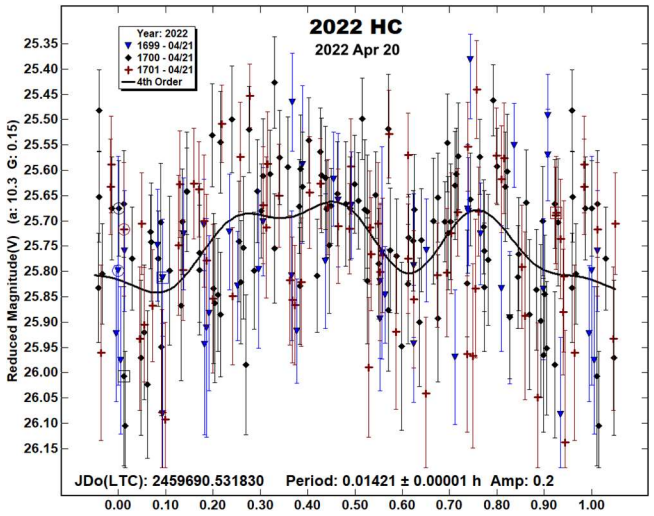

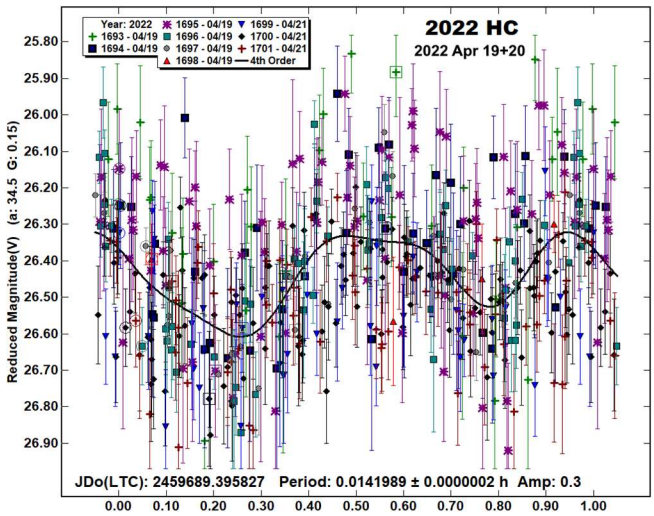

2022 JL. Another Apollo, it was discovered at mag +16 by the Catalina Sky Survey on 2022 May 3 (Melnikov et al., 2022a) just a few hours past its closest approach to 6 LD. With H = 23.36, it has an estimated size of ~63 m. Even though receding from Earth, with increasing elongation from the Sun and decreasing phase angle, its magnitude peaked about 0.5 mags brighter two days after discovery. It was observed for 7.5 minutes starting on 2022 May 4.91 UTC to measure astrometry and with motion of 35 arcsec/min, 72 usable images were obtained with 4 s exposures. Images were visually checked for any rapid change in brightness but nothing was obvious. Exposures were then increased immediately afterwards to 14.3-15 s, for an extended run of 3.3 h to gather images for photometry. When both set of images were measured it was obvious that the rotation period was actually very short. The linearly scaled period spectrum spanning 10 s to 3.6 minutes indicates the best fitting solution has a rotation period of P = 0.014 h (52 s).

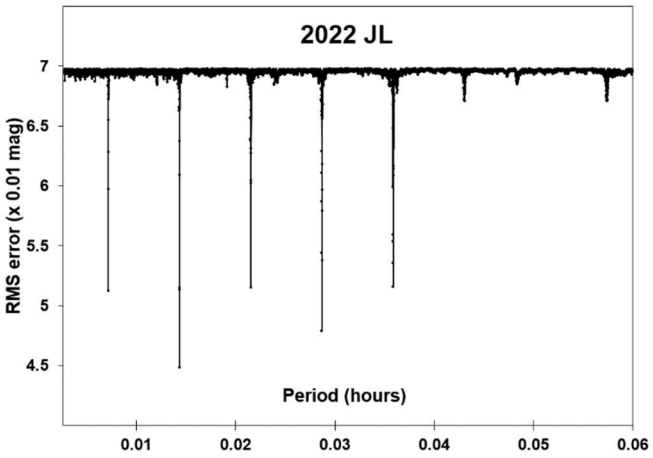

This result implies the exposure length, Δt, during the photometry run was long enough to cause significant lightcurve smoothing, where Δt/P reached 0.290. The next night provided another opportunity to observe 2022 JL and this time exposure length was set at 8 s, where Δt/P = 0.155 was chosen as a good compromise between maximising signal to noise ratio (at Δt/P = 0.185) and minimising lightcurve smoothing (Pravec et al., 2000). The resulting lightcurves, from exposure lengths of 4 s, then 14.3-15 s, both from 2022 May 4.91-5.06 UTC, and finally 8 s from 2022 May 5.95-6.01 UTC, show the effects of lightcurve smoothing on the shape of the lightcurve due to the different exposure lengths, the rotation period itself being secure in each analysis. Three independent phased reductions are given, the first, with Δt = 4 s shows a small minimum occurring at phase = 0.84 and a third maximum at phase = 0.94 in what would otherwise be a bimodal lightcurve, with amplitude 0.32.

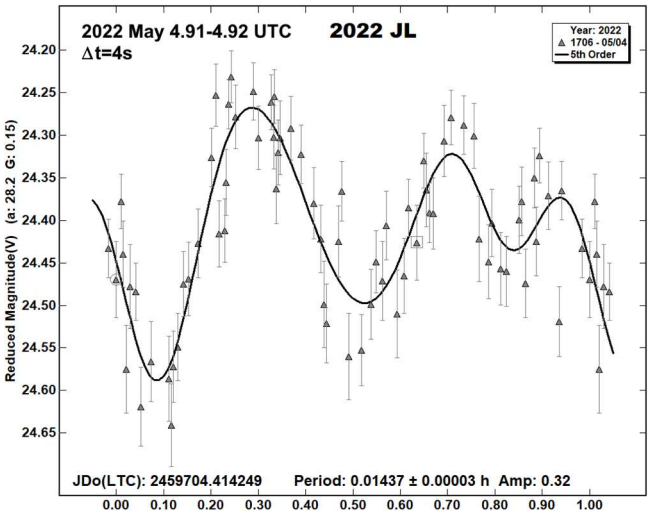

The second set of observations, with Δt = 14.3-15 s was started by chance about 8.7 minutes = 10.1 rotations later than the start of the first lightcurve, so the main features are similarly positioned in the two phased diagrams. There is no dip at the equivalent point in the second lightcurve, at phase = 0.75, indeed the Fourier curve shows a small hump in the overall descent between phase 0.64 and 0.98. The amplitude is also significantly smaller at 0.17.

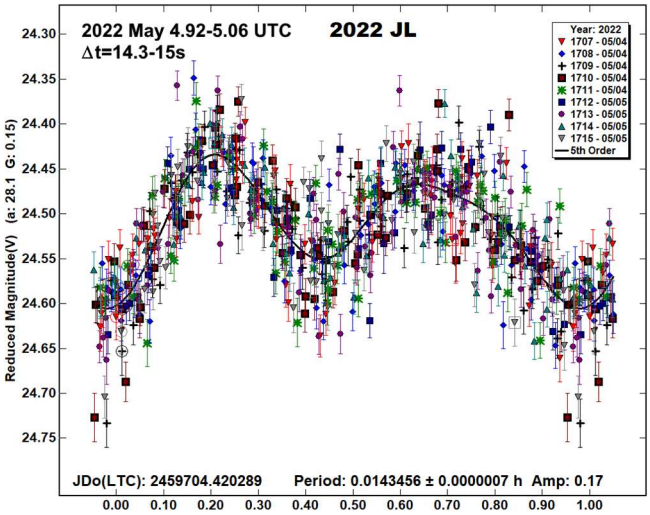

The third phased plot, centred on 2022 May 5.98 UTC, with Δt = 8 s and with a different zero point for the phased curve, does again show the small minimum, this time at phase = 0.28 and a small increase in overall amplitude from the previous lightcurve, at 0.21.

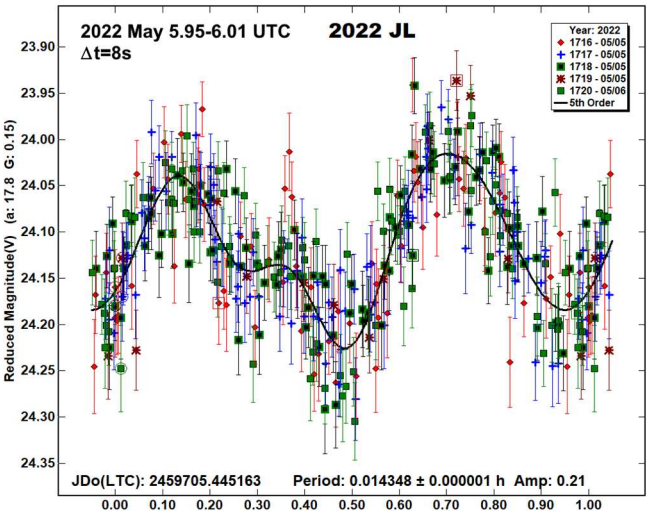

To model the effects of lightcurve smoothing, the factors $f_1 - f_5$ that would be expected to reduce the first five Fourier coefficients of the true lightcurve for the range of exposures used were calculated and are listed in Table I, together with the corresponding fraction of the rotation period.

Δt	Δt/P	f_1	f_2	f_3	f_4	f_5
4	0.077	0.99	0.96	0.91	0.85	0.77
8	0.155	0.96	0.85	0.68	0.48	0.27
14.3	0.277	0.88	0.57	0.19	-0.10	-0.21
15	0.290	0.87	0.53	0.14	-0.13	-0.22

Table I. Factors f_n reducing the strength of the first five harmonics in the lightcurve of 2022 JL for exposure length values of Δt (seconds) and rotation period of 51.64 s. (see Pravec et al., 2000).

It can be seen that the factors for Δt = 14.3 and 15 s are significant, e.g., for the normally dominant 2nd harmonic its strength will be almost halved, the 3rd harmonic reduced to less than 20% of its true strength and for the 4th and 5th harmonics, the factors are negative, indicating that their contribution to the smoothed lightcurve will be in the opposite sense of their true value.

Taking the observed Δt = 4 s curve as the least affected by smoothing, its calculated Fourier coefficients were adjusted by $1/f$ to approximate the true coefficients before smoothing. These were then reduced using the factors f_n for values of Δt = 14.3 and 15.0 s on the first night and Δt = 8 s on the second night to produce estimates of the smoothing of the Δt = 4 s curve due to the longer exposure times. The "Calculated smoothing" phased plot for May 4.99 UTC shows Fourier curves taken directly from the *MPO Canopus* reductions of the Δt = 4 s measurements (thin black line) and Δt = 14.3 – 15 s (dashed red line). Two almost coincident thicker blue lines are calculated from the Δt = 4 s curve by applying the factors for Δt = 14.3 and 15.0 s as described above, simulating how the Δt = 4 s curve would appear if the longer exposures had been used.

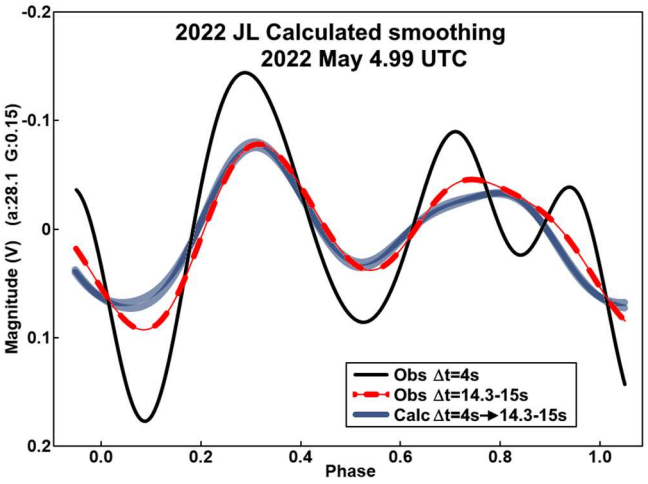

The calculated curve represents the observed lightcurve for Δt = 14.3-15 s well, including the disappearance of the small minimum at phase = 0.84 and a reduction in amplitude to 0.15. A similar phased diagram for May 5.98 UTC shows the equivalent comparison of the observed curves for Δt = 4 s (thin black line) and 8 s (dotted red line) together with a thick blue line calculated from the Δt = 4 s curve by applying the factors for Δt = 8 s.

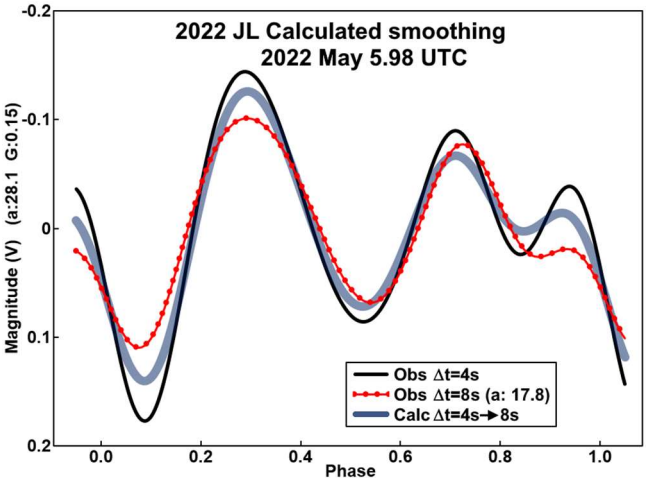

The Δt = 4 s feature at phase = 0.84 is evident in the calculated curve but reduced in scale. As expected, the calculated overall amplitude is reduced due to smoothing, to 0.27, though not as much as the observed amplitude of 0.21 for the Δt = 8 s curve. However, on that second night, 2022 JL was at phase angle a = 17.8°, and therefore the amplitude observed on that date would be expected to be somewhat smaller than the previous night, when a = 28.1°.

Using the measurements from both nights, the period is further refined, though the lightcurve shape has extra scatter due to the different degrees of lightcurve smoothing. Small zero-point adjustments with an RMS of 0.06 were applied to the 15 *MPO Canopus* sessions (for each time the telescope was repositioned), to reduce the overall scatter.

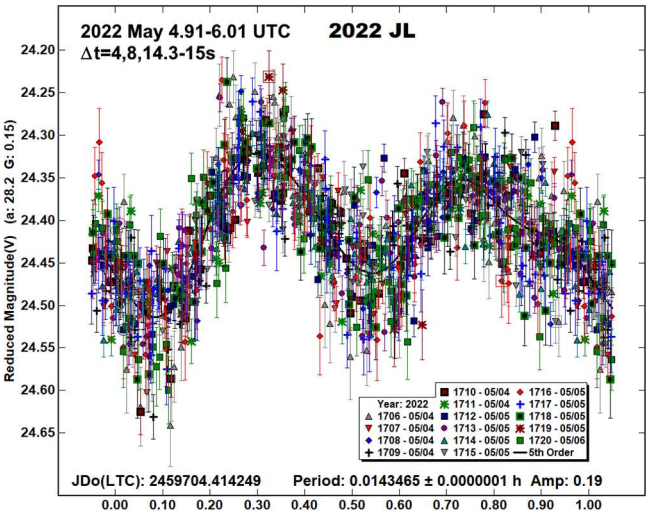

Mid-time	Δt	Pts/ Flds	Span (h)	Period(h)	P.E	Rotns	Amp
4.92	4	72/1	0.12	0.01437	0.00003	8	0.32
4.99	15	630/9	3.34	0.0143456	0.0000007	232	0.17
5.98	8	362/5	1.56	0.014348	0.000001	108	0.21

Table II. Details of periods of observation of 2022 JL, where Mid-time is the day in 2022 May (UTC), Δt is the longest exposure utilized (seconds), Pts is the number of data points used in the reduction, Flds is the number of times the telescope was repositioned to different fields, Span is the time from first to last measurement used, Rotns is the number of rotations completed during the Span and Amp is the Amplitude from the Fourier curve derived from the observations.

2022 KK5. This Apollo was another discovery made by the 1.05-m Schmidt at the Tokyo-Kiso station, first detected on 2022 May 29.56 UTC at mag +17 and less than four hours after an approach to with 3.5 LD of Earth (Melnikov et al., 2022b). Pre-discovery astrometry was reported from the Catalina Sky Survey from 2.4 days before and orbit solutions from Sentry (JPL 2022a) list 2022 KK5 as a virtual impactor with the earliest possible impact predicted for May 2043 with a probability of 1 in 7,700. It was observed from Great Shefford on 2022 May 31.96 UTC and 2022 June 1.98 UTC, on both occasions for just over one hour and on both nights large amplitude magnitude variations were apparent over a timescale of a few minutes. It had faded by about 0.5 mag on the second night as it receded from Earth but on both nights was visible on all images, where exposures ranged from 8 to 16 seconds. The period spectrum shows the best fit solution has a period of just under 5 minutes and the lightcurve indicates an amplitude of nearly 1 magnitude. About 13 rotations occurred during the first period of observation and 14 rotations during the second. Assuming a phase-relation slope parameter G = 0.15, the absolute magnitude (H) derived from the solution is 24.87 ± 0.19 which implies a diameter about 10% larger than the ~28 m diameter inferred from the value of H = 25.09 ± 0.40 given in the Small-Body Database Lookup (JPL 2022b).

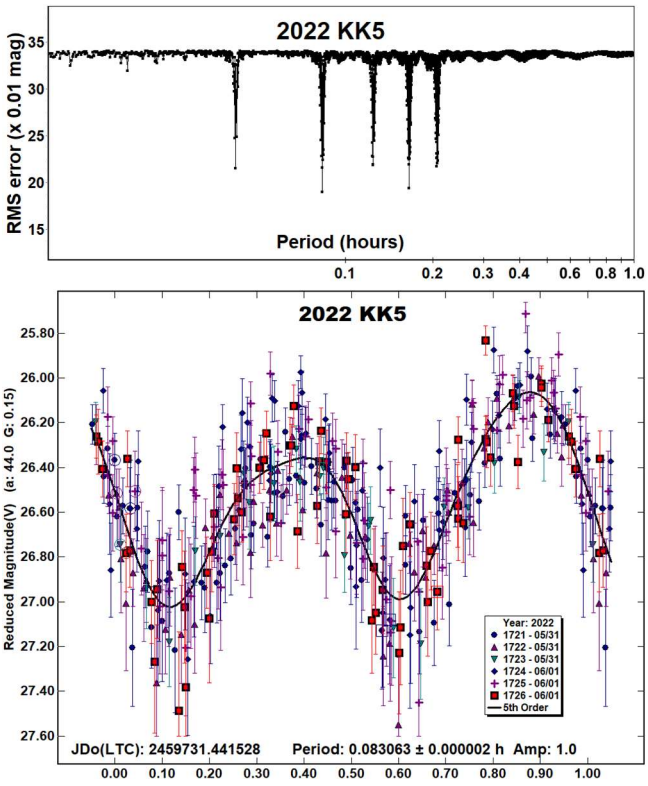

2022 MP. This Aten was discovered at mag 18 at the ATLAS Mauna Loa facility on 2022 June 21 (Bacci et al., 2022c). It was observed on 2022 June 21 and June 22 and was seen to show large magnitude variations in 10s of seconds but was too faint for reliable photometry. When 2022 MP was next observed, on 2022 June 25, it was within 0.1 mags of its peak brightness for the apparition at mag +16.

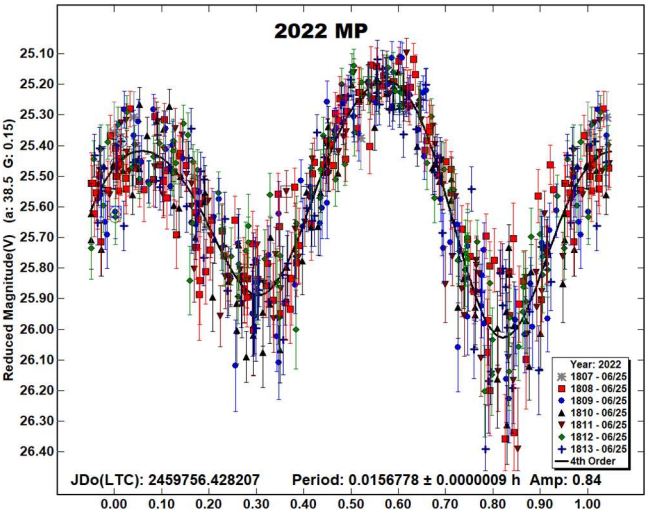

	2022 mm/ dd	Phase	L_{PAB}	B_{PAB}	Period(h)	P.E.	Amp	A.E	H
2022 GY2	04/07-04/10	37.4-28.7	181	2	9.26	0.01	0.6	0.1	21.69
2022 HA	04/18-04/19	42.5-47.5	198	20	0.31732	0.00008	1.3	0.2	24.39
2022 HC	04/19-04/21	34.3-9.9	203	9	0.0141989	0.0000002	0.3	0.3	25.10
2022 JL	05/04-05/06	28.2-17.3	223	12	0.0143465	0.0000001	0.32*	0.08*	23.38
2022 KK5	05/31-06/02	43.9-45.0	255	22	0.083063	0.000002	1.0	0.3	25.09
2022 MP	06/25-06/25	38.4-38.3	261	15	0.0156778	0.0000009	0.8	0.2	23.97
2022 MN1	06/27-06/27	71.9-73.0	248	24	0.015032	0.000009	0.8	0.3	27.30

Table III. Observing circumstances and results. The phase angle is given for the first and last date. If preceded by an asterisk, the phase angle reached an extrema during the period. LPAB and BPAB are the approximate phase angle bisector longitude/latitude at mid-date range (see Harris et al., 1984). Amplitude error (A.E.) is calculated as √2 * (lightcurve RMS residual). H is the absolute magnitude at 1 au from Sun and Earth taken from the Small-Body Database Lookup (JPL, 2022b). Note: * Values are taken from the lightcurve from 2022 May 4.91-4.92 UTC (with minimal lightcurve smoothing).

A set of 6 and 8 second exposures were obtained over a period of 1.6 h and the analysis of the 573 usable images shows a large amplitude asymmetrical bimodal lightcurve with a period of 56.4 seconds, indicating that 101 rotations occurred during image capture. About 76% of the images were from 6 s exposures, the remainder 8 s. The 6 and 8 s exposure lengths as a fraction of the period are 0.106 and 0.142, respectively, and therefore no significant smoothing of the lightcurve shape is to be expected (Pravec et al., 2000). The 6 s exposure length is likely to have caused the observed amplitude to be ~0.07 mags less than the real amplitude and the 8 s exposure length equivalently ~0.15 mags less, both reductions being smaller than the likely error in amplitude of 0.16 due to measurement uncertainty.

2022 MP was also observed by Radar from Goldstone on 2022 June 25 (Benner, 2022), where it is noted that T. Lister had reported a rotation period of 28 s (or possible 56 s) and a lightcurve amplitude of 0.5 magnitudes. These figures are in good agreement with the results determined in this paper. The Radar result includes the statement, "*If we adopt the preliminary period of 28 seconds reported by T. Lister, then the bandwidth of ~300 Hz places a lower bound on the maximum pole-on extent of 23 meters (or double that if the period is 56 seconds).*" Taking the 56 s period derived in this paper and a value of H = 23.97 ± 0.31 (JPL, 2022b), the size estimate of 46 m implies an albedo of 0.23 ± 0.06 for 2022 MP.

2022 MN1. The Pan-STARRS 2 team discovered this Apollo at mag +22 almost exactly one week before it passed Earth at 0.9 LD (Wainscoat et al., 2022). With H = 27.3, its diameter is ~10 m. It was followed during its approach on 2022 June 27 for 28 minutes, when it was mag +17, at a range of 1.3 LD, and moving at 160 arcsec/min. Exposures were limited to 3.2 s or less to keep trailing of the object within the measurement annulus of *Astrometrica*.

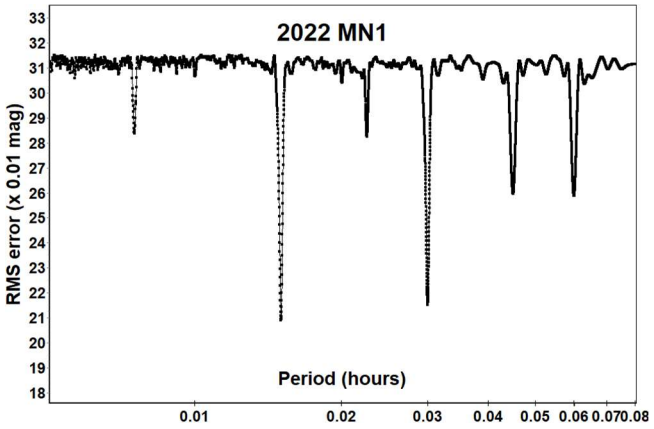

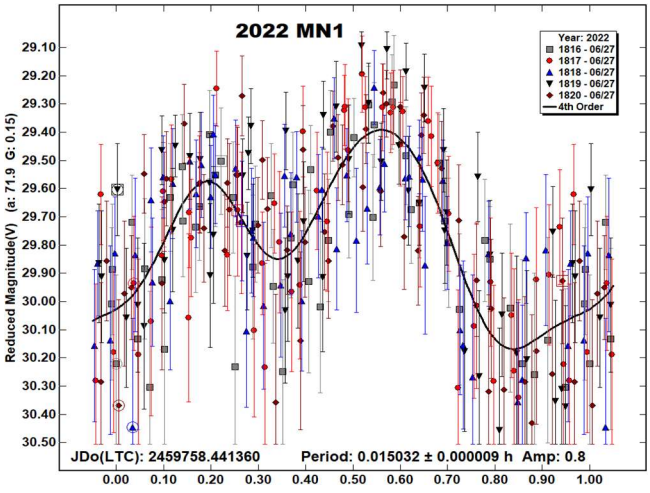

Although relatively faint, it was showing obvious variations in brightness between consecutive images taken with a cadence of 4-5 s and a period spectrum indicates the best fit to the data is a solution with a period of 54 s. The overall RMS residual of the lightcurve is 0.2 mag, contributing to another rather noisy lightcurve.

	Integration Times				
Name	Min/Max	intg/Pd	a/b	Pts	Flds
2022 GY2	621Σ	0.019	1.3	154	27
2022 HA	9.6-10.1	0.009	1.7	585	13
2022 HC	2-8	0.157	1.2	469	9
2022 JL	4-15	0.290	1.2	1064	15
2022 KK5	8-16	0.054	1.5	348	6
2022 MP	6,8	0.142	1.4	573	7
2022 MN1	3.1,3.2	0.059	1.3	264	5

Table IV. Ancillary information, listing the integration times used (seconds), the fraction of the period represented by the longest integration time (Pravec et al., 2000), the calculated minimum elongation of the asteroid (Kwiatkowski et al., 2010), the number of data points used in the analysis and the number of times the telescope was repositioned to different fields. Note: Σ = Longest elapsed integration time for stacked images (start of first to end of last exposure used).

Acknowledgements

The author gratefully acknowledges a Gene Shoemaker NEO Grant from the Planetary Society (2005) and a Ridley Grant from the British Astronomical Association (2005), both of which facilitated upgrades to observatory equipment used in this study.

References

ADS (2022). Astrophysics Data System. *https://ui.adsabs.harvard.edu/*

Bacci, P.; Maestripieri, M.; Tesi, L.; Fagioli, G.; Coffano, A.; Marinello, W.; Micheli, M.; Pizzetti, G.; Soffiantini, A.; Buzzi, L.; Ikari, Y.; Dupouy, P.; Emmerich, M.; Melchert, S.; Koch, B.; and 40 colleagues (2022a). "2022 HA." *MPEC* **2022-H08**. *https://minorplanetcenter.net/mpec/K22/K22H08.html*

Bacci, P.; Maestripieri, M.; Tesi, L.; Fagioli, G.; Buzzi, L.; Beniyama, J.; Ikari, Y.; Emmerich, M.; Melchert, S.; Koch, B.; Lindner, P.; Jahn, J.; Urbanik, M.; Birtwhistle, P.; Gerhard, C.; and 11 colleagues (2022b). "2022 HC." *MPEC* **2022-H12**. *https://minorplanetcenter.net/mpec/K22/K22H12.html*

Bacci, P.; Maestripieri, M.; Tesi, L.; Fagioli, G.; Dupouy, P.; Urbanik, M.; De Pieri, A.; Holmes, R.; Linder, T.; Horn, L.; Losse, F.; Birtwhistle, P.; Sioulas, N.; Lombardo, M.; Lombardo, K.; and 13 colleagues (2022c). "2022 MP." *MPEC* **2022-M35**. *https://minorplanetcenter.net/mpec/K22/K22M35.html*

Benner, L.A.M. (2022). "Goldstone Radar Observations Planning: (441987) 2010 NY65, 2022 LV, and 2022 MP." *https://echo.jpl.nasa.gov/asteroids/2010NY65/2010NY65.2022.goldstone.planning.html*

Harris, A.W.; Young, J.W.; Scaltriti, F.; Zappala, V. (1984). "Lightcurves and phase relations of the asteroids 82 Alkmene and 444 Gyptis." *Icarus* **57**, 251-258.

Harris, A.W.; Young, J.W.; Bowell, E.; Martin, L.J.; Millis, R.L.; Poutanen, M.; Scaltriti, F.; Zappala, V.; Schober, H.J.; Debehogne, H.; Zeigler, K. (1989). "Photoelectric Observations of Asteroids 3, 24, 60, 261, and 863." *Icarus* **77**, 171-186.

JPL (2022a). Sentry: Earth Impact Monitoring. *https://cneos.jpl.nasa.gov/sentry/*

JPL (2022b). Small-Body Database Lookup. *https://ssd.jpl.nasa.gov/tools/sbdb_lookup.html*

Kwiatkowski, T.; Buckley, D.A.H.; O'Donoghue, D.; Crause, L.; Crawford, S.; Hashimoto, Y.; Kniazev, A.; Loaring, N.; Romero Colmenero, E.; Sefako, R.; Still, M.; Vaisanen, P. (2010). "Photometric survey of the very small near-Earth asteroids with the SALT telescope - I. Lightcurves and periods for 14 objects." *Astron. Astrophys.* **509**, A94.

Melnikov, S.; Hoegner, C.; Laux, U.; Ludwig, F.; Stecklum, B.; Bacci, P.; Maestripieri, M.; Tesi, L.; Fagioli, G.; Aschi, S.; Pettarin, E.; Kowalski, R.A.; Christensen, E.J.; Fay, D.; Fazekas, J.B.; and 32 colleagues (2022a). "2022 JL." *MPEC* **2022-J30**. *https://minorplanetcenter.net/mpec/K22/K22J30.html*

Melnikov, S.; Hoegner, C.; Laux, U.; Ludwig, F.; Stecklum, B.; Beniyama, J.; Wada, S.; Pettarin, E.; Hogan, J.K.; Gray, B.; Rankin, D.; Shelly, F.C.; Dupouy, P.; Jahn, J.; Holmes, R.; and 13 colleagues (2022b). "2022 KK5." *MPEC* **2022-K158**. *https://minorplanetcenter.net/mpec/K22/K22KF8.html*

Pravec, P.; Hergenrother, C.; Whiteley, R.; Sarounova, L.; Kusnirak, P.; Wolf, M. (2000). "Fast Rotating Asteroids 1999 TY2, 1999 SF10, and 1998 WB2." *Icarus* **147**, 477-486

Raab, H. (2018). *Astrometrica* software, version 4.12.0.448. *http://www.astrometrica.at/*

Serrano, A.; Christensen, E.J.; Farneth, G.A.; Fazekas, J.B.; Fuls, D.C.; Gibbs, A.R.; Grauer, A.D.; Groeller, H.; Hogan, J.K.; Kowalski, R.A.; Larson, S.M.; Leonard, G.J.; Rankin, D.; Seaman, R.L.; Shelly, F.C.; and 42 colleagues (2022). "2022 GY2." *MPEC* **2022-G114**. *https://minorplanetcenter.net/mpec/K22/K22GB4.html*

Wainscoat, R.; Wells, L.; Burdullis, T.; Weryk, R.; Bulger, J.; Lowe, T.; Schultz, A.; Smith, I.; Chambers, K.; Dukes, T.; Chastel, S.; de Boer, T.; Fairlamb, J.; Gao, H.; Huber, M.; and 7 colleagues (2022). "2022 MN1." *MPEC* **2022-M61**. *https://minorplanetcenter.net/mpec/K22/K22M61.html*

Warner, B.D.; Harris, A.W.; Pravec, P. (2009). "The Asteroid Lightcurve Database." *Icarus* **202**, 134-146. Updated 2021 Dec. *https://minplanobs.org/mpinfo/php/lcdb.php*

Warner, B.D. (2022). MPO Software, *MPO Canopus* version 10.8.6.9. Bdw Publishing, Eaton, CO.

Zacharias, N.; Finch, C.T.; Girard, T.M.; Henden, A.; Bartlett, J.L.; Monet, D.G.; Zacharias, M.I. (2013). "The Fourth US Naval Observatory CCD Astrograph Catalog (UCAC4)." *Astron. J.*, **145**, 44-57.

LIGHTCURVE ANALYSIS OF L5 TROJAN ASTEROIDS AT THE CENTER FOR SOLAR SYSTEM STUDIES: 2022 JUNE

Robert D. Stephens
Center for Solar System Studies (CS3)
11355 Mount Johnson Ct., Rancho Cucamonga, CA 91737 USA
rstephens@foxandstephens.com

Daniel R. Coley
Center for Solar System Studies (CS3)
Corona, CA

Brian D. Warner
Center for Solar System Studies (CS3)
Eaton, CO

(Received: 2022 July 5)

Lightcurves for three Jovian Trojan asteroids were obtained at the Center for Solar System Studies (CS3) in 2022 June.

For several years, the Center for Solar System Studies (CS3, MPC U81) has been conducting a study of Jovian Trojan asteroids. This paper reports CCD photometric observations of three Trojan asteroids from the L_5 (Trojan) Lagrange point starting in 2022 June.

All observations were made using either a 0.35-m f/10 or 0.4-m f/10 Schmidt-Cassegrain telescope with an FLI Proline 1001E CCD camera. Images were unbinned with no filter and had master flats and darks applied. The exposures were 300 seconds.

Image processing, measurement, and period analysis were done using *MPO Canopus* (Bdw Publishing), which incorporates the Fourier analysis algorithm (FALC) developed by Harris (Harris et al., 1989). The Comp Star Selector feature in *MPO Canopus* was used to limit the comparison stars to near solar color. Night-to-night calibration was done using field stars from the ATLAS catalog (Tonry et al., 2018), which has Sloan *griz* magnitudes that were derived from the GAIA and Pan-STARR catalogs and are the "native" magnitudes of the catalog.

The Y-axis of lightcurves gives ATLAS SR "sky" (catalog) magnitudes. During period analysis, the magnitudes were normalized to the phase angle and value for *G* given in the parentheses. The X-axis rotational phase ranges from –0.05 to 1.05.

The amplitude indicated in the plots (e.g., Amp. 0.23) is the amplitude of the Fourier model curve and not necessarily the adopted amplitude of the lightcurve.

For brevity, only some of the previously reported rotational periods may be referenced. A complete list is available at the lightcurve database (LCDB; Warner et al., 2009).

1172 Aneas. This L_5 Trojan has been observed many times in the past (Stephens 2017, and references therein.; Pál et al. 2020; McNeill et al. 2021). Using data from the ATLAS survey, Ďurech et al. (2020) found a sideral period of 8.7024 h. The results this year are in good agreement with those prior findings.

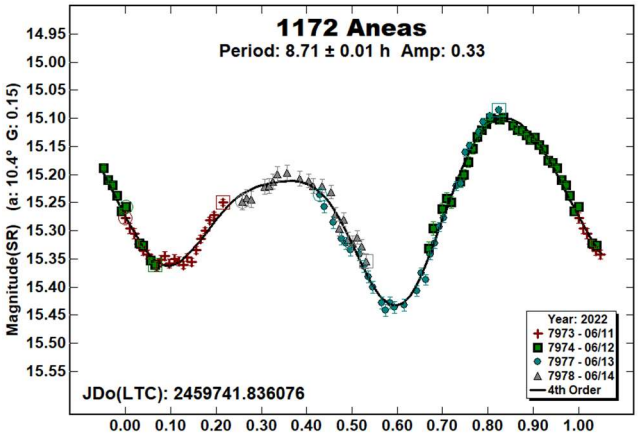

3317 Paris. This L_5 Trojan has been observed several times in the past (Mottola et al., 2011; Stephens et al., 2021, and references therein). All of these previous periods were near 7.08 h. Our result this year is in good agreement with the prior results.

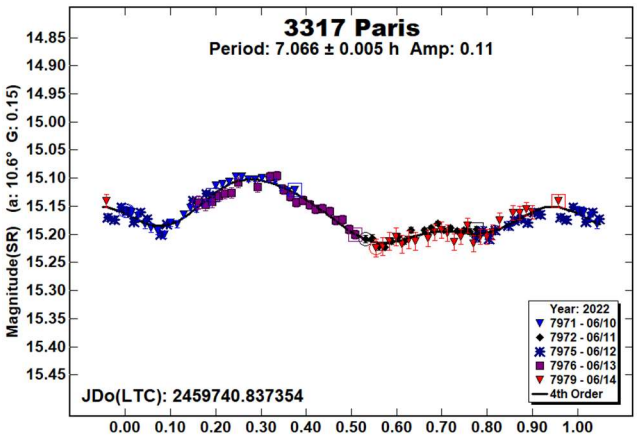

3451 Mentor. We observed Mentor several times in the past (Stephens and Warner; 2020, and references therein), each time finding a period near 7.7 h. More recently, using ATLAS data, McNeill et al. (2021) found a period of 7.697 h. Finally, using Gaia and Lowell data, Ďurech et al. (2019) found a sidereal period of 7.69659 h. Our result this year is in good agreement with those prior results.

Number	Name	2022/mm/dd	Phase	L_{PAB}	B_{PAB}	Period(h)	P.E.	Amp	A.E.
1172	Aneas	06/11-06/13	10.5,10.2	310	15	8.71	0.01	0.33	0.02
3317	Paris	06/10-06/14	10.6,10.1	309	7	7.066	0.005	0.11	0.02
3451	Mentor	06/26-07/01	10.7,10.2	329	16	7.7	0.002	0.42	0.01

Table I. Observing circumstances and results. The phase angle is given for the first and last dates. If preceded by an asterisk, the phase angle reached an extremum during the period. L_{PAB} and B_{PAB} are the approximate phase angle bisector longitude/latitude at mid-date range (see Harris et al., 1984).

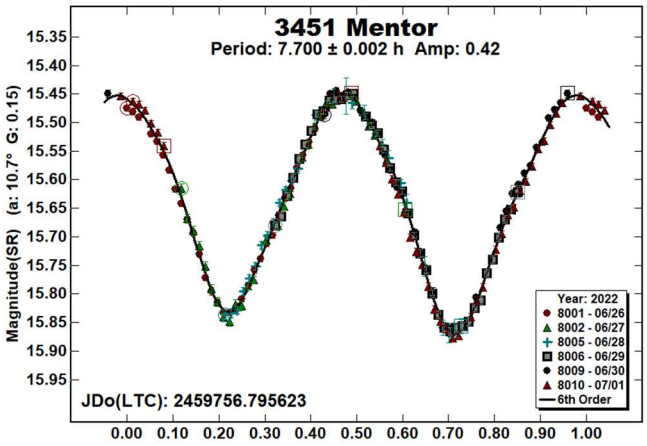

Acknowledgements

This work includes data from the Asteroid Terrestrial-impact Last Alert System (ATLAS) project. ATLAS is primarily funded to search for near earth asteroids through NASA grants NN12AR55G, 80NSSC18K0284, and 80NSSC18K1575; byproducts of the NEO search include images and catalogs from the survey area. The ATLAS science products have been made possible through the contributions of the University of Hawaii Institute for Astronomy, the Queen's University Belfast, the Space Telescope Science Institute, and the South African Astronomical Observatory.

The purchase of a FLI-1001E CCD camera was made possible by a 2013 Gene Shoemaker NEO Grant from the Planetary Society.

References

Ďurech, J.; Hanuš, J.; Vančo, R. (2019). "Inversion of asteroid photometry from Gaia DR2 and the Lowell Observatory photometric database." *Astron. Astrophys.* **631**, A2.

Ďurech, J.; Tonry, J.; Erasmus, N.; Denneau, L.; Heinze, A.N.; Flewelling, H.; Vančo, R. (2020). "Asteroid models reconstructed from ATLAS photometry." *Astron. Astrophys.* **643**, A59.

Harris, A.W.; Young, J.W.; Scaltriti, F.; Zappala, V. (1984). "Lightcurves and phase relations of the asteroids 82 Alkmene and 444 Gyptis." *Icarus* **57**, 251-258.

Harris, A.W.; Young, J.W.; Bowell, E.; Martin, L.J.; Millis, R.L.; Poutanen, M.; Scaltriti, F.; Zappala, V.; Schober, H.J.; Debehogne, H.; Zeigler, K.W. (1989). "Photoelectric Observations of Asteroids 3, 24, 60, 261, and 863." *Icarus* **77**, 171-186.

McNeill, A.; Erasmus, N.; Trilling, D.E.; Emery, J.P.; Tonry, J.L.; Denneau, L.; Flewelling, H.; Heinze, A.; Stalder, B.; Weiland, H.J. (2021). "Comparison of the Physical Properties of the L4 and L5 Trojan Asteroids from ATLAS Data." *PSJ* **2**, A6.

Mottola, S.; Di Martino, M.; Erikson, A.; Gonano-Beurer, M.; Carbognani, A.; Carsenty, U.; Hahn, G.; Schober, H.; Lahulla, F.; Delbò, M.; Lagerkvist, C. (2011). "Rotational Properties of Jupiter Trojans. I. Light Curves of 80 Objects." *Astron. J.* **141**, A170.

Pál, A.; Szakáts, R.; Kiss, C.; Bódi, A.; Bognár, Z.; Kalup, C.; Kiss, L.L.; Marton, G.; Molnár, L.; Plachy, E.; Sárneczky, K.; Szabó, G.M.; Szabó, R. (2020). "Solar System Objects Observed with TESS - First Data Release: Bright Main-belt and Trojan Asteroids from the Southern Survey." *Ap. J.* **247**, A26.

Stephens, R.D. (2017). "Lightcurve Analysis of Trojan Asteroids at the Center for Solar System Studies 2016 October - December." *Minor Planet Bull*. **44**, 123-125.

Stephens, R.D.; Warner, B.D. (2020). "Lightcurve Analysis of L5 Trojan Asteroids at the Center for Solar System Studies: 2020 April to June." *Minor Planet Bull*. **47**, 285-289.

Stephens, R.D.; Coley, D.R.; Warner, B.D. (2021). "Lightcurve Analysis of L4 and L5 Trojan Asteroids at the Center for Solar System Studies: 2021 April to June." *Minor Planet Bull*. **48**, 398-402.

Tonry, J.L.; Denneau, L.; Flewelling, H.; Heinze, A.N.; Onken, C.A.; Smartt, S.J.; Stalder, B.; Weiland, H.J.; Wolf, C. (2018). "The ATLAS All-Sky Stellar Reference Catalog." *Astrophys. J.* **867**, A105.

Warner, B.D.; Harris, A.W.; Pravec, P. (2009). "The Asteroid Lightcurve Database." *Icarus* **202**, 134-146. Updated 2021 Dec. *http://www.MinorPlanet.info/php/lcdb.php*

ROTATION PERIODS FOR ASTEROIDS FROM CARL SAGAN OBSERVATORY: 2021 NOVEMBER - 2022 MAY

P. A. Loera-González, L. Olguín, J. C. Saucedo, M.E. Contreras
Departamento de Investigación en Física, Universidad de Sonora
pabloloerag@tutanota.com

R. Nuñez-López
Departamento de Física, Matemáticas e Ingeniería,
Universidad de Sonora,
Caborca, Sonora, MEXICO

Rafael Domínguez-González
Hermosillo, Sonora, México

O. E. Angulo, S. D. Chapetti, D. E. Córdova, R. A. Cortez,
M. A. Ramírez, P. S. Vázquez
Departamento de Física, Universidad de Sonora
Hermosillo, Sonora, MEXICO

(Received: 2022 July 14 Revised: 2022 July 24)

We present photometric visible wavelength lightcurves and derive rotation periods for a sample of four asteroids:190 Ismene (6.5195 ± 0.0002 h), 5009 Sethos (2.688 ± 0.001 h), (7335) 1989 JA (2.590 ± 0.002 h) and (11512) 1991 AB2 (2.93275 ± 0.00025 h). Observations were carried out at the Observatorio Astronómico Carl Sagan (OACS) of the Universidad de Sonora in Hermosillo, México.

As part of our permanent campaign of asteroid observation at the Carl Sagan Astronomical Observatory, we obtained photometric data for three main-belt asteroids (190 Ismene, 5009 Sethos and 1991 AB2) and one Near Earth Asteroid (1989 JA). Asteroid observation provides an excellent opportunity to prepare students in observational techniques and data reduction as well as obtaining results such as lightcurves and rotation periods, and a way to fully take advantage of nearby astronomical facilities. This campaign was aimed to accomplish the above-mentioned objectives.

The equipment used at the OACS was a 512×512×20 µm SBIG ST-9 CCD camera mounted on a Meade LX- 200GPS 0.41-m *f*/10 telescope. Images yielding a final plate scale of 1.03 arcsec/pix and an effective 9×9 arcmin FOV. Data reduction was made with *IRAF* or *MaximDL* following standard procedures to correct for bias, dark current and flat-field effects. Photometry and lightcurve analysis were made using *MPO Canopus (*V.9.5.0.14*,* Warner*,* 2017) software package, which allowed us to obtain the synodic period for each object.

190 Ismene was discovered in 1878 Sep 22 by C.H.F. Peters at the Litchfield Observatory in Clinton, NY, (Schmadel, 2003). Ismene is a member of the Hilda family and has a size of 159 km, absolute magnitude H=7.71 and albedo of 0.066. We observed Ismene for 8 nights during 2021 November and December. A period of P = 6.5195 ± 0.0002 h was obtained with a lightcurve amplitude of A = 0.1 mag. These values are similar to those reported earlier by Warner et al. (2021), P=6.5198 ± 0.0003 h with A=0.15 mag; Warner and Stephens (2020), P=6.521 ± 0.0008 h. with A=0.16; Shevchenko et al. (2008), P=6.5192 ± 0.0002 h with A=0.1 mag; and Dahlgren et al. (1998), P=6.52 h. Changes in lightcurve shape and amplitude among different authors/epochs can be appreciated, presumably due to different viewing angles.

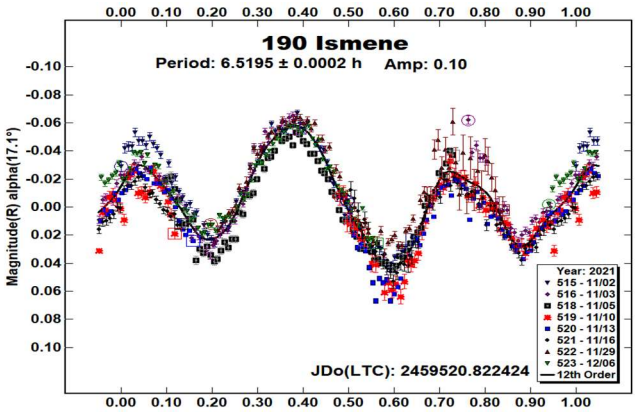

5009 Sethos. Discovered by C.J. van Houten and I. van Houten-Groeneveld at Palomar Observatory on 1960 Sep 24 (Schmadel, 2003). This Hilda asteroid has an estimated size of 4.3 km, an absolute magnitude H=14.03 and a geometric albedo of 0.455. We observed Sethos during 4 nights in 2022 May. A period of P = 2.688 ± 0.001 h was obtained with a lightcurve amplitude of A = 0.09 mag. Similar results, P = 2.6907 ± 0.0003 h with A=0.08, were obtained by Waszczak et al. (2015) from an incomplete lightcurve.

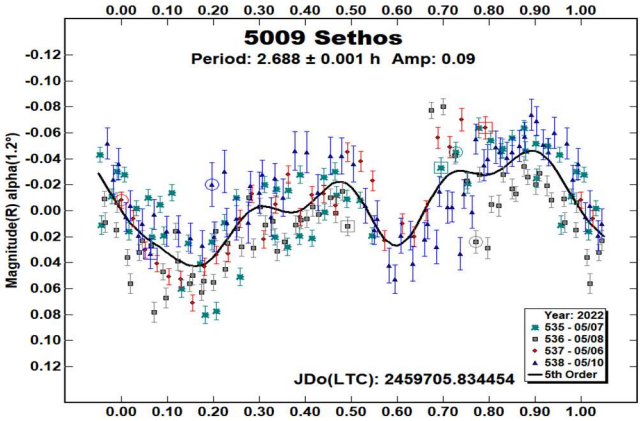

(7335) 1989 JA is an Apollo-type NEO and PHA discovered by E.F. Helin in 1989 May 1 at Palomar (Schmadel, 2003). It is 1.8 km in size, with an absolute magnitude H=17.61 and a geometric albedo of 0.448. We observed 1989 JA during late 2022 April and obtained a period of P = 2.59 ± 0.002 h and a lightcurve amplitude of A=0.11 mag. The only published result for this asteroid is given by Mahapatra et al. (2002) where an upper limit of P=12 h was obtained from radar observations. The period of 1989 JA is marked as inconclusive at the JPL Horizons Small-Body Database.

Number	Name	yyyy mm/dd	Phase	L_{PAB}	B_{PAB}	Period(h)	P.E.	Amp	A.E.	Grp
190	Ismene	2021 11/02-12/06	17.1,13.1	116.1	-6.2	6.5195	0.0002	0.10	0.05	MB-H
5009	Sethos	2022 05/07-05/10	0.9,2.7	224.7	0	2.688	0.001	0.09	0.04	MB-H
7335	1989 JA	2022 04/26-04/29	26.8	220.6	19.3	2.59	0.0002	0.11	0.05	NEO
11512	1991 AB2	2022 04/07-04/25	15.6,22.6	172.9	0.6	2.93275	0.00025	0.24	0.05	MB-I

Table I. Observing circumstances and results. The phase angle is given for the first and last date. If preceded by an asterisk, the phase angle reached an extrema during the period. L_{PAB} and B_{PAB} are the approximate phase angle bisector longitude/latitude at mid-date range (see Harris et al., 1984). Grp is the asteroid family/group (Warner et al., 2009).

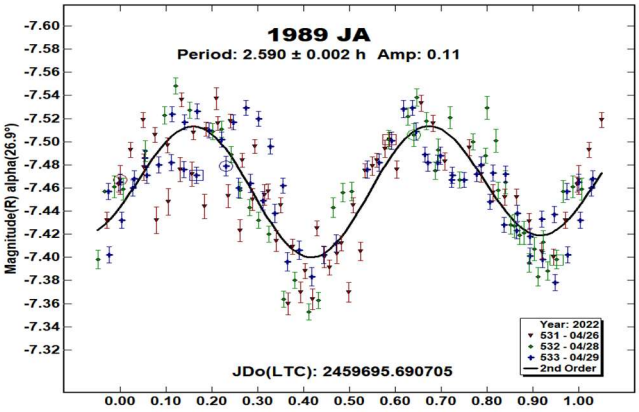

(11512) 1991 AB2 is an inner-main-belt asteroid with an estimated size of 4.3 km, an absolute magnitude H=13.89 and a geometric albedo of 0.373. We observed 1991 AB2 during three nights in 2022 April. A period of P = 2.93275 ± 0.00025 h was derived with a lightcurve amplitude A = 0.24 mag. This result is in close agreement with the reported value by Hess and Ditteon (2016) who obtained a period of P =2.933 ± 0.002h.

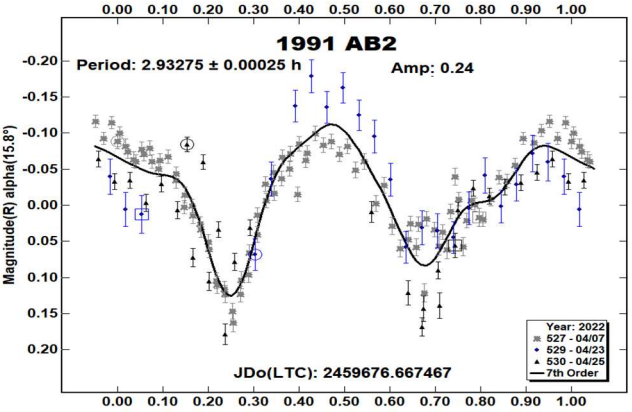

References

Dahlgren, M.; Lahulla, J.F.; Lagerkvist, C.-I.; Lagerros, J.; Mottola, S.; Erikson, A.; Gonano-Beurer, M.; Di Martino, M. (1998). "A study of Hilda asteroids. V. Lightcurves of 47 Hilda asteroids." *Icarus* **133**, 247-285.

Harris, A.W.; Young, J.W.; Scaltriti, F.; Zappala, V. (1984). "Lightcurves and phase realtions of the asteroids 82 Alkemene and 444 Gyptis." *Icarus* **57**, 251-258.

Hess, K.; Ditteon, R. (2016). "Asteroid Lightcurve Analysis at the Oakley Southern Sky Observatory: 2015 February." *Minor Planet Bulletin* ***43***. 87-87.

Mahapatra, P.R.; Benner, L.A.M.; Ostro, S.J.; Jurgens, R.F.; Giorgini, J.D.; Yeomans, D.K.; Chandler, J.F.; Shapiro I.I. (2002), "Radar Observations of asteroid 7335 (1989 JA)", *Planet. Space Sci*. **50**, 257-260.

Schmadel, L.D. (2003). *Dictionary of Minor Planet Names. (5th edition).* pp. 992. Springer, Berlin Heidelberg New York.

Shevchenko, V.G.; Chiorny, V.G.; Gaftonyuk, N.M.; Krugly, Y.N.; Belskaya, I.N.; Tereschenko, I.A.; Velichko, F.P. (2008). "Asteroid observations at low phase angles. III. Brightness behavior of dark asteroids." *Icarus* **196**, 601-611.

Small-Body Database at NASA JPL/California Institute of Technology, last time consulted in 2022 July 12. *https://ssd.jpl.nasa.gov/horizons/*

Warner, B.D.; Harris, A.W.; Pravec, P. (2009). "The Asteroid Lightcurve Database." *Icarus* **202**, 134-146. Updated 2021 Dec. *http://www.minorplanet.info/lightcurvedatabase.html*

Warner, B.D. (2017). MPO Canopus Software. *http://bdwpublishing.com*

Warner, B.D.; Stephens, R.D. (2020). "Lightcurve analysis of Hilda asteroids at the Center for Solar System Studies: 2019 November." *Minor Planet Bulletin* **47**, 123-124.

Warner, B.D.; Stephens, R.D.; Coley, D.R. (2021). "Lightcurve analysis of Hilda asteroids at the Center for Solar System Studies." *Minor Planet Bulletin* **48-3**, 303-308.

Waszczak, A.; Chang, C.-K.; Ofek, E.O.; Laher, R.; Masci, F.; Levitan, D.; Surace, J.; Cheng, Y.-C.; Ip, W.-H.; Kinoshita, D.; Helou, G.; Prince, T.A.; Kulkarni, S. (2015). "Asteroid light curves from the Palomar Transient Factory Survey: rotation periods and phase functions from sparse photometry." *Astron. J.* **150**, A75.

PHOTOMETRIC OBSERVATIONS AND ROTATION PERIODS OF ASTEROIDS 2376 MARTYNOV, (7335) 1989 JA, 12923 ZEPHYR, AND (85184) 1991 JG1

Sergei Schmalz, Anastasia Schmalz,
Viktor Voropaev, Artem Mokhnatkin
Keldysh Institute of Applied Mathematics of
Russian Academy of Sciences
Moscow, RUSSIA
sergiuspro77@gmail.com

Artyom Novichonok
Petrozavodsk State University, Petrozavodsk, RUSSIA

Alexandr Ivanov, Viktor Ivanov, Natalia Ivanova,
Anatoliy Barkov, Vadim Lysenko, Nikolay Yakovenko,
Nikita Gorbunov, German Kurbatov, Pavel Shchukin
Kuban State University, Krasnodar, RUSSIA

Inna Reva, Alexander Serebryanskiy, Chingis Omarov
Fesenkov Astrophysical Institute, Almaty, KAZAKHSTAN

Ricardo Celaya Arenas, Tatiana Kokina
Universidad Autónoma de Sinaloa, Culiacán, MEXICO

Filippo Graziani, Riccardo di Roberto
GAUSS Srl, Rome, ITALY

(Received: 2022 July 6)

Photometric observations of asteroids 2376 Martynov, (7335) 1989 JA, 12923 Zephyr, and (85184) 1991 JG1 were conducted in order to determine their synodic rotation period, the absolute brightness with its amplitude, and estimate their diameter. For 2376 Martynov we found P = 11.133 ± 0.005 h, H = 11.07 ± 0.05 mag, A = 0.38 ± 0.05 mag, D = 47.583 ± 0.529 km (for albedo a = 0.0364) and D = 39.212 ± 0.588 km (for albedo a = 0.0536). For (7335) 1989 JA we found P = 5.177 ± 0.005 h, H = 17.48 ± 0.05 mag, A = 0.27 ± 0.05 mag, D = 0.849 ± 0.009 km (for albedo a = 0.25) and D = 0.748 ± 0.010 km (for albedo a = 0.322). For 12923 Zephyr we found P = 3.894 ± 0.002 h, H = 15.73 ± 0.05 mag, A = 0.21 ± 0.05 mag, D = 2.260 ± 0.025 km (for albedo a = 0.1764) and D = 2.072 ± 0.027 km (for albedo a = 0.21). For (85184) 1991 JG1 we found P = 24.14 ± 0.02 h, H = 18.37 ± 0.07 mag, A = 0.65 ± 0.07 mag, D = 0.631 ± 0.008 km (for albedo a = 0.20).

We observed asteroids 2376 Martynov, (7335) 1989 JA, 12923 Zephyr, and (85184) 1991 JG1 in order to determine their synodic rotation period, the absolute brightness with its amplitude, and estimate their diameter. Observations took place at six observatories: Simeiz Observatory (MPC code 094) in Crimea, ISON-Kitab Observatory (MPC code 186) in Uzbekistan, Kuban State University Astrophysical Observatory (MPC code C40) in Russia, ISON-Castelgrande Observatory (MPC code L28) in Italy, Tien-Shan Astronomical Observatory (MPC code N42) in Kazakhstan, and UAS-ISON Observatory (MPC code V26) in Mexico.

For data processing we used the following software: *Tycho v.9.0.6* (Parrott, 2022) at C40; *APEX v.2021.01.4* (Kouprianov, 2008; Devyatkin et al., 2010) at L28, N42 and V26; *Astrometrica v.4.11.1.442* (Raab, 2018) and *FoCAs v.3.66* (Roig et al., 2011) at 186. All images were calibrated with dark and flat-field frames. Photometry was done in the Gaia G band against reference stars from the Gaia DR3 catalog with near-solar color indices $(G_{BP} - G_{RP})$ = 0.818 ± 10% (Gaia Collaboration, 2022). For the calculation of the absolute brightness, we used a phase slope parameter G = 0.15. For the rotation period search we used a custom-written Python script with the PDM algorithm imported from the *PyAstronomy* package (Czesla et al., 2019); the underlying orbital data was retrieved from the NASA JPL Horizons System (JPL, 2022a) by the imported *Astroquery* package (Ginsburg et al., 2019).

For the conversion from Gaia G to Johnson-Cousins V band we used the transformation:

$$G - V = -0.02704 + 0.01424 * (G_{BP} - G_{RP}) - 0.2156 * (G_{BP} - G_{RP})^2 + 0.01426 * (G_{BP} - G_{RP})^3$$

where: *G:* Gaia G magnitude; *V:* Johnson-Cousins V magnitude; and $(G_{BP} - G_{RP})$: Gaia BP-RP color index (ESA, 2022).

For the estimation of the asteroid diameter, we used the formula:

$$D = 10^{(3.1236 - 0.5 * \log(a) - 0.2 * H)}$$

where: D: asteroid diameter in km, a: geometric albedo of asteroid, and H: absolute brightness of asteroid in Johnson-Cousins V magnitudes (JPL, 2022b).

Table I shows the observing circumstances and results.

2376 Martynov was discovered on 1977 August 22 at the Crimean Astrophysical Observatory by N. S. Chernykh; it was named in honor of Dmitrij Yakovlevich Martynov, an outstanding astrophysicist, for many years the director of the Sternberg Astronomical Institute in Moscow, author of widely used texts on astrophysics (MPC, 1983). It is a main belt asteroid with a semi-major axis of a = 3.20 au, eccentricity e = 0.119, inclination i = 3.84°, and an orbital period P = 5.73 years; its absolute magnitude has a value of H = 11.03 (MPC, 2022a), other reported values range from H = 10.47 (Colazo et al., 2021) to H = 11.13 (Masiero et al., 2020). A search of the Asteroid Lightcurve Database (Warner et al., 2009) did not find any reported rotation period for asteroid 2376 Martynov.

CCD photometric observations of the asteroid were carried out on five nights in 2021 March 6 to March 23 at three observatories: 094, 186, and L28. At 094 we used a 1-m *f*/12.7 Cassegrain telescope with a FLI ML-09000 CCD camera without filters at 3×3 binning and 0.58 arcsec/pix pixel scale with 60 s exposure times during the nights 2021 March 6 and 9; at 186 we used a 0.36-m *f*/8 Ritchey-Chrétien telescope with a FLI PL 09000 CCD camera without filters at 2×2 binning and 1.72 arcsec/pix pixel scale with 60 s exposure times during the nights 2021 March 8, 11 and 23; and at L28 we used a 0.22-m *f*/2.38 Newton-Hamilton telescope with a FLI PL-16803 CCD camera without filters at 1×1 binning and 3.54 arcsec/pix pixel scale with 120 s exposure times during the night 2021 March 15. In the course of the entire observation campaign, the phase angle of 2376 Martynov changed from 7.8° to 2.8°. For the analysis we collected 381 usable data points.

Number	Name	20yy/mm/dd	Phase	L_{PAB}	B_{PAB}	Period(h)	P.E.	Amp	A.E.	D	Grp
2376	Martynov	21/03/07-21/03/23	7.8,2.8	191	3	11.133	0.005	0.38	0.05	47.583 39.212	MBA
7335	1989 JA	22/05/14-22/05/24	26.9,35.1	227	11	5.177	0.005	0.27	0.05	0.849 0.748	NEA
12923	Zephyr	21/05/10-21/06/20	17.2,51.0	215	9	3.894	0.002	0.21	0.05	2.260 2.072	NEA
85184	1991 JG1	20/05/12-20/05/23	20.5,40.0	229	19	24.14	0.02	0.65	0.07	0.631	NEA

Table I. Observing circumstances and results. The phase angle is given for the first and last exposure time. L_{PAB} and B_{PAB} are the approximate phase angle bisector longitude/latitude at mid-date range (see Harris et al., 1984). Grp is the asteroid family/group (Warner et al., 2009).

We found a synodic rotation period P = 11.133 ± 0.005 h, median absolute brightness H = 10.83 ± 0.05 mag in Johnson-Cousins V band, and brightness amplitude of the folded lightcurve A = 0.38 ± 0.05 mag. For the smallest reported albedo, a = 0.0364 (Mainzer et al., 2011), we estimated the diameter to be D = 47.583 ± 0.529 km; for the largest reported albedo, a = 0.0536 (Tedesco et al., 2004), we estimated the diameter as D = 39.212 ± 0.588 km. The first figure shows the folded lightcurve. The second plot shows the PDM power spectrum in a rotation period range between 2 and 12 hours with a red dashed line indicating the best probable rotation period at 5.566 h, which produced a monomodal folded lightcurve, though; the second-best probable rotation period at 11.133 h is the one which we consider the real rotation period.

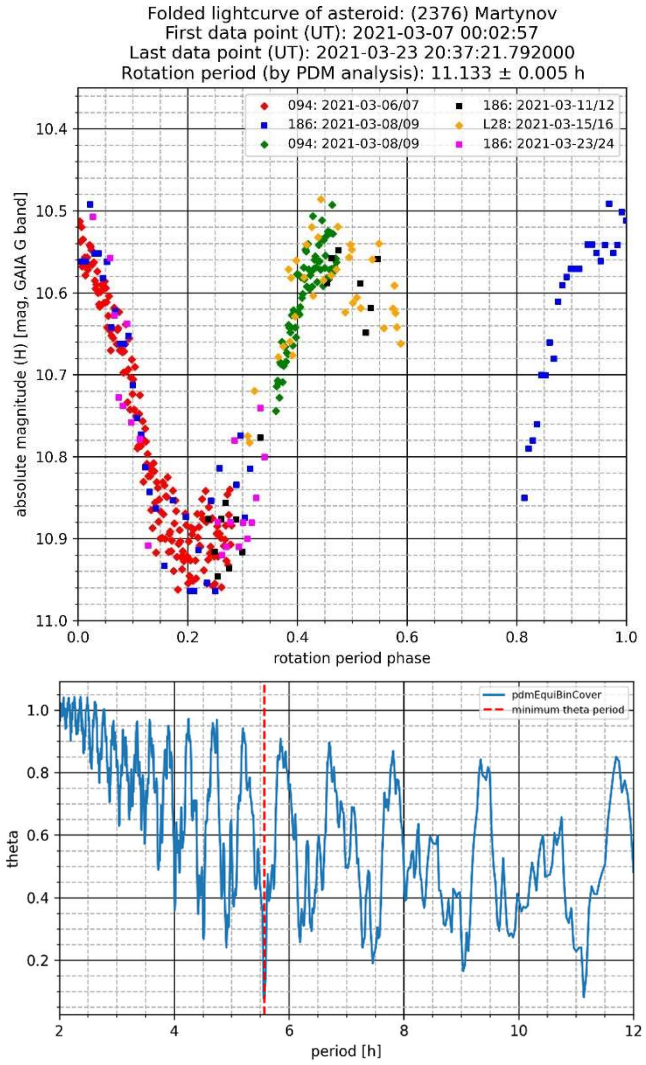

(7335) 1989 JA was discovered on 1989 May 1 at the Palomar Observatory by E.F. Helin (MPC, 1989). It is a potentially hazardous asteroid of the Apollo family with a semi-major axis of a = 1.77 au, eccentricity e = 0.484, inclination i = 15.19°, and orbital period of P = 2.36 years; its absolute magnitude has a value of H = 17.76 (MPC, 2022b), other reported values are: H = 17.8 (Wisniewski et al., 1997), H = 17.0 (Mainzer et al., 2011; 2019), and H = 17.82 (Nugent et al., 2016). A search of the Asteroid Lightcurve Database (Warner et al., 2009) did not find any precise rotation period reported for asteroid (7335) 1989 JA; there is only one report of a rotation period "less than half a day" based on radar observations (Mahapatra et al., 2002).

CCD photometric observations were carried out on nine nights in 2022 May 14 to May 24 at three observatories: 186, C40, and L28. At 186 we used a 0.36-m *f*/8 Ritchey-Chrétien telescope with a FLI PL-09000 CCD camera without filters at 2×2 binning and 1.72 arcsec/pix pixel scale with 20 s exposure times during the night 2022 May 23; at C40 we used a 0.51-m *f*/7.93 Ritchey-Chrétien telescope with a FLI PL-16803 CCD camera without filters at 1×1 binning and 1.22 arcsec/pix pixel scale with 10 s exposure times during the nights 2022 May 14-16 and 19-21, and a 0.2-m *f*/2.0 Schmidt telescope with a FLI ML-8300 CCD camera without filters at 1×1 binning and 2.83 arcsec/pix pixel scale with 10 s exposure times during the night 2022 May 24; and at L28 we used a 0.22-m *f*/2.38 Newton-Hamilton telescope with a FLI PL-16803 CCD camera without filters at 1×1 binning and 3.54 arcsec/pix pixel scale with 10 and 20 s exposure times during the nights 2022 May 21-24. In the course of the entire observation campaign the phase angle of (7335) 1989 JA changed from 26.9° to 35.1°. For the analysis we collected 3493 usable data points.

We found a synodic rotation period P = 5.177 ± 0.005 h, median absolute brightness H = 17.48 ± 0.05 mag in Johnson-Cousins V band, and brightness amplitude of the folded lightcurve A = 0.27 ± 0.05 mag. For the smallest reported albedo, a = 0.25 (Nugent et al., 2016), we estimated a diameter D = 0.849 ± 0.009 km; for the largest reported albedo, a = 0.322 (Mainzer et al., 2011; 2019), we estimated a diameter D = 0.748 ± 0.010 km. The PDM power spectrum covers a rotation period range between 2 and 12 hours with a red dashed line indicating the best probable rotation period corresponding to the one we found; the second-best probable rotation period at 2.589 h didn't produce a well-fitted folded lightcurve, so we could exclude this solution.

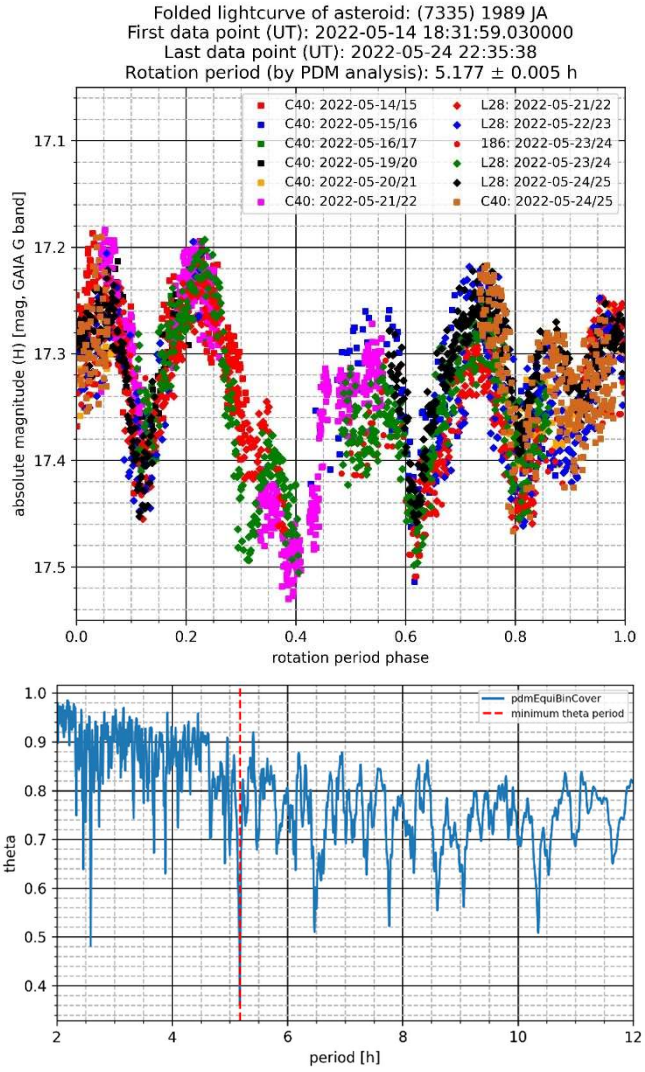

12923 Zephyr was discovered at the Anderson Mesa Station on 1994 November 11 by LONEOS; its name was suggested by M. Smitherman. The word "zephyr" derives from the name of the ancient Greek god of the west wind, Zephyros (MPC, 2004). It is a potentially hazardous asteroid of the Apollo family with a semi-major axis a = 1.96 au, eccentricity e = 0.492, inclination i = 5.31°, and orbital period P = 2.75 years; its absolute brightness has a value of H = 15.82 (MPC, 2022c). Other reported values range from H = 15.21 (Mahlke et al., 2021) to H = 15.93 (Pravec et al., 2012). In the Asteroid Lightcurve Database (Warner et al., 2009) we found two reported rotation periods for asteroid 12923 Zephyr: 3.891 h (Pravec et al., 1999web) and 3.893 ± 0.002 h (Warner et al., 2021).

CCD photometric observations of asteroid 12923 Zephyr were carried out on 22 nights in 2021 May 10 to June 20 at three observatories: 186, C40 and N42. At 186 we used a 0.36-m *f*/8 Ritchey-Chrétien telescope with a FLI PL-09000 CCD camera without filters at 2×2 binning and 1.72 arcsec/pix pixel scale with 60 s exposure times during the nights 2021 May 10, 11, 13, 14 and June 5, 6; at C40 we used a 0.51-m *f*/7.93 Ritchey-Chrétien telescope with a FLI PL-16803 CCD camera without filters at 3×3 binning and 1.37 arcsec/pix pixel scale with 40 s exposure times during the nights 2021 May 30 and June 5-18, 20; and at N42 we used a 1-m *f*/6.6 Cassegrain telescope with an Apogee Alta U16M D9 CCD camera without filters at 2×2 binning and 0.56 arcsec/pix pixel scale with 60 s exposure times during the night 2021 May 29. In the course of the entire observation campaign, the phase angle of 12923 Zephyr changed from 17.2° to 51.0°. For the analysis we collected 409 usable data points.

We found a synodic rotation period P = 3.894 ± 0.002 h, median absolute brightness H = 15.73 ± 0.05 mag in Johnson-Cousins V band, and brightness amplitude of the folded lightcurve A = 0.21 ± 0.05 mag. For the smallest reported albedo, a = 0.1764 (Pravec et al., 2012), we estimated a diameter D = 2.260 ± 0.025 km; for the largest reported albedo, a = 0.21 (Harris et al., 2011), we estimated a diameter D = 2.072 ± 0.027 km. The PDM power spectrum covers a rotation period range between 2 and 12 hours with a red dashed line indicating the best probable rotation period corresponding to the one we found.

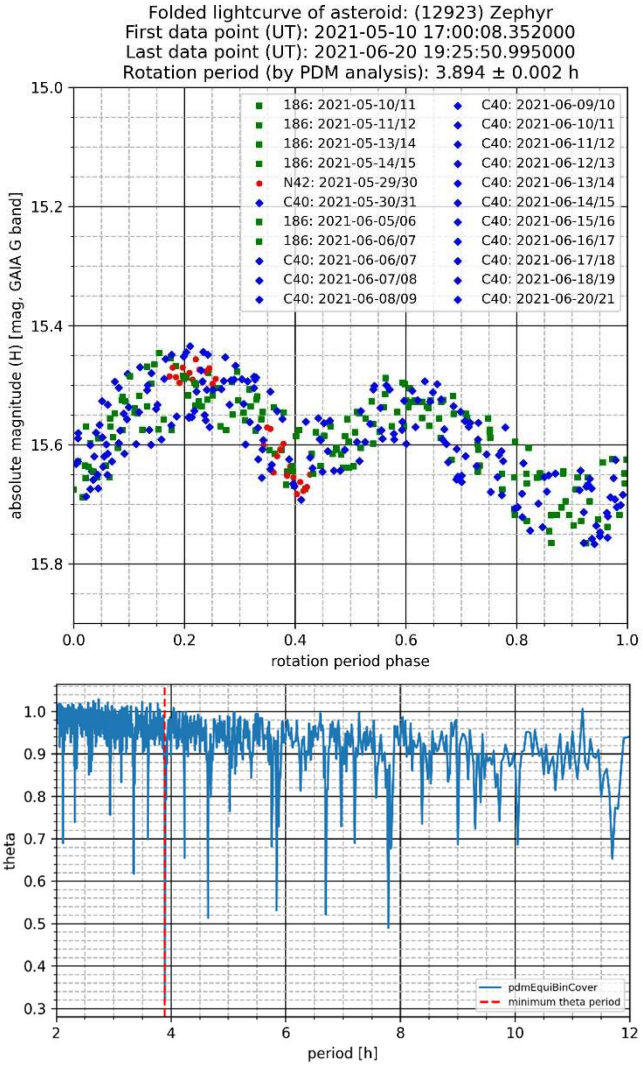

(85184) 1991 JG1 was discovered on 1991 May 9 at the Palomar Observatory by E.F. Helin (MPC, 1991). It is a near-Earth asteroid of the Amor family with a semi-major axis a = 1.37 au, eccentricity e = 0.185, inclination i = 33.88°, and orbital period P = 1.61 years; its absolute magnitude is H = 18.42 (MPC, 2022d). (Pravec et al., 1999web) reported H = 18.14. In the Asteroid Lightcurve Database (Warner et al., 2009) we found a reported rotation period of 24.02 ± 0.05 h (Pravec et al., 1999web), and a series of four different solutions: 22.56 ± 0.05 h, 25.08 ± 0.04 h, 23.63 ± 0.03 h, and 24.19 ± 0.02 h (Warner and Stephens, 2020).

CCD photometric observations of asteroid (85184) 1991 JG1 were carried out on eight nights in 2020 May 12 to May 23 at four observatories: 186, C40, N42 and V26. At 186 we used a 0.36-m *f*/8 Ritchey-Chrétien telescope with a FLI ML-09000 CCD camera without filters at 2×2 binning and 1.72 arcsec/pix pixel scale with 60 s exposure times during the nights 2020 May 12, 14, 16, 17 and 22; at C40 we used a 0.51-m *f*/7.93 Ritchey-Chrétien telescope with a FLI PL-16803 CCD camera without filters at 3×3 binning and 1.37 arcsec/pix pixel scale with 20 s exposure times during the nights 2020 May 13 and 15; at N42 we used a 1-m *f*/6.6 Cassegrain telescope with an Apogee Alta U16M D9 CCD camera without filters at 2×2 binning and 0.56 arcsec/pix pixel scale with 60 s exposure times during the night 2020 May 23; and at V26 we used a 0.40-m *f*/4.2 Ritchey-Chrétien telescope with a FLI PL-09000 CCD camera without filters at 2×2 binning and 2.87 arcsec/pix pixel scale with 60 s exposure times during the nights 2020 May 14, 15 and 23. In the course of the entire observation campaign, the phase angle of (85184) 1991 JG1 changed from 20.5° to 40.0°. For the analysis we collected 1194 usable data points.

We found a synodic rotation period P = 24.14 ± 0.02 h, median absolute brightness H = 18.37 ± 0.07 mag in Johnson-Cousins V band, and brightness amplitude of the folded lightcurve A = 0.65 ± 0.07 mag. For a theoretical albedo a = 0.20, we estimated a diameter D = 0.631 ± 0.008 km. The PDM power spectrum covers a rotation period range between 2 and 36 hours with a red dashed line indicating the best probable rotation period corresponding to the one we found.

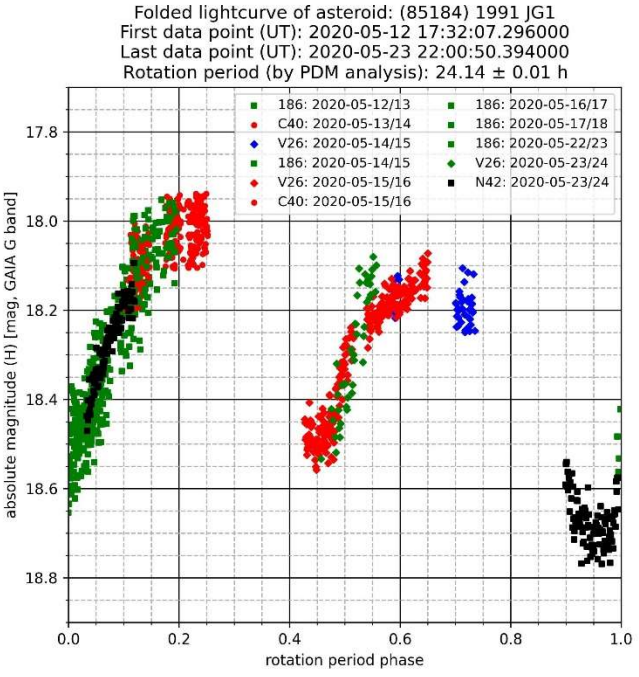

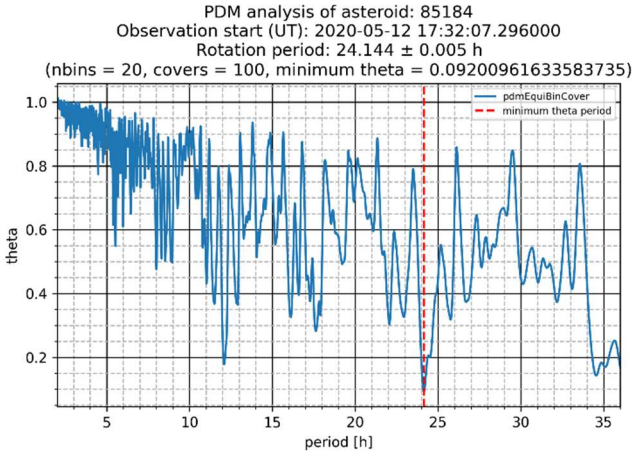

References

Colazo, M.; Duffard, R.; Weidmann, W. (2021). "The determination of asteroid H and G phase function parameters using Gaia DR2." *MNRAS* **504**, 761-768.

Czesla, S.; Schröter, S.; Schneider, C.P.; Huber, K.F.; Pfeifer, F.; Andreasen, D.T.; Zechmeister, M. (2019). "*PyA: Python astronomy-related packages*." Astrophysics Source Code Library, record ascl:1906.010. *https://github.com/sczesla/PyAstronomy*

Devyatkin, A.V.; Gorshanov, D.L.; Kouprianov, V.V.; Verestchagina, I.A. (2010). "Apex I and Apex II software packages for the reduction of astronomical CCD observations." *Solar System Research* **44**, 68-80.

ESA (2022). "5.5.1 Relationships with other photometric systems." Gaia Data Release 3. Documentation Release 1.1. *https://gea.esac.esa.int/archive/documentation/GDR3/Data_processing/chap_cu5pho/cu5pho_sec_photSystem/cu5pho_ssec_photRelations.html*

Gaia Collaboration: Creevey, O.L.; Sarro, L.M.; Lobel, A.; and 444 colleagues (2022). "Gaia Data Release 3: A Golden Sample of Astrophysical Parameters." *Astronomy & Astrophysics* (accepted). *https://arxiv.org/abs/2206.05870*

Ginsburg, A.; Sipöcz, B.M.; Brasseur, C.E.; and 22 colleagues. "*astroquery*: An Astronomical Web-querying Package in Python." *The Astronomical Journal* **157**, id. 98.

Harris, A.W.; Young, J.W.; Scaltriti, F.; Zappala, V. (1984). "Lightcurves and phase relations of the asteroids 82 Alkmene and 444 Gyptis." *Icarus* **57**, 251-258.

Harris, A.W.; Mommert, M.; Hora, J.L.; and 14 colleagues (2011). "ExploreNEOs. II. The Accuracy of the Warm Spitzer Near-Earth Object Survey." *The Astronomical Journal* **141**, id. 75.

JPL (2022a). Horizons. *https://ssd.jpl.nasa.gov/horizons/*

JPL (2022b). Asteroid Size Estimator. *https://cneos.jpl.nasa.gov/tools/ast_size_est.html*

Kouprianov, V. (2008). "Distinguishing features of CCD astrometry of faint GEO objects." *Advances in Space Research* **41**, 1029-1038.

Mahapatra, P.R.; Benner, L.A.M.; Ostro, S.J.; Jurgens, R.F.; Giorgini, J.D.; Yeomans, D.K.; Chandler, J.F.; Shapiro, I.I. (2002). "Radar observations of asteroid 7335 (1989 JA)." *Planetary and Space Science* **50**, 257-260.

Mahlke, M.; Carry, B.; Denneau, L. (2021). "Asteroid phase curves from ATLAS dual-band photometry." *Icarus* **354**, id. 114094.

Mainzer, A.; Grav, T.; Masiero, J.; Hand, E.; Bauer, J.; Tholen, D.; McMillan, R.S.; Spahr, T.; Cutri, R.M.; Wright, E.; Watkins, J.; Mo, W.; Maleszewski, C. (2011). "NEOWISE Studies of Spectrophotometrically Classified Asteroids: Preliminary Results." *The Astrophysical Journal* **741**, id 90.

Mainzer, A.K.; Bauer, J.M.; Cutri, R.M.; Grav, T.; Kramer, E.A.; Masiero, J.R.; Sonnett, S.; Wright, E.L. (2019). "NEOWISE Diameters and Albedos V2.0." *NASA Planetary Data System*.

Masiero, J.R.; Mainzer, A.K.; Bauer, J.M.; Cutri, R.M.; Grav, T.; Kramer, E.; Pittichová, J.; Sonnett, S.; Wright, E.L. (2020). "Asteroid Diameters and Albedos from NEOWISE Reactivation Mission Years 4 and 5." *The Planetary Science Journal* **1**, id 5.

MPC (1983). *Minor Planet Circular* **7783**.

MPC (1989). *Minor Planet Circular* **14556**.

MPC (1991). *Minor Planet Circular* **18342**.

MPC (2004). *Minor Planet Circular* **52768**.

MPC (2022a). Orbits Database. *https://minorplanetcenter.net/db_search/show_object?object_id=2376*

MPC (2022b). Orbits Database. *https://minorplanetcenter.net/db_search/show_object?object_id=7335*

MPC (2022c). Orbits Database. *https://minorplanetcenter.net/db_search/show_object?object_id=12923*

MPC (2022d). Orbits Database. *https://minorplanetcenter.net/db_search/show_object?object_id=85184*

Nugent, C.R.; Mainzer, A.; Bauer, J.; Cutri, R.M.; Kramer, E.A.; Grav, T.; Masiero, J.; Sonnett, S.; Wright, E.L. (2016). "NEOWISE Reactivation Mission Year Two: Asteroid Diameters and Albedos." *The Astronomical* Journal **152**, id 63.

Parrott, D. (2022). *Tycho software*. *https://www.tycho-tracker.com*

Pravec, P.; Wolf, M.; Sarounova, L. (1999web). Ondrejov Asteroid Photometry Project. *http://www.asu.cas.cz/~ppravec/neo.htm*

Pravec, P.; Harris, A.W.; Kušnirák, P.; Galád, A.; Hornoch, K. (2012). "Absolute magnitudes of asteroids and a revision of asteroid albedo estimates from WISE thermal observations." *Icarus* **221**, 365-387.

Raab, H. (2018). *Astrometrica* software. *http://www.astrometrica.at*

Roig, J.C.; Nogues, R.N.; Lorenz, E.S.; Gonzalez, J.L.S. (2011). *Fotometrica Con Astrometrica*, a Software Tool. *http://www.astrosurf.com/cometas-obs*

Tedesco, E.F.; Noah, P.V.; Noah, M.; Price, S.D. (2004). "IRAS Minor Planet Survey V6.0." NASA Planetary Data System, id. IRAS-A-FPA-3-RDR-IMPS-V6.0.

Warner, B.D.; Harris, A.W.; Pravec, P. (2009). "The Asteroid Lightcurve Database." *Icarus* **202**, 134-146. Updated 2022 Jul. *http://www.minorplanet.info/lightcurvedatabase.html*

Warner, B.D.; Stephens, R.D. (2020). "Near-Earth Asteroid Lightcurve Analysis at the Center for Solar System Studies: 2020 April - June." *The Minor Planet Bulletin* **47**, 290-304.

Warner, B.D.; Stephens, R.D.; Coley, D.R. (2021). "Near-Earth Asteroid Lightcurve Analysis at the Center for Solar System Studies: 2021 March - April." *The Minor Planet Bulletin* **48**, 337-340.

Wisniewski, W.Z.; Michalowski, T.M.; Harris, A.W.; McMillan, R.S. (1997). "Photometric Observations of 125 Asteroids." *Icarus* **126**, 395-449.

ROTATIONAL PERIOD AND LIGHTCURVE DETERMINATION OF FOUR ASTEROIDS

Andrzej Armiński
Marina Sky Observatory, Nerpio (Z06)
P.O. Box 730, 70-952 Szczecin, Poland
aa@aarminski.com.pl

(Received: 2022 June 17 Revised: 2022 July 9)

Photometric observations were conducted of four main-belt asteroids. The results of lightcurve analysis gave synodic rotation periods and amplitudes shown in the table below.

I report lightcurve and period of rotation of asteroids studied in 2022 February with Marina Sky Observatory 17-inch robotic telescope (Marina Sky, 2022). All images were taken with a Planewave CDK 0.432-m *f*/6.8 telescope and Finger Lake Instruments Proline 16803 CCD camera using Sloan r filter. The images were binned at 2×2 yielding an image scale of 1.28 arcsec/pixel and the field of view 43 × 43 arcmin.

The exposure time of each image was 150 seconds. To remove Residual Bulk Image (RBI), the NRI pre-flash was applied before each exposure. Images were calibrated with bias, dark for -20°C, and sky flat frames.

Astrometric plate solving of acquired images was achieved using *PinPoint* (DC3 Dreams, 2022) with star positions from ATLAS catalogue (Tonry et al., 2018). In photometry analysis, a couple dozen of carefully selected comparison stars sourced from ATLAS catalogue were used having SLOAN r magnitudes in range 12 - 16, B-V color index in range 0.45 - 0.9, and SNR usually between 50 and 450.

Tycho Tracker software (Parrot, 2022) and *Photometric Workflow* (Dose, 2020; 2021) were used for data processing and photometric analysis.

(5456) Merman 1979 HH3. This Vesta family (410) asteroid was discovered at Nauchnyj on 1979 April 25 by N. S. Chernykh. The determined orbit (MPC, 2022) has a semi-major axis of 2.3572709 au, eccentricity of 0.0513055, and inclination of 7.03068 degrees. According to JPL Small-Body Database (JPL, 2022), the asteroid diameter is 4.220 km, absolute magnitude H = 13.38, and geometric albedo 0.626. The asteroid sky motion during imaging was 0.66 arcsec/minute.

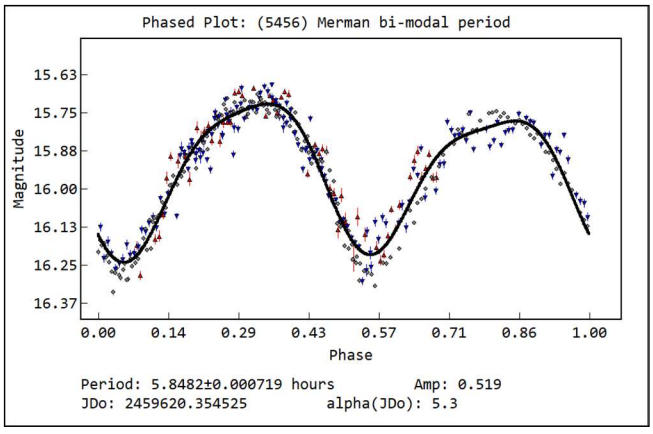

Observations were made on 2022 February 9-11. The number of images taken during first, second and third night respectively used in analysis were 187, 61 and 163.

The three observational nights allowed establishing for asteroid (5456) Merman a Sloan r magnitude range 15.72 - 16.24 and a bi-modal period of rotation of 5.8482 ± 0.0007 h that is in agreement with period of 5.85286 h calculated by (Ďurech et. al., 2020).

The periodogram shows that a single-mode lightcurve rotational period of 2.9236 ± 0.0007 h, being exactly half of a bi-modal period, gives an equally good match. The amplitude and shape of both parts of bi-modal lightcurve are very similar, which allows the possibility of a single-mode solution. However, given the amplitude of 0.52 mag and low phase angle, the true solution is almost certain to be near 5.8 h (Harris et al., 2014).

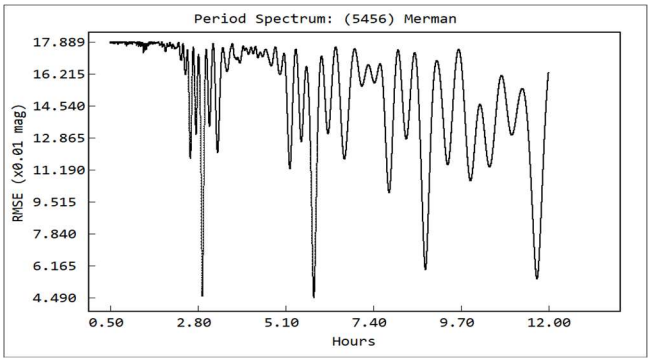

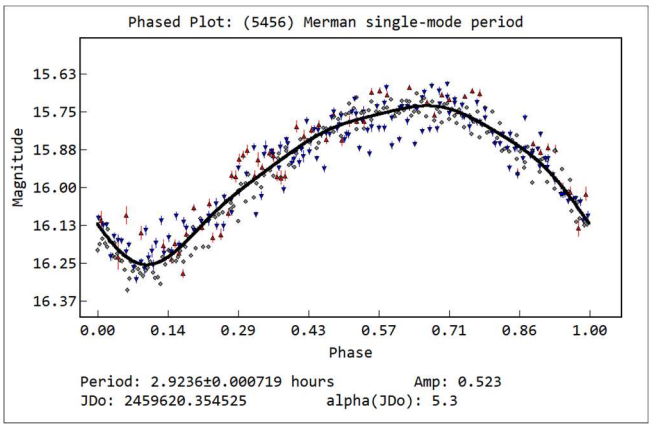

(6920) Esaki 1993 JE. This Vesta family (410) asteroid was discovered at Kitami on 1993 May 14 by K. Endate and K. Watanabe. The determined orbit (MPC, 2022) has a semi-major axis of 2.3873927 au, eccentricity of 0.0801087, and inclination of 6.71374 degrees. According to the JPL Small-Body Database (JPL, 2022), the diameter is 4.962 km, absolute magnitude H = 13.36, and the geometric albedo is 0.413. Asteroid speed during imaging was 0.64 arcsec/minute. The rotational period for this body has not been found in previously published data (Warner et al., 2009).

I report lightcurve and period of rotation of asteroid (6920) Esaki as studied on 2022 February 20, 21, and 28. The number of images taken and used in the analysis for the three nights were 116, 138, and 156, respectively. The three observational nights allowed establishing a period of rotation of 3.0695 ± 0.0007 h and Sloan r magnitude range 13.62 - 13.89.

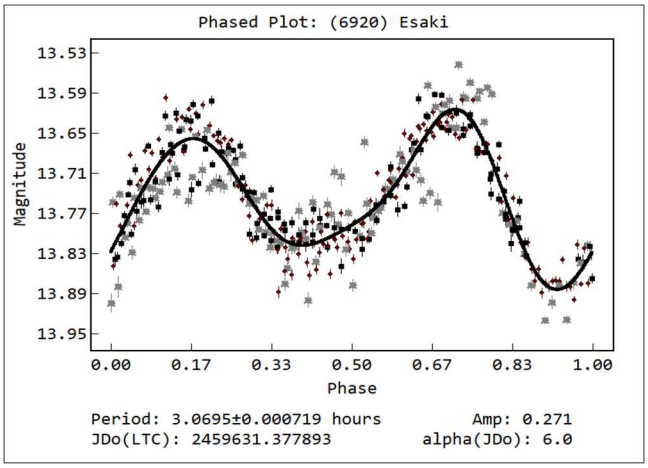

(13078) 1991 WD. This main-belt (LCDB orbital group 9105) asteroid was discovered at Kiyosato on 1991 Nov 17 by S. Otomo. The determined orbit (MPC, 2022) has a semi-major axis of 2.6161104 au, eccentricity of 0.2200691, and inclination of 13.87726 degrees. According to the JPL Small-Body Database (JPL, 2022), the diameter is 5.091 km, the absolute magnitude is H = 13.89, and the geometric albedo = 0.247. The sky motion during imaging was 0.64 arcsec/minute.

The rotational period for this body has not been found in previously published data (Warner et al., 2009). I report a lightcurve and period of rotation for the asteroid as studied on 2022 February 6-8. The number of images taken and used in analysis for the three nights were 74, 187, and 196, respectively. Analysis of the data found a period of rotation of 7.0945 ± 0.0007 h and Sloan r magnitude range 16.08 - 16.24.

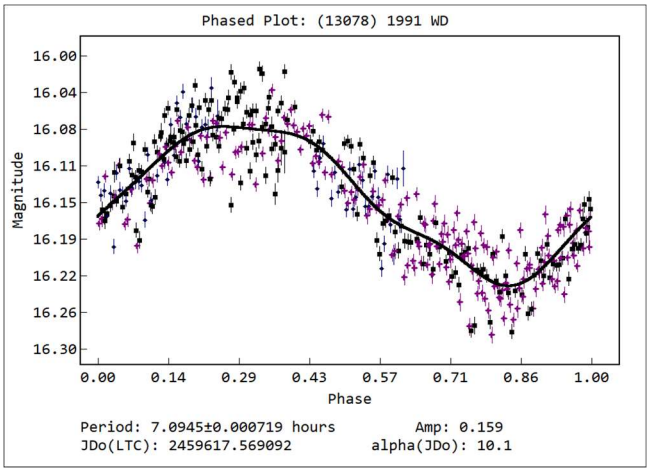

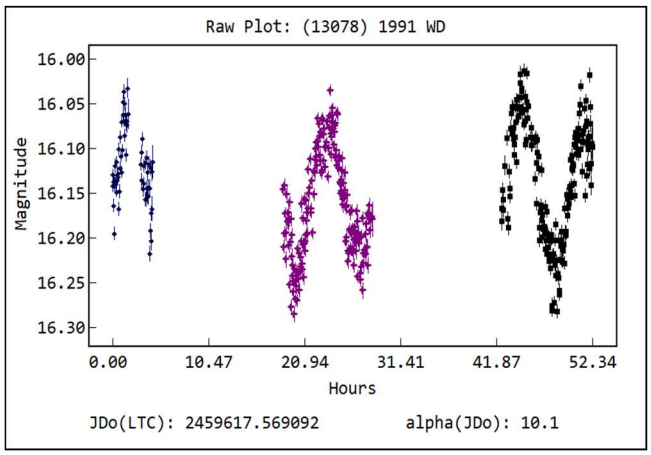

(49937) 1999 XO180. This inner main-belt (LCDB orbital group 9104) asteroid was discovered at Socorro on 1999 December 10 by LINEAR. The determined orbit (MPC, 2022) has a semi-major axis of 2.3806048 au, eccentricity of 0.1701859, and inclination of 9.73216 degrees. According to JPL Small-Body Database (JPL, 2022), the diameter is 3.421 km, absolute magnitude H = 14.23, geometric albedo 0.456. The sky motion during imaging was 0.63 arcsec/minute.

The rotational period for this body has not been found in previously published data (Warner et al., 2009). I report lightcurve and period of rotation based on data obtained on 2022 February 2 and 3. During the first and second night, 212 and 82 images were taken, while 207 and 71 observations, respectively, were used in analysis.

The two observational nights allowed establishing a period of rotation of 2.9488 ± 0.0007 h and Sloan r magnitude range 16.31-16.41.

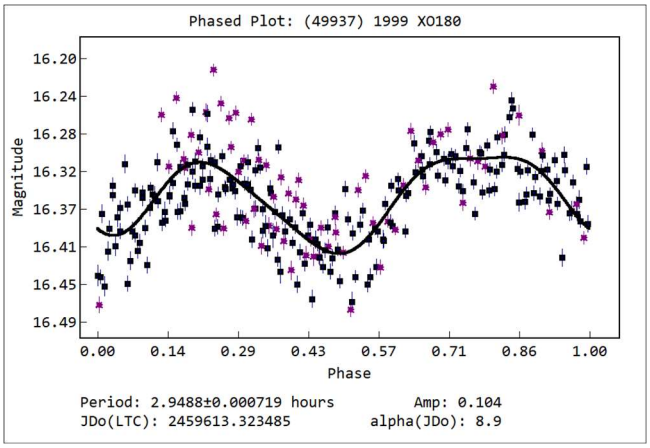

Number	Name	yyyy mm/dd	Phase	L_{PAB}	B_{PAB}	Period(h)	P.E.	Amp	A.E.	Grp
5456	Merman	2022 02/09-02/11	5.30,5.39	141	10	5.8482	0.0007	0.52	0.03	401
6920	Esaki	2022 02/20-02/28	6.01,5.52	157	9	3.0695	0.0007	0.27	0.03	401
13078	1991 WD	2022 02/06-02/08	10.12,9.99	142	16	7.0945	0.0007	0.16	0.03	MB-M
49937	1999 XO180	2022 02/02-02/03	8.88,8.85	135	14	2.9488	0.0007	0.10	0.03	MB-I

Table I. Observing circumstances and results. The phase angle is given for the first and last date. If preceded by an asterisk, the phase angle reached an extrema during the period. L_{PAB} and B_{PAB} are the approximate phase angle bisector longitude/latitude at mid-date range (see Harris et al., 1984). Grp is the asteroid family/group (Warner et al., 2009).

Acknowledgments

Marina Sky Observatory uses, with thanks, the Top 50 Asteroids website and associated database (Kluwak, 2022) as asteroid ephemeris generator during planning and observing.

References

DC3 Dreams. (2022). PinPoint Astrometric Engine. *http://pinpoint.dc3.com*

Dose, E.V. (2020). "A New Photometric Workflow and Lightcurves of Fifteen Asteroids." *Minor Planet Bull.* **47**, 324-330.

Dose, E.V. (2021). "MP2021 Photometric Workflow" repository. *https://github.com/edose/mp2021*

Ďurech, J.; Tonry, J.; Erasmus, N.; Denneau, L.; Heinze, A.N.; Flewelling, H.; Vančo, R. (2020). "Asteroid models reconstructed from ATLAS photometry." *Astronomy & Astrophysics* **643**, A59.

Harris, A.W.; Young, J.W.; Scaltriti, F.; Zappala, V. (1984). "Lightcurves and phase relations of the asteroids 82 Alkmene and 444 Gyptis." *Icarus* **57**, 251-258.

Harris, A.W.; Pravec, P.; Galad, A.; Skiff, B.A.; Warner, B.D.; Vilagi, J.; Gajdos, S.; Carbognani, A.; Hornoch, K.; Kusnirak, P.; Cooney, W.R.; Gross, J.; Terrell, D.; Higgins, D.; Bowell, E.; Koehn, B.W. (2014). "On the maximum amplitude of harmonics on an asteroid lightcurve." *Icarus* **235**, 55-59.

JPL Small-Body Database. (2022). *https://ssd.jpl.nasa.gov/tools/sbdb_lookup.html#/?sstr=49937*

Kluwak, T. (2022). "Top 50 Asteroids for K80 Lusowko Platanus Observatory." *https://platanus.pl/services*

Marina Sky Observatory, IAU code Z06. (2022). *http://marinasky.org*

MPC Objects. (2022). *https://minorplanetcenter.net/db_search/show_object?object_id=49937*

Parrot, D. (2022). Tycho Tracker software. *https://www.tycho-tracker.com*

Tonry, J.L.; Denneau, L.; Heinze, A.N.; Stalder, B.; Smith, K.W.; Smartt, S.J.; Stubbs, C.W.; Weiland, H.J.; Rest, A. (2018). "ATLAS: A High-cadence All-sky Survey System." *PASP* **130**, 064505.

Warner, B.D.; Harris, A.W.; Pravec, P. (2009). "The Asteroid Lightcurve Database." *Icarus* **202**, 134-146. Updated 2021, Sep. *http://www.minorplanet.info/lightcurvedatabase.html*

LIGHTCURVES FOR SIXTEEN MINOR PLANETS

Tom Polakis
Command Module Observatory
121 W. Alameda Dr.
Tempe, AZ 85282
tpolakis@cox.net

(Received: 2022 June 23)

Photometric measurements of CCD observations on 16 main-belt asteroids were made from 2022 April through May. Phased lightcurves were created for twelve asteroids, while four did not yield period solutions. All the data have been submitted to the ALCDEF database.

CCD photometric observations of 16 main-belt asteroids were performed at Command Module Observatory (MPC V02) in Tempe, AZ. Images were taken using a 0.32-m *f*/6.7 Modified Dall-Kirkham telescope, SBIG STXL-6303 CCD camera, and a 'clear' glass filter. Exposure time for all the images was 2 minutes. The image scale after 2×2 binning was 1.76 arcsec/pixel. Table I shows the observing circumstances and results. All of the images for these asteroids were obtained between 2022 April and May.

Images were calibrated using a dozen bias, dark, and flat frames. Flat-field images were made using an electroluminescent panel. Image calibration and alignment was performed using *MaxIm DL* software.

Data reduction and period analysis were done using *MPO Canopus* (Warner, 2020). The 45′×30′ field of the CCD typically enables the use of the same field center for three consecutive nights. In these fields, the asteroid and three to five comparison stars were measured. Comparison stars were selected with colors within the range of $0.5 < B\text{-}V < 0.95$ to correspond with color ranges of asteroids. In order to reduce the internal scatter in the data, the brightest stars of appropriate color that had peak ADU counts below the range where chip response becomes nonlinear were selected. *MPO Canopus* plots instrumental vs. catalog magnitudes for solar-colored stars, which is useful for selecting comp stars of suitable color and brightness.

Since the sensitivity of the KAF-6303 chip peaks in the red, the clear-filtered images were reduced to Sloan r′ to minimize error with respect to a color term. Comparison star magnitudes were obtained from the ATLAS catalog (Tonry et al., 2018), which is incorporated directly into *MPO Canopus*. The ATLAS catalog derives Sloan *griz* magnitudes using a number of available catalogs. The consistency of the ATLAS comp star magnitudes and color-indices usually allowed the separate nightly runs to be linked with no zero-point shifts and occasionally only a few hundredths of a magnitude.

A 9-pixel (16 arcsec) diameter measuring aperture was used for asteroids and comp stars. It was typically necessary to employ star subtraction to remove contamination by field stars. For the asteroids described here, I note the RMS scatter on the phased lightcurves, which gives an indication of the overall data quality including errors from the calibration of the frames, measurement of the comp stars, the asteroid itself, and the period-fit. Period determination was done using the *MPO Canopus* Fourier-type FALC fitting method (cf. Harris et al., 1989). Phased lightcurves show the maximum at phase zero. Magnitudes in these plots are apparent and scaled by *MPO*

Canopus to the first night. In cases where rotation periods could not be determined, raw lightcurves are presented, with "Raw" appearing in the upper right-hand corner of the plots.

Asteroids were selected from the CALL website (Warner, 2011a), either for having uncertain periods or for needing more lightcurves for shape modeling. In this set of observations, 1 of the 16 asteroids had no previous period analysis, 2 had U = 1, and 6 had U=2. The Asteroid Lightcurve Database (LCDB; Warner et al. (2009) was consulted to locate previously published results. All the new data for these asteroids can be found in the ALCDEF database.

233 Asterope was discovered by Alphonse Borrelly at Marseille in 1883. Papers showing similar rotational periods include Hanus et al. (2016, 19.69801 h) and Hanus et al. (2017, 19.69803 ± 0.00002 h. During four nights, 249 data points were gathered to determine a period of 19.772 ± 0.009 h, agreeing with previous values. The amplitude of the lightcurve is 0.40 ± 0.01 mag.

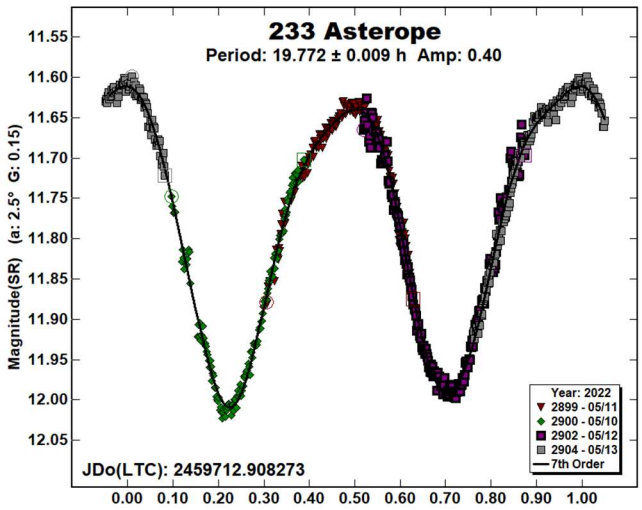

240 Vanadis. This middle main-belt asteroid is another of Borrelly's discoveries, this one in 1884. Its eccentric orbit brought it to an unfavorable opposition in 2022. Denchev (2000) computed a rotation period of 10.64 h and Alton (2016) published 10.57 ± 0.01 h. A total of 905 images were taken in eight nights, producing a period of 10.543 ± 0.009 h and an amplitude of 0.08 ± 0.02 mag. The monomodal lightcurve results in a solution that matches previous values, and a "split halves" plot does not support the bimodal solution.

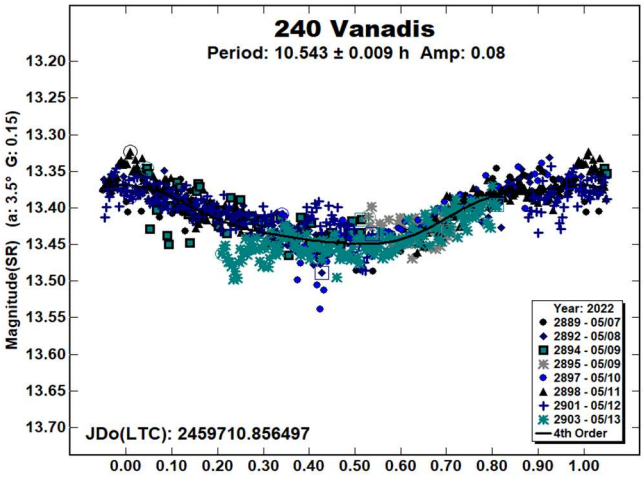

275 Sapentia was discovered by Johann Palisa in 1888 at Vienna. Warner (2007) published a period of 14.766 ± 0.006 h and Pilcher (2016) computed 14.932 ± 0.001 h. Three nights and 187 images were sufficient to produce a period solution of 14.886 ± 0.022 h. The amplitude of the lightcurve is 0.11 mag, with an RMS error on the fit of 0.009 mag.

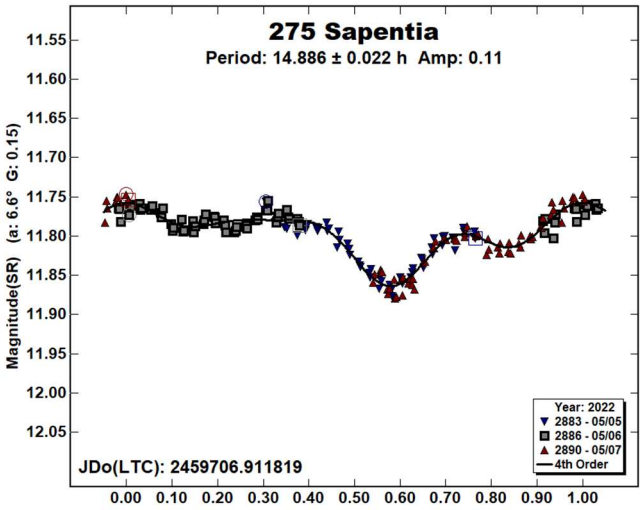

282 Clorinde lies in the inner main belt. It was discovered at Nice by Auguste Charlois in 1889. The period shown by Durech et al. (2020) is 49.365 ± 0.002 h while Bonamico and van Belle (2021) published 49.352 ± 0.004 h. In three nights, 177 images were taken. The raw lightcurve was flat, so no further imaging was done because a period solution could not be determined.

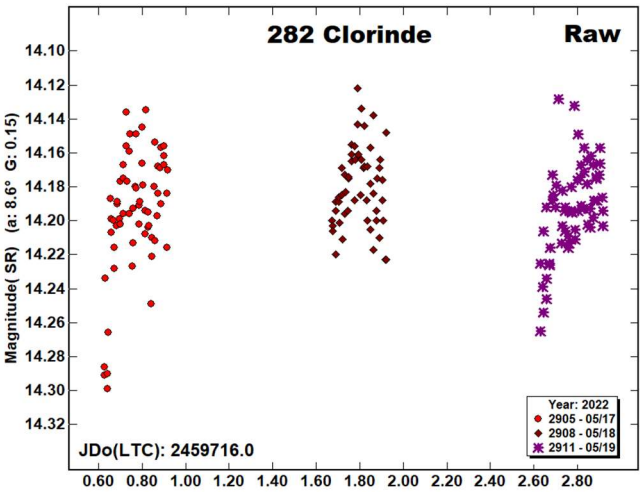

323 Brucia is a Phocea-family minor planet in a highly inclined and eccentric orbit. It had an unfavorably distant, but northerly opposition in 2022. Discovered at Heidelberg in 1891, it was Max Wolf's first of his 248 asteroid discoveries. Seven agreeing period solutions appear in the LCDB. The most recent are Warner (2018, 9.458 ± 0.008 h); Behrend (2021web, 9.463 ± 0.001 h); and Stephens et al. (2021, 9.457 ± 0.002 h). A three-night run with 196 images produced a similar rotational period of 9.530 ± 0.033 h and an amplitude of 0.07 ± 0.014 mag.

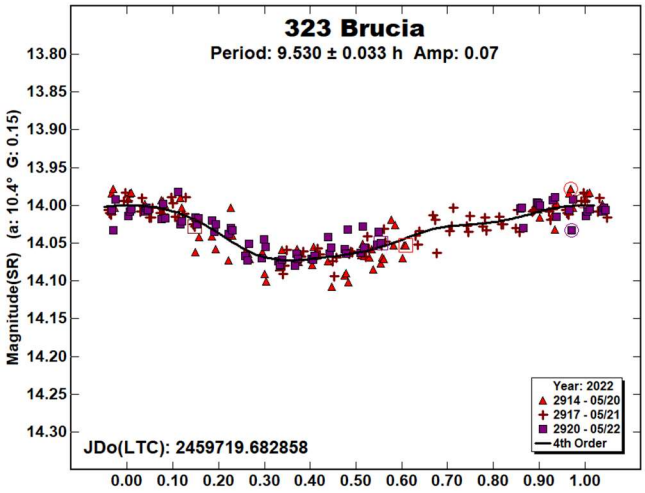

513 Centesima is another of Max Wolf's discoveries. Durech et al. (2016) published a period of 5.32399 ± 0.00001 h and Behrend (2021web) shows 4.794 ± 0.001 h. During three nights, 181 data points were acquired to produce a period solution of 4.790 ± 0.002 h, in agreement with Behrend. The lightcurve has an amplitude of 0.35 ± 0.03 mag.

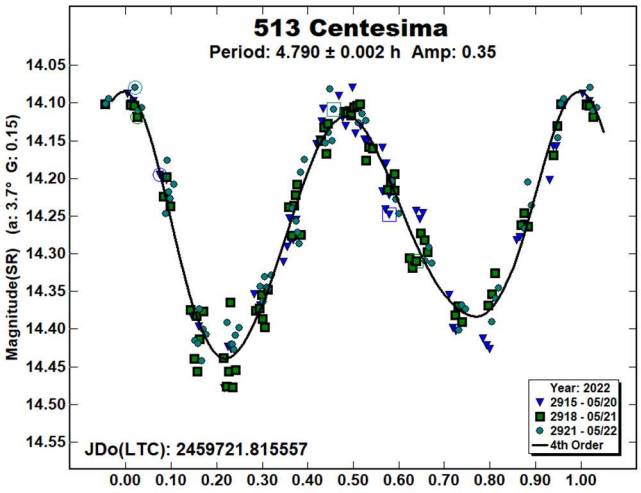

795 Fini was discovered at Vienna in in 1914 by Johann Palisa. Several uncertain period solutions appear in the LCDB, including Warner (2011b, 7.49 ± 0.02 h), Pravec (2012web, 4.65 h), and Waszczak et al. (2015, 26.971 ± 0.0557 h). A total of 600 images were taken during 11 nights. These produced a synodic period of 51.40 ± 0.20 h, disagreeing with all previous assessments. The amplitude is 0.11 ± 0.01 mag.

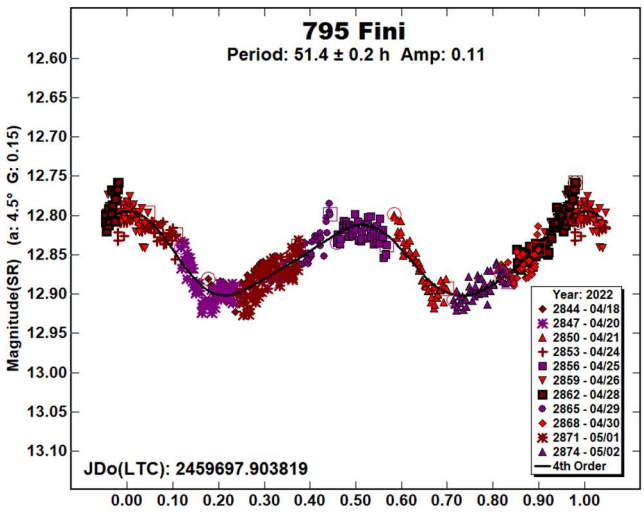

1055 Tynka is a Flora-family asteroid in an eccentric orbit. discovered by Emil Buchar at Algiers in 1912. The most recent period solutions are Stephens (2012, 11.75 ± 0.01 h) and Durech et al. (2020, 5.94680 ± 0.00002 h). During three nights, 180 images were gathered, but the lightcurve remained too flat to achieve a period solution.

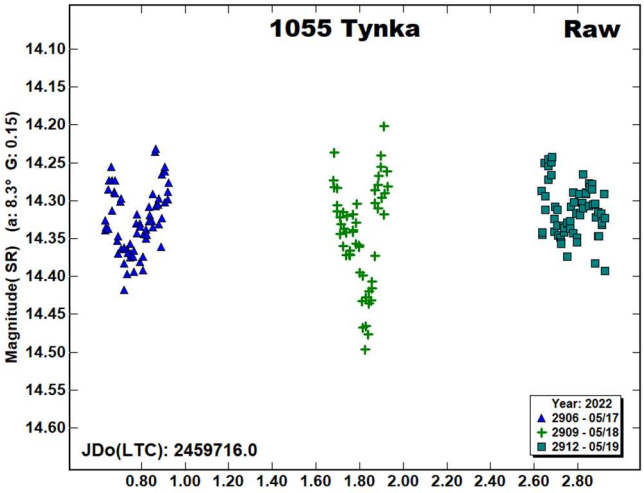

1237 Genevieve was discovered by Guy Reiss in 1951 at Algiers. Polakis (2018) shows a period of 16.48 ± 0.02 h and Durech et al. (2019) published 24.6982 ± 0.002 h. The asteroid was observed on four nights, and 213 images were obtained, yielding a synodic rotation period of 16.31 ± 0.04 h. The lightcurve has an amplitude of 0.22 mag and an RMS error on the fit of 0.031 mag.

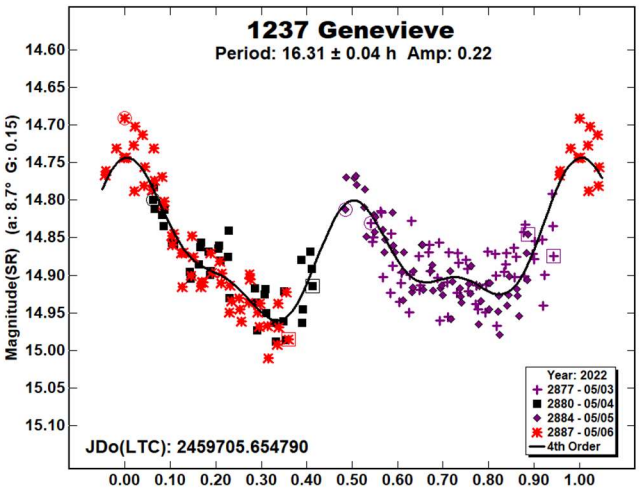

1319 Disa. This outer-belt asteroid was discovered by Cyril Jackson at Johannesburg in 1934. Period solutions in the LCDB include Warner (2006, 7.080 ± 0.003 h) and Waszczak et al. (2015, 7.082 ± 0.0077 h. After three nights, 281 images were used to calculate a synodic period of 7.082 ± 0.004 h, in agreement with previous solutions. The amplitude of the lightcurve is 0.22 mag with an RMS error of 0.022 mag.

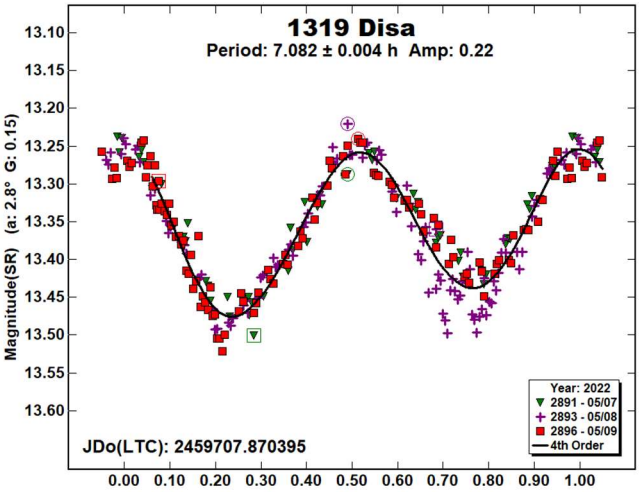

1783 Albitskij is an Adeona-family asteroid, first identified by Grigory Neujmin in 1935 at Simeis. Durech et al. (2020) published a period of 19.9375 ± 0.0001 h. A total of 222 images were taken during four nights, producing a rotational period of 19.93 ± 0.04 h and amplitude of 0.72 ± 0.04 mag.

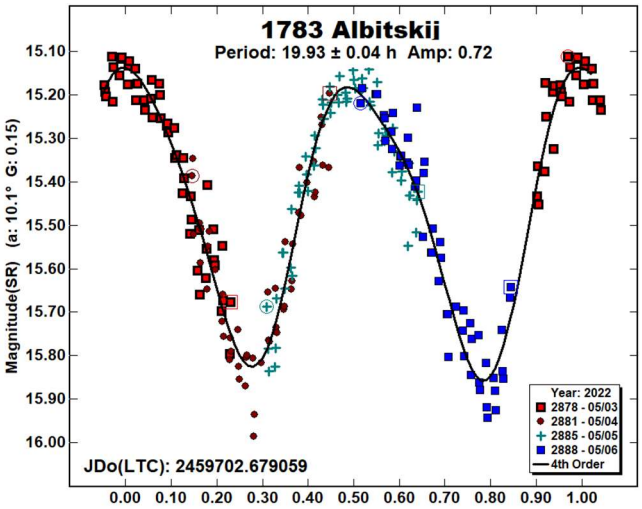

2685 Masursky is a Eunomia-family asteroid that was discovered by Edward Bowell at Flagstaff in 1981. No period solutions appear in the LCDB. It became apparent after taking 111 images during two nights that the scatter would be too high to derive a period solution from Tempe. The raw lightcurve is provided.

Number	Name	yy/mm/dd	Phase	L_{PAB}	B_{PAB}	Period(h)	P.E.	Amp	A.E.	Grp
233	Asterope	22/05/10-05/14	13.5,12.6	235	1	19.772	0.009	0.40	0.01	MB-O
240	Vanadis	22/05/07-05/13	3.5,1.4	235	2	10.543	0.009	0.08	0.02	MB-O
275	Sapentia	22/05/05-05/07	6.6,7.4	214	6	14.886	0.022	0.11	0.01	MB-O
282	Clorinde	22/05/17-05/19	8.6,9.2	223	12	--	--	--	--	MB-M
323	Brucia	22/05/20-05/22	10.4,10.7	224	23	9.530	0.033	0.07	0.01	MB-O
513	Centesima	22/05/20-05/22	3.7,4.1	235	9	4.790	0.002	0.35	0.03	MB-M
795	Fini	22/04/18-05/02	4.5,10.6	199	-3	51.40	0.20	0.11	0.01	MB-O
1055	Tynka	22/05/17-05/19	8.3,9.2	225	7	--	--	--	--	MB-M
1237	Genevieve	22/05/03-05/06	8.7,9.8	203	6	16.31	0.04	0.22	0.03	PHO
1319	Disa	22/05/07-05/09	2.8,3.7	222	-2	7.082	0.004	0.22	0.02	MB-O
1783	Albitskij	22/05/03-05/06	10.1,11.3	203	5	19.93	0.04	0.72	0.04	MB-O
2685	Masursky	22/05/03-05/04	8.8,9.2	205	-2	--	--	--	--	MB-O
2689	Bruxelles	22/04/18-05/02	4.8,12.9	202	2	101.6	0.3	0.76	0.06	MB-O
3224	Irkutsk	22/04/20-05/02	2.3,8.1	206	-2	33.08	0.02	0.45	0.04	MARS
3306	Byron	22/05/20-05/22	2.1,2.8	235	3	6.999	0.011	0.29	0.05	MB-M
3469	Bulgakov	22/05/17-05/19	1.5,1.8	235	3	--	--	--	--	MB-M

Table I. Observing circumstances and results. The phase angle is given for the first and last date. If preceded by an asterisk, the phase angle reached an extrema during the period. LPAB and BPAB are the approximate phase angle bisector longitude/latitude at mid-date range (see Harris et al., 1984). Grp is the asteroid family/group (Warner et al., 2009).

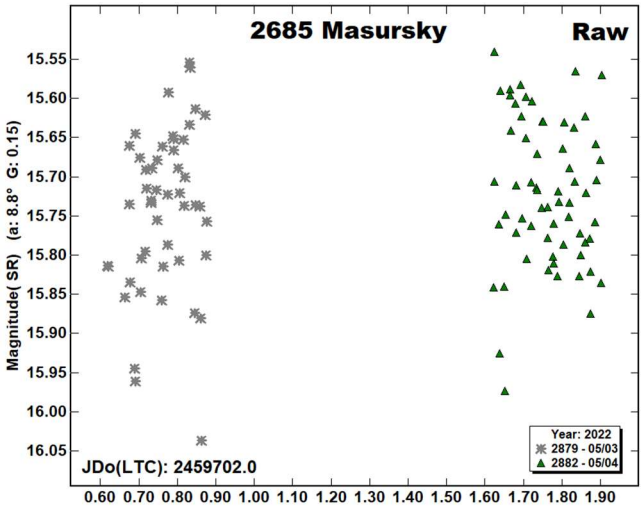

2689 Bruxelles. This Flora-family minor planet was discovered in 1935 at Uccle by Sylvain Arend. Two period solutions were found in the LCDB. Hess and Ditteon (2016) reported a period of 8.71 ± 0.05 h, and Dose (2021) computed a much longer period: 101.800 ± 0.026 h. The asteroid was observed on 11 nights, and 626 images were taken. The calculated period is 101.6 ± 0.3 h, supporting Dose's value. The amplitude is 0.76 ± 0.060 mag.

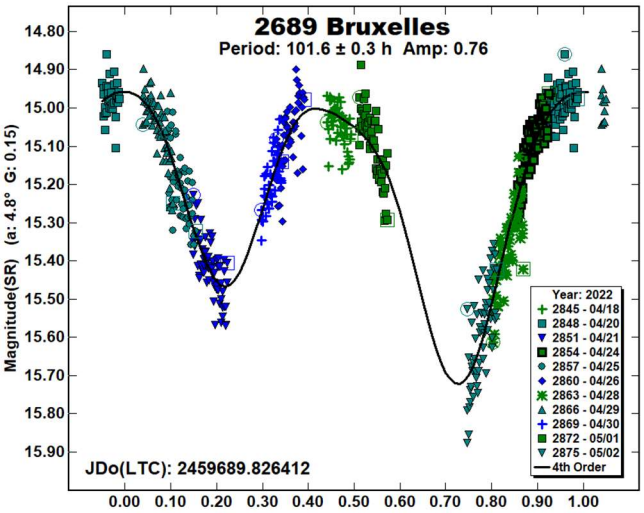

3224 Irkutsk was identified by Nikolai Chernykh at Nauchnyj in 1977. Its eccentric orbit brought it to a favorable 2022 opposition. Period solutions include Waszczak et al. (2015, 33.140 ± 0.0630 h) and Durech et al. (2019, 33.1038 ± 0.0002 h). Over the course of 10 nights, 532 images were used to compute a synodic period of 33.08 ± 0.02 h, in line with published values. The lightcurve amplitude is 0.45 ± 0.04 mag.

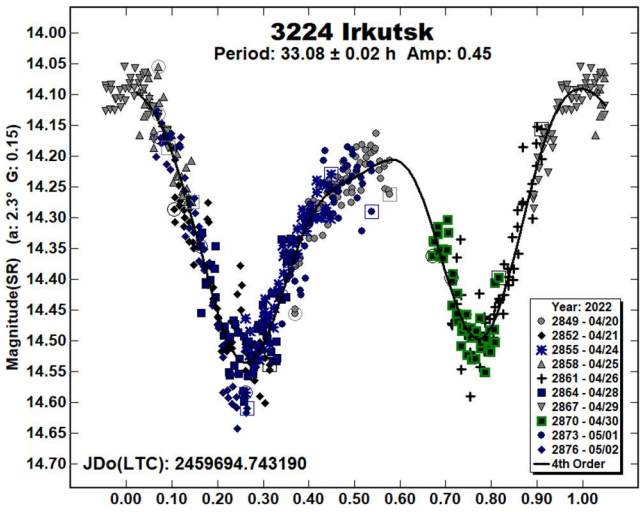

3306 Byron is an Eos-family asteroid that was discovered by Nikolai Chernykh in 1979. Moravec et al. (2013) show a rotation period of 7.321 ± 0.005 h and Polakis (2020) computed 6.999 ± 0.005 h. After three nights, 152 data points had been acquired, resulting in a period solution of 6.999 ± 0.011 h, with an amplitude of 0.29 ± 0.05 mag.

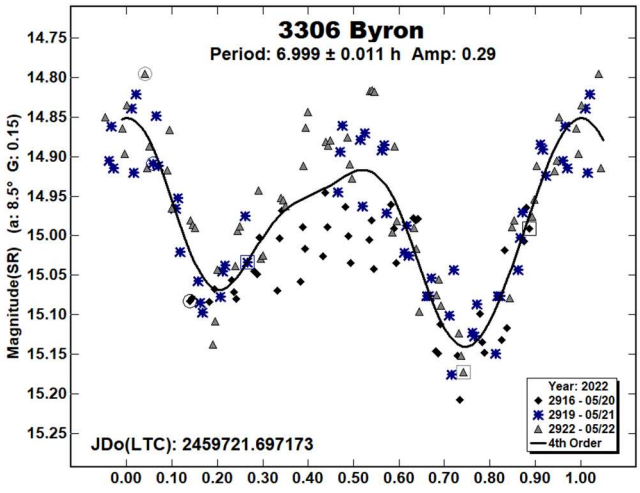

3469 Bulgakov. Ludmilla Karachkina discovered this asteroid in in 1982 at Nauchnyj. Durech et al. (2020) computed a synodic rotation period of 180.76 ± 0.01 h. However, Behrend (2021web) shows a much shorter period of 6.48 ± 0.05 h. During three nights, 176 images were taken, producing a flat lightcurve, from which no period solution was obtained.

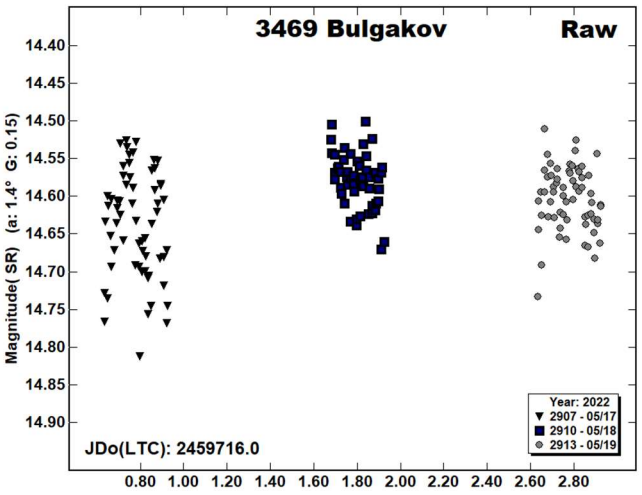

Acknowledgements

The author would like to express his gratitude to Brian Skiff for his indispensable mentoring in data acquisition and reduction. Thanks also go out to Brian Warner for support of his *MPO Canopus* software package.

References

Alton, K.B. (2016). "CCD Lightcurve for the Main-belt Asteroid 240 Vanadis." *Minor Planet Bull.* **43**, 217-218.

Behrend, R. (2021web). Observatoire de Geneve web site. *http://obswww.unige.ch/~behrend/page_cou.html*

Bonamico, R.; van Belle, G. (2021), "Determining the Rotational Period of Main-Belt Asteroid 282 Clorinde." *Minor Planet Bull*. **43**, 210.

Denchev, P. (2000). "Photometry of 11 asteroids during their 1998 and 1999 apparitions." *Planet. Space Sci.* **48**, 987-992.

Dose, E. (2021). "Lightcurves of Eighteen Asteroids." *Minor Planet Bull*. **48**, 125-132.

Durech, J.; Hanus, J.; Oszkiewsicz, D.; Vanco, R. (2016). *"A*steroid models from the Lowell photometric database.*" Astron. Astrophys*. **587**, A48-53.

Durech, J.; Hanus, J.; Vanco, R. (2019). "Inversion of asteroid photometry from Gaia DR2 and the Lowell Observatory photometric database." *Astron. Astrophys* **631**, A2-5.

Durech, J.; Tonry, J.; Erasmus, N.; Denneau, L.; Heinze, A.N.; Flewelling, H.; Vanco, R. (2020). "Asteroid models reconstructed from ATLAS photometry." *Astron. Astrophys.* **643**, A59-63.

Hanuš, J.; Ďurech, J.; Oszkiewicz, D.A.; and 166 colleagues (2016). "New and updated convex shape models of asteroids based on optical data from a large collaboration network." *Astron. Astrophys.***586**, 108-131.

Hanuš, J.; and 13 colleagues (2017). "Volumes and bulk densities of forty asteroids from ADAM shape modeling." *Astron. Astrophys.* **601**, 114-155.

Harris, A.W.; Young, J.W.; Scaltriti, F.; Zappala, V. (1984). "Lightcurves and phase relations of the asteroids 82 Alkmene and 444 Gyptis." *Icarus* **57**, 251-258.

Harris, A.W.; Young, J.W.; Bowell, E.; Martin, L.J.; Millis, R.L.; Poutanen, M.; Scaltriti, F.; Zappala, V.; Schober, H.J.; Debehogne, H.; Zeigler, K.W. (1989). "Photoelectric Observations of Asteroids 3, 24, 60, 261, and 863." *Icarus* **77**, 171-186.

Hess, K.; Ditteon, R. (2016). "Asteroid Lightcurve Analysis at the Oakley Southern Sky Observatory: 2015 February." *Minor Planet Bull*. **43**, 87.

Moravec, P.; Letfullina, A.; Ditteon, R. (2013). "Asteroid Lightcurve Analysis at the Oakley Observatories: 2012 May - June." *Minor Planet Bull*. **40**, 17-20.

Pilcher, F. (2016). "Rotation Period Determination for 269 Justitia, 275 Sapientia 331 Etheridgea, and 609 Fulvia." *Minor Planet Bull*. **43**, 135-136.

Polakis, T. (2018). "Lightcurve Analysis for Fourteen Main-belt Minor Planets." *Minor Planet Bull*. **45**, 347-352.

Polakis, T. (2020). "Photometric Observations of Ten Minor Planets." *Minor Planet Bull*. **47**, 13-17.

Pravec, P.; Wolf, M.; Sarounova, L. (2012web). Ondrejov Asteroid Photometry Project web site. *http://www.asu.cas.cz/~ppravec/neo.htm*

Stephens, R.D. (2012). "Asteroids Observed from Santana, CS3 and GMARS Observatories: 2012 April - June." *Minor Planet Bull*. **39**, 226-228.

Stephens, R.D.; Coley, D.R.; Warner, B.D. (2021) "Main-belt Asteroids Observed from CS3: 2021 April - May." *Minor Planet Bull*. **48**, 380-387.

Tonry, J.L.; Denneau, L.; Flewelling, H.; Heinze, A.N.; Onken, C.A.; Smartt, S.J.; Stalder, B.; Weiland, H.J.; Wolf, C. (2018). "The ATLAS All-Sky Stellar Reference Catalog." *Astrophys. J.* **867**, A105.

Warner, B.D. (2006). "Asteroid lightcurve analysis at the Palmer Divide Observatory: February - March 2006." *Minor Planet Bull*. **33**, 82-84.

Warner, B.D. (2007). "Asteroid Lightcurve Analysis at the Palmer Divide Observatory - December 2006 - March 2007." *Minor Planet Bull.* **34**, 72-77.

Warner, B.D.; Harris, A.W.; Pravec, P. (2009). "The Asteroid Lightcurve Database." *Icarus* **202**, 134-146. Updated 2020 Aug. *http://www.minorplanet.info/lightcurvedatabase.html*

Warner, B.D. (2011a). Collaborative Asteroid Lightcurve Link website. *http://www.minorplanet.info/call.html*

Warner, B.D. (2011b). "Asteroid Lightcurve Analysis at the Palmer Divide Observatory: 2010 September - December." *Minor Planet Bull*. **38**, 82-86.

Warner, B.D. (2018). "Asteroid Lightcurve Analysis at CS3-Palmer Divide Station: 2018 April - June." *Minor Planet Bull*. **45**, 380-386.

Warner, B.D. (2020). *MPO Canopus* software. *http://bdwpublishing.com*

Waszczak, A.; Chang, C.-K.; Ofek, E.O.; Laher, R.; Masci, F.; Levitan, D.; Surace, J.; Cheng, Y.-C.; Ip, W.-H.; Kinoshita, D.; Helou, G.; Prince, T.A.; Kulkarni, S. (2015). "Asteroid Light Curves from the Palomar Transient Factory Survey: Rotation Periods and Phase Functions from Sparse Photometry." *Astron. J.* **150**, A75.

ASTEROID PHOTOMETRY AND LIGHTCURVE ANALYSIS FOR SIX ASTEROIDS

Milagros Colazo
Instituto de Astronomía Teórica y Experimental
(IATE-CONICET), Argentina
Facultad de Matemática, Astronomía y Física
Universidad Nacional de Córdoba, Argentina
Grupo de Observadores de Rotaciones de Asteroides
(GORA), Argentina
https://aoacm.com.ar/gora/index.php
milirita.colazovinovo@gmail.com

Damián Scotta, Bruno Monteleone, Mario Morales,
Giuseppe Ciancia, Alberto García, Raúl Melia, Néstor Suárez,
Aldo Wilberger, César Fornari, Ricardo Nolte,
Ezequiel Bellocchio, Aldo Mottino, Carlos Colazo.

Grupo de Observadores de Rotaciones de Asteroides
(GORA), Argentina

Observatorio de Sencelles (MPC K14) - Sencelles
(Mallorca-Islas Baleares-España)

Observatorio Los Cabezones (MPC X12) - Santa Rosa
(La Pampa-Argentina)

Observatorio Galileo Galilei (MPC X31) - Oro Verde
(Entre Ríos-Argentina)

Observatorio Antares (MPC X39) - Pilar
(Buenos Aires-Argentina)

Observatorio Río Cofio (MPC Z03) - Robledo de Chavela
(Madrid-España)

Observatorio AstroPilar (GORA APB) - Pilar
(Buenos Aires-Argentina)

Osservatorio Astronómico "La Macchina del Tempo"
(GORA BM1) - Ardore Marina (Reggio Calabria-Italia)

Specola "Giuseppe Pustorino 1" (GORA GC1) -
Palizzi Marina (Reggio Calabria-Italia)

Specola "Giuseppe Pustorino 2" (GORA GC2) -
Palizzi Marina (Reggio Calabria-Italia)

Specola "Giuseppe Pustorino 3" (GORA GC3) -
Palizzi Marina (Reggio Calabria-Italia)

Observatorio de Damián Scotta 1 (GORA ODS) -
San Carlos Centro (Santa Fe-Argentina)

Observatorio Ricardo Nolte (GORA ORN) - Córdoba
(Córdoba-Argentina)

Observatorio de Raúl Melia (GORA RMG) - Gálvez
(Santa Fe-Argentina)

(Received: 2022 June 9)

Synodic rotation periods and amplitudes are reported for: 705 Erminia, 748 Simeisa, 914 Palisana, 983 Gunila, 1043 Beate, and (138971) 2001 CB21

The periods and amplitudes of asteroid lightcurves currently presented are the product of collaborative work by GORA (Grupo de Observadores de Rotaciones de Asteroides) group. In all the studies we have applied relative photometry assigning V magnitudes to the calibration stars.

The image acquisition was performed without filters and with exposure times of a few minutes. All images used were corrected using dark frames and, in some cases, bias and flat-field were also used. Photometry measurements were performed using *FotoDif* software and for the analysis, we employed *Periodos* software (Mazzone, 2012).

Below, we present the results for each asteroid under study. The lightcurve figures contain the following information: the estimated period and period error and the estimated amplitude and amplitude error. In the reference boxes, the columns represent, respectively, the marker, observatory MPC code, or - failing that - the GORA internal code, session date, session offset, and several data points.

Targets were selected based on the following criteria: 1) those asteroids with magnitudes accessible to the equipment of all participants, 2) those with favorable observation conditions from Argentina or Spain and Italy, i.e., with negative or positive declinations δ, respectively, and 3) objects with few periods reported in the literature and/or with light curve Database (LCDB) (Warner et al., 2009b) quality codes (U) of less than 3.

705 Erminia is an X-type asteroid, discovered in 1910 by Ernst Heidelberg. We found in the literature two rather different periods calculated for this object: P = 53.96 ± 0.01 h with Δm = 0.12 ± 0.01 mag (Koff et al., 2006), and P = 7.22 h with Δm = 0.07 mag (Di Martino et al., 1995). The results we obtained are P = 53.416 ± 0.005 h and Δm = 0.09 ± 0.01 mag. Our period well agrees with the one measured by Koff et al. (2006).

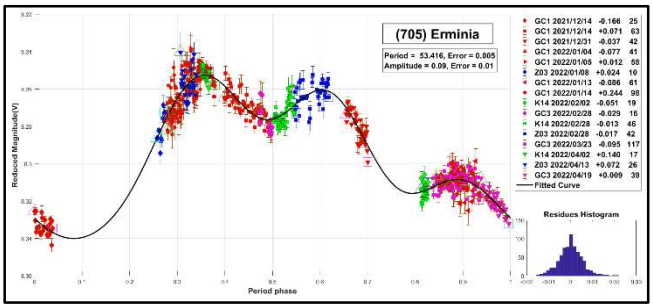

748 Simeisa is a P-type asteroid, discovered in 1913 by G. Neujim. We determined a period of 11.904 ± 0.011 h with Δm = 0.24 ± 0.02 mag. These results well agree with those reported by Dahlgren et al., (1998), P = 11.88 h with Δm = 0.22 mag and Behrend (2011web), P = 11.919 ± 0.002 h with Δm = 0.36 ± 0.03 mag. As a further contribution, our lightcurve provides more coverage on the rotational phase space.

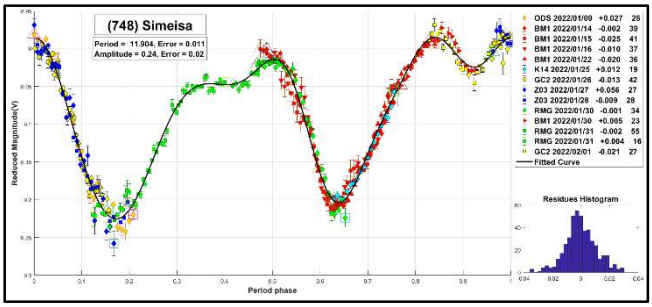

914 Palisana was discovered in 1919 by Wolf, M. We determined a period of 8.681 ± 0.010 h with Δm = 0.11 ± 0.01 mag. However, different authors have reported longer periods: P = 14 h with Δm = 0.02 mag (Tedesco, 1979) and P = 15.922 ± 0.004 h with Δm = 0.04 ± 0.01 mag (Warner, 2009a). In this paper, we present full light curve coverage, with observations made by overlapping different nights and telescopes, thus giving confidence to our result.

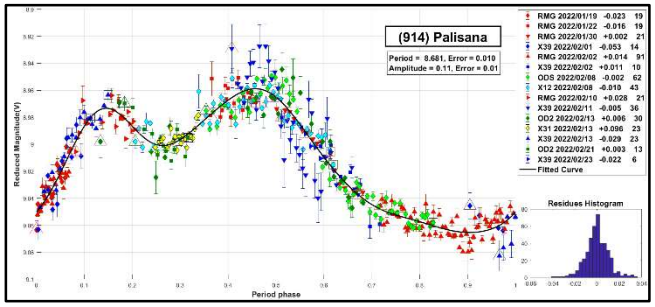

983 Gunila was discovered in 1922 by K. Reinmuth. Different authors attempted to measure the period of this asteroid without success (Warner, 2011; Albers et al., 2010; Shipley et al., 2008). The first reported period for this asteroid was published in 2014 by Hayes-Gehrke et al. (2014), resulting in P = 8.37 ± 0.12 h with Δm = 0.11 ± 0.01 mag. However, years later, Polakis (2019) published a new period, with a value doubling the previous one: P = 16.633 ± 0.023 h with Δm = 0.12 ± 0.02 mag. Our results, P = 16.092 ± 0.012 h with Δm = 0.12 ± 0.02 mag, well agree with those from Polakis (2019).

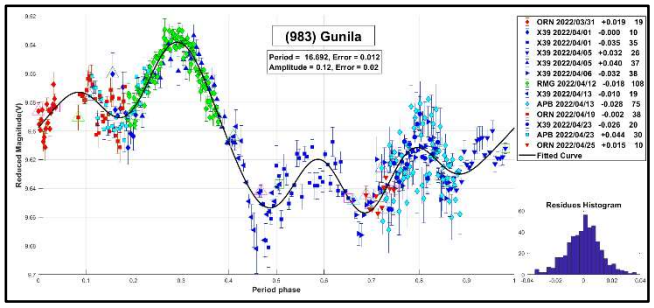

1043 Beate is an S-type asteroid, discovered in 1925 by K. Reinmuth. In the literature, we found only one reported period for this asteroid: P = 44.1 ± 0.1 h (Warner and Higgins, 2006). However, in the same paper, the authors propose a shorter period corresponding to 22.05 ± 0.10 h, though it was considered less plausible. Our study supports the longer period and yielded the following data: P = 43.751 ± 0.011 h with Δm = 0.21 ± 0.02 mag.

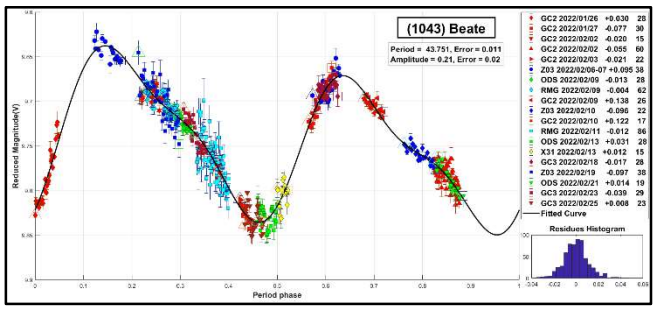

(138971) 2001 CB21 is a near-Earth asteroid, discovered in 2001 by LINEAR. According to the period previously reported, it is a fast rotator, with P = 3.3020 ± 0.0008 h and Δm = 0.12 ± 0.02 mag (Galád et al., 2005). Our observations also support the short-period scenario: P = 3.160 ± 0.034 h with Δm = 0.24 ± 0.05 mag.

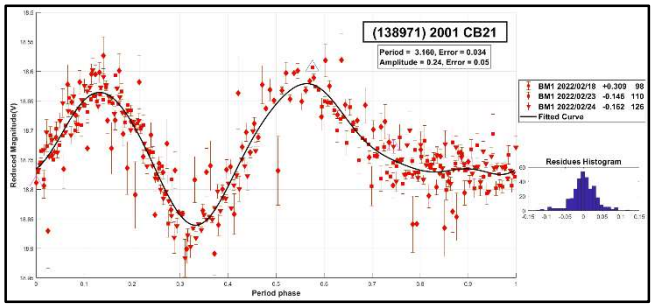

Acknowledgements

We want to thank Julio Castellano as we use his *FotoDif* program for preliminary analyses, Fernando Mazzone for his *Periodos* program, used in final analyses, and Matías Martini for his *CalculadorMDE_v0.2* used for generating ephemerides used in the planning stage of the observations. This research has made use of the Small Bodies Data Ferret (*http://sbn.psi.edu/ferret/*), supported by the NASA Planetary System. This research has made use of data and/or services provided by the International Astronomical Union's Minor Planet Center.

References

Albers, K.; Kragh, K.; Monnier, A.; Pligge, Z.; Stolze, K.; West, J.; Yim, A.; Ditteon, R. (2010). "Asteroid Lightcurve Analysis at the Oakley Southern Sky Observatory: 2009 October thru 2010 April." *Minor Planet Bulletin*, *37*, 152-158.

Behrend, R. (2011web). Observatoire de Geneve web site. *http://obswww.unige.ch/~behrend/page_cou.html*

Dahlgren, M.; Lahulla, J.F.; Lagerkvist, C.-I.; Lagerros, J.; Mottola, S.; Erikson, A.; Gonano-Beurer, M.; Di Martino, M. (1998). "A Study of Hilda Asteroids: V. Lightcurves of 47 Hilda Asteroids." *Icarus* ***133*****(2)**, 247-285.

Di Martino, M.; Dotto, E.; Cellino, A.; Barucci, M.A.; Fulchignoni, M. (1995). "Intermediate size asteroids: Photoelectric photometry of 8 objects." *Astronomy and Astrophysics Supplement Series* **112**, 1.4.

Galád, A.; Pravec, P.; Kušnirák, P.; Gajdoš, Š.; Kornoš, L.; Világi, J. (2005). "Joint lightcurve observations of 10 near-earth Asteroids from Modra and Ondřejov." *Earth, Moon, and Planets* **97(1)**, 147-163.

Harris, A.W.; Young, J.W.; Scaltriti, F.; Zappala, V. (1984). "Lightcurves and phase relations of the asteroids 82 Alkmene and 444 Gyptis." *Icarus* **57(2)**, 251-258.

Hayes-Gehrke, M.; Berenhaus, J.; Mascone, A.; Lopez-Lahocki, M.; Levantis, G.; Haigh, E.; Yang, Z.; Guerci, J.; Wasli, Z.; Koester, K. (2014). "Rotation Period of 983 Gunila." *Minor Planet Bulletin*, **41(2)**, 77.

Number	Name	yy/ mm/dd- yy/ mm/dd	Phase	L_{PAB}	B_{PAB}	Period(h)	P.E.	Amp	A.E.	Grp
705	Erminia	21/12/14-22/04/19	*18.7,20.5	136	23	53.416	0.005	0.09	0.01	MB-O
748	Simeisa	22/01/09-22/02/01	10.5,03.7	143	-02	11.904	0.011	0.24	0.02	HIL
914	Palisana	22/01/19-22/02/23	16.7,12.3	161	-30	8.681	0.010	0.11	0.01	MB-I
983	Gunila	22/03/31-22/04/25	*07.7,07.1	203	-14	16.692	0.012	0.12	0.02	MB-O
1043	Beate	22/01/26-22/02/25	*06.2,05.1	142	-03	43.751	0.011	0.21	0.02	MB-O
138971	2001 CB21	22/02/18-22/02/25	42.6,54.5	172	20	3.160	0.034	0.24	0.05	NEA

Table I. Observing circumstances and results. The phase angle is given for the first and last date. If preceded by an asterisk, the phase angle reached an extremum during the period. L_{PAB} and B_{PAB} are the approximate phase angle bisector longitude/latitude at mid-date range (see Harris et al., 1984). Grp is the asteroid family/group (Warner et al., 2009b). HIL Hilda; MB-O: main-belt outer; MB-I: main-belt inner.

Observatory	Telescope	Camera
K14 Obs.Astr.de Sencelles	Newtoniano (D=250mm; f=4.0)	CCD SBIG ST-7XME
X12 Obs.Astr.Los Cabezones	Newtoniano (D=200mm; f=5.0)	CMOS QHY 174M GPS
X31 Obs.Astr.Galileo Galilei	RCT ap (D=405mm; f=8.0)	CCD SBIG STF8300M
X39 Obs.Astr.Antares	Newtoniano (D=250mm; f=4.7)	CCD QHY9 Mono
Z03 Obs.Astr.Río Cofio	SCT (D=254mm; f=6.3)	CCD SBIG ST8-XME
APB Obs.Astr.AstroPilar	Refractor (D=150mm; f=7.0)	CCD ZWO-ASI183
BM1 Oss.Astr.La Macchina del Tempo	Ritchey-Chretien (D250mm; f=8)	CMOS ZWO ASI 1600 MM
GC1 Specola Giuseppe Pustorino 1	Newtoniano (D=254mm; f=4.7)	CCD Atik 383l+Mono
GC2 Specola Giuseppe Pustorino 2	RC (D=400mm; f=8.0)	CCD Atik 383l+Mono
GC3 Specola Giuseppe Pustorino 3	RC (D=400mm; f=5.7)	CCD Atik 383l+Mono
ODS Obs.Astr.de Damián Scotta 1	Newtoniano (D=300mm; f=4.0)	CMOS QHY 174M
ORN Obs.Astr.de Ricardo Nolte	Newtoniano (D=200mm; f=5.0)	CMOS Neptune-M
RMG Obs.Astr.de Raúl Melia	Newtoniano (D=254mm; f=4.7)	CMOS QHY 174M GPS

Table II. List of observatories and equipment.

Koff, R.A.; Pravec, P.; Goncalves, R.; Antonini, P.; Behrend, R.; Pray, D.P. (2006). "Lightcurve photometry of asteroid 705 Erminia." *Minor Planet Bulletin* **33**, 44.

Mazzone, F.D. (2012). Periodos software, version 1.0. *http://www.astrosurf.com/salvador/Programas.html*

Polakis, T. (2019). "Lightcurve Analysis for Seven Main-belt Minor Planets." *Minor Planet Bulletin* **46**, 78-80.

Shipley, H.; Dillard, A.; Kendall, J.; Reichert, M.; Sauppe, J.J.; Shafer, N.; Kleeman, T.; Ditteon, R. (2008). "Asteroid Lightcurve Analysis at the Oakley Observatory - September 2007." *The Minor Planet Bulletin* ***35***, 99-102.

Tedesco, E.F. (1979). *A Photometric Investigation of the Colors, Shapes and Spin Rates of Hirayama Family Asteroids* (Doctoral dissertation, New Mexico State University).

Warner, B.D.; Higgins, D. (2006). "The lightcurves of 1043 Beate and 1186 Turnera." *Minor Planet Bulletin* **33**, 104-105.

Warner, B.D. (2009a). "Asteroid Lightcurve Analysis at the Palmer Divide Observatory: 2008 September-December." *Minor Planet Bulletin* **36**, 70-73.

Warner, B.D.; Harris, A.W.; Pravec, P. (2009b). "The Asteroid Lightcurve Database." *Icarus* **202**, 134-146. Updated 2022 Feb. *http://www.minorplanet.info/lightcurvedatabase.html*

Warner, B.D. (2011). "Upon Further Review: IV. An Examination of Previous Lightcurve Analysis from the Palmer Divide Observatory." *Minor Planet Bulletin* ***38***, 52-54.

PHOTOMETRY OF 25 LARGE MAIN-BELT ASTEROIDS WITH TRAPPIST-NORTH AND -SOUTH

Marin Ferrais, Pierre Vernazza, Laurent Jorda
Aix Marseille Université, CNRS, LAM, Laboratoire d'Astrophysique de Marseille, Marseille, France
marin.ferrais@lam.fr

Emmanuël Jehin, Francisco J. Pozuelos, Jean Manfroid
Space sciences, Technologies & Astrophysics Research (STAR) Institute
Université de Liège
Allée du 6 Août 19, 4000 Liège, Belgium

Youssef Moulane
Physics Department, Auburn University, AL 36832, USA

Khalid Barkaoui
Astrobiology Research Unit, Université de Liège,
Allée du 6 Août 19C, 4000 Liège, Belgium
Department of Earth, Atmospheric and Planetary Science, Massachusetts Institute of Technology, 77 Massachusetts Avenue, Cambridge, MA 02139, USA
Instituto de Astrofísica de Canarias (IAC), Vía Láctea, 38205 La Laguna, Tenerife, Spain

Zouhair Benkhaldoun
Oukaïmenden Observatory,
Cadi Ayyad University, Marrakech, Morocco

(Received: 2022 June 8)

Densely sampled lightcurves of 25 large main-belt asteroids were obtained with the TRAPPIST-South (TS) and TRAPPIST-North (TN) telescopes from 2017 to 2021. Those observations took place in support of an ESO large program aiming at observing a representative sample of large asteroids with the ESO VLT for precise shape determination from adaptive optics high-resolution imaging. Synodic rotation periods and lightcurve amplitudes have been determined for all but one target. Six asteroids were observed during two different apparitions. The data have been submitted to the ALCDEF database.

Observations were acquired with the robotic telescopes TRAPPIST-North (TN, Z53) and TRAPPIST-South (TS, I40) of the Liège University (Jehin et al., 2011). They are located, respectively, at the Oukaïmeden Observatory in Morocco and the ESO La Silla Observatory in Chile. Both are 0.6-m Ritchey-Chrétien telescopes operating at f/8 on German Equatorial mounts. The TN camera is an Andor IKONL BEX2 DD (0.60 arcsec/pixel) and the one of TS is an FLI ProLine 3041-BB (0.64 arcsec/pixel).

The raw images were calibrated with corresponding flat fields, bias, and dark frames, and photometric measurements were obtained using *IRAF* (Tody, 1986) scripts. The differential photometry and lightcurves were made with Python scripts. All the stars with a high enough SNR were used and checked to discard the variable stars for the differential photometry. Various apertures were tested to maximize the SNR. The absolute calibration in the Johnson-Cousins Rc band was then performed using the *Photometry Pipeline* developed by Mommert (2017). This pipeline allows photometric zero-point calibration by matching field stars with catalogs. The photometric catalogs PanSTARRS DR1 and SDSS-R9 were used to match up to 100 stars with solar colors for each image. The rotation periods were determined with the software *Peranso* (Vanmunster, 2018), which implements the FALC algorithm (Harris et al., 1989).

The ESO large program (ID 199.C-0074; PI P. Vernazza) supported by these observations acquired high angular resolution images of 42 large (D > 100km) main-belt asteroids with the adaptive optics instrument (AO) SPHERE at the VLT. It aimed mainly at reconstructing the 3D shape, and therefore density of those bodies to better constrain their formation and evolution. Multiple 3D reconstruction algorithms were used, notably *ADAM* and *SAGE* (Viikinkoski et al., 2015; Bartczak and Dudzinski, 2018). They combine the AO images with data from other sources, most importantly photometric lightcurves, which help to cover the viewing geometries not seen by the AO images. The final results of the program were recently published in Vernazza et al. (2021).

In the lightcurves below the Rc magnitude is plotted as a function of the rotational phase using the period indicated on the plot. The zero phase corresponds to the maximum of the curve and to the Julian Date indicated on the plot (JDo). The solid black line represents a Fourier fit up to an order indicated in the legend, and from which are computed the residuals shown in the bottom panel. The reported amplitude is from the Fourier model curve. For all our targets, the derived synodic periods agreed with previously published results found in the asteroid lightcurve database (LCDB; Warner et al., 2009). All data have been submitted to the ALCDEF database.

7 Iris is an S-type asteroid and the fourth brightest main-belt object due to its bright surface (albedo ~0.28) and small distance from the Sun. It was observed at an angular size of 0.33 arcsec by SPHERE in 2017, revealing its cratered surface (Hanuš et al., 2019). We observed it in 2020 at V ~9 mag.

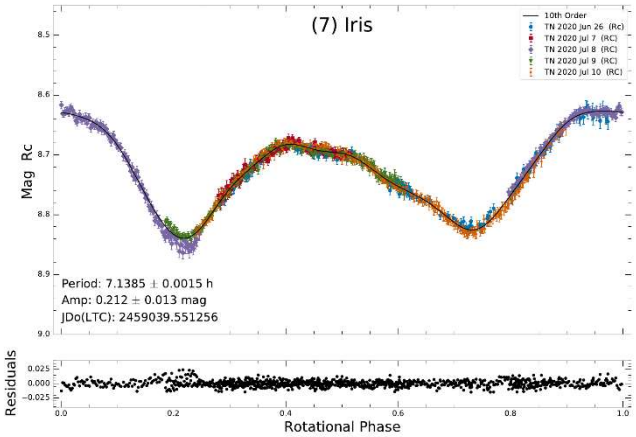

13 Egeria. The whole rotation (period of ~7h) of this Ch-type asteroid was covered in one night with TS in 2019 Aug 19.

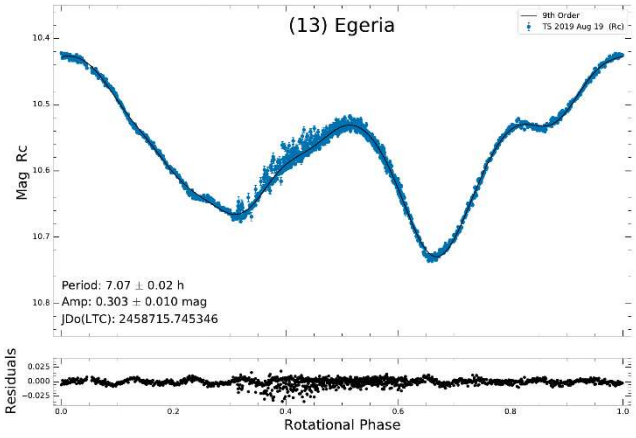

15 Eunomia is an S-type asteroid featuring an elongated shape resulting in the large observed amplitude of the lightcurve of ~0.46 mag while it was in equator-on viewing configuration.

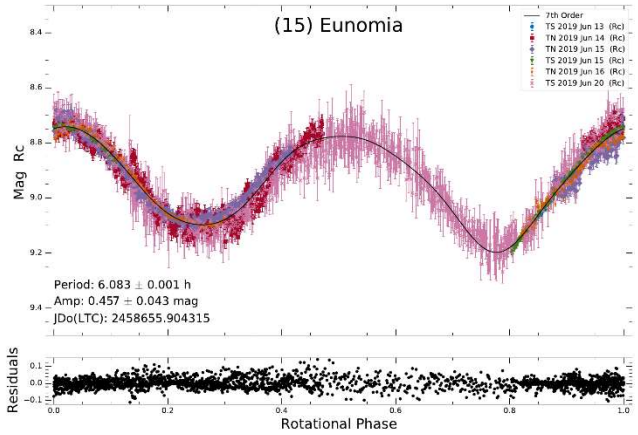

16 Psyche is a very interesting object that will be explored in-situ by a NASA space mission in 2026 (Elkins-Tanton et al., 2017). Psyche has an M-type classification, features metal at its surface and is one of the densest large asteroids known (Ferrais et al., 2020). We observed it in 2018 while it was viewed from its north pole. This explains the small amplitude of the lightcurve that shows only one maximum.

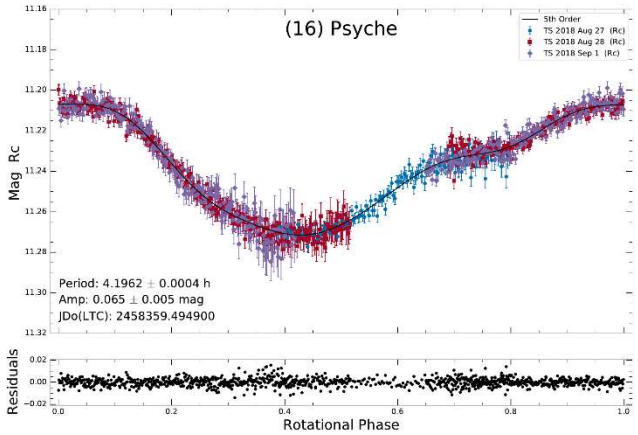

18 Melpomene is an S-type asteroid and is another example of a relatively large amplitude with ~0.3 mag.

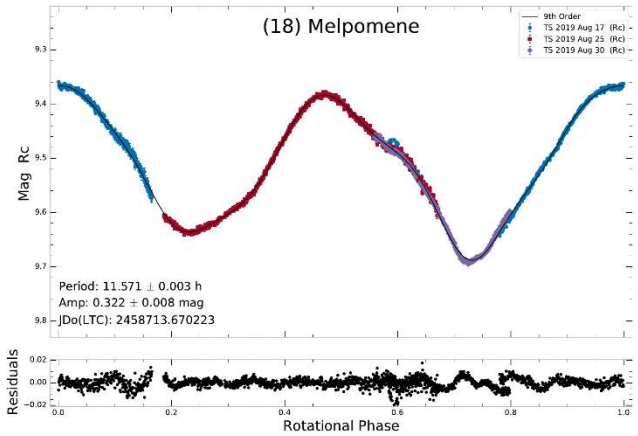

20 Massalia. We observed this S-type asteroid in 2017 and then for another night in 2019. Its rotation period is very close to 8 h, making it challenging to cover the whole rotation with data from consecutive nights. In this context, the combination of observations from both TN and TS was highly beneficial.

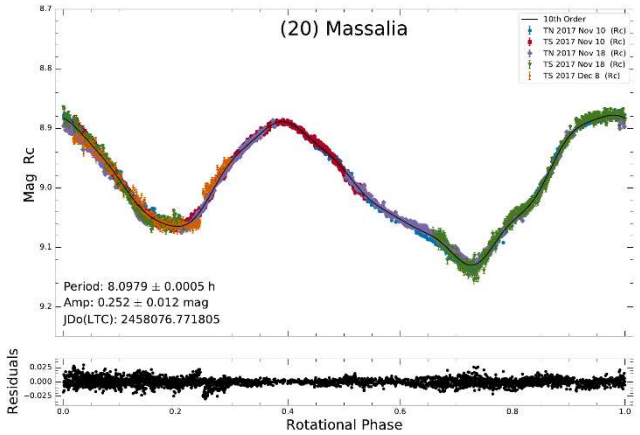

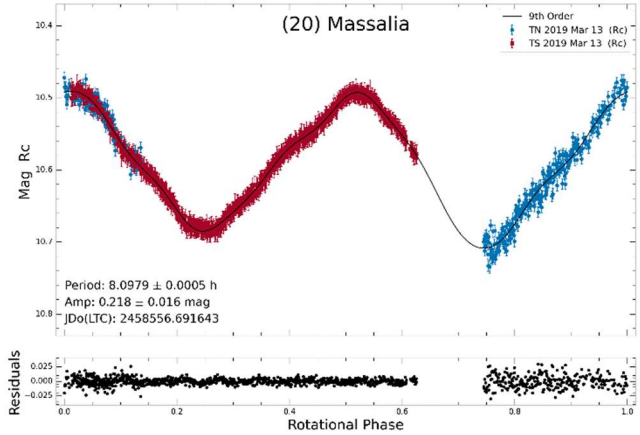

21 Lutetia was the second smallest object of our program (D = 98 km) but was visited by the ESA Rosetta space mission during its journey to comet 67P/C-G (Sierks et al., 2011). We covered the rotation on 2019 Sep. 11 using both TN and TS.

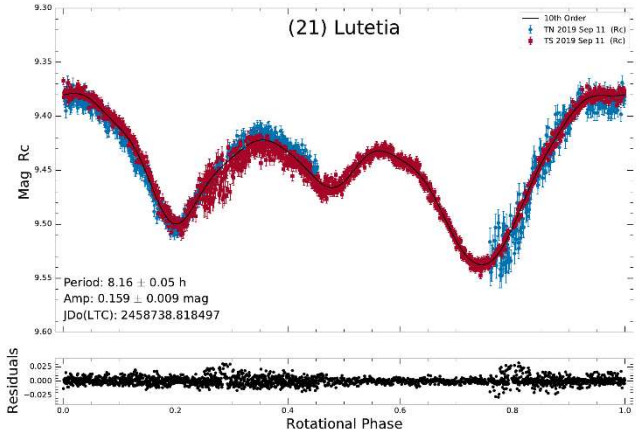

22 Kalliope is a dense M-type asteroid with a probably differentiated interior (Ferrais et al., 2022) and a relatively large companion 28 km in diameter named Linus. Our observations in 2018 were almost pole-on which explains the practically flat lightcurve.

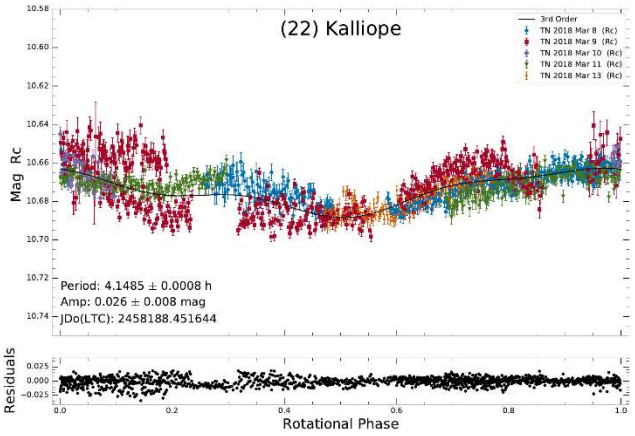

24 Themis is a carbonaceous asteroid and the parent body of one of the largest family. Themis has a relatively spherical shape which resulted in lightcurves of modest amplitudes featuring many bumps for both our 2017 and 2019 observations.

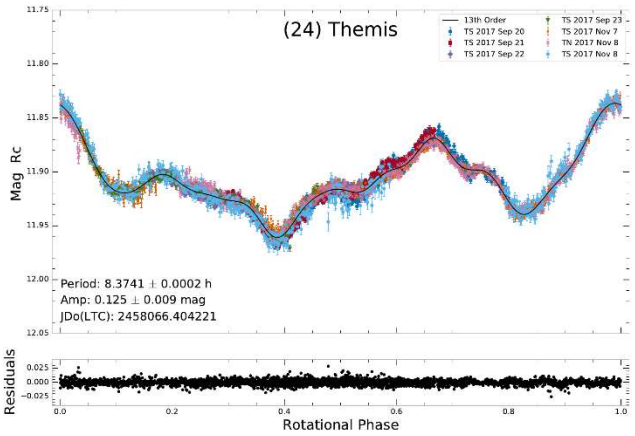

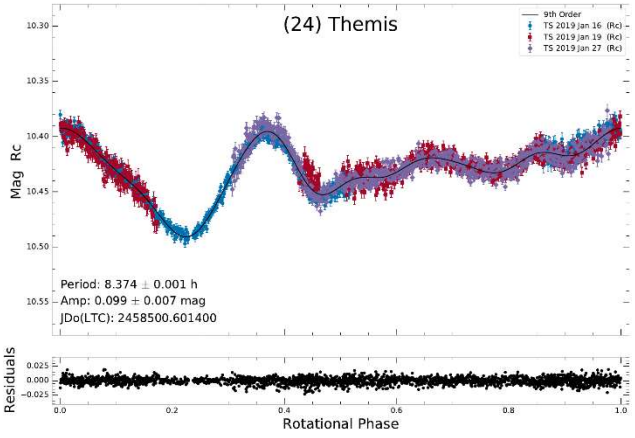

30 Urania is an S-type and with a diameter of 88 km, and it is the smallest asteroid in our sample. Its shape is irregular, and our lightcurve shows an amplitude of 0.26 mag.

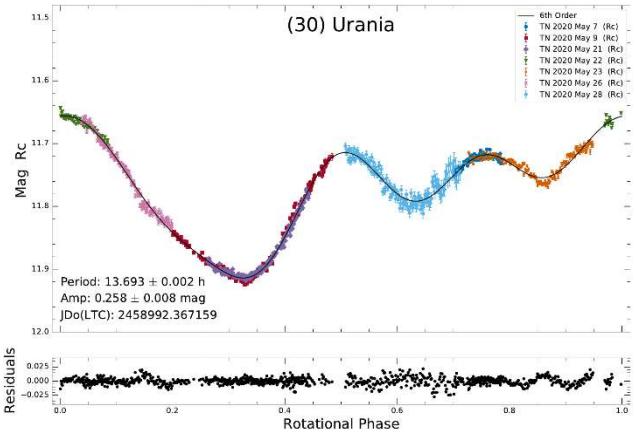

45 Eugenia is a carbonaceous asteroid with two moons. Its short rotation period of ~5.65 h was covered in one night on 2018 Mar 6.

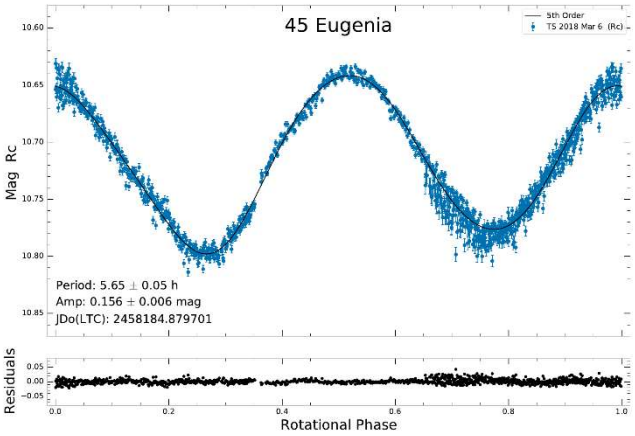

51 Nemausa is a C-type asteroid that we observed in 2019.

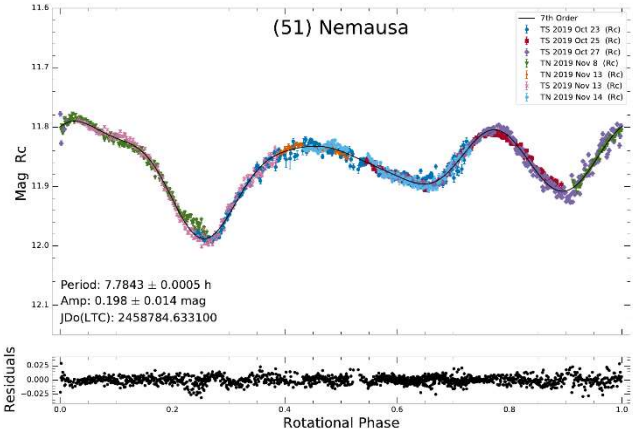

52 Europa is a C-type asteroid with a short period of ~5.58 h that was covered in one night on 2019 Aug. 26.

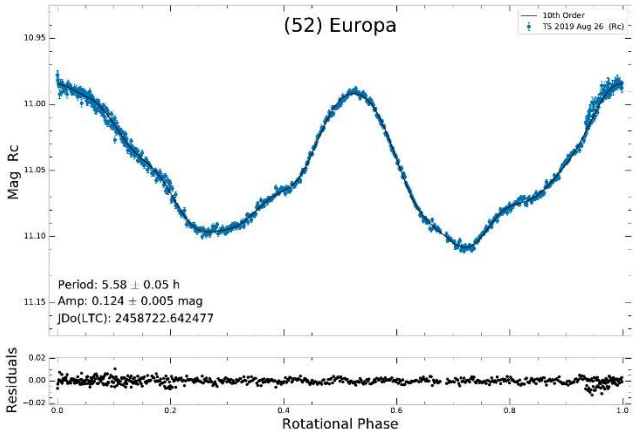

87 Sylvia is a large asteroid located in the outer region of the main belt and the first triple asteroid to be discovered (Marchis et al., 2005). Sylvia is a relatively fast rotator and has an elongated shape as shown by our lightcurve with a period of 5.1837 h and an amplitude of ~0.32 mag.

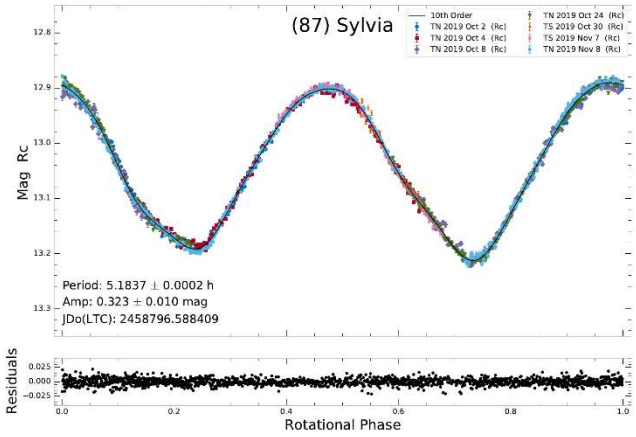

88 Thisbe is a C-type asteroid that we observed during its 2019 apparition.

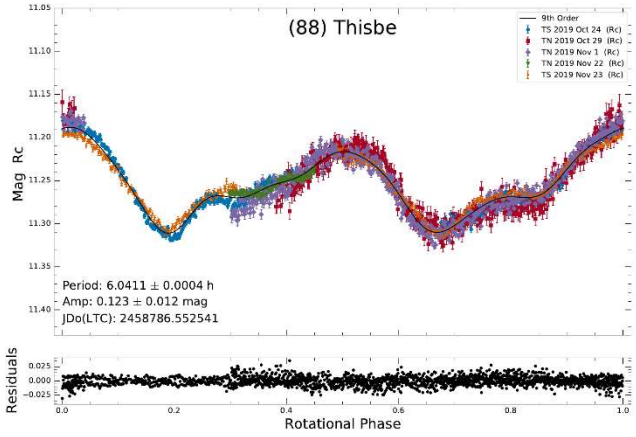

105 Artemis is a C-type asteroid with a period of ~37 h. We acquired 14 series of observations between 2020 Jan. 10 and 2020 Feb. 1 with TN and TS to fully cover its rotational lightcurve.

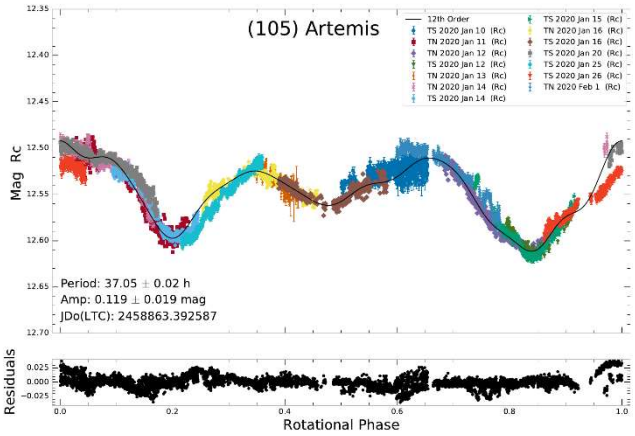

128 Nemesis is a C-type asteroid and a slow rotator. Scaltriti et al. (1979) measured a rotation period of P = 39 h and Pilcher (2015) measured a value double of that, with P = 77.81 ± 0.01 h. Recently, Colazo et al. (2022) published the period P = 38.907 ± 0.006 h. We observed Nemesis in 2021 Feb. and Mar. with TN and TS. Our analysis yields a period P = 38.904 ± 0.006 h that closely agrees with that of Colazo et al. (2022). It must be noted that our data and the shape model of Vernazza et al. (2021) favour the shorter period of ~39h but the double period still cannot be completely ruled out. Finally, we acquired BVRI sequences during five different nights to measure Nemesis' colors. The obtained color indexes are: BV = 0.406 ± 0.032, VR = 0.795 ± 0.014, VI = 0.718 ± 0.028.

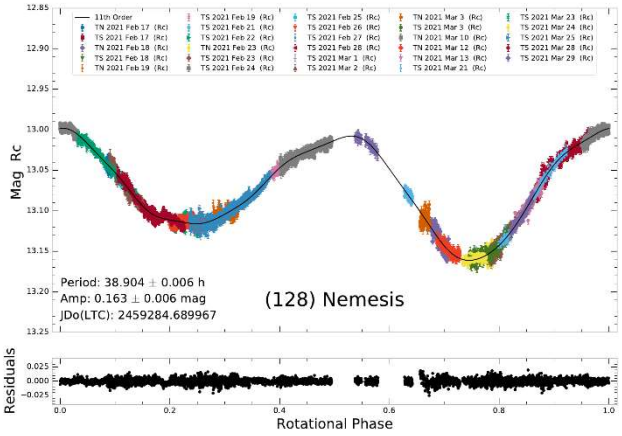

145 Adeona is a C-type asteroid that we observed in 2018. The lightcurve amplitude is small (0.064 mag) but Adeona was bright at that time with V ~11.6, resulting in good quality data.

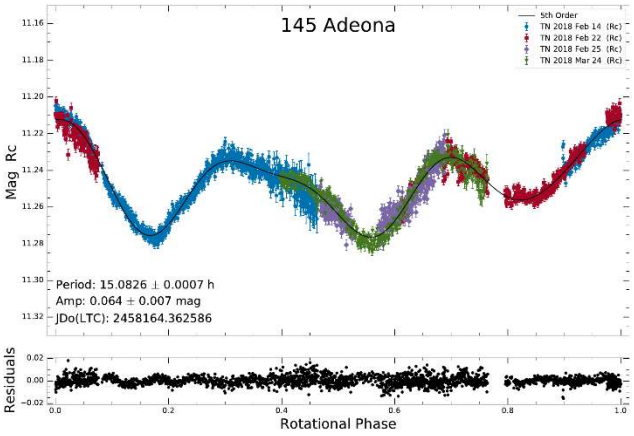

187 Lamberta. The lightcurve of this C-type asteroid was covered in two nights in May 2018 with TS.

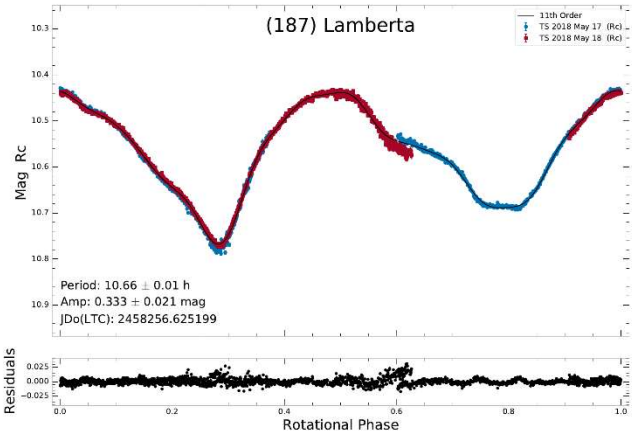

216 Kleopatra. A very smooth lightcurve was obtained from our 2021 observations of this fascinating M-type, dog-bone shaped asteroid with two moons (see e.g., Marchis et al., 2021).

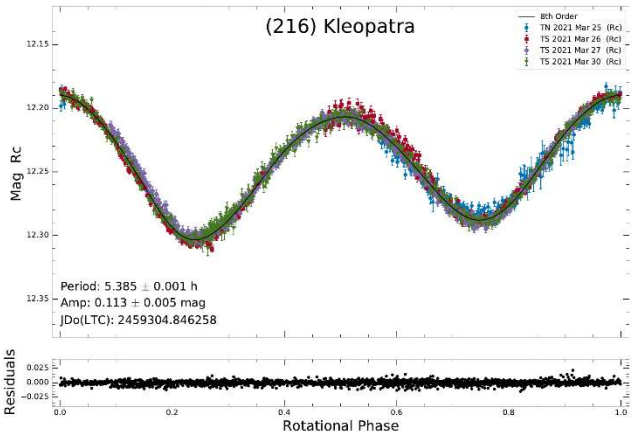

324 Bamberga is a large C-type asteroid with a regular and spherical shape. It results in small brightness changes during its rotation and makes more challenging the shape and spin axis determination. To help constrain these parameters, we regularly observed Bamberga during two months in 2019, from Feb. 19 to Apr. 18, and in Feb. 2020. In total we acquired more than 15000 data points. A spin solution was found by *SAGE* and presented in Vernazza et al. (2021).

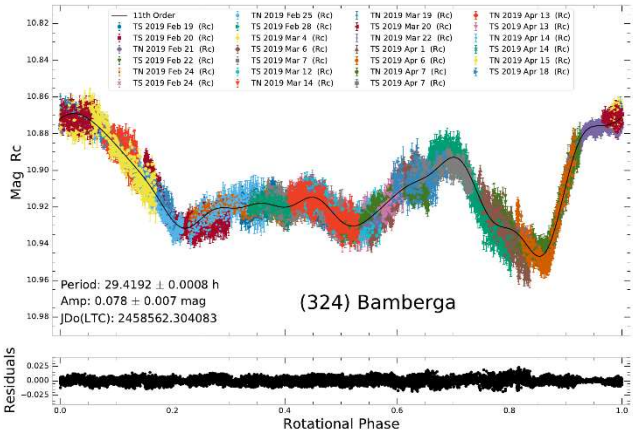

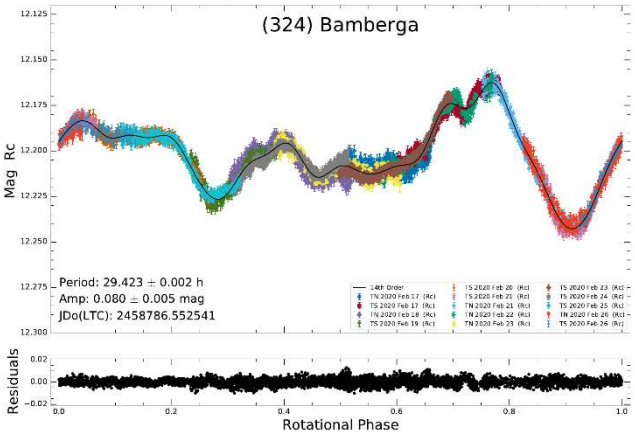

354 Eleonora is a stony asteroid that we observed in 2020 with TN. While the first four observations were taken within nine days, 19 days separate them from the last one on May 27. The solar phase angle increased from 12 to 18 degrees and the shape of the last curve has slightly changed.

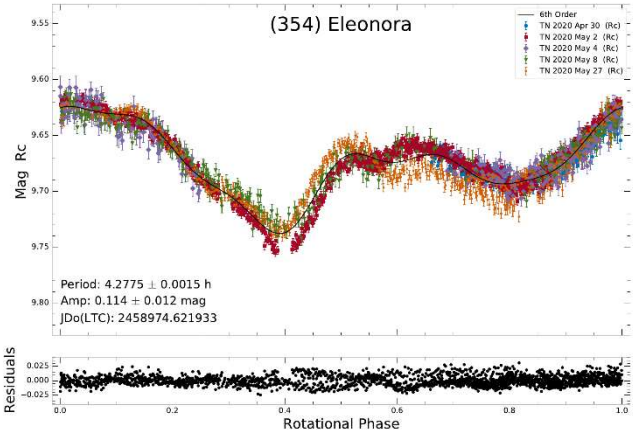

476 Hedwig. Three series of data were obtained for this long period asteroid in 2017 resulting in an incomplete lightcurve. The plot below shows the absolute magnitude H.

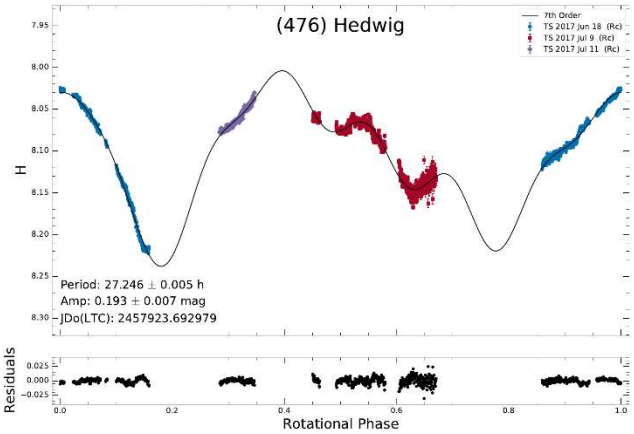

596 Scheila was observed during two nights in 2017 and more densely during its 2019 apparition. The two lightcurves show small amplitudes of 0.061 and 0.070 mag, respectively.

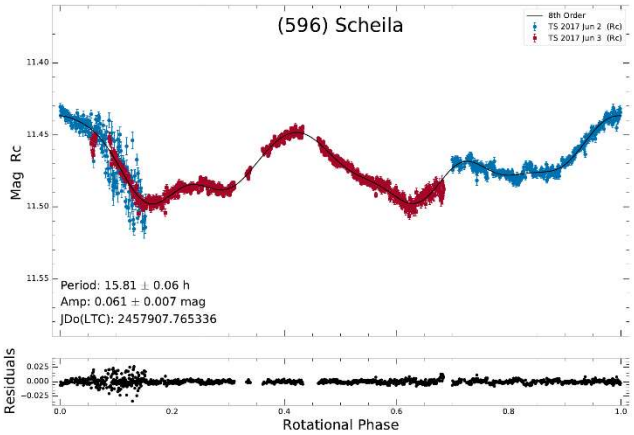

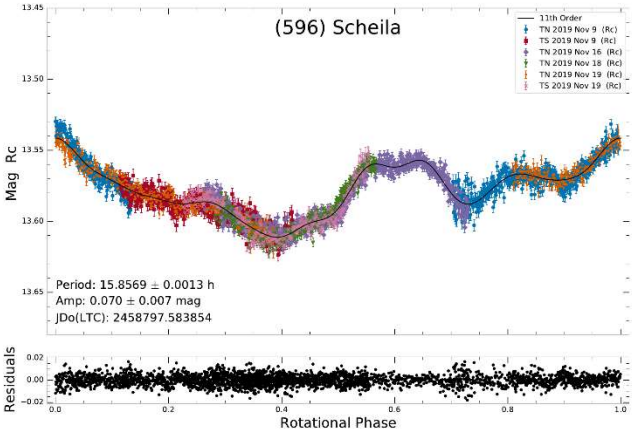

704 Interamnia is the fifth largest main-belt asteroid with a diameter of 332 km and a regular shape. We observed Interamnia in 2018 and 2019 and obtained dense lightcurves with amplitudes of 0.042 and 0.043 mag, respectively. A shape model and spin-state solution are presented in Hanuš et al. (2020).

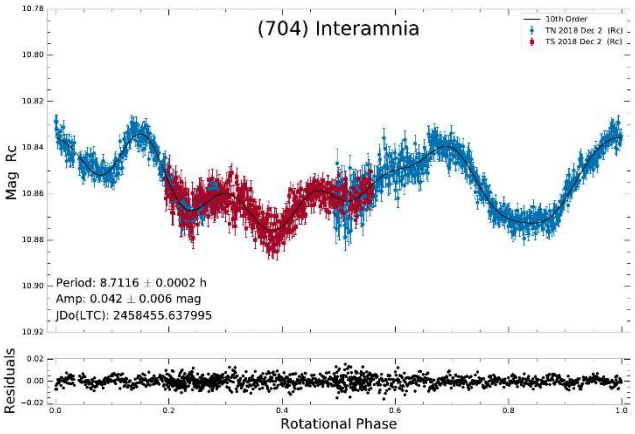

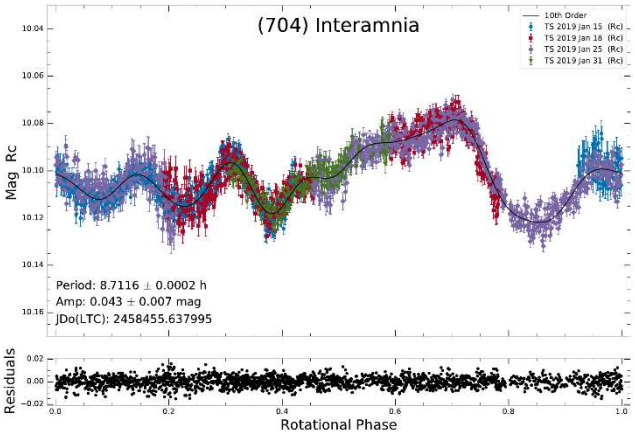

Acknowledgements

TRAPPIST is a project funded by the Belgian Fonds (National) de la Recherche Scientifique (F.R.S.-FNRS) under grant PDR T.0120.21. TRAPPIST-North is a project funded by the University of Liège, in collaboration with the Cadi Ayyad University of Marrakech (Morocco). E. Jehin is FNRS Senior Research Associate. The website of the TRAPPIST project can be visited at *https://www.trappist.uliege.be*.

References

Bartczak, P.; Dudzinski, G. (2018). "Shaping asteroid models using genetic evolution (SAGE)." *MNRAS* **473**, 5050-5065.

Colazo, M.; Morales, M.; Fornari, C.; and 21 colleagues (2022). "Photometry and Light Curve Analysis of Eight Asteroids by GORA'S Observatories." *Minor Planet Bull.* **49**, 48-51.

Elkins-Tanton, L.T.; Asphaug, E.; Bell, J.F.; and 21 colleagues (2017). "Asteroid (16) Psyche: Visiting a Metal World." *Lunar Planet. Sci. Conf.* **48**, 1718.

Ferrais, M.; Vernazza, P.; Jorda, L.; and 34 colleagues (2020). "Asteroid (16) Psyche's primordial shape: A possible Jacobi ellipsoid." *Astronomy & Astrophysics* **638**, L15.

Ferrais, M.; Jorda, L.; Vernazza, P.; and 49 colleagues (2022). "M-type (22) Kalliope: A tiny Mercury." *Astronomy & Astrophysics*, forthcoming article.

Number	Name	yyyy mm/dd	Pts	Phase	L_{PAB}	B_{PAB}	Period (h)	P.E.	Amp	A.E.
7	Iris	2020 06/26-07/10	1010	1.1, 6.1	277	2.3	7.1385	0.0015	0.21	0.01
13	Egeria	2019 08/20	1340	9.5	337	-20	7.07	0.02	0.30	0.01
15	Eunomia	2019 06/13-06/20	2681	21.0,19.8	316	3	6.083	0.001	0.46	0.04
16	Psyche	2018 08/27-09/01	1028	18.0,17.7	239	3	4.1962	0.0004	0.07	0.01
18	Melpomene	2019 08/17-08/30	1934	22.4,25.7	284	7	11.571	0.003	0.32	0.01
20	Massalia	2017 11/10-12/09	3228	15.8, 5.0	84	-1	8.0979	0.0005	0.25	0.01
20	Massalia	2019 03/14	1185	21.9	235	0	8.0979	0.0005	0.22	0.02
21	Lutetia	2019 09/11	2177	9.6	3	-4	8.16	0.05	0.16	0.01
22	Kalliope	2018 02/08-03/13	1391	10.0, 8.6	190	14	4.1485	0.0008	0.03	0.01
24	Themis	2017 09/21-11/08	3264	*9.6, 7.1	27	0	8.3741	0.0002	0.12	0.01
24	Themis	2019 01/17-01/28	2099	1.4, 6.0	113	1	8.3740	0.0010	0.10	0.01
30	Urania	2020 05/07-05/28	944	22.0,22.9	167	-2	13.693	0.002	0.26	0.01
45	Eugenia	2018 03/07	1155	5.3	177	4	5.65	0.05	0.16	0.01
51	Nemausa	2019 10/23-11/14	1478	23.4,22.7	319	5	7.7843	0.0005	0.20	0.01
52	Europa	2019 08/27	635	11.1	5	-7	5.58	0.05	0.12	0.01
87	Sylvia	2019 10/03-11/09	1557	15.1,15.2	11	26	5.1837	0.0002	0.32	0.01
88	Thisbe	2019 10/25-11/24	1966	13.5,2.4	66	4	6.0411	0.0004	0.12	0.01
105	Artemis	2020 01/11-02/01	5893	11.7,15.0	106	-27	37.05	0.02	0.12	0.02
128	Nemesis	2021 02/18-03/30	5529	18.8,17.1	235	3	38.904	0.006	0.17	0.01
145	Adeona	2019 02/14-03/24	2272	17.0,25.0	116	11	15.0826	0.0007	0.06	0.01
187	Lamberta	2018 05/17-05/18	2415	15.2,15.6	337	-9	10.66	0.01	0.33	0.01
216	Kleopatra	2021 03/26-03/31	1763	16.0,15.5	247	6	5.385	0.001	0.11	0.01
324	Bamberga	2019 02/20-03/18	10393	12.5,19.9	123	4	29.4192	0.0008	0.08	0.01
324	Bamberga	2020 02/18-02/27	5043	10.7, 8.4	185	-7	29.423	0.002	0.08	0.01
354	Eleonora	2020 05/01-05/27	2167	12.2,18.0	205	22	4.2275	0.0015	0.11	0.01
476	Hedwig	2017 06/19-07/12	1132	*6.1, 5.2	280	-2	27.246	0.005	0.19	0.01
596	Scheila	2017 06/02-06/03	1342	1.8, 2.3	249	0	15.81	0.06	0.06	0.01
596	Scheila	2019 11/09-11/20	2837	6.9, 3.5	68	-2	15.8569	0.0013	0.07	0.01
704	Interamnia	2018 12/02-12/03	1395	14.8,14.7	114	-2	8.7116	0.0002	0.04	0.01
704	Interamnia	2019 01/16-02/01	2112	2.1, 7.0	114	-6	8.7116	0.0002	0.04	0.01

Table I. Observing circumstances and results. Pts is the number of data points. The phase angles are given for the first and last date and a * indicates if it reached a minimum during the period. L_{PAB} and B_{PAB} are the approximate phase angle bisector longitude and latitude at mid-date range (see Harris et al., 1984).

Hanuš, J.; Marsset, M.; Vernazza, P.; and 35 colleagues (2019). "The shape of (7) Iris as evidence of an ancient large impact?" *Astronomy & Astrophysics* **624**, A121.

Hanuš, J.; Vernazza, P.; Viikinkoski, M.; and 56 colleagues (2020). "(704) Interamnia: a transitional object between a dwarf planet and a typical irregular-shaped minor body." *Astronomy & Astrophysics* **633**, A65.

Harris, A.W.; Young, J.W.; Scaltriti, F.; Zappala, V. (1984). "Lightcurves and phase relations of the asteroids 82 Alkmene and 444 Gyptis." *Icarus* **57**, 251-258.

Harris, A.W.; Young, J.W.; Bowell, E.; Martin, L.J.; Millis, R.L.; Poutanen, M.; Scaltriti, F.; Zappala, V.; Schober, H.J.; Debehogne, H.; Zeigler, K.W. (1989). "Photoelectric Observations of Asteroids 3, 24, 60, 261, and 863." *Icarus* **77**, 171-186.

Jehin, E.; Gillon, M.; Queloz, D.; Magain, P.; Manfroid, J.; Chantry V.; Lendl, M.; Hutsemékers, D.; Udry, S. (2011). "TRAPPIST: TRAnsiting Planets and PlanetesImals Small Telescope." *The Messenger* **145**, 2-6.

Marchis, F.; Descamps, P.; Hestroffer, D.; and Berthier, J. (2005). "Discovery of the triple asteroidal system 87 Sylvia." *Nature* **436**, 822.

Marchis, F.; Jorda, L.; Vernazza, P.; and 36 colleagues (2021). "(216) Kleopatra, a low density critically rotating M-type asteroid." *Astronomy & Astrophysics* **653**, A57.

Mommert, M. (2017). "PHOTOMETRYPIPELINE: An Automated Pipeline for Calibrated Photometry." *Astronomy and Computing* **18**, 47-53.

Pilcher, F. (2015) "New Photometric Observations of 128 Nemesis, 249 Ilse, and 279 Thule." *Minor Planet Bull.* **42**, 190-192.

Scaltriti, F.; Zappala, V.; Schober, H.J. (1979). "The Rotations of 128 Nemesis and 393 Lampetia: The Longest Known Periods to Date." *Icarus* **37**, 133-141.

Sierks, H.; Lamy, P.; Barbieri, C.; and 55 colleagues (2011). "Images of Asteroid 21 Lutetia: A Remnant Planetesimal from the Early Solar System." *Science* **334**, 487.

Tody, D. (1986). "The IRAF Data Reduction and Analysis System." *Proc. SPIE Instrumentation in Astronomy VI* **627**, 733.

Vanmunster, T. (2018). *Peranso* software. *www.cbabelgium.com/peranso/*

Vernazza, P.; Ferrais, M.; Jorda, L.; and 40 colleagues (2021). "VLT/SPHERE imaging survey of the largest main-belt asteroids: Final results and synthesis." *Astronomy & Astrophysics* **654**, A56.

Viikinkoski, M.; Kaasalainen, M.; Durech, J. (2015), "ADAM: a general method for using various data types in asteroid reconstruction." *Astronomy & Astrophysics*, **676**, A8.

Warner, B.D.; Harris, A.W.; Pravec, P. (2009). "The Asteroid Lightcurve Database." *Icarus* **202**, 134-146. Updated 2021 Dec. *http://www.MinorPlanet.info/php/lcdb.php*

MAIN-BELT ASTEROIDS OBSERVED FROM CS3: 2022 APRIL-JUNE

Robert D. Stephens
Center for Solar System Studies (CS3)
11355 Mount Johnson Ct., Rancho Cucamonga, CA 91737 USA
rstephens@foxandstephens.com

Daniel R. Coley
Center for Solar System Studies (CS3)
Corona, CA

Brian D. Warner
Center for Solar System Studies (CS3)
Eaton, CO

(Received: 2022 July 5)

CCD photometric observations of 22 main-belt asteroids were obtained at the Center for Solar System Studies (CS3) from 2022 April-June. One revised period from observations obtained in 2005 is also reported.

The Center for Solar System Studies (CS3) has nine telescopes which are normally used in program asteroid family studies. The focus is on near-Earth asteroids, Jovian Trojans and Hildas. When it is not the season to study a family, or when a nearly full moon is too close to the family targets being studied, targets of opportunity amongst the main-belt families were selected.

Table I lists the telescopes and CCD cameras that were used to make the observations. Images were unbinned with no filter and had master flats and darks applied. The exposures depended upon various factors including magnitude of the target, sky motion, and Moon illumination.

Telescope	Camera
0.30-m f/6.3 Schmidt-Cass	FLI Microline 1001E
0.35-m f/9.1 Schmidt-Cass	FLI Microline 1001E
0.35-m f/9.1 Schmidt-Cass	FLI Microline 1001E
0.35-m f/9.1 Schmidt-Cass	FLI Microline 1001E
0.40-m f/10 Schmidt-Cass	FLI Proline 1001E
0.40-m f/10 Schmidt-Cass	FLI Proline 1001E
0.50-m F8.1 R-C	FLI Proline 1001E

Table I: List of CS3 telescope/CCD camera.

Image processing, measurement, and period analysis were done using *MPO Canopus* (Bdw Publishing), which incorporates the Fourier analysis algorithm (FALC) developed by Harris (Harris et al., 1989). The Comp Star Selector feature in *MPO Canopus* was used to limit the comparison stars to near solar color. Night-to-night calibration was done using field stars from the ATLAS catalog (Tonry et al., 2018), which has Sloan *griz* magnitudes that were derived from the GAIA and Pan-STARR catalogs and are "native" magnitudes of the catalog. Those adjustments are usually ≤ ±0.03 mag. The rare greater corrections may have been related in part to using unfiltered observations, poor centroiding of the reference stars, and not correcting for second-order extinction.

The Y-axis values are ATLAS SR "sky" magnitudes. The two values in the parentheses are the phase angle (a) and the value of *G* used to normalize the data to the comparison stars used in the earliest session. This, in effect, made all the observations seem to be made at a single fixed date/time and phase angle, leaving any variations due only to the asteroid's rotation and/or albedo changes. The X-axis shows rotational phase from -0.05 to 1.05. If the plot includes the amplitude, e.g., "Amp: 0.65", this is the amplitude of the Fourier model curve and *not necessarily the adopted amplitude for the lightcurve*.

For brevity, only some of the previously reported rotational periods may be referenced. A complete list is available at the asteroid lightcurve database (LCDB; Warner et al., 2009).

864 Aase. Rotational periods for this member of the Flora dynamical family have been observed several times in the past. Kryszczyńska et al. (2012), Pilcher (2017), Behrend (2019web), and Erasmus et al. (2020) all reported periods near 3.23 h. This year's result is in good agreement with those prior findings.

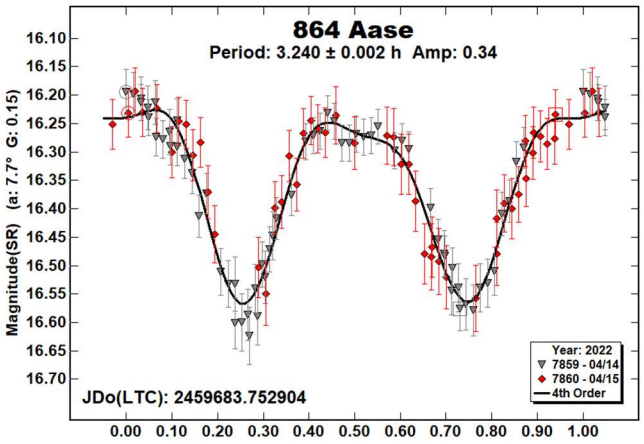

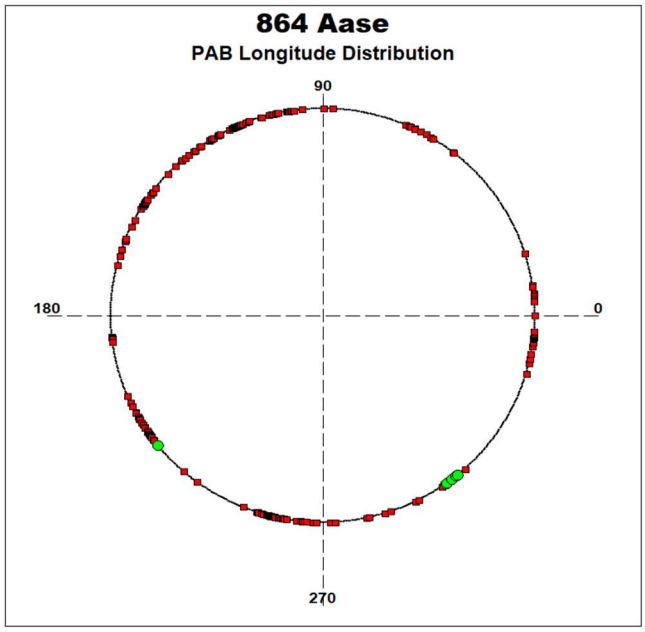

Because of the availability of the Pilcher data on the Asteroid Lightcurve Data Exchange Format database (ALCDEF, 2020) web site, we attempted to create a pole/shape model. We added these two dense data sets to additional sparse data from the AstDyS-2 site (AstDyS-2, 2020). We were able to use sparse data from the ATLAS, Zwicky Transient Factory, and USNO surveys. The following plots show the PAB longitude, latitude and phase angle distributions. Green dots represent the three dense datasets, and red dots represent sparse data from the three surveys.

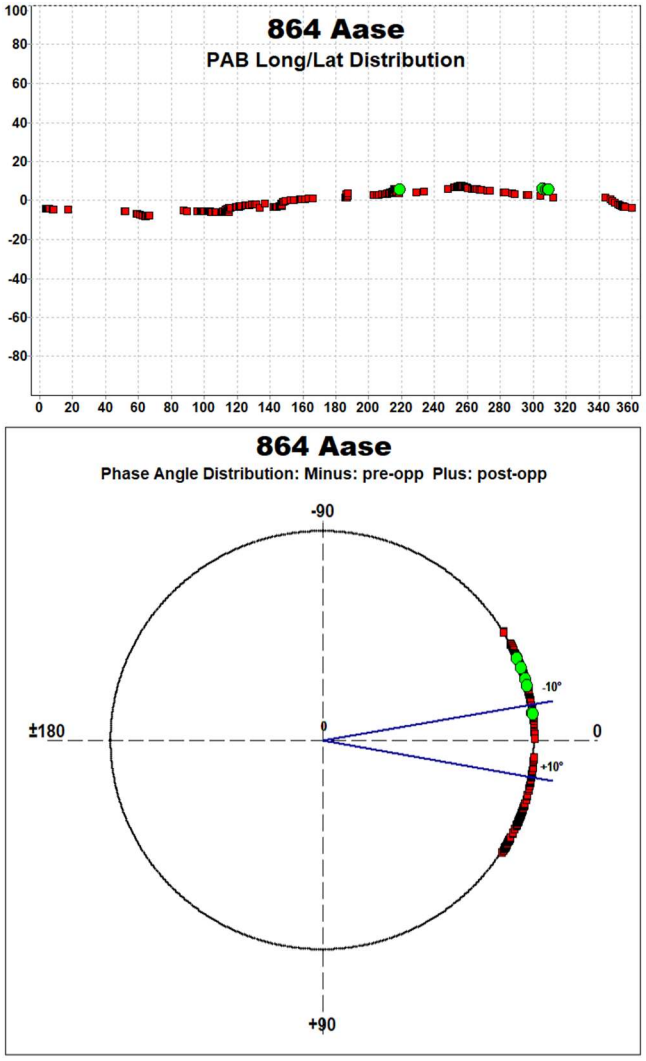

The data were combined using *MPO LCInvert* (Bdw Publishing). This Windows-based program incorporates the algorithms developed by Kaasalainen and Torppa (2001) and Kaasalainen et al. (2001) and converted by Josef Durech from the original FORTRAN to C. A period search was made over a sufficiently wide range to assure finding a global minimum in χ^2 values. The sparse data were weighted between 30% and 50%.

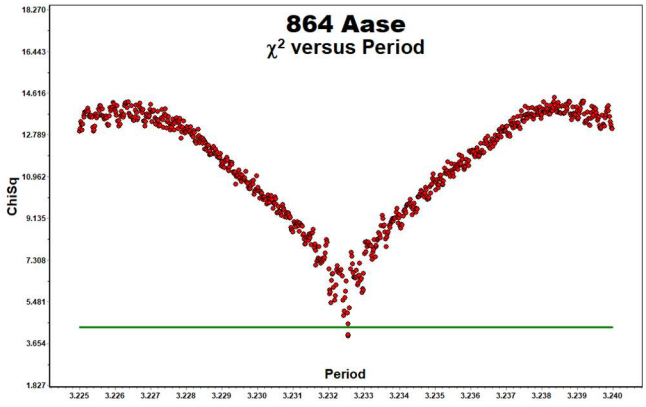

As is often the case, the pole model showed two possible solutions 180° apart; (λ, β, P) = (64°, -77°, 3.23256 h) and (λ, β, P) = (246°, -66°, 3.23256 h). Both solutions are very close to the south ecliptic pole indicating the rotation is retrograde, but makes the longitude of the spin axis hard to find with certainty. Our preferred solution is the (64°, -77°) pole position.

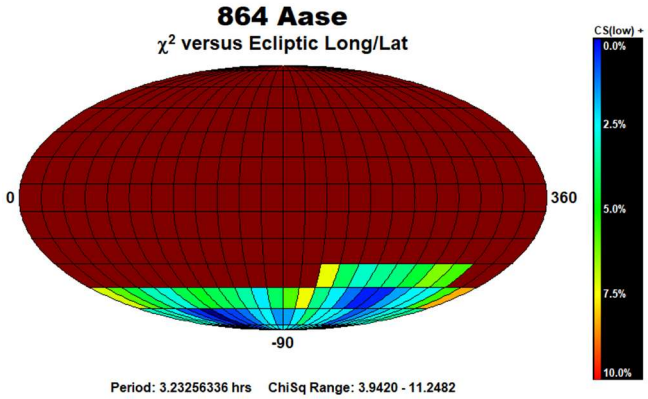

The two pole solutions created similar models, both with a/b ratios of 1.3 and a/c ratios of 1.3 or 1.4.

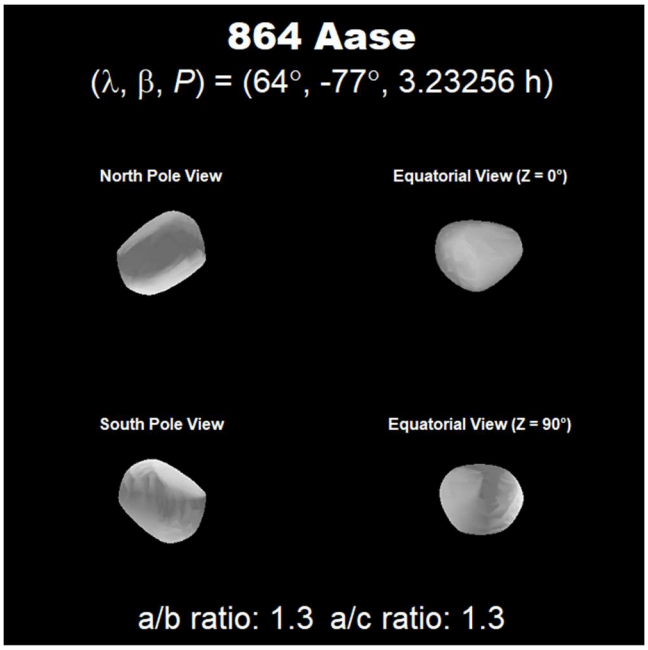

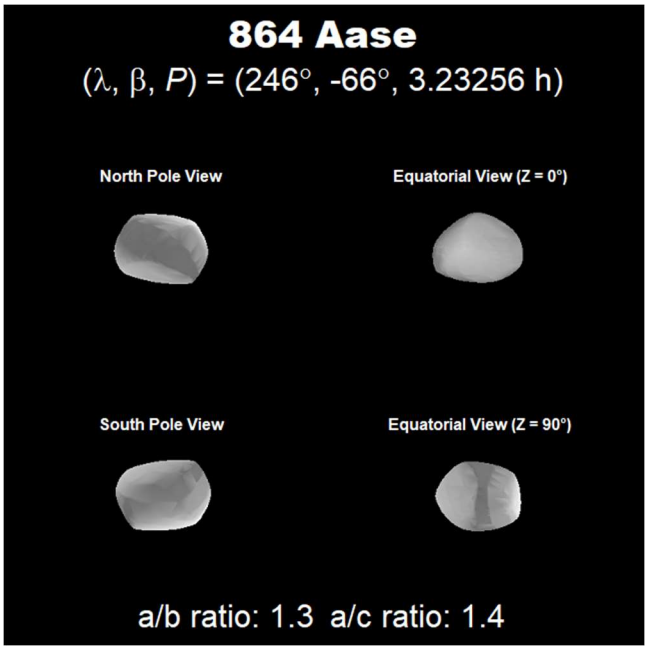

To test the model, the dense datasets were plotted against the predicted lightcurve for each dataset. Each plot resulted in a very good match, giving confidence in the pole/shape model result.

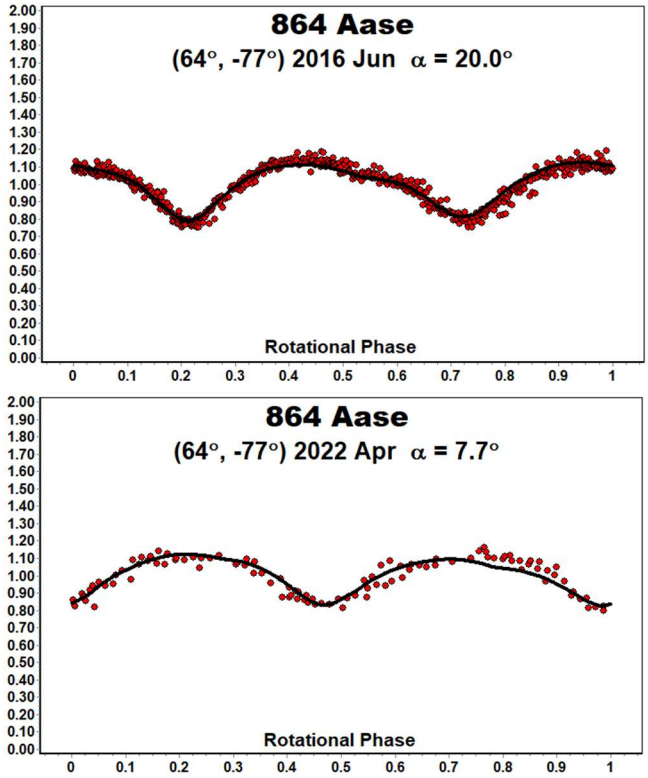

To further refine the model, the next favorable opposition is in 2023 December.

1806 Derice. This member of the Flora dynamical family has been observed many times in the past by the Photometric Survey for Asynchronous Binary Asteroids (Pravec et al., 2009web; 2011web; 2012web; 2016web) as a 'Prime Suspect' of being a binary asteroid, each time finding a period near 3.224 h. We observed it in 2020 (Stephens and Warner; 2020) finding a period of 3.2243 h with slight deviations from the lightcurve, but no indication of a secondary period. Our result this year is in good agreement with those prior results. The sparser data set this year also did not show any indication of a secondary frequency.

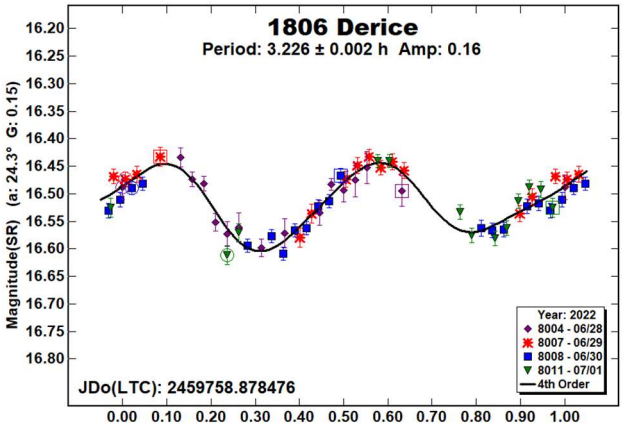

2048 Dwornik. Several periods are reported in the LCDB for this member of the Hungaria dynamical family Warner (2016; and references therein) and Skiff et al. (2019a) report many periods near 3.7 h with an amplitude rarely exceeding 0.16 h. Our result this year is a little faster than those prior results, but the low amplitude and proximity to the galactic bulge makes the result less certain.

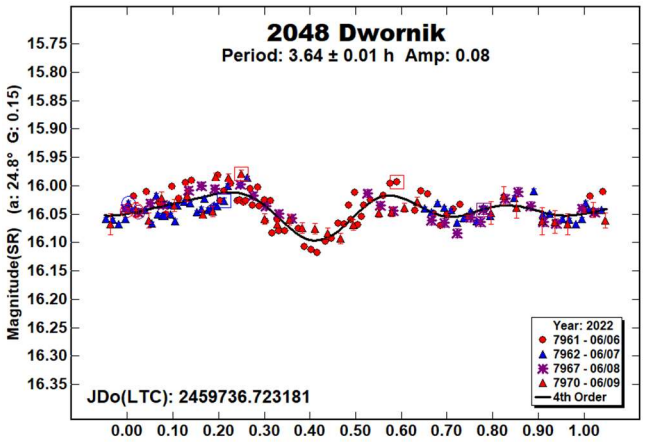

2069 Hubble. We first observed this outer Main-belt asteroid in 2005, obtaining a very noisy dataset where the error bars met or exceeded the amplitude of the lightcurve; the derived period was 32.52 h. Polakis (2022) reported a period of 44.62 h using a much higher-quality data set. This prompted us to revisit our work by first remeasuring the images and using SR (Sloan r′) magnitudes from the ATLAS catalog (Tonry et al., 2018). This gave a significantly cleaner data set with nightly zero-point shifts less than 0.04 mag. Our revised period of 87.3 h is nearly double that found by Polakis. Given our sparse dataset, the two results are in good agreement.

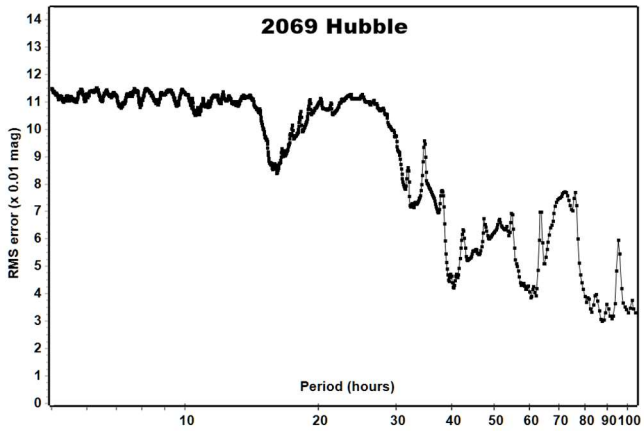

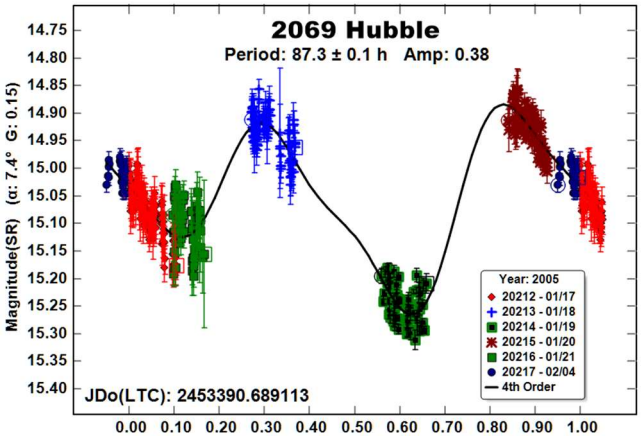

2093 Genichesk. This member of the Baptistina dynamical family has been observed three times in the past. Behrend (2002web) and Warner (2008c) found periods near 11.02 h. Using data from the Palomar Transient Factory Survey, Waszczak et al. (2015) also found a period near 11.02 h. Our result this year is in good agreement with those prior results.

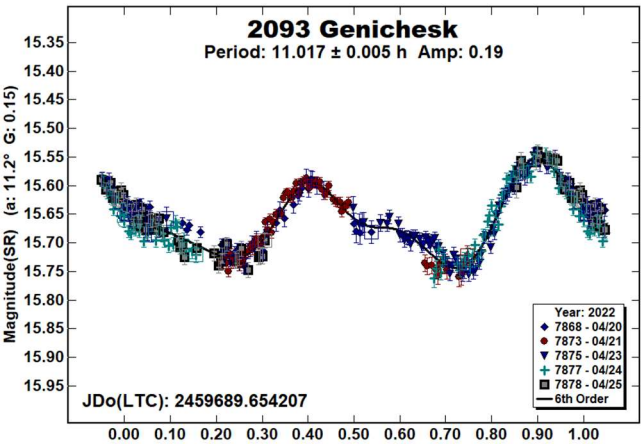

2784 Domeyko. This inner Main-belt asteroid has been observed twice in the past. Almeida et al. (2004) reported a period of 5.98 h. Polakis (2019) found a period of 6.025. Our result this year was a full moon project, and because the period is commensurate with an Earth day, could not completely cover the lightcurve. Still, it is in good agreement with those prior results.

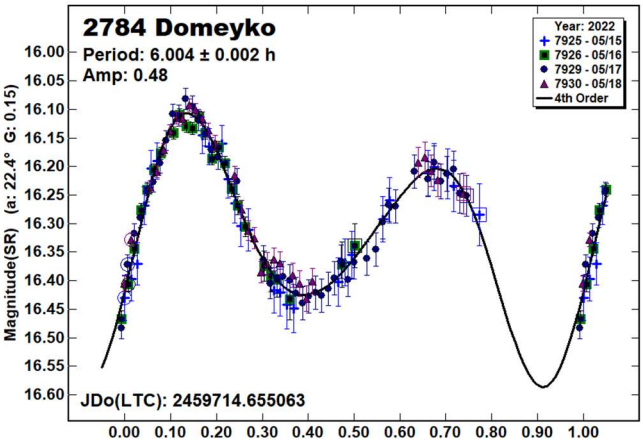

2858 Carlosporter. Carbognani (2014) reported a period of 3.336 h for this member of the Baptistina dynamical family. That period was derived from two sets of observations, two months apart. The first set was a single night, and the second set on three nights spanning two weeks. That second set had a night in which the magnitude of the asteroid dropped, then rose 0.45 magnitude over the course of 30 minutes. While it is possible that was caused by a mutual event, it seems unlikely and was not repeated on any of the other three nights. It is more likely the drop was caused by an observational effect. The earlier single night of observations a month earlier was cleaner and seems to have an amplitude of about 0.10 mag.

Our observations this year occurred near a full moon when the asteroid was also near the galactic bulge. That hampered getting high quality data points. Compounding the situation, the lightcurve was also very low amplitude. A period search suggested a number of possibilities, with the strongest being between 3 and 4 hours. With an amplitude of only 0.05 mag, there is no assurance of a bimodal lightcurve (Harris et al., 2014). However, given Carbognani's first session, it is likely the true period is less than 4 hours.

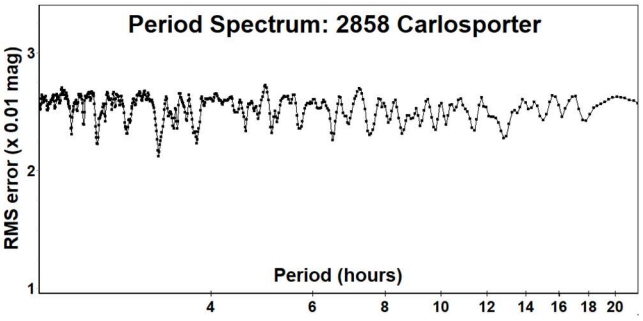

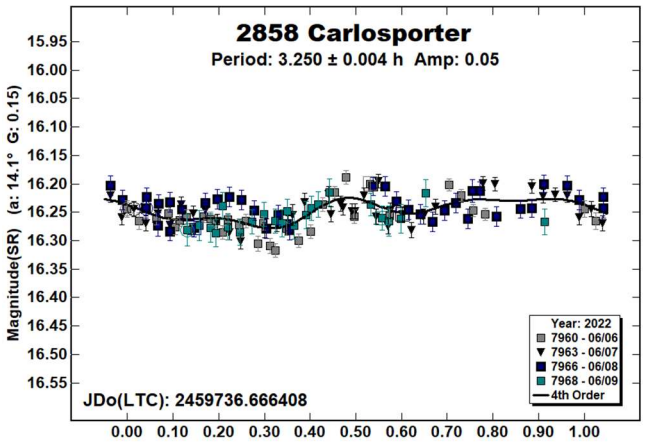

3470 Yaronika. There are only two prior periods in the LCDB for this inner Main-belt asteroid. Ditteon (2019) reported a period of 6.63 h. Also, using data from the ATLAS survey, Ďurech et al. (2020) created a pole/shape model with a sideral period of 6.63157 h. Our results this year is in good agreement with those prior results.

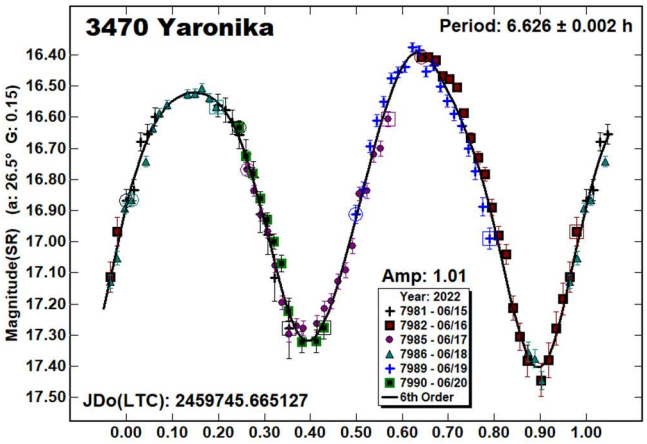

3569 Kumon. This member of the Eunomia family (Nesvorny, 2015; Nesvorny et al., 2015) was observed once before. Clark (2019) reported a period of 7.49 h, but commented that the scatter in the data precluded any reasonable period determination.

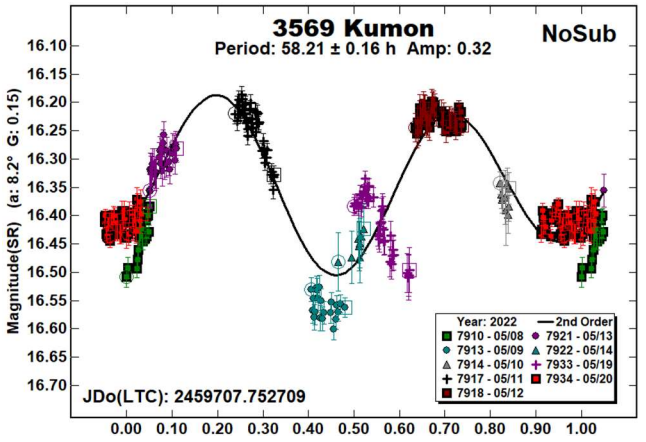

Our observations immediately suggested a long period. The initial analysis showed that the solution was dominated by a period near 58 hours. However, our data showed very distinctive signs of being in a tumbling state ("NoSub" plot). There were signs of a second period, one that was unlikely due to a satellite.

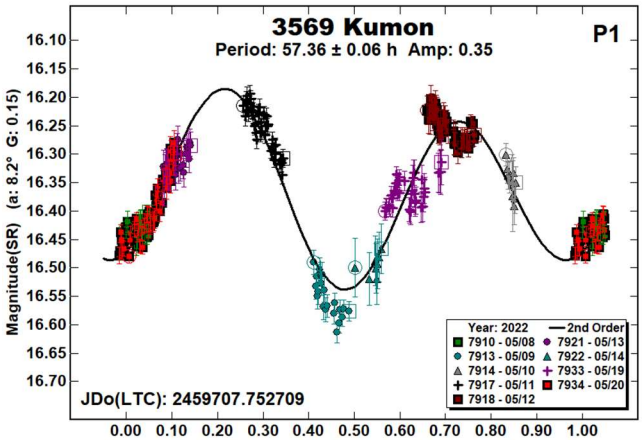

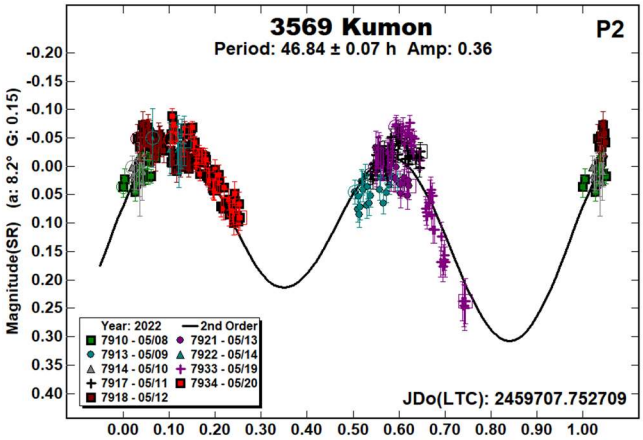

A dual-period search was done using *MPO Canopus*, which is not equipped to work with tumbling asteroids. This resulted in a pretty good fit to a period of 57.36 h ("P1"), close to the single-period solution. It is highly unlikely that the secondary period lightcurve near 47 h ("P2") has a physical cause, other than the asteroid being a tumbler.

3894 Williamcooke. This member of the Eunomia dynamical family has been observed three times in the past. Macias (2015) found a period of 3.10 h, but it was a quadrimodal lightcurve with an amplitude of 0.09 mag. With an amplitude of only 0.10 mag., there is no assurance of a bimodal lightcurve (Harris et al., 2014).

In 2018 July, we found a period of 4.16 h with an amplitude of 0.20 mag. (Stephens 2019). The 2015 Macias period is a 3:4 alias of the 4.16 h period we found in 2018. Also in 2018 July, Behrend (2018web) reported a period of 8.3343 h. That lightcurve had six extrema and is a 2:1 alias of our period.

Our period this year is in good agreement with our prior result, with the lowest amplitude seen to date. The period spectrum shows possible solutions near 2.6 h, 4.2 h, and 5.2 h, and with such a low amplitude, single modal, bimodal, trimodal, and quadrimodal lightcurves are all possible. We tried rephasing the lightcurve to the 3.10 h Macias period, and excluded it as a possibility. The 2.6 h period produced a bimodal lightcurve. Our 2018 data could not be phased to that period. By the process of elimination, a 4.173 h period was the only period that could be phased to both our 2018 and 2022 data.

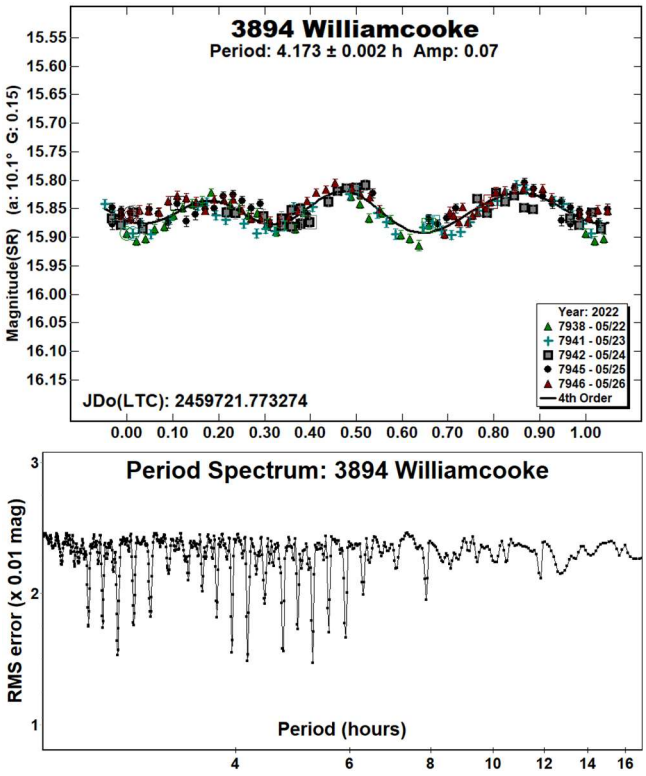

3936 Elst. There is only one previously reported period in the LCDB for this Vestoid. Pravec et al. (2007web) reported a period of 6.6322 h. Our result this year is in good agreement with the Pravec et al. period.

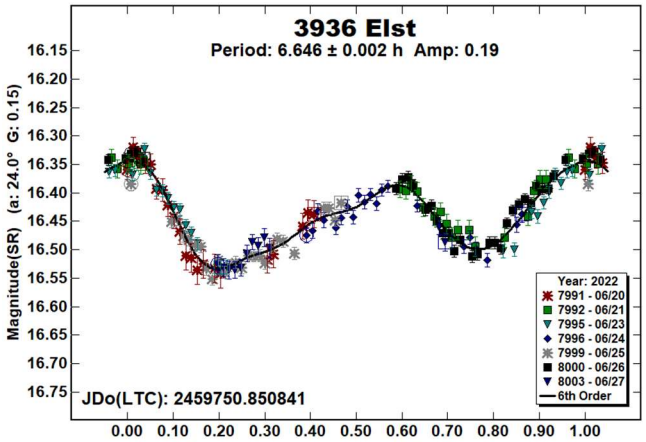

5720 Halweaver. Two rotational periods were found in the LCDB for this Mars-crosser. Warner (2008b) reported a period of 3.8883 h. Using data from the TESS spacecraft, Pál et al. (2020) found a period of 3.88689 h. This year's result is in good agreement with those prior findings.

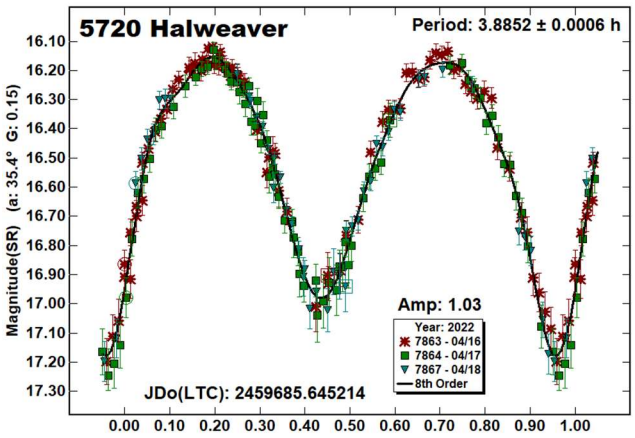

Because of our previous data from 2008, the availability of the Pál et al. data, and other unpublished data from Hopkins on the Asteroid Lightcurve Data Exchange Format database (ALCDEF, 2020) web site, we attempted to create a pole/shape model. We added additional sparse data from the AstDyS-2 site (AstDyS-2, 2020). We were able to use sparse data from ATLAS, Zwicky Transient Factory and the Catalina Sky Survey. The following plots show the PAB longitude, latitude and phase angle distributions. Green dots represent the three dense datasets, and red dots represent sparse data from the three surveys. The Pál et al. data is located at (PABL = 244°, PABB = -10°, Phase = 5.2°).

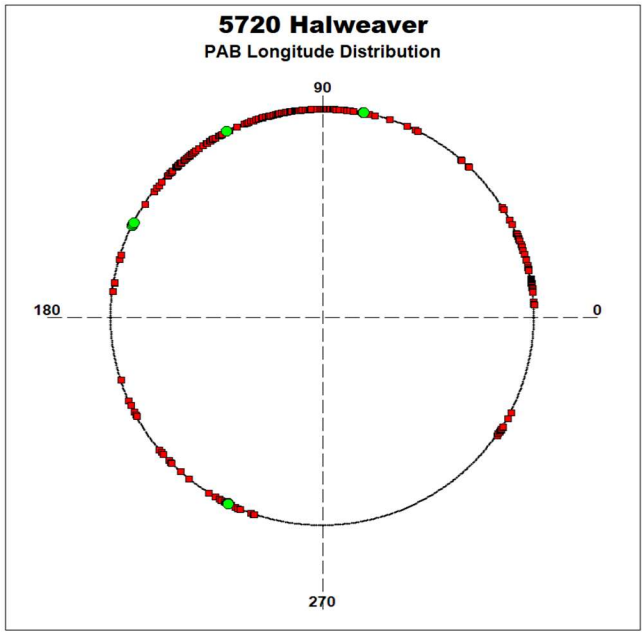

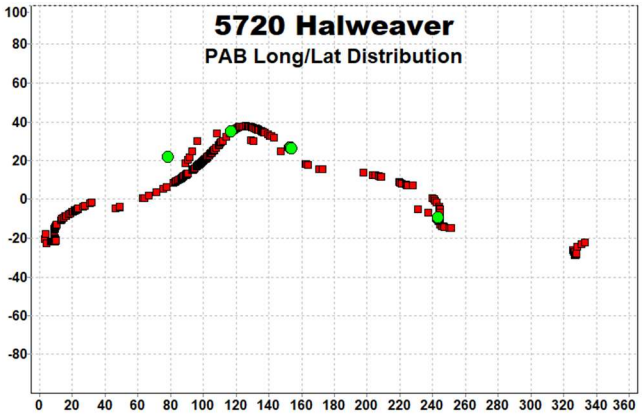

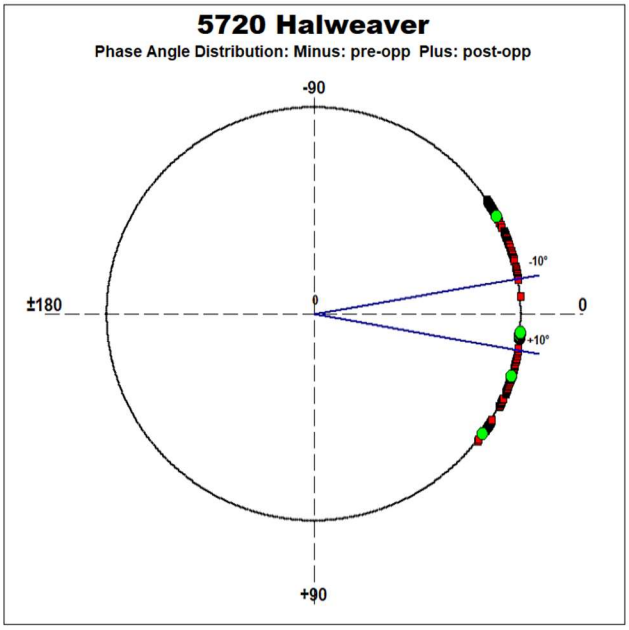

The data were combined using *MPO LCInvert* (Bdw Publishing) described in the 864 Aase section of this article. Only two unique periods below the 10% χ^2 line was found.

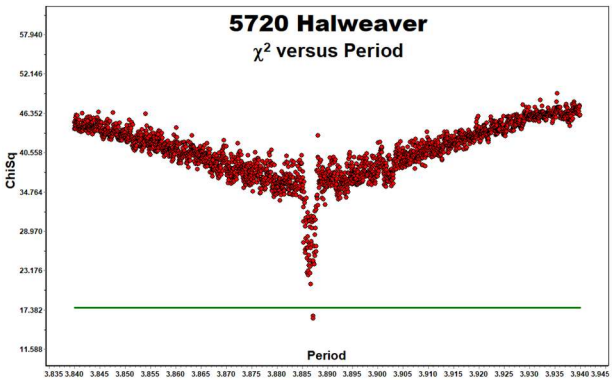

Only one unique solution was found (172°, -80°). It was within 10 degrees of the south ecliptic pole, indicating the rotation is retrograde, but because of its proximity to the pole, the longitude can be ambiguous.

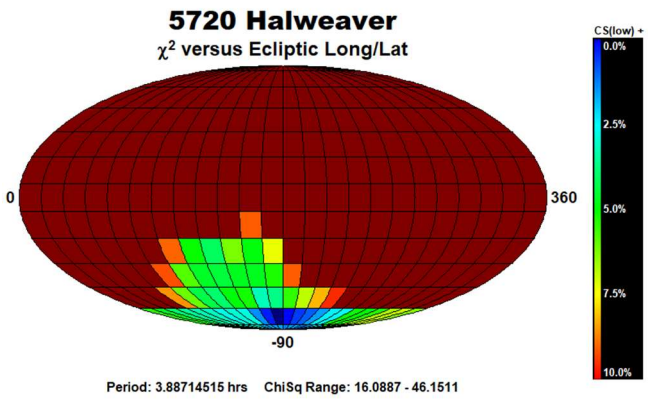

The resulting model presents an elongated body. This is expected given that all of the amplitudes reported in the LCDB are between 0.45 and 1.02 mag.

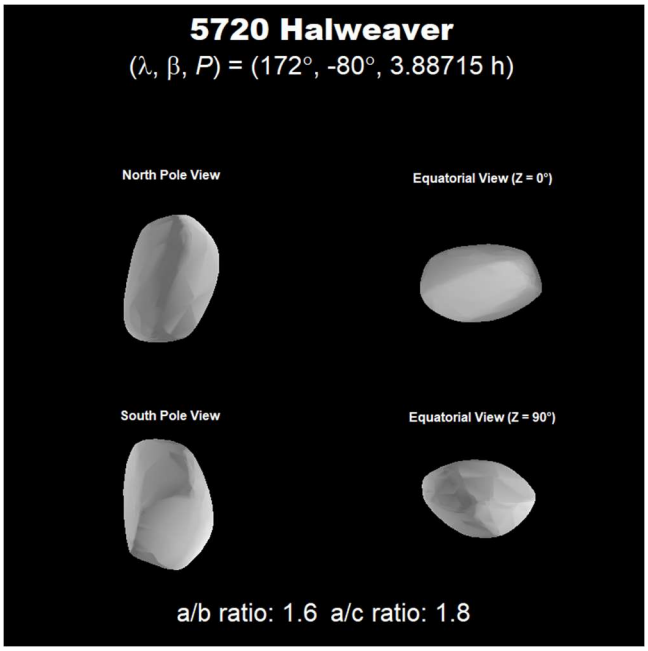

To test the model, these dense datasets were plotted against the predicted lightcurve for each dataset. Each plot for the (172°, -80°) pole position resulted in a good match. Even the Pál et al data from the TESS spacecraft, which had an expected number of outliers, was a good match to the predicted lightcurve giving high confidence in the pole/shape model result. The 2022 Jan. plot was a single night, unpublished lightcurve found in the Asteroid Lightcurve Data Exchange Format database.

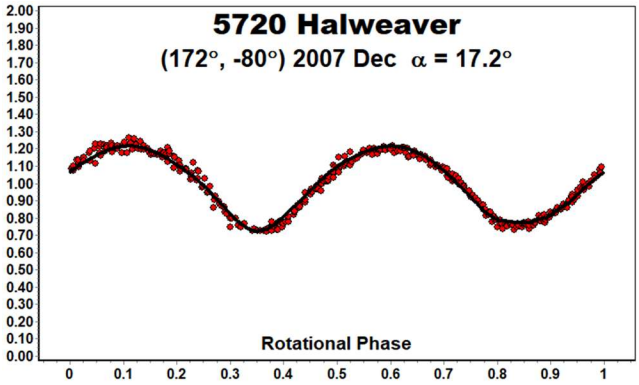

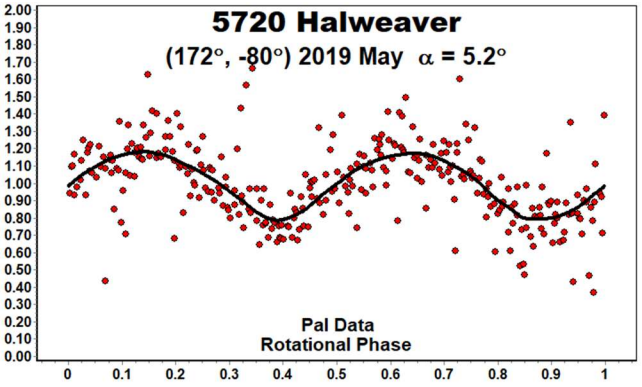

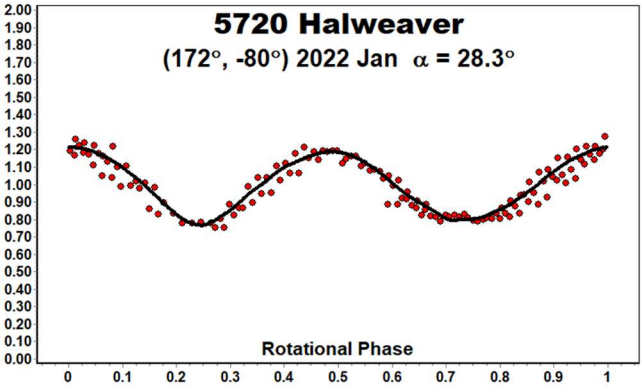

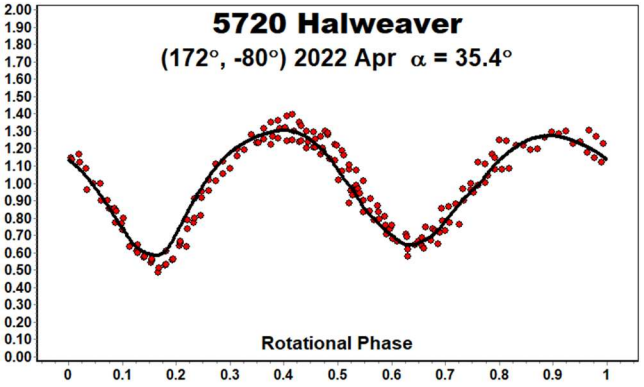

It will be several years before its next favorable opposition for northern hemisphere observers.

6384 Kervin. This Hungaria member has been observed numerous times in the past. Pravec et al. (2006web) found a period of 3.6200 h. We observed the asteroid five times before as part of the continuing program on the Hungaria asteroids. All results were close to 3.62 h. The 2022 data produced a period of 3.6192 h if assuming a monomodal lightcurve.

However, given the low amplitude of only 0.10 mag, the true lightcurve might be bimodal or even multimodal (Harris et al., 2014). The maximum amplitude found in the LCDB is only 0.16 mag, which can still make the modality of the lightcurve uncertain.

We present an alternate period of 7.236 h with a bimodal lightcurve. However, the so-called *Split Halves* plot (see Harris et al., 2014) shows that the two halves of the lightcurve are essentially identical, which significantly reduces the likelihood of the longer period being the correct solution.

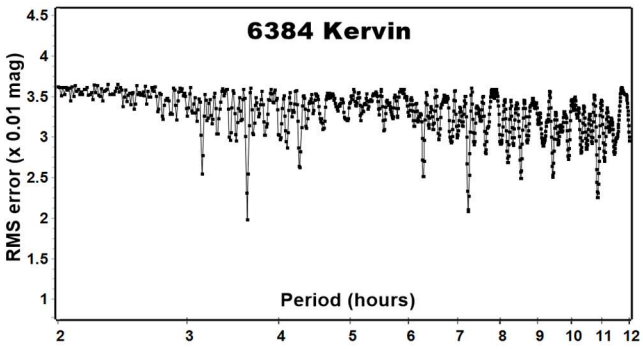

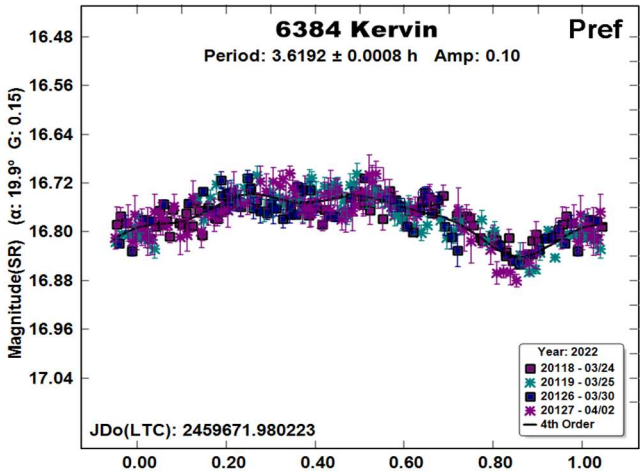

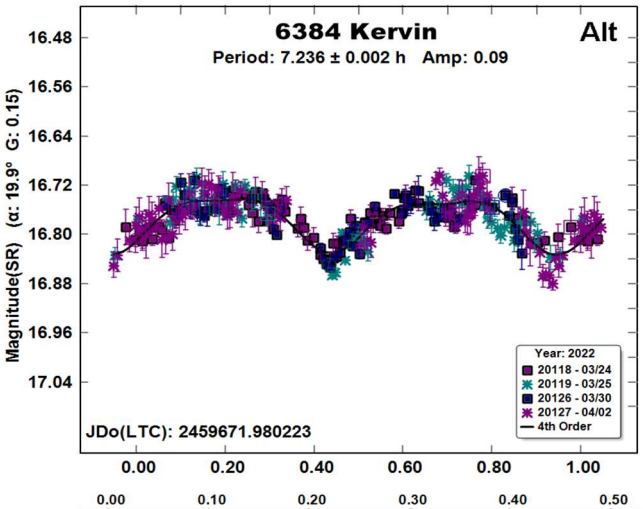

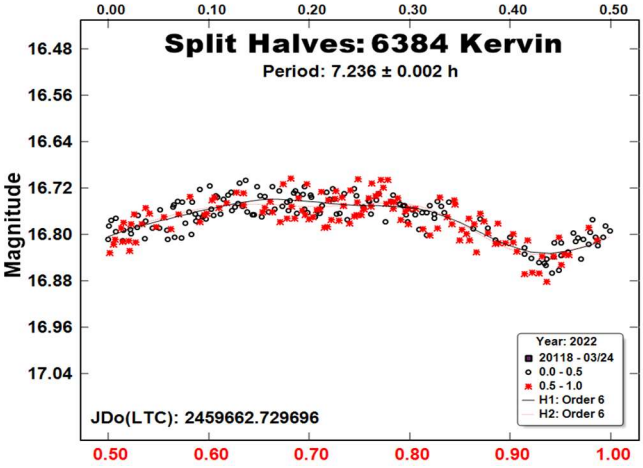

7516 Kranjc. This inner Main-Belt asteroid has been observed four times in the past. As part of a campaign for the Photometric Survey of Asynchronous Binary Asteroids (Pravec et al., 2006), Oey et al. (2009) observed it over two months finding a period of 3.96776 ± 0.00005 h. They detected a single mutual event spanning a dozen data points over 1-1/2 h. No other mutual event was ever detected in any other datasets.

About the same time, Warner (2009) observed it finding a period of 3.982 h. More recently, the Photometric Survey of Asynchronous Binary Asteroids observed it again (Pravec et al., 2019web) finding a period of 3.9702 h. Our result this year is in good agreement with those prior results.

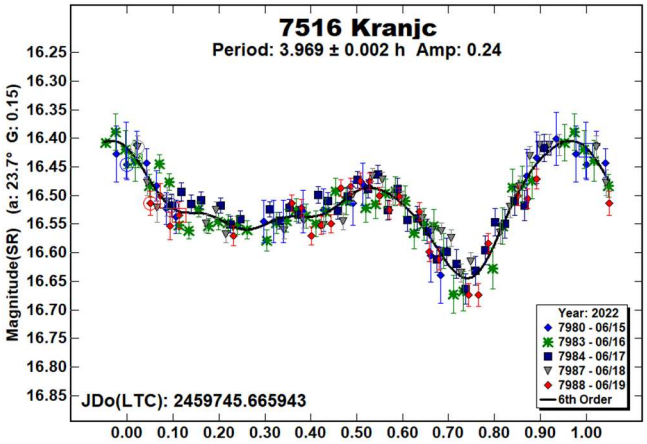

9698 Idzerda. This member of the Vesta dynamical family has been observed twice by surveys in the past. Using data from the Asteroid Terrestrial-impact Last Alert System (ATLAS) survey, Erasmus et al. (2020) found a period of 5.475 h. With data from the TESS spacecraft, Pál et al. (2020) found a period of 5.47439 h. Our result this year is in good agreement with those prior survey results.

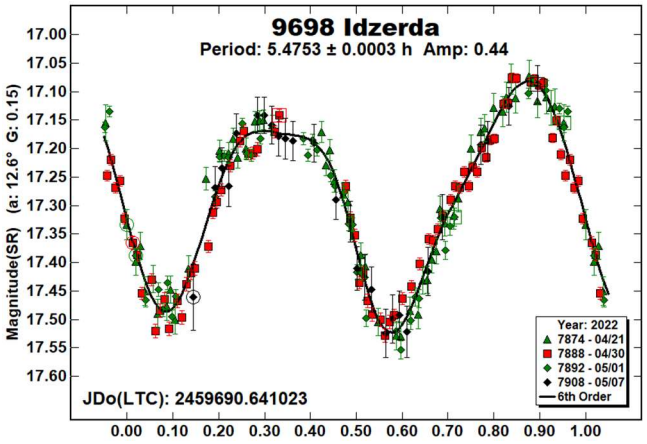

(1992) 1997 TG19. This Mars-crosser has been observed twice in the past. Higgins et al. (2006) reported a period of 5.7402 h. Using data from the Palomar Transient Factory Survey, Waszczak et al. (2015) found a period near 5.730 h. Our period this year is in good agreement with those prior results.

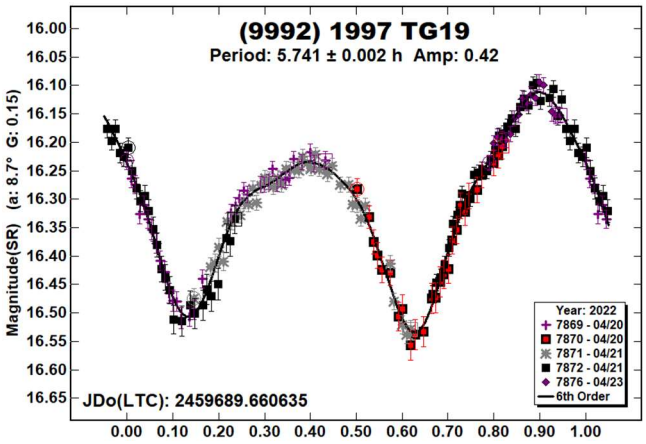

11450 Shearer. Using data from the Palomar Transient Factory Survey, Waszczak et al. (2015) reported a period of 5.422 h. Our period this year is in good agreement with that prior result.

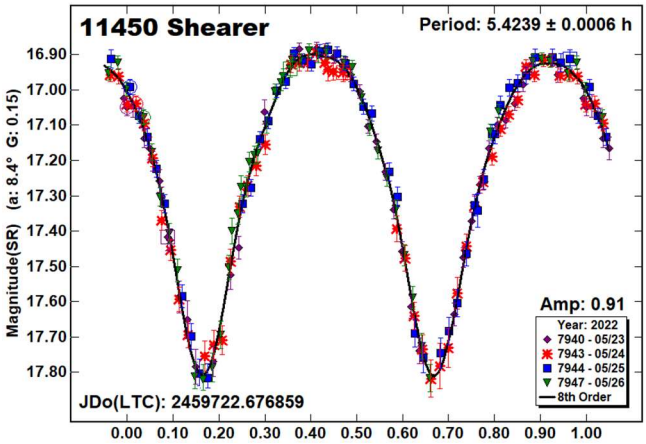

16214 Venkatachalam. Using data from the Palomar Transient Factory Survey, Waszczak et al. (2015) reported a period of 6.272 h. Our period this year is in good agreement with that prior result.

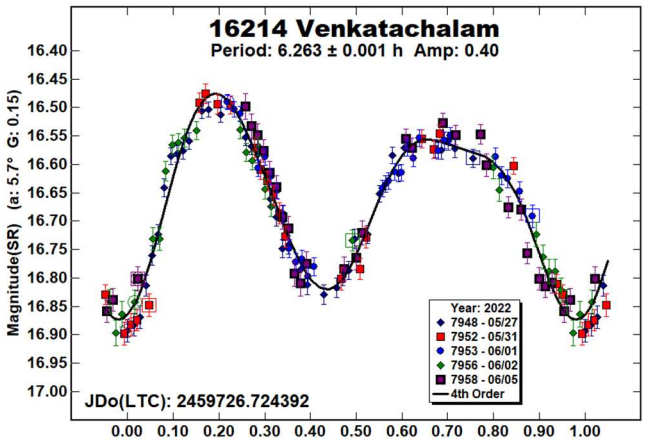

(24029) 1999 RT198. This Mars-crosser was observed at Lowell in 2010 and 2017 (Skiff et al., 2019b), both times finding a period near 5.49 h and an amplitude over 0.7 mag. The period we found this year is in good agreement with those prior results.

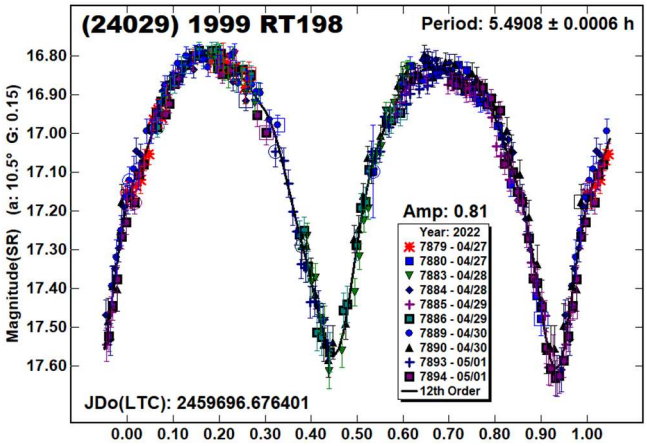

(27262) 1999 XT184. Using data from the TESS spacecraft, Pál et al. (2020) previously reported a period of 5.74263 h for this Vestoid. Our period this year is in good agreement with that prior result.

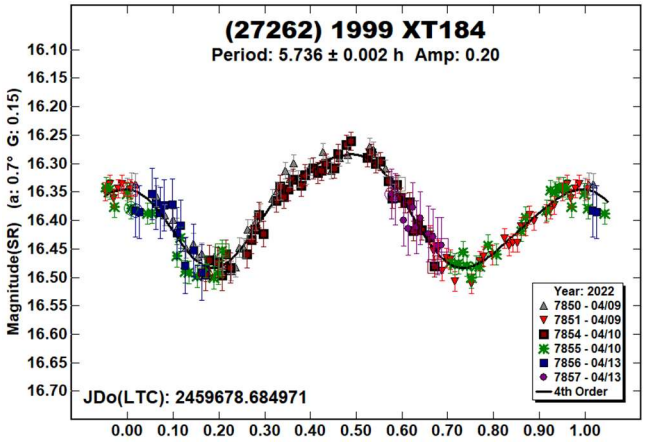

(42811) 1999 JN81. This member of the Hungaria dynamical family has been observed several times in the past. Warner (2008a, 2012), Benishek (2018), Skiff et al. (2019b), and Pál et al. (2020) all found periods near 3.9 h. The period we found this year is in good agreement with those prior results.

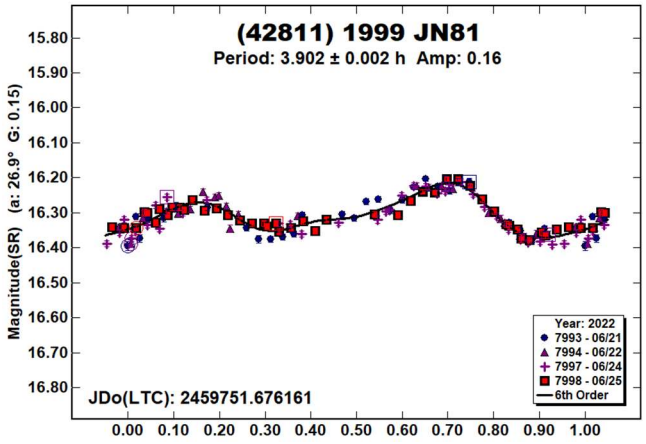

49699 Hidetakasato. There are no entries in the LCDB for this dynamical member of the Phocaea family (Nesvorny, 2015; Nesvorny et al., 2015). We observed it in 2022 March and April. Initial observations pointed towards a long period, but a decisive wobble suggestive of a tumbling state was quickly apparent. That is not a surprise given its long period and that the asteroid is tumbling, which is likely given the damping time is between 1 - 3 Gy (Pravec et al., 2005; 2014).

The initial analysis showed that the solution was dominated by a period near 68 hours ("NoSub"), but there were signs of a second period, one that was unlikely due to a satellite.

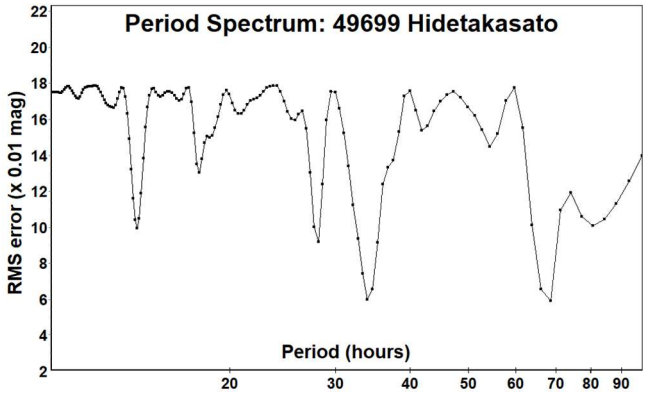

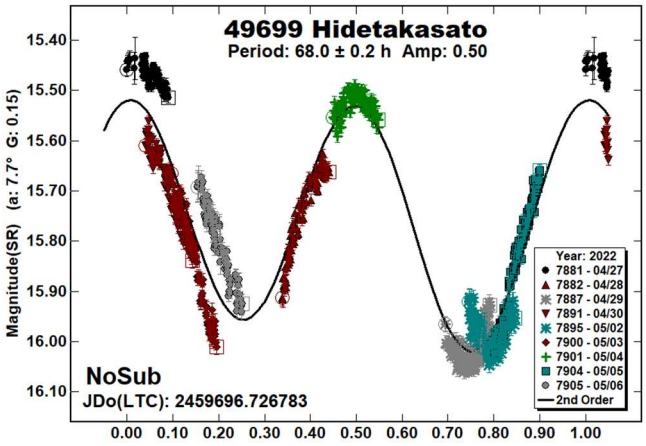

The tumbling frequencies cannot be confirmed from our data set alone, but we attempted to solve for the dominant period of the solution using *MPO Canopus*, which is not equipped to work with tumbling asteroids. The plot labeled "P1" is the dominant frequency, after subtracting a secondary frequency of 52.91 h.

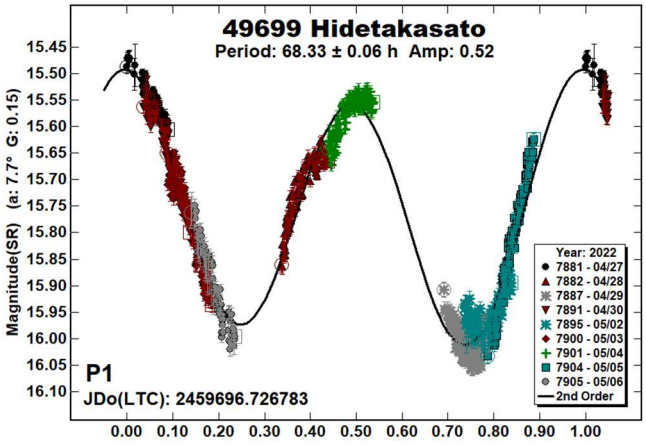

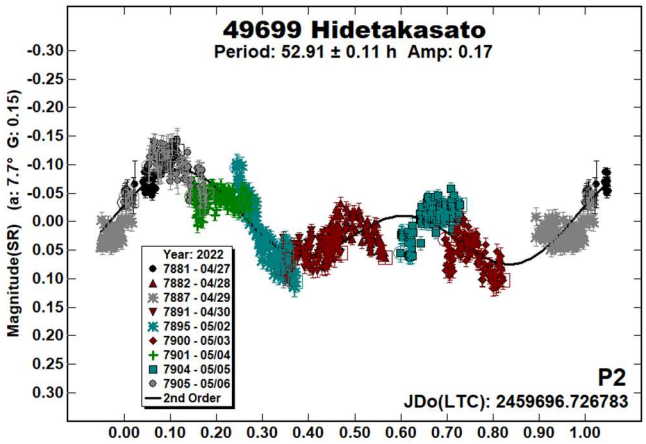

The cleanup on P1 is noteworthy with P2 being reasonable compared to P1. There's a limit to the difference in periods based on the amplitude. As a rule of thumb, the rotation and wobble frequencies cannot be separated by more than a factor of about the inverse amplitude of variation (Alan Harris, *private communication*). Thus, for something varying by 0.5 mag., the two periods must be within 200% of each other. So, the two periods are plausible. The inability for *MPO Canopus* to work accurately with tumbling asteroids could well be the reason for the shape and amplitude of the P2 lightcurve.

Acknowledgements

This work includes data from the Asteroid Terrestrial-impact Last Alert System (ATLAS) project. ATLAS is primarily funded to search for near earth asteroids through NASA grants NN12AR55G, 80NSSC18K0284, and 80NSSC18K1575; byproducts of the NEO search include images and catalogs from the survey area. The ATLAS science products have been made possible through the contributions of the University of Hawaii Institute for Astronomy, the Queen's University Belfast, the Space Telescope Science Institute, and the South African Astronomical Observatory.

The authors gratefully acknowledge Shoemaker NEO Grants from the Planetary Society (2007, 2013). These were used to purchase some of the telescopes and CCD cameras used in this research.

References

AstDys-2 (2020). Asteroids - Dynamic web site. *https://newton.spacedys.com/astdys/*

ALCDEF (2020). Asteroid Lightcurve Data Exchange Format database. *http://www.alcdef.org/*

Almeida, R.; Angeli, C.A.; Duffard, R.; Lazzaro, D. (2004). "Rotation periods for small main-belt asteroids." *Astron. Astrophys.* **415**, 403-406.

Number	Name	2021/mm/dd	Phase	L_{PAB}	B_{PAB}	Period(h)	P.E.	Amp	A.E.
864	Aase	04/14-04/15	7.8,7.3	219	6	3.240	0.002	0.34	0.05
1806	Derice	06/28-07/01	24.3,24.1	341	4	3.226	0.002	0.16	0.02
2048	Dwornik	06/06-06/09	24.8,24.3	277	33	3.64	0.01	0.08	0.01
2069	Hubble 2005	01/17-02/04	7.3,13.5	104	10	87.3	0.1	0.34	0.03
2093	Genichesk	04/20-04/25	11.2,13.8	192	6	11.017	0.005	0.19	0.02
2784	Domeyko	05/15-05/18	22.4,23.3	192	9	6.004	0.002	0.48	0.05
2858	Carlosporter	06/06-06/09	*14.1,15.5	190	7	3.250	0.004	0.05	0.02
3470	Yaronika	06/15-06/20	26.5,27.3	213	-1	6.626	0.002	1.01	1.02
3569	Kumon	05/08-05/20	*8.2,8.0	234	17	T57.36	0.06	0.35	0.01
						46.84	0.007	0.36	0.05
3894	Williamcooke	05/22-05/26	10.1,9.3	255	17	4.173	0.002	0.07	0.01
3936	Elst	06/20-06/27	*24.0,22.2	271	6	6.646	0.002	0.19	0.02
5720	Halweaver	04/18-04/18	35.4	154	26	3.8852	0.0006	1.03	0.01
6384	Kervin 2022	03/24-04/02	*19.9,19.8	187	35	A3.6192	0.0008	0.10	0.01
						7.236	0.002	0.09	0.01
7516	Kranjc	06/15-06/19	23.8,25.2	227	10	3.969	0.002	0.24	0.01
9698	Idzerda	04/21-05/07	12.7,19.0	189	-2	5.4753	0.0003	0.44	0.02
9992	1997 TG19	04/20-04/23	8.8,10.8	198	1	5.741	0.002	0.42	0.02
11450	Shearer	05/23-05/26	8.4,9.3	235	11	5.4239	0.0006	0.91	0.01
16214	Venkatachalam	05/27-06/05	5.7,8.5	244	9	6.263	0.001	0.40	0.02
24029	1999 RT198	04/27-05/01	10.5,12.3	196	1	5.4908	0.0006	0.81	0.01
27262	1999 XT184	04/09-04/10	0.7,1.2	198	1	5.736	0.002	0.20	0.02
29606	1998 QN94	05/02-05/21	25.9,30.1	192	26	2.8965	0.0001	0.17	0.01
42811	1999 JN81	06/21-06/25	27.0,27.2	277	35	3.902	0.002	0.16	0.02
49699	Hidetakasato	04/27-05/06	*7.7,8.1	218	10	T68.33	0.06	0.52	0.50
						52.91	0.11	0.17	0.03

Table II. Observing circumstances and results. TDominant period for a tumbling asteroid. The phase angle is given for the first and last date. If preceded by an asterisk, the phase angle reached an extremum during the period. L_{PAB} and B_{PAB} are the approximate phase angle bisector longitude/latitude at mid-date range (see Harris et al., 1984). If more than one line for an asteroid, the first line gives the dominant solution and has a T superscript. Subsequent lines are additional, not alternate, periods. See the text for more details.

Number	Name	λ	β	Period	λ	β	Period	a/b ratio	a/c ratio
864	Aase	**64**	**-77**	**3.23256**	246	-66	3.23256	1.3	1.3
5720	Halweaver	**172**	**-80**	**3.88715**				1.6	1.8

Table III. Results of Pole/Shape modeling. The preferred solution is listed first in bold text. For the ratios, c = 1.0.

Behrend, R. (2002web, 2018web, 2019web) Observatoire de Geneve web site.
http://obswww.unige.ch/~behrend/page_cou.html.

Benishek, V. (2018). "Lightcurve and Rotation Period Determinations for 29 Asteroids." *Minor Planet Bull.* **45**, 82-91.

Carbognani, A. (2014). "Asteroids Lightcurves at Oavda: 2012 June - 2013 March." *Minor Planet Bull.* **41**, 4-8.

Clark, M. (2019). "Asteroid Photometry from the Preston Gott Observatory." *Minor Planet Bull.* **46**, 346-349.

Ditteon, T. (2019). "Lightcurve Analysis of Minor Planets Observed at the Oakley Southern Sky Observatory: 2018 January - March." *Minor Planet Bull.* **46**, 127-129.

Ďurech, J.; Tonry, J.; Erasmus, N.; Denneau, L.; Heinze, A.N.; Flewelling, H.; Vančo, R. (2020). "Asteroid models reconstructed from ATLAS photometry." *Astron. Astrophys.* **643**, A59.

Erasmus, N.; Navarro-Meza, S.; McNeill, A.; Trilling, D.E.; Sickafoose, A.A.; Denneau, L.; Flewelling, H.; Heinze, A.; Tonry, J.L. (2020). "Investigating Taxonomic Diversity within Asteroid Families through ATLAS Dual-band Photometry." *Ap. J. Suppl. Ser.* **247**, A13.

Harris, A.W.; Young, J.W.; Scaltriti, F.; Zappala, V. (1984). "Lightcurves and phase relations of the asteroids 82 Alkmene and 444 Gyptis." *Icarus* **57**, 251-258.

Harris, A.W.; Young, J.W.; Contreiras, L.; Dockweiler, T.; Belkora, L.; Salo, H.; Harris, W.D.; Bowell, E.; Poutanen, M.; Binzel, R.P.; Tholen, D.J.; Wang, S. (1989). "Phase relations of high albedo asteroids: The unusual opposition brightening of 44 Nysa and 64 Angelina." *Icarus* **81**, 365-374.

Harris, A.W.; Pravec, P.; Galad, A.; Skiff, B.A.; Warner, B.D.; Vilagi, J.; Gajdos, S.; Carbognani, A.; Hornoch, K.; Kusnirak, P.; Cooney, W.R.; Gross, J.; Terrell, D.; Higgins, D.; Bowell, E.; Koehn, B.W. (2014). "On the maximum amplitude of harmonics on an asteroid lightcurve." *Icarus* **235**, 55-59.

Higgins, D.; Pravec, P.; Kusnirak, P.; Galad, A.; Kornos, L.; Pray, D.; Koff, R.A. (2006). "Asteriod lightcurve analysis at Hunters Hill Observatory and collaborating stations - autumn 2006." *Minor Planet Bull.* **33**, 89-91.

Kaasalainen, M.; Torppa J. (2001). "Optimization Methods for Asteroid Lightcurve Inversion. I. Shape Determination." *Icarus* **153**, 24-36.

Kaasalainen, M.; Torppa J.; Muinonen, K. (2001). "Optimization Methods for Asteroid Lightcurve Inversion. II. The Complete Inverse Problem." *Icarus* **153**, 37-51.

Kryszczyńska, A.; Colas, F.; Polińska, M.; Hirsch, R.; Ivanova, V.; Apostolovska, G.; Bilkina, B.; Velichko, F.P.; Kwiatkowski, T.; Kankiewicz, P.; Vachier, F.; Umlenski, V.; Michałowski, T.; Marciniak, A.; Maury, A.; Kamiński, K.; Fagas, M.; Dimitrov, W.; Borczyk, W.; Sobkowiak, K.; Lecacheux, J.; Behrend, R.; Klotz, A.; Bernasconi, L.; Crippa, R.; Manzini, F.; Poncy, R.; Antonini, P.; Oszkiewicz, D.; Santana-Ros, T. (2012). "Do Slivan states exist in the Flora family? I. Photometric survey of the Flora region." *Astron. Astrophys*. **546**, A72.

Macias, A.A. (2015). "Asteroid Lightcurve Analysis at Isaac Aznar Observatory Aras De Los Olmos, Valencia, Spain." *Minor Planet Bull.* **42**, 4-6.

Nesvorny, D. (2015). "Nesvorny HCM Asteroids Families V3.0." NASA Planetary Data Systems, id. EAR-A-VARGBET-5-NESVORNYFAM-V3.0.

Nesvorny, D.; Broz, M.; Carruba, V. (2015). "Identification and Dynamical Properties of Asteroid Families." In *Asteroids IV* (P. Michel, F. DeMeo, W.F. Bottke, R. Binzel, Eds.). Univ. of Arizona Press, Tucson, also available on astro-ph.

Oey, J.; Cooney, W.; Gross, J.; Terrell, D.; Marchis, F.; Stewart, H.; Stephens, E.D.; Brinsfield, J.W.; Vilagi, J., Gajdos, S.; Crawford, G. (2009). "Photometry of Asteroids 7516 Kranjc, 7965 Katsuihiko, and (15515) 1999 VN80 from Leura and Other Collaborating Observatories." *Minor Planet Bull.* **36**, 50-51.

Pál, A.; Szakáts, R.; Kiss, C.; Bódi, A.; Bognár, Z.; Kalup, C.; Kiss, L.L.; Marton, G.; Molnár, L.; Plachy, E.; Sárneczky, K.; Szabó, G.M.; Szabó, R. (2020). "Solar System Objects Observed with TESS - First Data Release: Bright Main-belt and Trojan Asteroids from the Southern Survey." *Ap. J.* **247**, A26.

Pilcher, D. (2017). "Rotation Period Determinations for 392 Wilhelmina and 854 Aase." *Minor Planet Bull*. **44**, 9.

Polakis, T. (2019). "Photometric Observations of Seventeen Minor Planets." *Minor Planet Bull.* **46**, 400-406.

Polakis, T. (2022). "Lightcurves for Fifteen Minor Planets." *Minor Planet Bull.* **49**, 179-184.

Pravec, P.; Harris, A.W.; Scheirich, P.; Kušnirák, P.; Šarounová, L.; Hergenrother, C.W.; Mottola, S.; Hicks, M.D.; Masi, G.; Krugly, Yu.N.; Shevchenko, V.G.; Nolan, M.C.; Howell, E.S.; Kaasalainen, M.; Galád, A.; Brown, P.; Degraff, D.R.; Lambert, J. V.; Cooney, W.R.; Foglia, S. (2005). "Tumbling asteroids." *Icarus* **173**, 108-131.

Pravec, P.; Scheirich, P.; Kusnirák, P.; Sarounová, L.; Mottola, S.; Hahn, G.; Brown, P.; Esquerdo, G.; Kaiser, N.; Krzeminski, Z.; and 47 coauthors (2006). "Photometric survey of binary near-Earth asteroids." *Icarus* **181**, 63-93.

Pravec, P.; Scheirich, P.; Durech, J.; Pollock, J.; Kusnirak, P.; Hornoch, K.; Galad, A.; Vokrouhlicky, D.; Harris, A.W.; Jehin, E.; Manfroid, J.; Opitom, C.; Gillon, M.; Colas, F.; Oey, J.; Vrastil, J.; Reichart, D.; Ivarsen, K.; Haislip, J.; LaCluyze, A. (2014). "The tumbling state of (99942) Apophis." *Icarus* **233**, 48-60.

Pravec, P.; Wolf, M.; Sarounova, L. (2006web, 2007web, 2009web, 2011web, 2012web, 2016web, 2019web).
http://www.asu.cas.cz/~ppravec/neo.htm

Skiff, B.A.; McLelland, K.P.; Sanborn, J.J.; Pravec, P.; Koehn, B.W. (2019a). "Lowell Observatory Near-Earth Asteroid Photometric Survey (NEAPS): Paper 3." *Minor Planet Bull.* **46**, 238-265.

Skiff, B.A.; McLelland, K.P.; Sanborn, J.J.; Pravec, P.; Koehn, B.W. (2019b). "Lowell Observatory Near-Earth Asteroid Photometric Survey (NEAPS): Paper 4." *Minor Planet Bull.* **46**, 458-503.

Stephens, R.D. (2019). "Asteroids Observed from CS3: 2018 July - September." *Minor Planet Bull.* **46**, 66-71.

Stephens, R.D.; Warner, B.D. (2020). "Main-belt Asteroids Observed from CS3: 2020 January to March." *Minor Planet Bull.* **47**, 224-230.

Tonry, J.L.; Denneau, L.; Flewelling, H.; Heinze, A.N.; Onken, C.A.; Smartt, S.J.; Stalder, B.; Weiland, H.J.; Wolf, C. (2018). "The ATLAS All-Sky Stellar Reference Catalog." *Astrophys. J.* **867**, A105.

Warner, B.D. (2008a). "Asteroid Lightcurve Analysis at the Palmer Divide Observatory - June - October 2007." *Minor Planet Bull.* **35**, 50-60.

Warner, B.D. (2008b). "Asteroid Lightcurve Analysis at the Palmer Divide Observatory: September - December 2007." *Minor Planet Bull*. **35**, 67-71.

Warner, B.D. (2008c). "Asteroid Lightcurve Analysis at the Palmer Divide Observatory: December 2007 - March 2008." *Minor Planet Bull.* **35**, 95-98.

Warner, B.D. (2009). "Asteroid Lightcurve Analysis at the Palmer Divide Observatory: 2008 May - September." *Minor Planet Bull.* **36**, 7-13.

Warner, B.D.; Harris, A.W.; Pravec, P. (2009). "The Asteroid Lightcurve Database." *Icarus* **202**, 134-146. Updated 2021 Dec. *http://www.minorplanet.info/lightcurvedatabase.html*

Warner, B.D. (2012). "Asteroid Lightcurve Analysis at the Palmer Divide Observatory: 2012 March - June." *Minor Planet Bull.* **39**, 245-252.

Warner, B.D. (2016). "Asteroid Lightcurve Analysis at CS3-Palmer Divide Station: 2015 December - 2016 April." *Minor Planet Bull.* **43**, 227-233.

Waszczak, A.; Chang, C.-K.; Ofek, E.O.; Laher, R.; Masci, F.; Levitan, D.; Surace, J.; Cheng, Y.-C.; Ip, W.-H.; Kinoshita, D.; Helou, G.; Prince, T.A.; Kulkarni, S. (2015). "Asteroid Light Curves from the Palomar Transient Factory Survey: Rotation Periods and Phase Functions from Sparse Photometry." *Astron. J.* **150**, A75.

ROTATIONAL PERIOD DETERMINATION AND TAXONOMIC CLASSIFICATION FOR ASTEROIDS 417 SUEVIA, 554 PERAGA, AND 747 WINCHESTER

Massimiliano Mannucci, Nico Montigiani
Associazione Astrofili Fiorentini
Osservatorio Astronomico Margherita Hack (A57)
Florence, ITALY
info@astrofilifiorentini.it

Davide Gabellini, Fabio Mortari
Osservatorio Astronomico Hypatia (L62)
Rimini, ITALY

(Received: 2022 June 26)

CCD photometric observations of three main-belt asteroids were made between 2022 January and March in order to measure their rotation periods and define their taxonomic class. The observations used instrumentation available at our two observatories.

CCD photometric observations of three main-belt asteroids were carried out in 2022 January and March at the Osservatorio Astronomico Margherita Hack (A57) and Osservatorio Astronomico Hypatia (L62). The Osservatorio Astronomico Margherita Hack is equipped with a 0.35-m *f*/8.25 Schmidt-Cassegrain telescope, an SBIG ST10 XME CCD camera, and Johnson-Cousins BVRc photometric filters. The pixel scale was 1 arcsec when binned at 2×2 pixels. The Osservatorio Astronomico Hypatia is equipped with a 0.25-m *f*/5.6 Ritchey-Chretien telescope and a Moravian G2-8300 CCD camera having the pixel scale of 0.81 arcsec at 1×1 binning, and Rc photometric filter. Data processing and analysis were done with *MPO Canopus* (Warner, 2021). All images were calibrated with dark and flat field frames using *Astroart 6.0*. and *MaximDL*. Table I shows the observing circumstances and results.

417 Suevia was discovered at Heidelberg on 1896 May 6 by M.F. Wolf. It is a main-belt asteroid with a semi-major axis of 2.800 au, eccentricity 0.135, inclination 6.65 deg, and orbital period of 4.69 years. Its absolute magnitude is H = 9.56 (JPL, 2022; MPC, 2022).

In this case, our observations were conducted in two steps. The first step consisted in collecting 192 data points during two nights on 2022 Feb 23 and 24. The period analysis shows a bimodal solution for a rotational period P = 7.034 ± 0.002 h with an amplitude A = 0.12 ± 0.02 mag. The split-halves plot let us resolve the potential ambiguity between monomodal and bimodal solution by showing that the two halves of the 7.034 h solution are not superimposable. This makes the bimodal solution much more probable. As a further check, we consulted the asteroid lightcurve database (LCDB; Warner et al., 2009) and found three previously reported periods: Barucci et al. (1992, 7.034 h), Fauvaud and Fauvaud (2013, 7.020 h), and Martikainen et al. (2021, 7.0185 h). The period we found seems to be in good agreement with those previous results.

Number	Name	2022 mm/dd	Pts	Phase	LPAB	BPAB	Period(h)	P.E.	Amp	A.E.	Grp
417	Suevia	02/22	192	3.37	152	-6	7.034	0.002	0.12	0.014	MBA
554	Peraga	01/13	391	6.53	103	1	13.715	0.002	0.18	0.01	MBA
747	Winchester	03/01	513	5.46	168	14	9.418	0.002	0.13	0.016	MBA

Table I. Observing circumstances and results. Pts is the number of data points. The phase angle is given for the first and last date. L_{PAB} and B_{PAB} are the approximate phase angle bisector longitude and latitude at mid-date range (see Harris *et al.*, 1984). Grp is the asteroid family/group (Warner *et al.*, 2009).

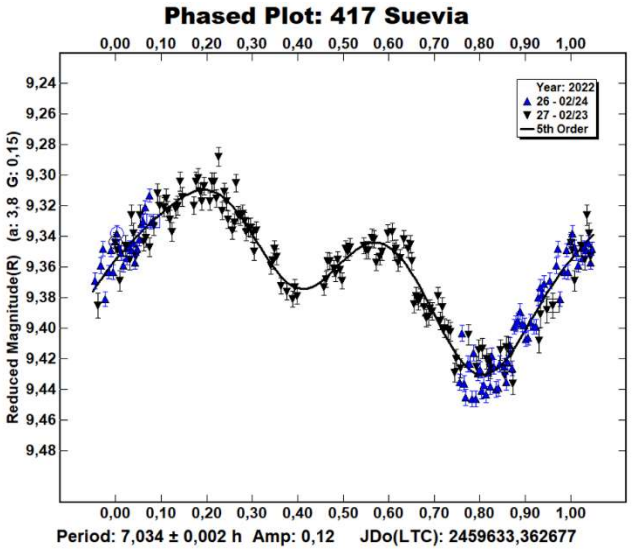

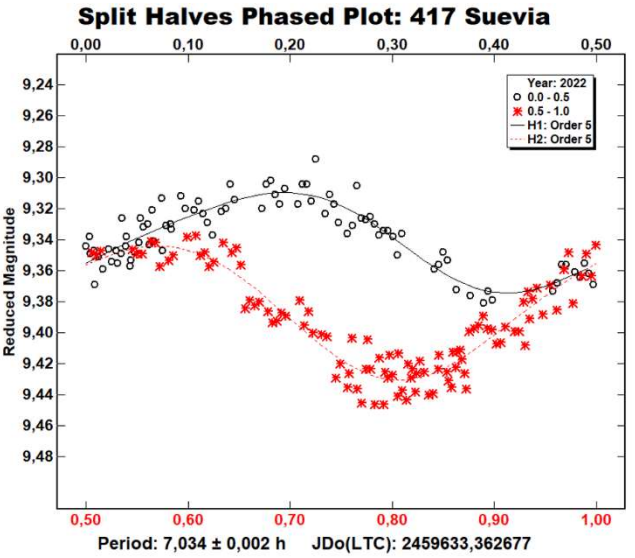

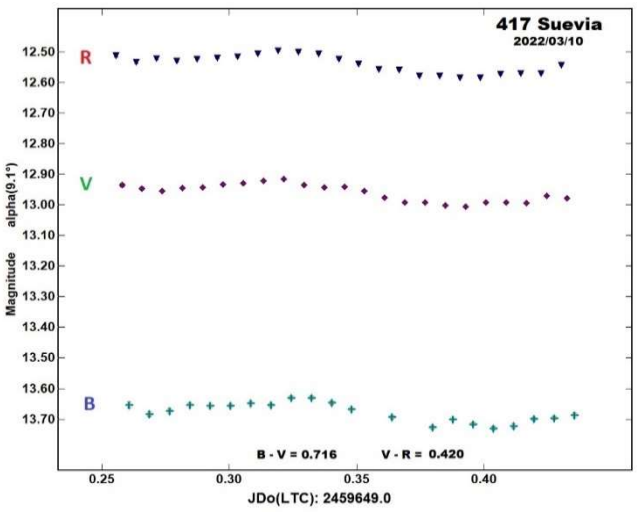

In the second step, we collected further 67 data points in one night using B, V, and Rc filters. This allowed us to determine the color indexes (V-R) = 0.420 ± 0.005 and (B-V) = 0.716 ± 0.008. These values are consistent with a medium albedo M-type taxonomic class (Shevchenko and Lupishko, 1998) and in good accordance with the previously published results in the LCDB. The albedo of 0.1637 (Warner, B.D. et al., 2009) is also consistent with a taxonomic class of type M (Shevchenko and Lupishko, 1998).

554 Peraga was discovered on 1905 Jan 8 at Heidelberg by P. Gotz. It was chosen from the list of lightcurve photometry opportunities in the *Minor Planet Bulletin* (Warner et al., 2022). It is a main-belt asteroid with a semi-major axis of 2.375 au, eccentricity 0.1519, inclination 2.935 deg, and orbital period of 3.66 years. Its absolute magnitude is $H = 9.13$ (JPL, 2022; MPC, 2022).

We consulted the asteroid lightcurve database (LCDB; Warner et al., 2009) and found five previous calculated periods: Scaltriti and Zappala (1979, 13.63 h), Behrend (2004web, 13.707 h; 2006web, 13.7 h), Higgins et al. (2007, 13.7128 h), and Stephens (2007, 13.71 h).

Our observations were again conducted in two steps. The first consisted of collecting 391 data points during three nights from 2022 Jan 13-22. The period analysis shows a bimodal solution for the rotational period with $P = 13.715 \pm 0.002$ h and an amplitude $A = 0.18 \pm 0.01$ mag. The split-halves plot resolved the potential ambiguity between a monomodal and bimodal solution by showing that the two halves of the 13.715 h solution are not superimposable. This makes the bimodal solution much more probable. The period we found seems to be in good agreement with the previous results.

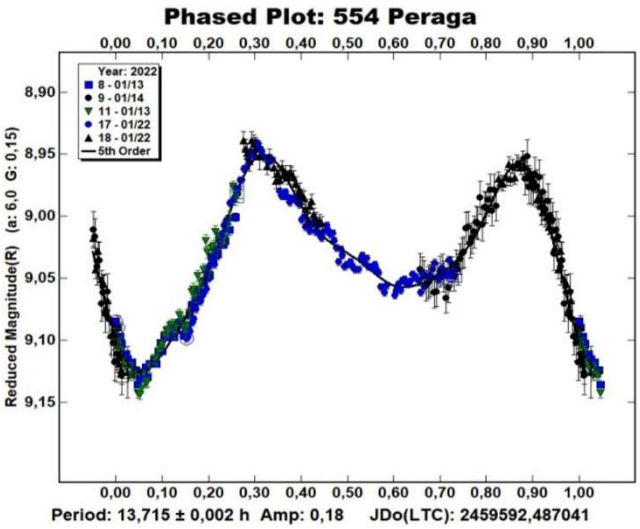

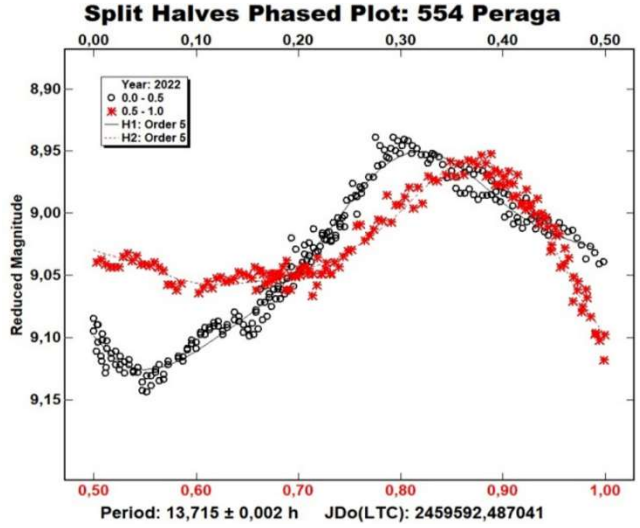

In the second step, we collected an additional 51 data points in one night using filters B, V and Rc. This allowed us to determine the color indexes (V-R) = 0.37 ± 0.004 and (B-V) = 0.691 ± 0.005. These values are consistent with a low albedo C-type taxonomic class (Shevchenko and Lupishko, 1998) and in good accordance with the previously published results in the LCDB. The albedo of 0.044 (Warner, B.D. et al., 2009) is also consistent with a taxonomic class of type C (Shevchenko and Lupishko, 1998).

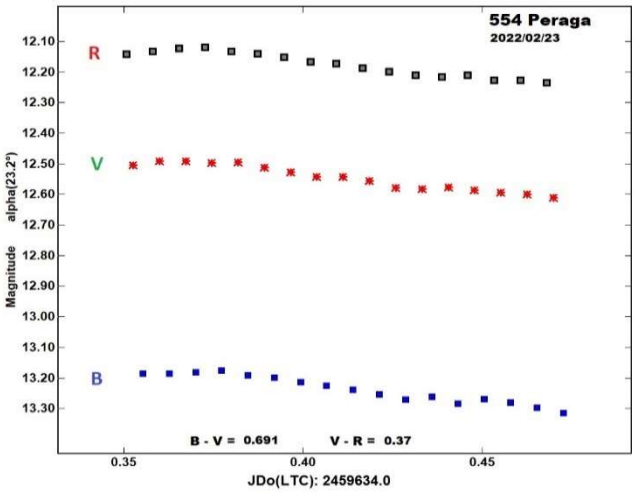

747 Winchester was discovered at Winchester on 1913 Mar 7 by J. H. Metcalf. It is a main-belt asteroid with a semi-major axis of 3.001 au, eccentricity 0.339, inclination 18.22 deg, and orbital period of 5.2 years. Its absolute magnitude is H = 7.84 (JPL, 2022; MPC, 2022).

Keeping with the method mentioned above, the first of two steps of observations collected 513 data points from 2022 Mar 2-12. Period analysis shows a bimodal solution with P = 9.418 ± 0.002 h and amplitude A = 0.13 ± 0.02 mag. The split-halves plot shows that the bimodal solution is the most probable. We found at least three previous results in the LCDB (Warner et al., 2009) in good agreement with ours: Warner (2007, 9.4146 h), Pilcher (2010; 9.414 h), and Ďurech et al. (2011; 9.414 h).

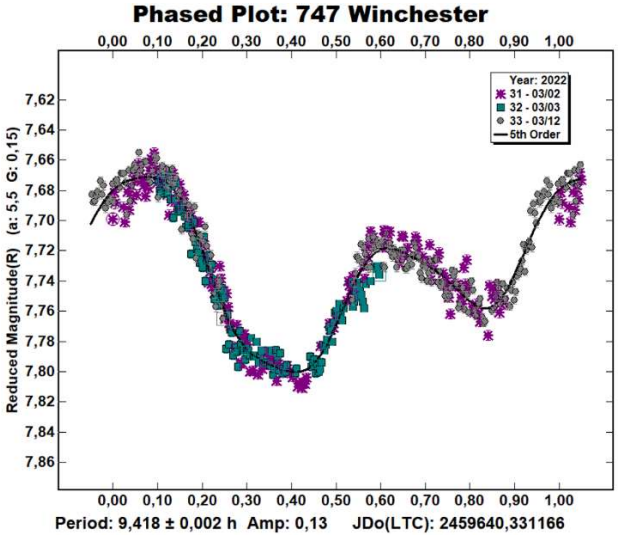

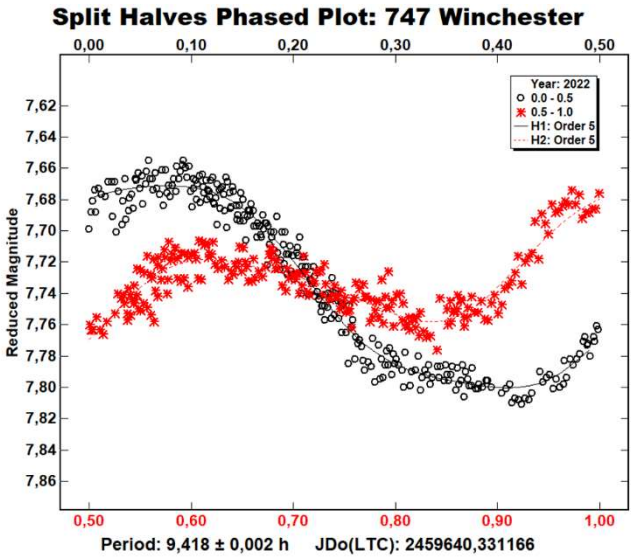

In the second step, we collected further 69 data points in one night using filters B, V and Rc. This allowed us to determine the color indexes (V-R) = 0.39 ± 0.02 and (B-V) = 0.66 ± 0.02. These values are consistent with a low albedo C-type taxonomic class (Shevchenko and Lupishko, 1998) and in good accordance with the previously published results in the LCDB. The albedo value of 0.0435 (Warner et al., 2009) is also consistent with a taxonomic class of type C (Shevchenko and Lupishko, 1998).

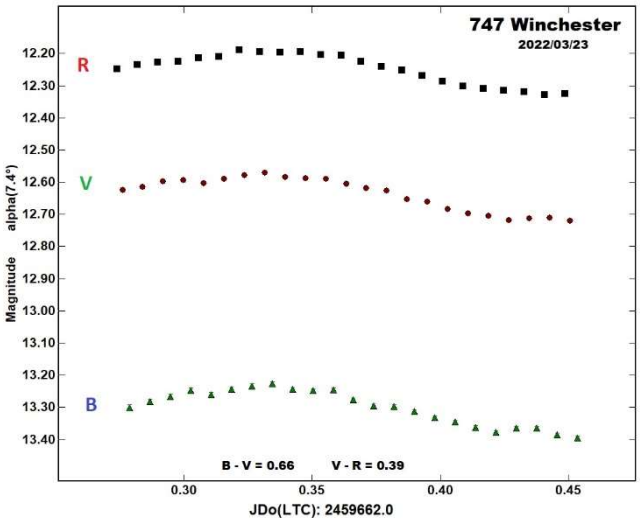

References

Barucci, M.A.; di Martino, M.; Fulchignoni, M. (1992). "Rotational Properties of Small Asteroids: Photoelectric Observations." *Astronomical Journal* **103**, 1679.

Behrend, R. (2004web; 2006web). "Courbes de rotation d'astéroïdes et de comètes, CdR." *https://obswww.unige.ch/~behrend/page2cou.html#000554*

Ďurech, J.; Kaasalainen, M.; Herald, D.; Dunham, D.; Timerson, B.; Hanuš, J.; Frappa, E.; Talbot, J.; Hayamizu, T.; Warner, B.D.; Pilcher, F.; Galád, A. (2011). "Combining asteroid models derived by lightcurve inversion with asteroidal occultation silhouettes." *Icarus* **214**, 652-670.

Fauvaud, S.; Fauvaud, M. (2013). "Photometry of Minor Planets. I. Rotation Periods from Lightcurve Analysis for Seven Main-belt Asteroids." *Minor Planet Bulletin* **40**, 224-229.

Harris, A.W.; Young, J.W.; Scaltriti, F.; Zappala, V. (1984). "Lightcurves and phase relations of the asteroids 82 Alkmene and 444 Gyptis." *Icarus* **57**, 251-258.

Higgins, D.; Warner, B.D.; Dymock, R.; Crow, M. (2007). "Asteroid Lightcurve Analysis of 554 Peraga." *Minor Planet Bulletin* **34**, 30.

JPL (2022). Small-Body Database Browser. *http://ssd.jpl.nasa.gov/sbdb.cgi#top*

Martikainen, J.; Muinonen, K.; Penttilä, A.; Cellino, A.; Wang, X. (2021). "Asteroid absolute magnitudes and phase curve parameters from Gaia photometry." *Astron. & Astrophys.* **649**, id. A98.

MPC (2022). MPC Database. *http://www.minorplanetcenter.net/db_search/*

Pilcher, F. (2010). "Period Determinations for 11 Parthenope, 35 Leukothea, 38 Leda 111 Ate, 194 Prokne, 262 Valda, 728 Leonisis, and 747 Winchester." *Minor Planet Bulletin* **37**, 119-122.

Scaltriti, F.; Zappala, V. (1979). "Photoelectric photometry and rotation periods of the asteroids 26 Proserpina, 194 Prokne, 287 Nephthys, and 554 Peraga." *Icarus* **39**, 124-130.

Shevchenko, V.G.; Lupishko, D.F. (1998). "Optical Properties of Asteroids from Photometric Data." *Solar System Research* **32**, 220.

Stephens, R.D. (2007). "Asteroid Lightcurve Photometry from Santana and GMARS Observatories - September to December 2006." *Minor Planet Bulletin* **34**, 31-32.

Warner, B.D. (2007). "Asteroid Lightcurve Analysis at the Palmer Divide Observatory: March - May 2007." *Minor Planet Bulletin* **34**, 104-107.

Warner, B.D.; Harris, A.W.; Pravec, P. (2009). "The Asteroid Lightcurve Database." *Icarus* **202**, 134-146. Updated 2018 June 23. *http://www.minorplanet.info/lightcurvedatabase.html*

Warner, B.D.; Harris, A.W.; Ďurech, J.; Benner, L.A.M. (2022). "Lightcurve photometry opportunities: 2022 January - March." *Minor Planet Bulletin* **49**, 61-65.

Warner, B.D. (2021). MPO Software, *MPO Canopus* v10.8.5.0. Bdw Publishing. *http://minorplanetobserver.com*

LIGHTCURVE ANALYSIS OF THREE MAIN BELT ASTREROIDS: 2265 VERBAANDERT, 3787 AIVAZOVSKIJ, AND 4528 BERG

Edward O. Wiley
Live Oaks Observatory (V62)
125 Mountain Creek Pass, Georgetown, TX 78633
ewiley@suddenlink.net

Frederick Pilcher
4438 Organ Mesa Loop
Las Cruces, NM 88011 USA
fpilcher35@gmail.com

(Received: 2022 July 5)

2265 Verbaandert was imaged on seven nights between 2022 Feb 13 and 2022 Apr 03. A period of 2.8143 ±0.0001 hours and amplitude of 0.105 magnitude are reported. 3787 Aivazovskij was imaged five nights between 2022 Jan 06 and 2022 Feb 07. A period of 2.9532±0.0001 hours and amplitude of 0.191 magnitude are reported. 4528 Berg was imaged on eight nights from 2022 Apr 07 to 2022 May 07. A period of 3.5630±0.0001 hours and amplitude of 0.345 magnitude are reported.

Photometric measurements of three main-belt asteroids were performed by first author Wiley at the Live Oaks Observatory near Pontotoc, Texas (MPC V62). Images were taken with a 0.36m f/ 7.2 corrected Dall-Kirkham telescope, SBIG Aluma 3200 CCD, and no filter. Nightly ephemeris positions were obtained from the Minor Planet Center. Exposure time of all images was 180 seconds. The image scale was 1.094 arcseconds/pixel binned 2×2. Images were calibrated with bias (N = 100), dark (N = 30) and flat frames (N = 21) in *MaxIm DL*. Flat images were taken using a full spectrum LED panel. Alignment, plate solving, and data reduction were preformed using *Tycho Tracker* (Parrott, 2021). Comparison stars (five minimum) were picked from *Tycho Tracker*'s "Find Comp Stars" which presents those stars in the FOV (19.6'×13.3') with suitable comp stars similar in color to the Sun, typically 0.55 < B-V < 0.90. Clear instrumental magnitudes are converted to Sloan r' (SR) magnitudes using the Atlas All-Sky Reference Catalog (Tonry et al., 2018) within *Tycho Tracker*. (Two runs are exceptions as noted below.) Fourier analysis was used to find the periods. For each asteroid an initial search was conducted for periods between one and eight hours to investigate aliases. A final step size between one and four hours with 30,000 steps was used to determine the periods and amplitudes. A fit order = 6 was used for 2265 Verbaandeert while a fit order = 4 was used for both 3787Aivazovskij and 4528 Berg. Figures were made in *MPO Canopus* (Warner, 2010) to conform to the Minor Planet Bulletin format by F. P. using ALCDEF files generated in *Tycho Tracker*.

2265 Verbaandert (1950 DB) was discovered by Sylvain J.V. Arend at the Observatoire royal de Belgique. It is a carbonaceous mid-main-belt (9105) asteroid of 12 km in diameter (JPL, 2022). Waszczask et al. (2015) estimated a rotation period of 2.990 ±0.0006 hours based on sparse photometric data.

Verbaandert was imaged over seven nights in 2022 from late February, late March and early April; see Table I for details. Fourier analysis in *Tycho Tracker* and a fit order of 6 reported a new period of 2.8143±0.0001 hours with an amplitude of 0.105 magnitude (Fig. 1). Photometric precision averaged 0.008 magnitude. Fitting a 2.8143-hour period to data from the existing ALCDEF yielded the

same fit as the analysis of our data but a slightly worse fit for the Waszczask et al. (2015) period. A period of 2.990 hours results is a poor fit to our data. The period spectrum is shown in Fig. 2.

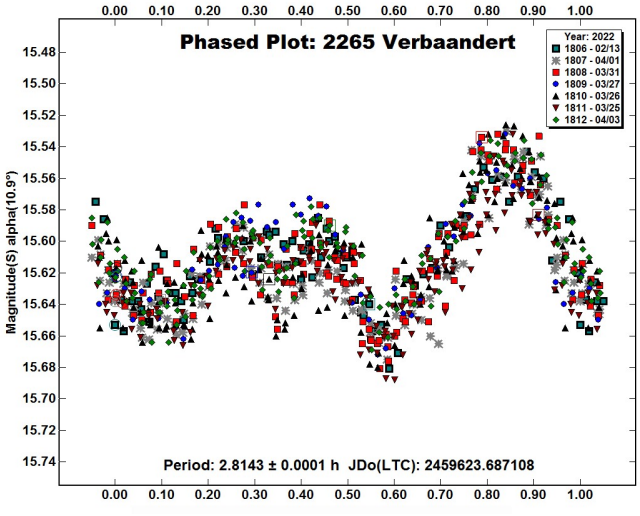

Figure 1. 2265 Verbaandert Phase Plot.

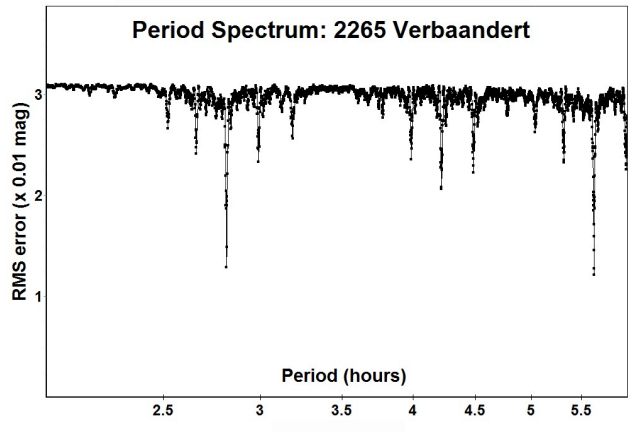

Figure 2. 2265 Verbaandert, period spectrum from 2 to 6 hours showing an alias at 5.6287 hours.

3787 Aivazovskij (1977 RG7) is an outer main-belt stony asteroid discovered by Nikolai Chernykh at the Crimean Astrophysical Observatory (Nauchnyj) belonging to the Itha family (633). It is about 12 kilometers in diameter and elongate. Period estimates in hours include Behrend (2018web: 2.95398±0.0007), Sada (2008: 2.97±0.01), Waszczak et al. (2015: 2.953±0.0005), and Hanus et al. (2016: 2.980807±0.000005) who also determined the spin axis (pole) and modeled the asteroid shape. The period listed in the Summary of the ALCDEF data page (Warner et al., 2009) is 2.95395 hours with an amplitude range of 0.18-0.24 magnitude.

Wiley picked this asteroid as a fast-rotating asteroid for training to perform asteroid lightcurves as the rotation period and amplitude seemed well established. To explore filters, Wiley used a Cousins R for two nights and no filter for three. Fourier analysis in *Tycho Tracker* and a fit order of 4 reported a period of 2.9532±0.0001 hours with an amplitude of 0.191 magnitude (Fig. 3). Photometric precision average 0.007 magnitude. Because there was a difference between the ALCDEF period and ours that exceeded errors we downloaded the ALCDEF file and reanalyzed the data with the same parameters used for our data. The period returned was 2.9533±0.0001 hours, within errors (in rounding) of our analysis. Given the period and amplitude shown in Table I, both similar to the re-analyzed period and amplitude in the ALCDEF gave confidence that Wiley could do further work with two asteroids that appeared on the January-March lightcurve opportunities list (Warner et al., 2022).

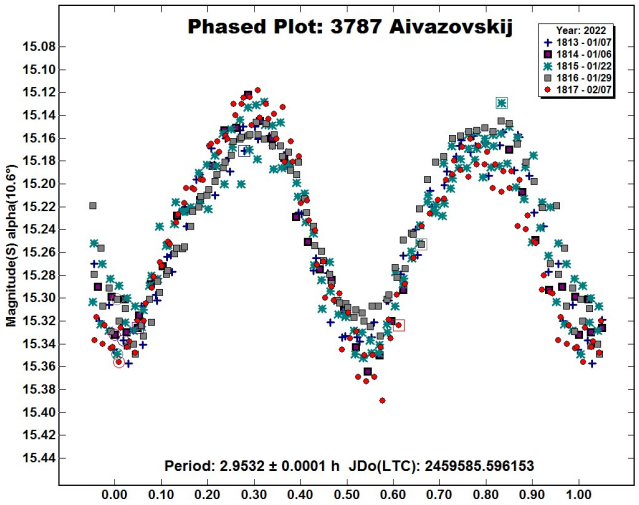

Figure. 3. 3787 Aivazovskij, Phase Plot.

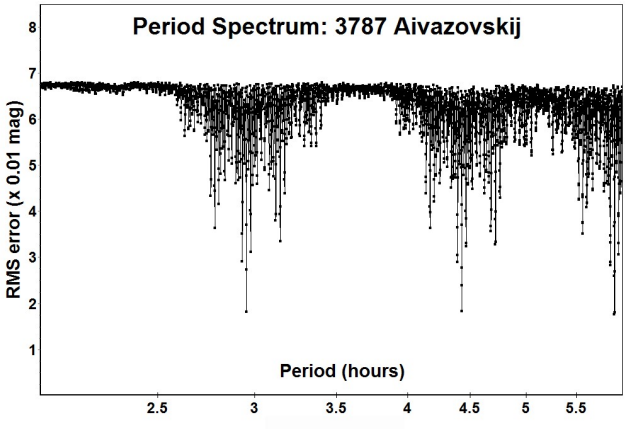

Figure 4. 3787 Aivazovskij, period spectrum from 2 to 6 hours showing aliases to period solution.

Number	Name	2022/mm/dd	Pts	Phase	L_{PAB}	B_{PAB}	Period(h)	P.E.	Amp	A.E.	Grp
2265	Verbaandert	02/13-04/03	811	16.9,10.9	162	16	2.8143	0.0001	0.105	0.0173	9105
3787	Aivazovskij	01/06-02/07	438	10.2,19.3	91	-14	2.9532	0.0001	0.191	0.0199	633
4528	Berg	04/07-05/07	587	22.9,21.7	169	3	3.5630	0.0002	0.345	0.0295	9104

Table I. Observing circumstances and results. Pts is the number of data points. The phase angle is given for the first and last dates. L_{PAB} and B_{PAB} are the approximate phase angle bisector longitude and latitude at mid-date range (see Harris et al., 1984). Grp is the asteroid family/grpup (Warner et al., 2009).

4528 Berg (1983 PP) is a main-belt asteroid discovered by Edward Bowell (Lowell Observatory) and named for the Austrian composer Alban Berg. It is 9 km in diameter (JPL, 2022). Behrend (2006web), using observations from Pierre Antonini posted a provisional rotation period of 3.5163±0.004 hours. Stecher et al. (2015) estimated a period of 3.47±0.47 hours. With almost complete coverage Polakis (2018) found the period to be 3.5626±0.0004 hours. Data from Polakis (2018) for one night in 2014 in Johnson V (Pts = 109) and six nights in 2018 in C (Pts = 342) were downloaded from the ALCDEF database. Fourier analysis resulted in the same period and uncertainty reported here. 4528 Berg was recently found to be binary (Benishek et al., 2022) using a much larger data set than reported here and reported a primary rotation period (3.5627 ± 0.0001 hr), a satellite orbital period (35.02 ± 0.02 hr) and a light curve amplitude (0.23 magnitude at solar phases 1-4 degrees).

Berg was imaged over eight nights between 2022 April 07 and 2022 May 07 with a total of 587 images covering all phases of the lightcurve. Precision was in the millimagnitudes in April (0.007) and decreased to an average 0.01 magnitude in May as the asteroid dimmed. Fourier analysis of fit = 4 in *Tycho Tracker* returned a rotation period of 3.5630 ± 0.0001 hr (Figs. 5, 6). This is close to the primary rotation period reported by Benishek et al. (2022). We note that the minima from two nights (2022/05/07, phase 0 and 2022/04/08 at phase 0.50) show a magnitude drop of ca. 0.10 magnitude. To explore these possible mutual events, we employed the dual period algorithm of MPO Canopus to extract the secondary period. Further analysis of our data was carried out using *MPO Canopus* (Warner, 2010) to investigate possible mutual events, using the dual period feature as detailed below. *Peranso* (Vanmunster, 2013) was used to estimate or calculate minima of mutual events.

Our primary lightcurve is shown in Fig. 7 and the satellite lightcurve in Fig. 8. Using the original data from both nights on which a mutual event was observed we were able to calculate a time of minimum HJD 2459706.67713 (2022 May 7, 04:15:4.03 UT) for the 05-07 date using the Kwee-van Woerden (1956) algorithm implemented in *Peranso*. There were insufficient data points to calculate the minimum for the April 8 mutual event, an estimate based on the minimum magnitude observed is HJD 2459677.72 (2022 April 8 05:16:48 UT). See Table I for details.

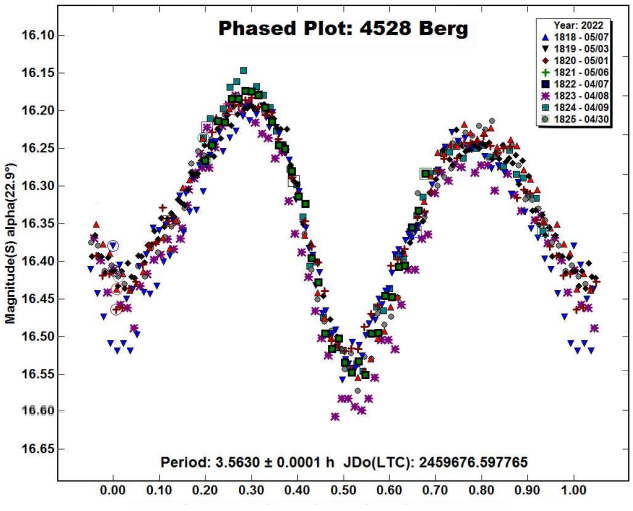

Figure 5. 4528 Berg, Phase plot.

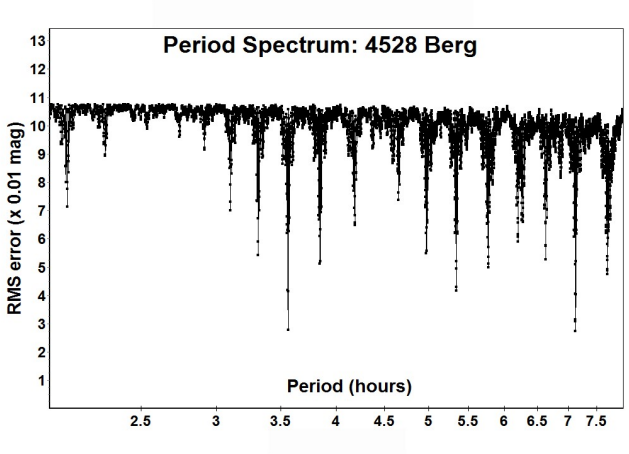

Figure 6. 4528 Berg, Period Spectrum from 2 to 8 hours showing alias at ca. 7.12 hours.

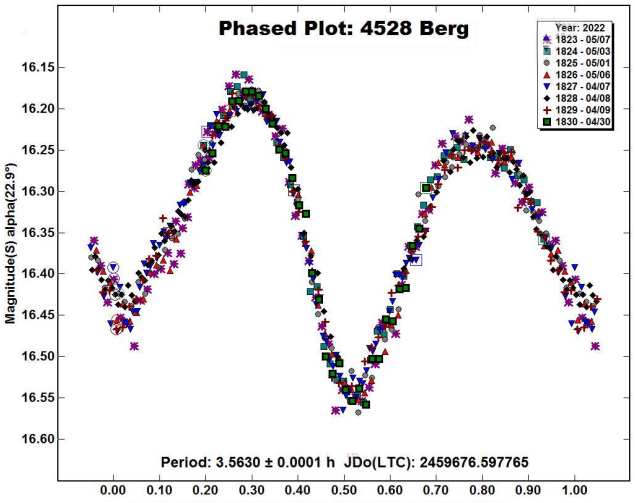

Figure. 7. 4528 Berg primary light curve.

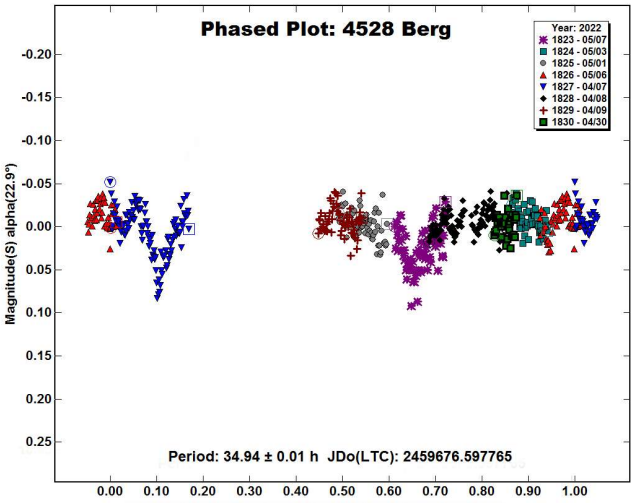

Figure. 8. Light curve of the 4528 Berg satellite showing the mutual events (Occultations, eclipses, or transits) based on the orbital period of the satellite from Benishek et al. (2022). Magnitude zero is the average magnitude of the primary.

Acknowledgements

EOW thanks FP for mentoring him through his first research in asteroid light curves. Thanks to Petr Pravec (Ondrejov Observatory), Vadimir Benishek (Belgrade Astronomical Observatory) and Russ Durkee (Shed of Science Observatory, V61) for comments to EOW. We acknowledge the Minor Planet Center, the Propulsion Laboratory Small Body Database and the ALCDEF Database for providing data used in this project.

References

Behrend, R. (2006web, 2018web). "Courbes de rotation d'astéroïdes et de comètes, CdR." *www.unige.ch/~behrend/ page_cou.html*

Benishek, V.; Pravec, P.; Scarfi, G.; Coffano, A.; Marinello, W.; and 14 collegues (2022). "(4528) Berg." *CBET* **5123**.

Hanus, J.; Durech, J.; Oszkiewicz, D.A.; Beherend, R.; Carry, B.; and 164 colleagues (2016). "New and updated convex shape models of asteroids based on optical data from a large collaboration network." *A&A* **586**, A108, 24pp.

Harris, A.W.; Young, J.W.; Scaltriti, F.; Zappala, V. (1984). "Lightcurves and phase relations of the asteroids 82 Alkmene and 444 Gyptis." *Icarus* **57**, 251-258.

JPL (2022). Small Body Database Search Engine. *https://ssd.jpl.nasa.gov*

Kwee, K.K.; van Woerden, H. (1956). "A method for computing accurately the epoch of minimum of an eclipsing variable." *Bull. Astron. Inst. Netherlands* **12**, 327.

Parrott, D. (2021) "Tycho Tracker: A New Tool to Facilitate the Discovery and Recovery of Asteroids Using Synthetic Tracking and Modern GPU Hardware." *JAAVSO* **48(2)**, 262.

Polakis, T. (2018). "Lightcurve analysis for eleven main-belt minor planets." *Minor Planet Bull.* **45**, 269-273.

Sada, P.V. (2008). "CCD Photometry of Three Short-period Asteroids from the Universidad de Monterrey Observatory." *Minor Planet Bull.* **35**, 161-162.

Strecher, G.; Ford, L.; Bluem, J.; Smith, B.; Fahey, S. (2015). "The Rotation Period of 4528 Burg." *Minor Planet Bull.* **42**, 148.

Tonry, J.L.; Denneau, L.; Flewelling, H.; Heinze, A.N.; Onken, C.A.; Smartt, S.J.; Stalder, B.; Weiland, H.J.; Wolf, C. (2018). "The ATLAS All-Sky Stellar Reference Catalog." *Astrophys. J.* **867**, A105.

Vanmunster, T. (2013). Light curve and period analysis software *Peranso,* v.2.50. *http://www.cbabelgium.com/peranso*

Warner, B.D.; Harris, A.W.; Pravec, P. (2009). "The Asteroid Lightcurve Database." *Icarus* **202**, 134-146. Updated 2021 May. *http://www.minorplanet.info/lightcurvedatabase.html*

Warner, B.D. (2010). MPO Software, *MPO Canopus*. Bdw Publishing, Colorado Springs, CO. *http://minorplanetobserver.com*

Warner, B.D.; Harris, A.W.; Ďurech, J.; Benner, L.A.M. (2022). "Lightcurve Photometry Opportunities: 2022 January - March." *Minor Planet Bull.* **49**, 61-64.

Waszczak, A.; Chang, C.-K.; Ofek, E.O.; Laher, R.; Masci, F.; Levitan, D.; Surace, J.; Cheng, Y.-C.; Ip, W.-H.; Kinoshita, D.; Helou, G.; Prince, T.A.; Kulkarni, S. (2015). "Asteroid Light Curves from the Palomar Transient Factory Survey: Rotation Periods and Phase Functions from Sparse Photometry." *Astron. J.* **150**, A75.

CCD PHOTOMETRY OF 35 ASTEROIDS AT SOPOT ASTRONOMICAL OBSERVATORY: 2021 NOVEMBER - 2022 JULY

Vladimir Benishek
Belgrade Astronomical Observatory
Volgina 7, 11060 Belgrade 38, SERBIA
vlaben@yahoo.com

(Received: 2022 July 10)

Lightcurves and synodic rotation periods were established for 35 asteroids using photometric observations carried out at Sopot Astronomical Observatory between 2021 November and 2022 July are presented in this paper.

Photometric observations of 35 asteroids were conducted at Sopot Astronomical Observatory (SAO) from 2021 November through 2022 July in order to determine the asteroids' synodic rotation periods. For this purpose, two 0.35-m *f*/6.3 Meade LX200GPS Schmidt-Cassegrain telescopes were employed. The telescopes are equipped with a SBIG ST-8 XME and a SBIG ST-10 XME CCD cameras. The exposures were unfiltered and unguided for all targets. Both cameras were operated in 2×2 binning mode, which produces image scales of 1.66 arcsec/pixel and 1.25 arcsec/pixel for ST-8 XME and ST-10 XME cameras, respectively. Prior to measurements, all images were corrected using dark and flat field frames.

Photometric reduction was conducted using *MPO Canopus* (Warner, 2018). Differential photometry with up to five comparison stars of near solar color ($0.5 \leq$ B-V ≤ 0.9) was performed using the Comparison Star Selector (CSS) utility. This helped ensure a satisfactory quality level of night-to-night zero-point calibrations and correlation of the measurements within the standard magnitude framework. Field comparison stars were calibrated using standard Cousins R magnitudes derived from the Carlsberg Meridian Catalog 15 (VizieR, 2022) Sloan r' magnitudes using the formula: R = r' - 0.22 in all cases presented in this paper. In some instances, small zero-point adjustments were necessary in order to achieve the best match between individual data sets in terms of achieving the most favorable statistical indicators of Fourier fit goodness.

Lightcurve construction and period analysis were performed using *Perfindia* custom-made software developed in the R statistical programming language (R Core Team, 2020) by the author. The essence of its algorithm is reflected in finding the most favorable solution for rotational period by minimizing the *residual standard error* of the lightcurve Fourier fit.

The lightcurve plots presented in this paper show so-called 2% error for rotational periods, i.e., an error that would cause the last data point in a combined data set by date order to be shifted by 2% (Warner, 2012) and represented by

$$\Delta P = (0.02 \cdot P^2) / T$$

where P and T are the rotational period and the total time span of observations, respectively. Both of these quantities must be expressed in the same units.

Some of the targets presented in this paper were observed within the Photometric Survey for Asynchronous Binary Asteroids (*BinAstPhot Survey*) under the leadership of Dr. Petr Pravec from Ondřejov Observatory, Czech Republic.

Table I gives the observing circumstances and results.

87 Sylvia. The rotation period derived from the 2022 March SAO observations, $P = 5.18 \pm 0.02$ h, is in full agreement with virtually all previously recorded values in the Asteroid Lightcurve Database (LCDB; Warner et al., 2009a), including 5.183 h (Schober and Surdej, 1979), 5.184 h (Foerster and Potthoff, 2001), 5.1833 h (Behrend, 2007web), and 5.1858 h (Behrend 2021web).

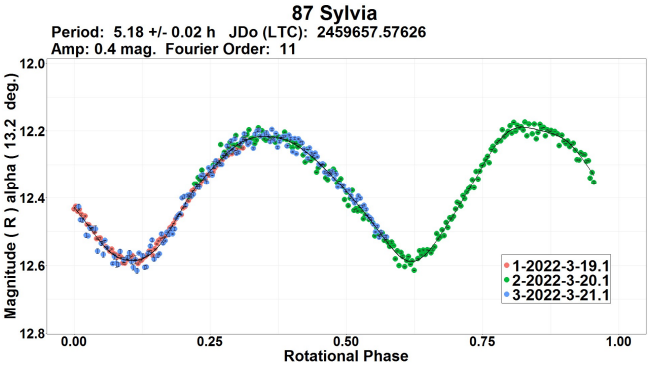

967 Helionape. Photometric data obtained at SAO in early 2022 February over four nights indicate a bimodal lightcurve solution with a corresponding period of $P = 3.233 \pm 0.002$ h, perfectly in line with previous higly-consistent results: 3.234 h (Apostolovska et al., 2009), 3.232 h (Kryszczynska et al., 2012), and 3.2341 h (Behrend, 2020web).

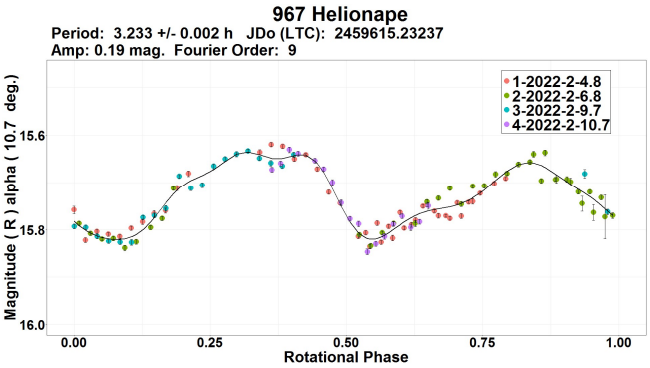

1019 Strackea. During the 2022 apparition, this Hungaria asteroid was observed at two different viewing geometries resulting in two separate data groups and two composite lightcurves different in shape. The first data group was obtained on two consecutive nights in 2022 April and show a bimodal lightcurve phased to a period of $P = 4.05 \pm 0.02$ h as a plausible solution.

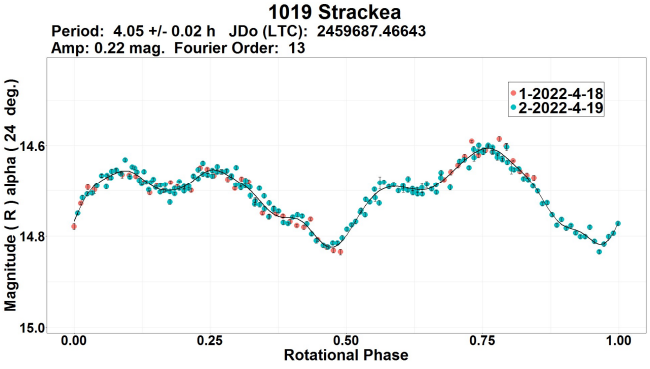

Another group of data acquired over 6 nights from mid-2022 June to early 2022 July also indicates a bimodal solution corresponding to the period of $P = 4.0460 \pm 0.0007$ h.

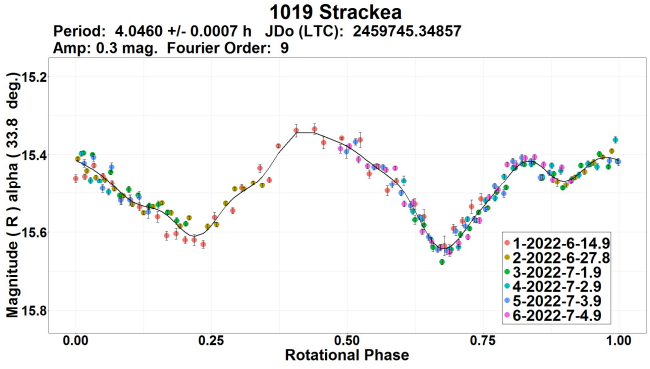

Both results are not only mutually consistent, but are also consistent with most previously established periods: 4.05 h (Behrend, 2006web), 4.044 h (Warner, 2009b), 4.047 h (Warner, 2011), 4.048 h (Stephens and Warner, 2019), and 4.04729 h (Pal, 2020).

1156 Kira. Data obtained on a single night in 2022 January were sufficient to achieve coverage of more than one rotation cycle and to establish at least a coarse period of $P = 2.71 \pm 0.05$ h. Nevertheless, it matches quite well the previous period results recorded in the LCDB: 2.79103 h, 2.79105 h, and 2.79113 h (Dykhuis et al., 2016), and 2.791 h (Polakis, 2021).

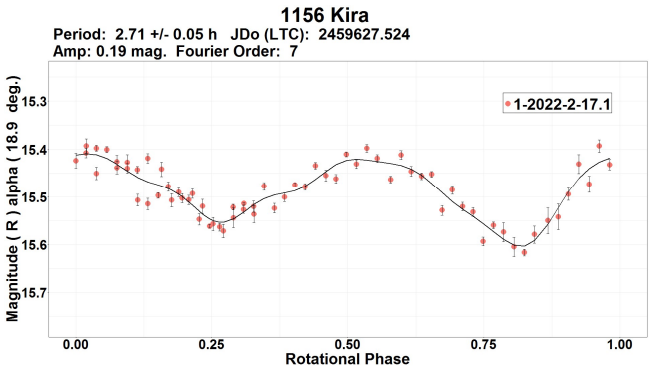

1346 Gotha. A bimodal period of $P = 2.640 \pm 0.002$ h is singled out as the most favorable result in the period analysis conducted upon the data collected over four nights in 2022 January. A search for previously determined periods in the LCDB finds a series of values in very good agreement with the newly established result, for example: 2.6548 h (Behrend, 2006web), 2.64067 h (Behrend, 2011web), 2.640 h (Waszczak et al., 2015), and 2.642 h (Aznar Macias, 2017).

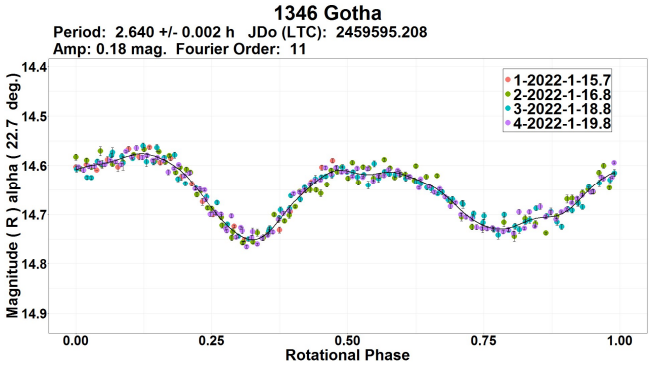

1664 Felix. In this case as well, the data are divided into two groups collected at two different viewing geometries during the same 2022 apparition. The first group was obtained over two consecutive nights in 2022 January while the second one was acquired on two consecutive nights two months later. Consequently, as a result of period analysis, two bimodal lightcurves of different shape phased to statistically identical period values of 3.345 ± 0.008 h and 3.344 ± 0.009 h were constructed. An insight into the LCDB database indicates a very good agreement with the new results and those previously determined by Higgins et al. (2008, 3.3454 h) and a sidereal rotation period by Durech et al. (2020, 3.344855 h).

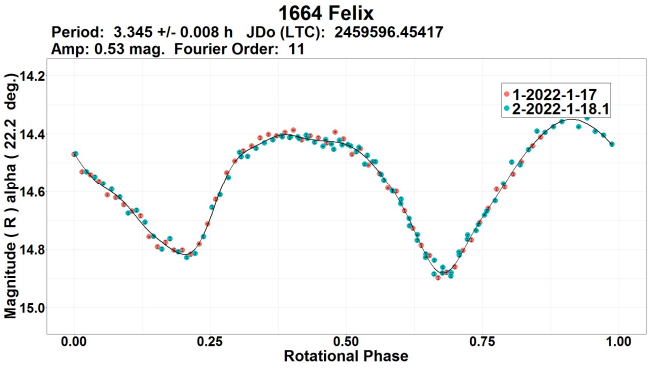

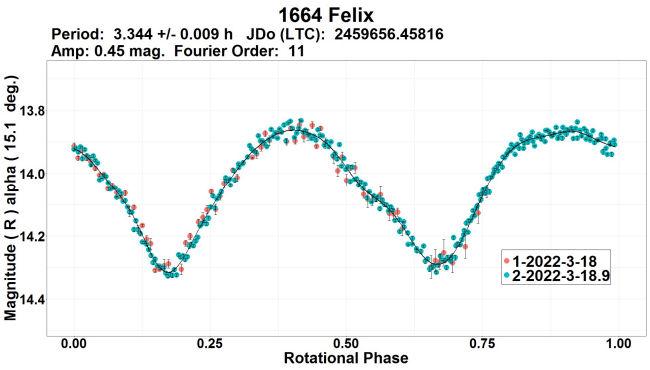

1816 Liberia. Data from two consecutive nights in 2022 May led to an unambiguous bimodal solution with a period of $P = 3.086 \pm 0.007$ h. The SAO data collected in the 2019 apparition showed an identical result of 3.08606 h (Benishek, 2020).

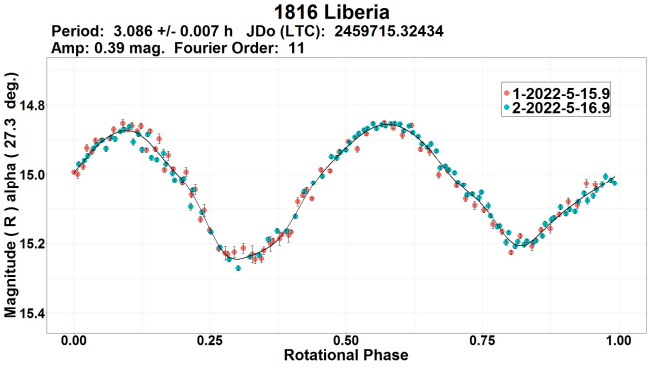

1878 Hughes. This was a *BinAstPhot Survey* target. According to the LCDB records on this asteroid, there is only one previously known rotation period, Molnar et al. (2018, 2.683 h). A bimodal period of $P = 2.6833 \pm 0.0003$ h found from the 2022 February-March SAO data apparently confirms the previous finding.

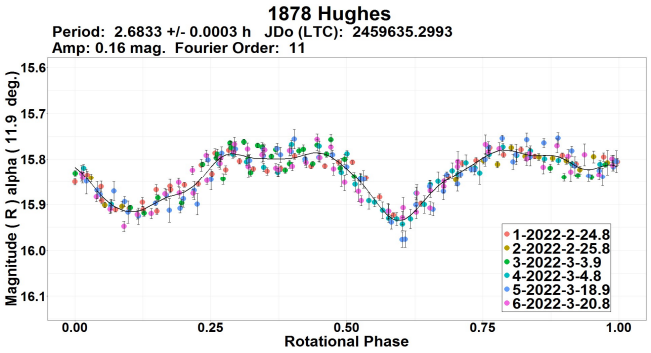

1884 Skip. Previously known rotation periods include Di Martino et al. (1994, 3.079 h), Behrend (2017web, 7.7477 h), Benishek and Rowe (2018, 2.89484 h), Skiff et al. (2019, 2.8887 h), and a sidereal period by Durech et al. (2020, 2.89442 h). The 2022 apparition SAO observations obtained on five nights in January and three nights in February produced two bimodal lightcurves with statistically equal periods of 2.894 ± 0.002 h (January) and 2.895 ± 0.004 h (February).

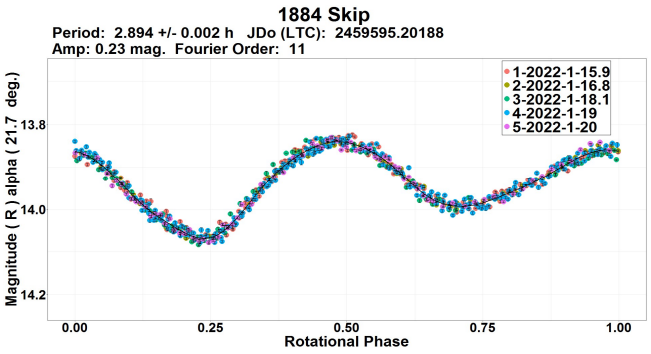

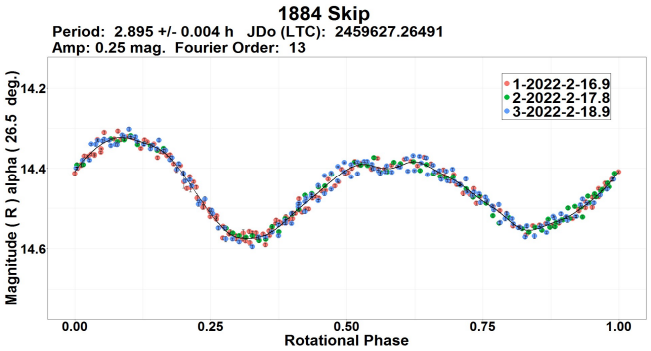

2635 Huggins. A rotation period result of P = 3.1320 ± 0.0007 h, found from SAO data obtained on three nights in 2022 April, corroborates a previous result by Waszczak et al. (2015, 3.129 h).

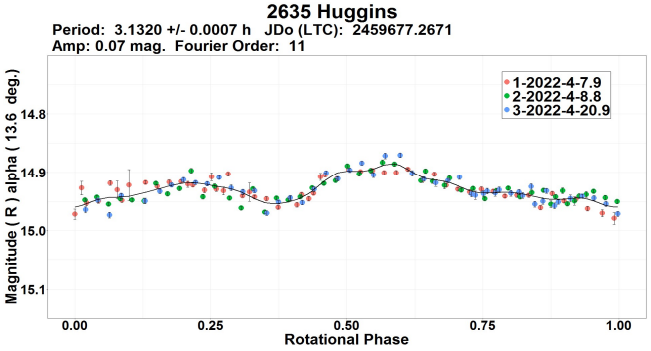

2714 Matti. A bimodal period solution of P = 9.27 ± 0.02 h was obtained from a data set obtained over two nights in 2022 April. Durech et al. (2020) found a sidereal rotation period of 9.27359 h.

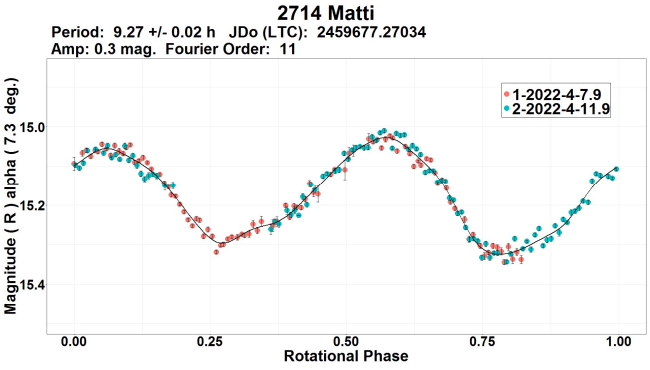

3057 Malaren. A period of 4.496 ± 0.002 h was found from data obtained on six nights in 2022 March-April. The result is identical to the only previous result of 4.496 h by Waszczak et al. (2015).

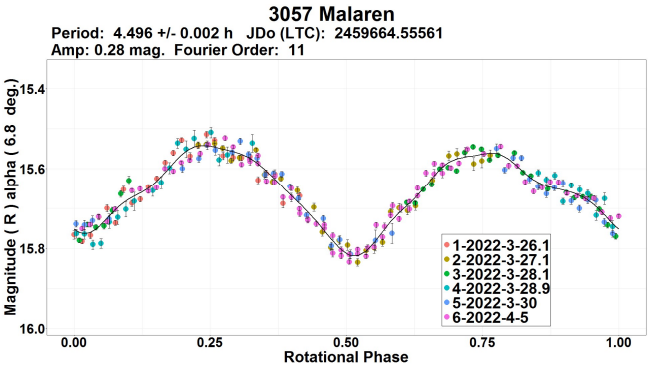

3263 Bligh was observed on four nights in late 2022 January. Period analysis led to a bimodal solution with P = 3.191 ± 0.002 h. This matches very well with the only previously known period determination by Casalnuovo (2014, 3.193 h).

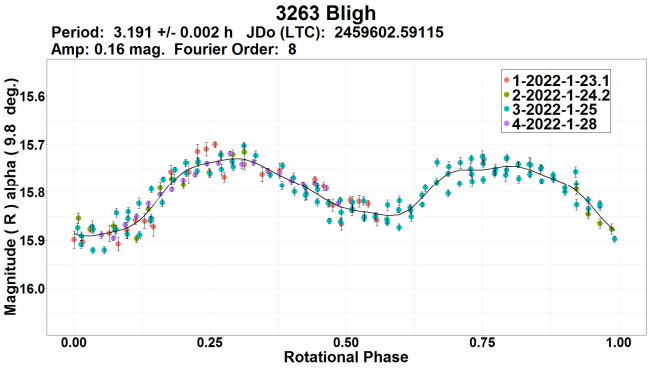

3388 Tsanginchi. A period of P = 3.2570 ± 0.0005 h was determined from observations made on four nights in 2022 January. An excellent match with a rotation period result found by Durkee (2011, 3.257 h) is obvious.

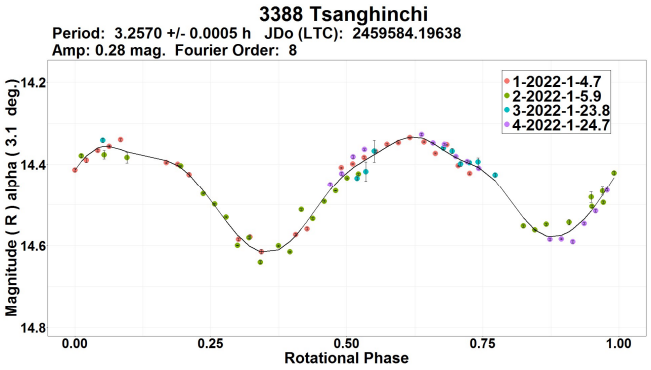

3477 Kazbegi. Period analysis conducted on the 2022 May-June combined data set yielded an unequivocal bimodal period solution of P = 8.401 ± 0.002 h.

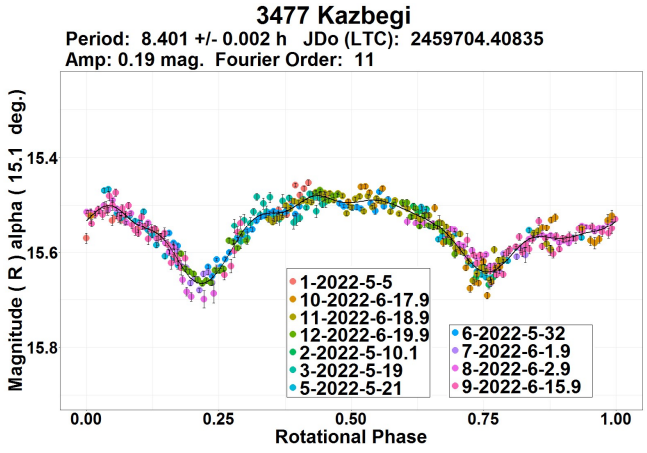

4235 Tatishchev. No records on previous rotation period determinations were found in the LCDB. Photometric observations taken with high cadence on two consecutive nights in 2022 March proved sufficient to unambiguously establish a bimodal lightcurve solution phased to a period of P = 5.07 ± 0.02.

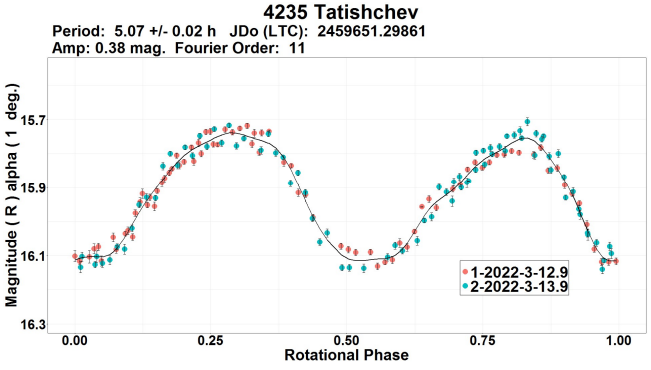

4935 Maslachkova. A period of P = 2.91 ± 0.03 h, determined from a single night of observations in 2021 November, is statistically consistent with the results found by Galad et al. (2009, 2.90192 h) and Waszczak et al. (2015, 2.903 h).

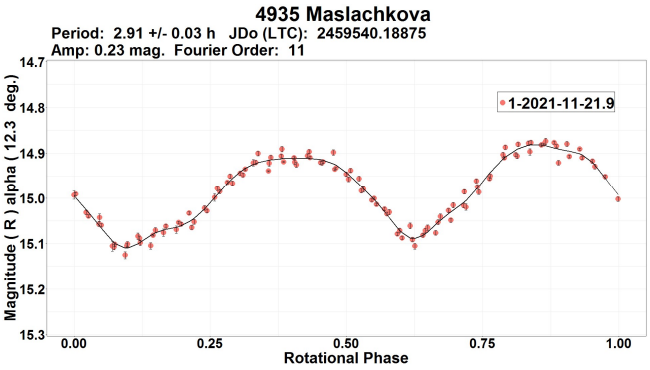

5129 Groom. This asteroid was a *BinAstPhot Survey* returning binary suspect. Data obtained on three nights in 2022 May show a synodic rotation period of P = 3.638 ± 0.002 h, a result that is in very good agreement with the vast majority of previously determined values: 3.636 h (Behrend, 2007web), 3.6378 h (Pravec, 2007web), 3.6374 h (Pravec, 2011web), 3.6362 h (Pravec, 2012web), 3.6371 h (Pravec, 2016web), 3.6376 h (Pravec, 2018web), and a sidereal period of 3.63759 h by Durech et al. (2020). No significant deviations in the lightcurve that could point to the existence of a secondary rotation component or mutual events were detected during the 2022 apparition.

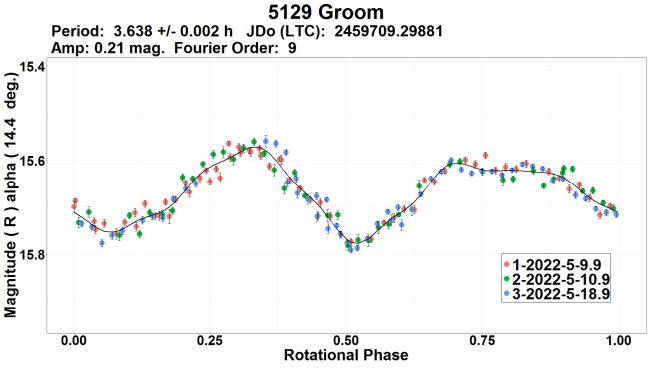

5182 Bray. Analysis of four nights of observations at SAO in 2022 late June to early July indicate a short rotation period bimodal solution of P = 2.884 ± 0.002 h, which is consistent with other values found to date, e.g., 2.883 h (Klinglesmith, 2014web), 2.884 h (Behrend, 2018web), and 2.86 h (Fauerbach, 2019).

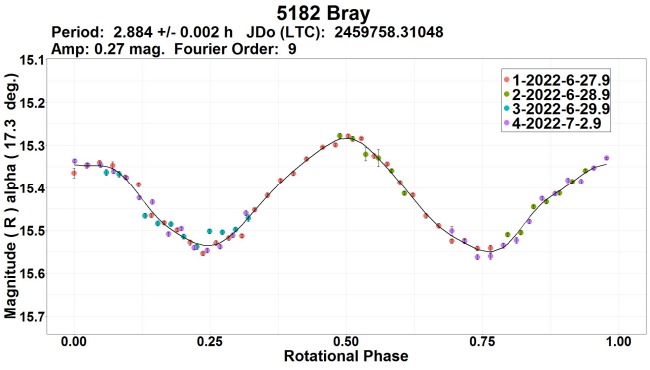

6714 Montreal. Prior to this rotation period determination there was only one sidereal period result reported by Durech (2020, 2.651089 h). Period analysis of the 2022 May SAO data taken on three nights yielded a synodic period of P = 2.651 ± 0.002 h.

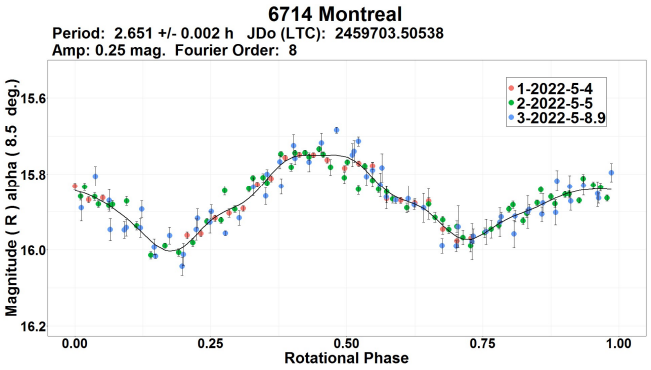

6729 Emiko. The only previously reported rotation period by Behrend (2016web, 3.13 h) is highly consistent with the value of $P = 3.14 \pm 0.03$ h shown here, which was obtained from the single night dense photometric data taken in 2022 mid-March.

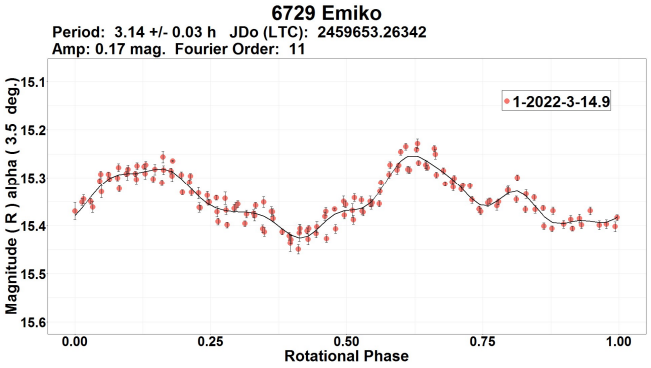

6920 Esaki. This is a Vestoid asteroid with no previously known spin rate. Four data sets obtained at SAO in 2022 February reveal a fairly fast rotation with a period of $P = 3.069 \pm 0.002$ h.

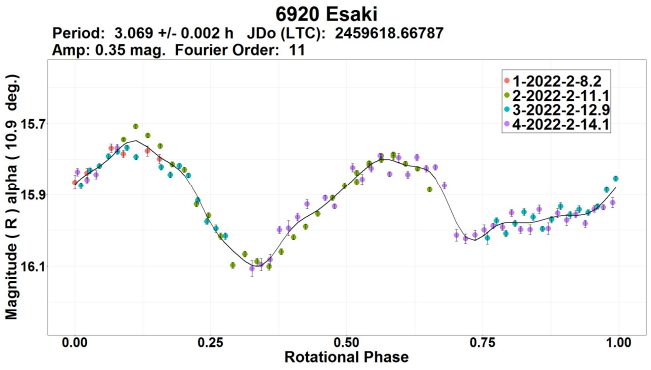

7172 Multatuli. Erasmus et al. (2020) report a value of 3.357 h for rotation period. The uncertainty score of U = 2- assigned in the LCDB indicates that the result, the only one previously reported, is mostly unreliable, i.e., barely statistically valid for rotation rate studies. The 2022 February dense cadence SAO combined data set obtained over four nights shows a somewhat different rotation period of $P = 3.479 \pm 0.003$ h based on a bimodal lightcurve solution.

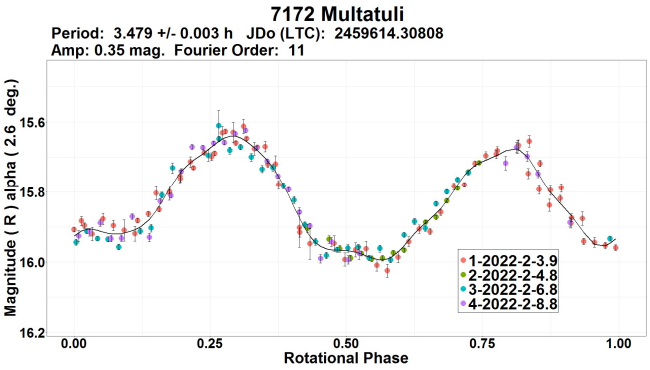

7516 Kranjc. This was a returning *BinAstPhot Survey* suspected binary asteroid. A unique bimodal rotation period solution of $P = 3.9690 \pm 0.0009$ h was determined from the SAO dense combined data set obtained over five nights in 2022 April. The newly found value corresponds very well to those previously known, such as 3.96769 h (Pravec, 2008web), 3.96776 h (Oey, 2009), 3.982 h (Warner, 2009c), and 3.9702 h (Pravec, 2019web). No significant attenuations in the rotational lightcurve that could be a binarity indicator were detected in the 2022 apparition data.

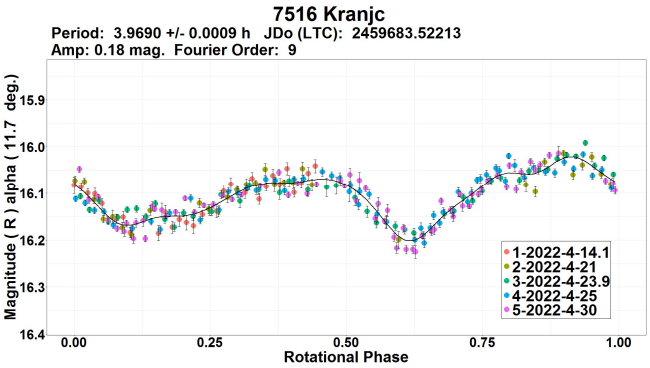

7736 Nizhnij Novgorod. Papini et al. (2019) reported a value of 2.858 h for rotational period. Period analysis of the SAO combined photometric data set obtained over five nights in 2022 May-June yielded a period $P = 2.8582 \pm 0.0004$ h, which is equal to the one previously determined.

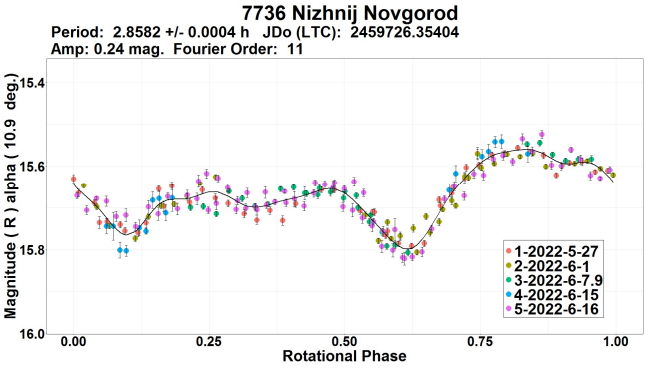

11001 Andrewulff. This was another returning *BinAstPhot Survey* binary suspect. The period of $P = 3.964 \pm 0.001$ h derived from the 2022 March-April SAO observations matches well with two previously reported results by Pravec (2012web, 3.9638 h) and Waszczak et al. (2015, 3.965 h). No signs of a possible satellite were observed.

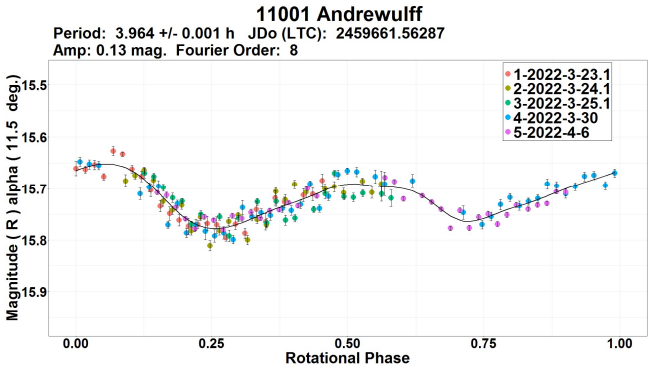

(11512) 1991 AB2. Hess and Ditteon (2016) found a period of 2.933 h. The period result obtained using 2022 February-March SAO data collected on three nights is $P = 2.9334 \pm 0.0004$ h.

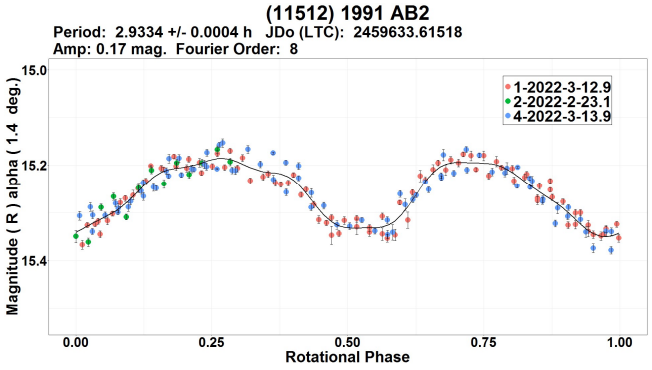

(13255) 1998 OH14. This was a *BinAstPhot Survey* target. The rotation period found in 2017 from the BinAstPhot Survey observations by Donald Pray is 3.2941 h (Pravec, 2017web). Any significant rotational lightcurve deviations were not detected at that time.

During the 2022 apparition, this target was observed at SAO in February and March. Due to viewing geometry changes over the time span of observations, the data were split into two separate groups, each producing a lightcurve of different shape from the other.

No significant deviations that could indicate the presence of a satellite were observed in either of the lightcurves. Results for rotation period obtained from both combined data sets in independent period analyzes are higly consistent with each other: 3.2927 ± 0.0007 h (2022 February, five nights) and 3.293 ± 0.003 h (2022 March, four nights).

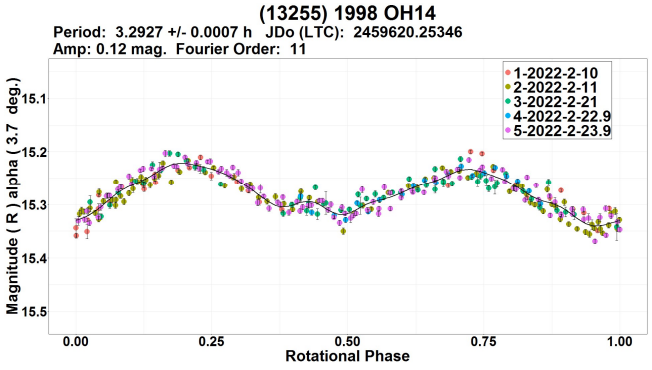

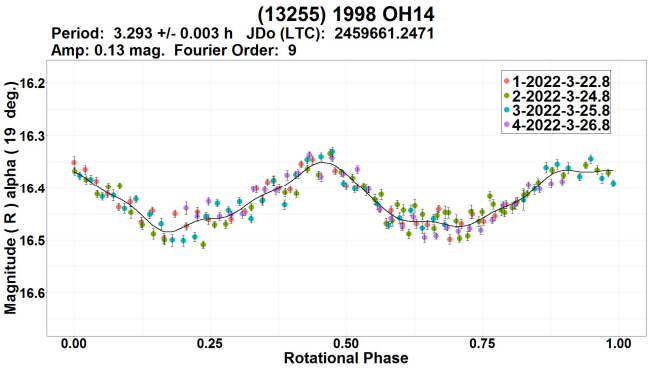

17170 Vsevustinov. This returning *BinAstPhot Survey* suspected binary asteroid was observed in the 2012 apparition without any sign of a satellite. During the 2022 apparition, observations were made in April and May for a total of eight nights. The 2012 result for a rotation period of 3.3750 h (Pravec, 2012web) is almost identical to the newly established result of $P = 3.3746 \pm 0.0005$ h derived from the 2022 data. As in 2012, the 2022 observations found no lightcurve deviations that would indicate a satellite.

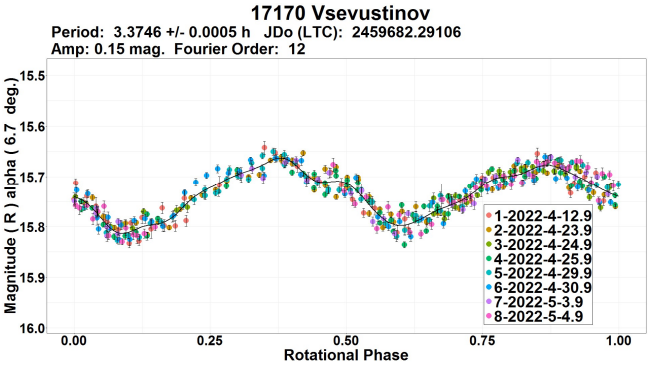

(21831) 1999 TX93. No previous rotation period reports were found in the LCDB. Photometric observations with dense cadence were carried out at SAO on three nights in 2022 February-March. Although the data analysis indicates a small lightcurve amplitude of only 0.1 mag, a reliable unique period of $P = 4.0940 \pm 0.0008$ h was established.

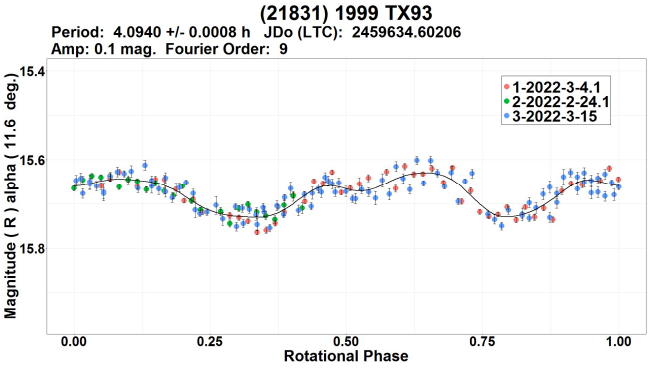

(23456) 1989 DB. A plausible rotation period of $P = 2.8040 \pm 0.0005$ h was found from the 2022 February-March combined data set obtained over five nights. The possibility of a harmonically related bimodal period solution of 5.609 ± 0.002 h, i.e., 2P, within the perod error, was ruled out since the two halves of the corresponding bimodal lightcurve were essentialy equal. According to the LCDB, this is the first reported period for the asteroid.

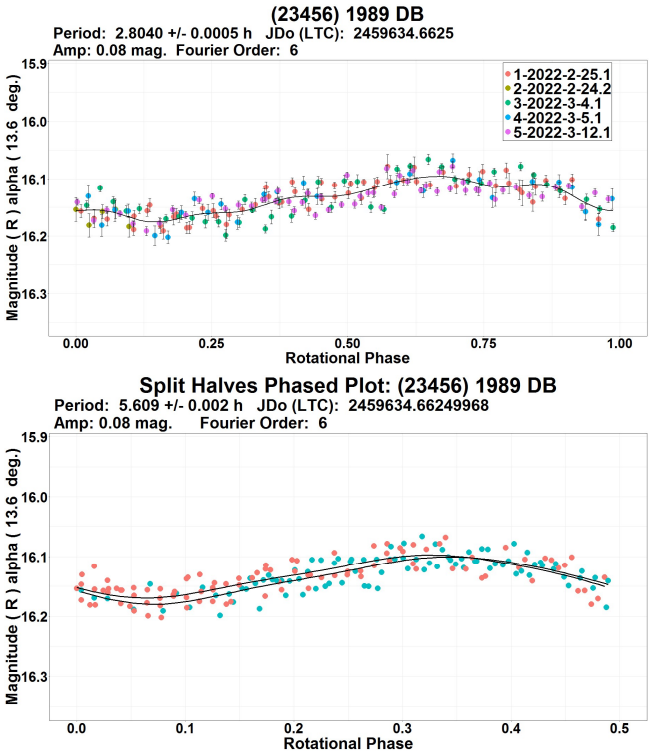

24779 Presque Isle. A search for of the LCDB found no previous results. Period analysis conducted on the 2022 June SAO combined data set shows a secure bimodal lightcurve with a period of $P = 4.4844 \pm 0.0008$ h.

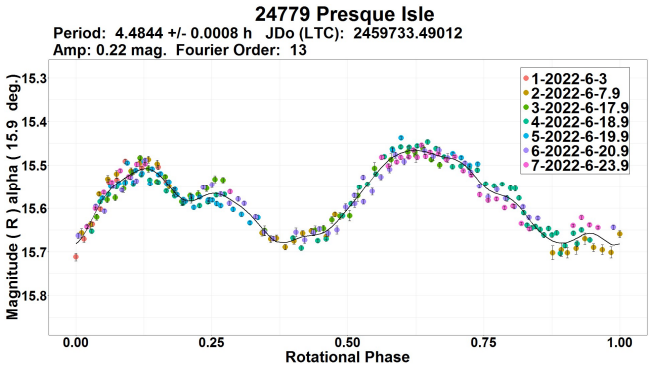

(36619) 2000 QE151. A period of $P = 2.5830 \pm 0.0007$ h was found from the 2022 January-February combined data set. This closely matches the only previous result of 2.58294 h found by Pal et al. (2020).

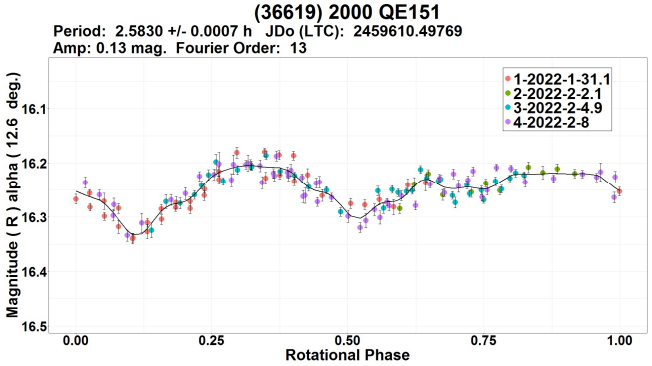

(42701) 1998 MD13. As in some cases described above, the data were divided into two groups and analyzed separately due to the changing viewing geometry and lightcurve shape over the observing span (2022 April-May). The established period values are exactly the same for both data groups (including the period errors): $P = 2.604 \pm 0.002$ h. Previously known period determinations include 2.602 h (Klinglesmith and Lovata, 2018), 2.603 h (Papini et al., 2019), and 2.603 h (Rowe, 2019).

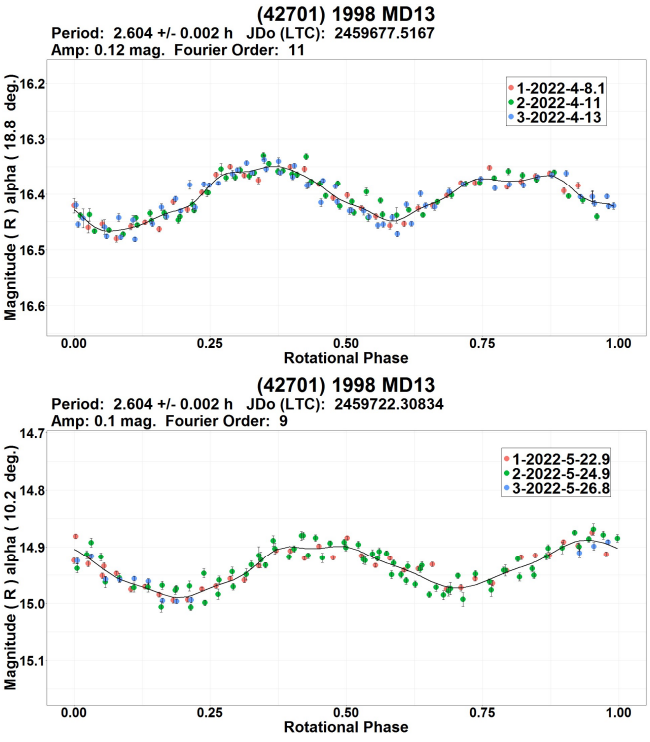

(170891) 2004 TY16. The rotation period presented here for this near-Earth asteroid ($P = 2.791 \pm 0.003$ h) is fully accordant with the only previously reported result by Carbognani (2008, 2.795 h).

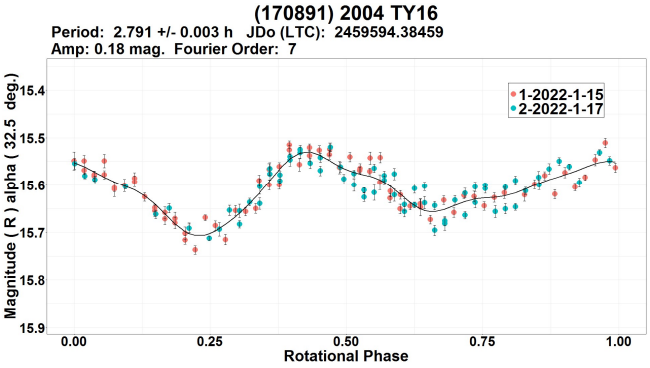

Acknowledgements

Observational work at Sopot Astronomical Observatory is generously supported by Gene Shoemaker NEO Grants awarded by the Planetary Society in 2018 and 2022.

References

Apostolovska, G.; Ivanova, V.; Kostov, A. (2009). "CCD Photometry of 967 Helionape, 3415 Danby, (85275) 1994 LY, 2007 DT103, and 2007 TU24." *Minor Planet Bull.* **36**, 27-28.

Number	Name	20yy/mm/dd	Phase	L_{PAB}	B_{PAB}	Period (h)	P.E.	Amp	A.E.	Grp
87	Sylvia	22/03/19-03/21	13.2,12.9	227	7	5.18	0.02	0.40	0.02	SYL
967	Helionape	22/02/04-02/10	10.7,13.1	112	4	3.233	0.002	0.19	0.02	FLOR
1019	Strackea	22/04/17-04/19	24.0,24.3	189	32	4.05	0.02	0.22	0.01	HUN
1019	Strackea	22/06/14-07/04	33.8,34.4	207	32	4.0460	0.0007	0.30	0.02	HUN
1156	Kira	22/02/17-02/17	18.9,18.9	186	2	2.71	0.05	0.19	0.03	MB-I
1346	Gotha	22/01/15-01/19	22.7,23.5	70	-17	2.640	0.002	0.18	0.02	EUN
1664	Felix	22/01/16-01/18	22.2,21.8	149	9	3.345	0.008	0.53	0.02	MB-I
		22/03/17-03/19	15.1,15.7	158	8	3.344	0.009	0.45	0.02	MB-I
1816	Liberia	22/05/15-05/17	27.3,27.4	184	24	3.086	0.007	0.39	0.02	PHO
1878	Hughes	22/02/24-03/20	12.0,18.1	127	-2	2.6833	0.0003	0.16	0.03	KOR
1884	Skip	22/01/15-01/20	21.7,22	106	30	2.894	0.002	0.23	0.02	MB-I
		22/02/16-02/19	26.5,26.9	113	24	2.895	0.004	0.25	0.02	MB-I
2635	Huggins	22/04/07-04/20	13.6,19.4	177	-6	3.1320	0.0007	0.07	0.02	FLOR
2714	Matti	22/04/07-04/12	7.3,9.4	188	7	2.604	0.002	0.12	0.02	MB-I
3057	Malaren	22/03/26-04-05	*6.8,6.4	191	10	4.496	0.002	0.28	0.02	MB-I
3263	Bligh	22/01/23-01/28	9.8,7.8	139	9	3.191	0.002	0.16	0.03	V
3388	Tsanghinchi	22/01/04-01/24	3.1,13.8	106	7	3.2570	0.0005	0.28	0.02	PHO
3477	Kazbegi	22/05/04-06/20	*15.1,11.5	251	9	8.401	0.002	0.19	0.02	V
4235	Tatishchev	22/03/12-03/14	1.0,1.4	170	0	5.07	0.02	0.38	0.03	MB-O
4935	Maslachkova	21/11/21-11/22	12.3,12.5	44	-8	2.91	0.03	0.23	0.02	FLOR
5129	Groom	22/05/09-05/18	14.4,17.8	205	10	3.638	0.002	0.21	0.01	MB-O
5182	Bray	22/06/27-07/02	17.3,18.7	250	19	2.884	0.002	0.27	0.01	MB-I
6714	Montreal	22/05/04-05/09	*8.5,7.9	231	17	2.651	0.002	0.25	0.03	MB-I
6729	Emiko	22/03/14-03/15	3.5,3.4	175	7	3.14	0.03	0.17	0.02	EUN
6920	Esaki	22/02/08-02/14	10.9,8.4	157	9	3.069	0.002	0.35	0.03	V
7172	Multatuli	22/02/03-02/08	2.6,5.2	132	3	3.479	0.003	0.35	0.02	HER
7516	Kranjc	22/04/14-04/30	11.7,6.0	222	8	3.9690	0.0009	0.18	0.03	MB-I
7736	Nizhnij Novgorod	22/05/26-06/16	*10.9,11.8	254	19	2.8582	0.0004	0.24	0.03	EUN
11001	Andrewulff	22/03/23-04/06	11.5,4.9	198	5	3.964	0.001	0.13	0.02	MB-I
11512	1991 AB2	22/02/23-03/14	*9.4,2.2	169	-1	2.9334	0.0004	0.17	0.03	MB
13255	1998 OH14	22/02/09-02/24	*3.7,6.0	146	3	3.2927	0.0007	0.12	0.02	MB-I
		22/03/22-03/26	19.0,20.5	150	4	3.293	0.003	0.13	0.03	MB-I
17170	Vsevustinov	22/04/12-05/05	6.7,15.7	201	9	3.3746	0.0005	0.15	0.02	FLOR
21831	1999 TX93	22/02/24-03/15	15.2,6.0	184	2	4.0940	0.0008	0.10	0.02	MB-I
23456	1989 DB	22/02/24-03/12	14.0,5.3	178	3	2.8040	0.0005	0.08	0.02	MB-I
24779	Presque Isle	22/06/02-06/24	15.9,10.8	273	18	4.4844	0.0008	0.22	0.03	MB-I
36619	2000 QE151	22/01/30-02/08	12.6,8.2	152	-2	2.5830	0.0007	0.13	0.03	FLOR
42701	1998 MD13	22/04/08-04/13	18.8,16.8	227	10	2.604	0.002	0.12	0.02	MB-I
		22/05/22-05/26	10.2,11.6	232	12	2.604	0.002	0.10	0.02	MB-I
170891	2004 TY16	22/01/14-01/17	32.5,31.9	138	10	2.791	0.003	0.18	0.03	NEA

Table I. Observing circumstances and results. Phase is the solar phase angle given at the start and end of the date range. If preceded by an asterisk, the phase angle reached an extrema during the period. L_{PAB} and B_{PAB} are the average phase angle bisector longitude and latitude. Grp is the asteroid family/group (Warner *et al.*, 2009a): SYL = Sylvia, HUN = Hungaria, FLOR = Flora, MB-I/O = main-belt inner / outer, PHO = Phocaea, V = Vestoid, NEA = near-Earth asteroid, HER = Hertha, EUN = Eunomia, KOR = Koronis.

Aznar Macias, A. (2017). "Lightcurve Analysis from APT Observatory Group for Nine Main-belt Asteroids: 2016 July - September. Rotation Period and Physical Parameters." *Minor Planet Bull.* **44**, 60-63.

Behrend, R. (2006web, 2007web, 2011web, 2016web, 2017web, 2018web, 2020web, 2021web). Observatoire de Geneve web site. *http://obswww.unige.ch/~behrend/page_cou.html*

Benishek, V. (2020). "Asteroid Photometry at Sopot Astronomical Observatory: 2019 June - October." *Minor Planet Bull.* **47**, 75-83.

Benishek, V.; Rowe, B. (2018). "New Lightcurve and Rotation Period Determination for 1884 Skip." *Minor Planet Bull.* **45**, 267-268.

Carbognani, A. (2008). "Lightcurve Photometry of NEAs 4450 Pan, (170891) 2004 TY16, 2002 RC118, and 2007 VD12." *Minor Planet Bull.* **35**, 109-110.

Casalnuovo, G.B. (2014). "Lightcurve Analysis of 3182 Shimanto and 3263 Bligh." *Minor Planet Bull.* **41**, 85-86.

Di Martino, M.; Dotto, E.; Barucci, M.A.; Fulchignoni, M.; Rotundi, A. (1994). "Photoelectric Photometry of Ten Small and Fast Spinning Asteroids." *Icarus* **109**, 210-218.

Durech, J.; Tonry, J.; Erasmus, N.; Denneau, L.; Heinze, A.N.; Flewelling, H.; Vanco, R. (2020). "Asteroid models reconstructed from ATLAS photometry." *Astron. Astrophys*. **643**, A59-A63.

Durkee, R.I. (2011). "Asteroids Observed from the Shed of Science Observatory 2010 October - 2011 April." *Minor Planet Bull.* **38**, 167-168.

Dykhuis, M.J.; Molnar, L.A.; Gates, C.J.; Gonzales, J.A.; Huffman, J.J.; Maat, A.R.; Maat, S.L.; Marks, M.I.; Massey-Plantinga, A.R.; McReynolds, M.D.; Schut, J.A.; Stoep, J.P.; Stutzman, A.J.; Thomas, B.C.; Vander Tuig, G.W. and 2 colleagues (2016). "Efficient spin sense determination of Flora-region asteroids via the epoch method." *Icarus* **267**, 174-203.

Erasmus, N.; Navarro-Meza, S.; McNeill, A.; Trilling, D.E.; Sickafoose, A.A.; Denneau, L.; Flewelling, H.; Heinze, A.; Tonry, J.L. (2020). "Investigating Taxonomic Diversity within Asteroid Families through ATLAS Dual-band Photometry." *Astrophys. J. Suppl. Series* **247**, 13.

Fauerbach, M. (2019). "Photometric Observations of Asteroids 570 Kythera, 1334 Lundmarka, 2699 Kalinin, and 5182 Bray." *Minor Planet Bull.* **46**, 3-4.

Foerster, I.; Potthoff, H. (2001). "Lightcurves of Asteroids 43, 87, 129, and 130." *Minor Planet Bull.* **28**, 25-26.

Galad, A.; Vilagi, J.; Kornos, L.; Gajdos, S. (2009). "Relative Photometry of Nine Asteroids from Modra." *Minor Planet Bull.* **36**, 116-118.

Hess, K.; Ditteon, R. (2016). "Asteroid Lightcurve Analysis at the Oakley Southern Sky Observatory: 2015 February." *Minor Planet Bull.* **43**, 87.

Higgins, D.; Pravec, P.; Kusnirak, P.; Hornoch, K.; Brinsfield, J.W.; Allen, B.; Warner, B.D. (2008). "Asteroid Lightcurve Analysis at Hunters Hill Observatory and Collaborating Stations: November 2007 - March 2008." *Minor Planet Bull.* **35**, 123-126.

Klinglesmith III, D.A. (2014web). Posting on CALL web site. *http://www.MinorPlanet.info/call.html*

Klinglesmith III, D.A.; Lovata, E.A. (2018). "Three Asteroids from Etscorn: 461 Saskia, 3800 Karayusuf, and (42701) 1998 MD13." *Minor Planet Bull.* **45**, 397-398.

Kryszczynska, A.; Colas, F.; Polinska, M.; Hirsch, R.; Ivanova, V.; Apostolovska, G.; Bilkina, B.; Velichko, F.P.; Kwiatkowski, T.; Kankiewicz, P. and 20 colleagues. (2012). "Do Slivan states exist in the Flora family? I. Photometric survey of the Flora region." *Astron. Astrophys.* **546**, A72.

Molnar, L.; Pal, A.; Sarneczky, K.; Szabo, R.; Vinko, J.; Szabo, Gy.M., Kiss, Cs.; Hanyecz, O.; Marton, G.; Kiss, L.L. (2018). "Main-belt Asteroids in the K2 Uranus Field." *Ap. J. Supl. Ser*. **234**, id.37.

Oey, J.; Cooney, W.; Gross, J.; Terrell, D.; Marchis, F.; Stewart, H.; Stephens, R.D.; Brinsfield, J.W.; Vilagi, J.; Gajdos, S.; Crawford, G. (2009). "Photometry of Asteroids 7516 Kranjc, 7965 Katsuihiko, and (15515) 1999 VN80 from Leura and Other Collaborating Observatories." *Minor Planet Bull.* **36**, 50-51.

Pal, A.; Szakáts, R.; Kiss, C.; Bódi, A.; Bognár, Z.; Kalup, C.; Kiss, L.L.; Marton, G.; Molnár, L.; Plachy, E.; Sárneczky, K.; Szabó, G.M.; Szabó, R. (2020). "Solar System Objects Observed with TESS - First Data Release: Bright Main-belt and Trojan Asteroids from the Southern Survey." *Ap. J. Supl. Ser*. **247**, 26-34.

Papini, R.; Banfi, M.; Salvaggio, F.; Marchini, A. (2019). "Rotation Period Determination of Asteroids 7736 Nizhnij Novgorod and (42701) 1998 MD13." *Minor Planet Bull.* **46**, 99-100.

Polakis, T. (2021). "Photometric Observations of Eight Minor Planets for Shape Modeling." *Minor Planet Bull.* **48**, 144-147.

Pravec, P. (2007web, 2008web, 2011web, 2012web, 2016web, 2017web, 2018web, 2019web). Photometric Survey for Asynchronous Binary Asteroids web site. *http://www.asu.cas.cz/~ppravec/newres.txt*

R Core Team (2020). R: A language and environment for statistical computing. R Foundation for Statistical Computing. Vienna, Austria. *https://www.R-project.org/*

Rowe, B. (2019). "Lightcurve Analysis of 6 Asteroids from RMS Observatory." *Minor Planet Bull.* **46**, 92-94.

Schober, H.J.; Surdej, J. (1979). "UBV photometry of the asteroids 9 Metis, 87 Sylvia, and 247 Eukrate during their oppositions in 1978 with respect to lightcurves." *Astronomy & Astrophysics Suppl. Ser.* **38**, 269.

Skiff, B.A.; McLelland, K.P.; Sanborn, J.J.; Pravec, P.; Koehn, B.W. (2019). "Lowell Observatory Near-Earth Asteroid Photometric Survey (NEAPS): Paper 3." *Minor Planet Bull.* **46**, 238-265.

Stephens, R.D.; Warner, B.D. (2019). "Main-Belt Asteroids Observed from CS3: 2019 January - March." *Minor Planet Bull.* **46**, 298-301.

VizieR (2022). *http://vizier.u-strasbg.fr/viz-bin/VizieR*

Warner, B.D.; Harris, A.W.; Pravec, P. (2009a). "The Asteroid Lightcurve Database." *Icarus* **202**, 134-146. Updated 2021 Dec14. *http://www.minorplanet.info/lightcurvedatabase.html*

Warner, B.D. (2009b). "Asteroid Lightcurve Analysis at the Palmer Divide Observatory: 2009 March - June." *Minor Planet Bull.***36**, 172-176.

Warner, B.D. (2009c). "Asteroid Lightcurve Analysis at the Palmer Divide Observatory: 2008 May - September." *Minor Planet Bull.* **36**, 7-13.

Warner, B.D. (2011). "Asteroid Lightcurve Analysis at the Palmer Divide Observatory: 2010 December - 2011 March." *Minor Planet Bull.* **38**, 142-149.

Warner, B.D. (2012). *The MPO Users Guide: A Companion Guide to the MPO Canopus/PhotoRed Reference Manuals*. BDW Publishing, Eaton, CO.

Warner, B.D. (2018). *MPO Canopus* software, version 10.7.11.3. *http://www.bdwpublishing.com*

Waszczak, A.; Chang, C.-K.; Ofek, E.O.; Laher, R.; Masci, F.; Levitan, D.; Surace, J.; Cheng, Y.-C.; Ip, W.-H.; Kinoshita, D.; Helou, G.; Prince, T.A.; Kulkarni, S. (2015). "Asteroid Light Curves from the Palomar Transient Factory Survey: Rotation Periods and Phase Functions from Sparse Photometry." *Astron. J.* **150**, A75.

COLLABORATIVE ASTEROID PHOTOMETRY FROM UAI: 2022 APRIL-JUNE

Lorenzo Franco
Balzaretto Observatory (A81), Rome, ITALY
lor_franco@libero.it

Alessandro Marchini, Riccardo Papini
Astronomical Observatory, DSFTA - University of Siena (K54)
Via Roma 56, 53100 - Siena, ITALY

Paolo Bacci, Martina Maestripieri
GAMP - San Marcello Pistoiese (104), Pistoia, ITALY

Nello Ruocco
Osservatorio Astronomico Nastro Verde (C82), Sorrento, ITALY

Giulio Scarfi
Iota Scorpii Observatory (K78), La Spezia, ITALY

Marco Iozzi
HOB Astronomical Observatory (L63),
Capraia Fiorentina, ITALY

Nico Montigiani, Massimiliano Mannucci
Osservatorio Astronomico Margherita Hack (A57)
Florence, ITALY

Giorgio Baj
M57 Observatory (K38), Saltrio, ITALY

Adriano Valvasori, Ernesto Guido
ALMO Observatory (G18), Padulle (BO), ITALY

Gianni Galli
GiaGa Observatory (203), Pogliano Milanese, ITALY

Luca Buzzi
Schiaparelli Observatory (204), Varese, ITALY

(Received: 2022 July 12)

Photometric observations of ten asteroids were made in order to acquire lightcurves for shape/spin axis modeling. The synodic period and lightcurve amplitude were found for 323 Brucia, 342 Endymion, 542 Susanna, 578 Happelia, 1656 Suomi, 4221 Picasso, (5693) 1993 EA, (7335) 1989 JA, 2022 BT and 2022 MP. We also found color indices for 323 Brucia and (7335) 1989 JA.

Collaborative asteroid photometry was done inside the Italian Amateur Astronomers Union (UAI; 2022) group. The targets were selected mainly in order to acquire lightcurves for shape/spin axis modeling. Table I shows the observing circumstances and results.

The CCD observations of ten asteroids were made in 2022 April-June using the instrumentation described in the Table II. Lightcurve analysis was performed at the Balzaretto Observatory with *MPO Canopus* (Warner, 2021). All the images were calibrated with dark and flat frames and converted to R magnitudes using solar colored field stars from CMC15 catalogue, distributed with *MPO Canopus*. For brevity, the following citations to the asteroid lightcurve database (LCDB; Warner et al., 2009) will be summarized only as "LCDB".

323 Brucia is an S-type (Tholen, 1984) inner main-belt asteroid. Collaborative observations were made over ten nights. The period analysis shows a synodic period of P = 9.459 ± 0.001 h with an amplitude A = 0.09 ± 0.02 mag. The period is close to the previously published results in the LCDB.

Multiband photometry was made by P. Bacci and M. Maestripieri (104) on 2022 April 28. We found the color indices (B-V) = 0.87 ± 0.02 and (V-R) = 0.50 ± 0.02, both are consistent with a S-type asteroid (Shevchenko and Lupishko, 1998).

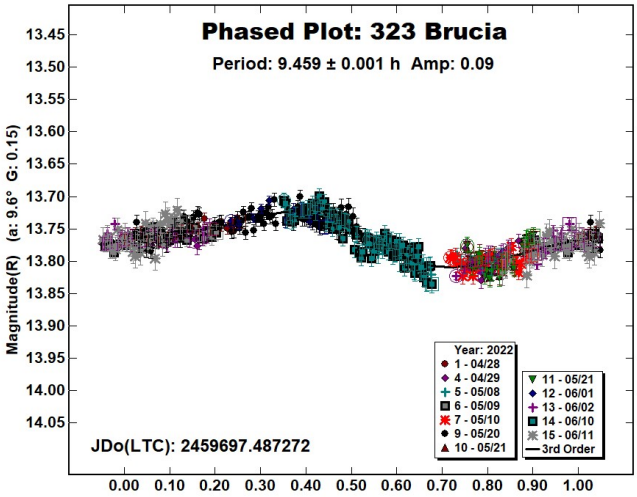

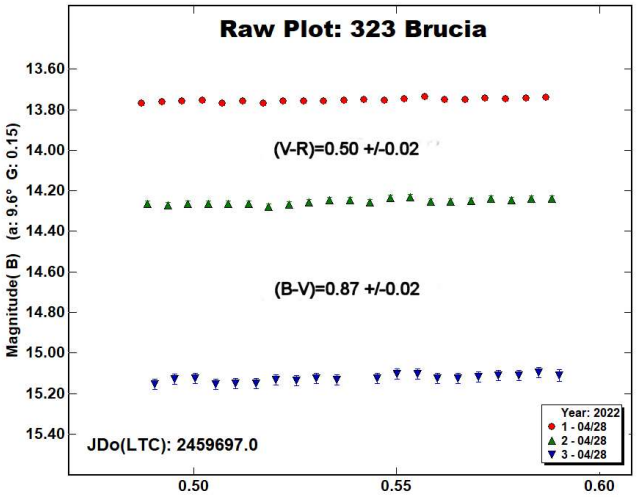

342 Endymion is a Ch-type (Bus and Binzel, 2002) middle main-belt asteroid. Collaborative observations were made over four nights. The period analysis shows a synodic period of P = 6.319 ± 0.002 h with an amplitude A = 0.12 ± 0.02 mag. The period is close to the previously published results in the LCDB.

Number	Name	2022 mm/dd	Phase	L_{PAB}	B_{PAB}	Period(h)	P.E.	Amp	A.E.	Grp
323	Brucia	04/28-06/11	*9.4,14.8	224	24	9.459	0.001	0.09	0.02	MB-I
342	Endymion	05/10-05/19	0.2,3.8	230	0	6.319	0.002	0.12	0.02	MB-M
542	Susanna	06/25-07/04	8.8,11.3	256	14	10.090	0.005	0.11	0.02	MB-O
578	Happelia	04/26-05/18	8.4,16.5	198	1	10.066	0.002	0.15	0.02	MB-M
1656	Suomi	04/26-05/21	16.8,21.2	219	27	2.589	0.001	0.11	0.06	H
4221	Picasso	04/28-05/10	9.4,14.6	203	9	3.3270	0.001	0.18	0.06	MB-M
5693	1993 EA	05/20-05/22	48.5,55.7	265	17	2.493	0.002	0.11	0.07	NEA
7335	1989 JA	05/20-05/24	26.4,34.8	227	3	2.588	0.001	0.21	0.05	NEA
	2022 BT	01/23-01/23	107.7,105.5	78	32	0.0366	0.0001	0.76	0.20	NEA
	2022 MP	06/25-06/26	*38.4,38.5	259	12	0.015678	0.000001	0.52	0.20	NEA

Table I. Observing circumstances and results. The first line gives the results for the primary of a binary system. The second line gives the orbital period of the satellite and the maximum attenuation. The phase angle is given for the first and last date. If preceded by an asterisk, the phase angle reached an extrema during the period. L_{PAB} and B_{PAB} are the approximate phase angle bisector longitude/latitude at mid-date range (see Harris et al., 1984). Grp is the asteroid family/group (Warner et al., 2009).

Observatory (MPC code)	Telescope	CCD	Filter	Asteroids Observed (#Sessions)
Astronomical Observatory of the University of Siena(K54)	0.30-m MCT f/5.6	SBIG STL-6303e (2x2)	C,Rc	323(1), 342(1), 542(6), 578(4), 1656(2), 5693(3)
GAMP (104)	0.60-m NRT f/4.0	Apogee Alta	C,B, V,Rc	323(1), 342(3), 7335(3), 2022 BT(1), 2022 MP(2)
Osservatorio Astronomico Nastro Verde (C82)	0.35-m SCT f/6.3	SBIG ST10XME (2x2)	C	1656(4), 4221(1), 7335(2)
Iota Scorpii(K78)	0.40-m RCT f/8.0	SBIG STXL-6303e (2x2)	Rc	323(2), 1656(2)
HOB Astronomical Observatory (L63)	0.20-m SCT f/6.8	ATIK 383L+	C,Rc	323(2), 578(2)
Osservatorio Astronomico Margherita Hack (A57)	0.35-m SCT f/8.3	SBIG ST10XME (2x2)	Rc	1656(1), 4221(3)
M57 (K38)	0.35-m RCT f/5.5	SBIG STT1603ME	Rc	323(4)
ALMO Observatory (G18)	0.30-m NRT f/4.0	Moravian G2-1600	Rc	323(1), 7335(1)
GiaGa Observatory (203)	0.36-m SCT f/5.8	Moravian G2-3200	C	5693(1)
Schiaparelli Observatory (204)	0.80-m RCT f/8.0	SBIG STX-16803	C	2022 BT(1)

Table II. Observing Instrumentations. MCT: Maksutov-Cassegrain, NRT: Newtonian Reflector, RCT: Ritchey-Chretien, SCT: Schmidt-Cassegrain.

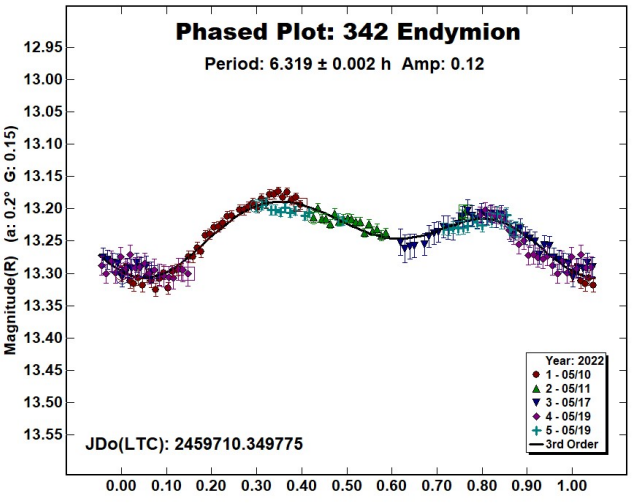

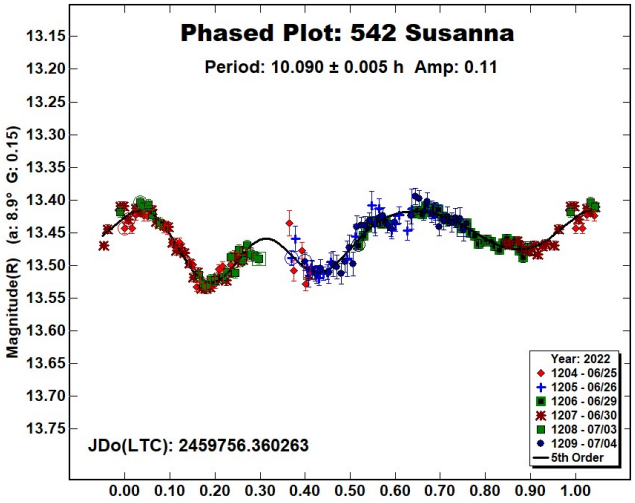

542 Susanna is an S-type (Tholen, 1984) outer main-belt asteroid. Observations were made over six nights by A. Marchini (K54). The period analysis shows a synodic period of $P = 10.090 \pm 0.005$ h with an amplitude $A = 0.11 \pm 0.02$ mag. The period is close to the previously published results in the LCDB.

578 Happelia is an Xc-type (Bus & Binzel, 2002) middle main-belt asteroid. Collaborative observations were made over five nights. We found a synodic period of $P = 10.066 \pm 0.002$ h with an amplitude $A = 0.15 \pm 0.02$ mag. The period is close to the previously published results in the LCDB.

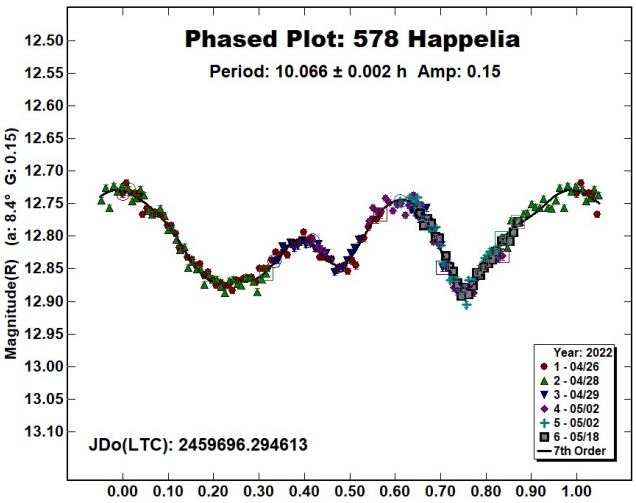

1656 Suomi is an S-type (Tholen, 1984) a binary asteroid (Warner et al., 2020) member of the Hungaria group. Collaborative observations were made over seven nights. We found a synodic period of P = 2.589 ± 0.001 h with an amplitude A = 0.11 ± 0.06 mag. Noteworthy is the attenuation event observed by N. Ruocco (C82) on 2022 May 18. The period is close to the previously published results in the LCDB.

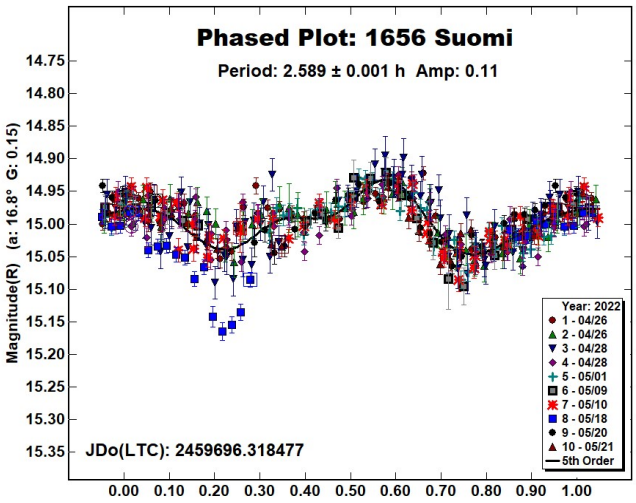

4221 Picasso is a medium albedo middle main-belt asteroid. Collaborative observations were made over four nights. We found a synodic period of P = 3.327 ± 0.001 h with an amplitude A = 0.18 ± 0.06 mag. The period agrees with that published by Clark (2019).

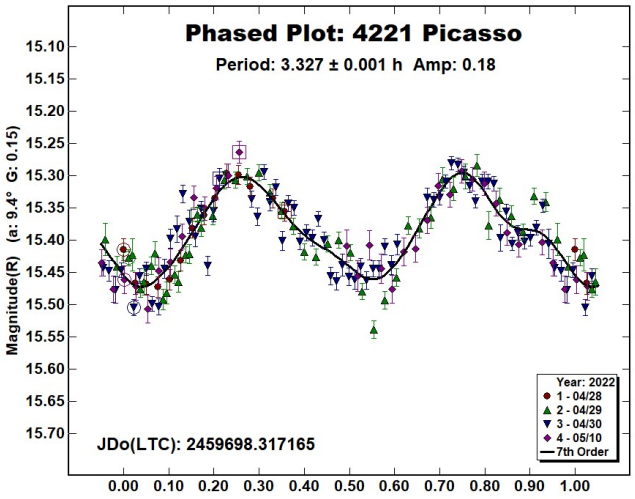

(5693) 1993 EA is an Apollo Near-Earth asteroid classified as Potentially Hazardous Asteroid (PHA). Collaborative observations were made over three nights. We found a synodic period of P = 2.493 ± 0.002 h with an amplitude A = 0.11 ± 0.07 mag. The period is close to the previously published results in the LCDB.

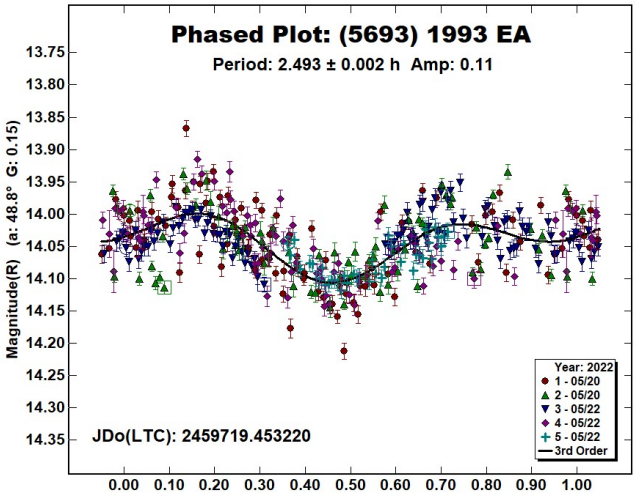

(7335) 1989 JA is an Apollo Near-Earth asteroid classified as Potentially Hazardous Asteroid (PHA). Collaborative observations were made over three nights. We found a quadrimodal lightcurve with a synodic period of P = 2.588 ± 0.001 h with an amplitude A = 0.21 ± 0.05 mag. This result differs from the upper limit of 12 hours reported in the LCDB. Multiband photometry was made by P. Bacci and M. Maestripieri (104) on 2022 May 23. We found the color indices (B-V) = 0.77 ± 0.05 and (V-R) = 0.45 ± 0.03, both consistent with an M-type asteroid (Shevchenko and Lupishko, 1998).

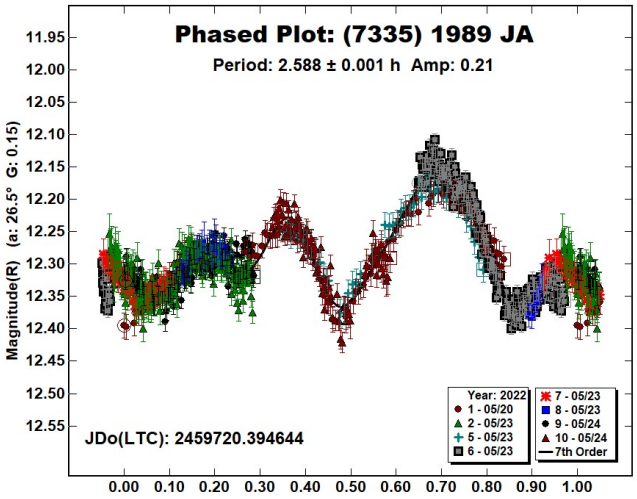

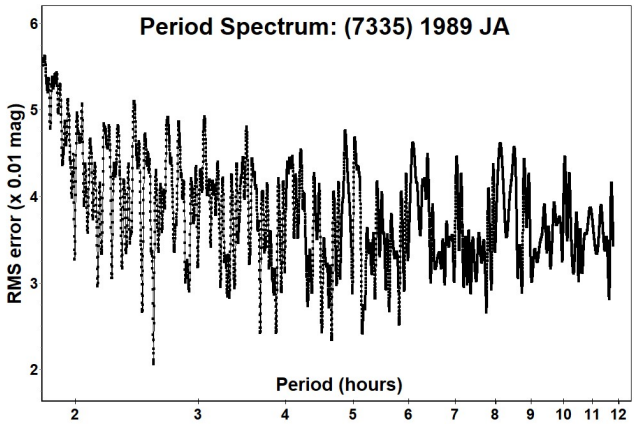

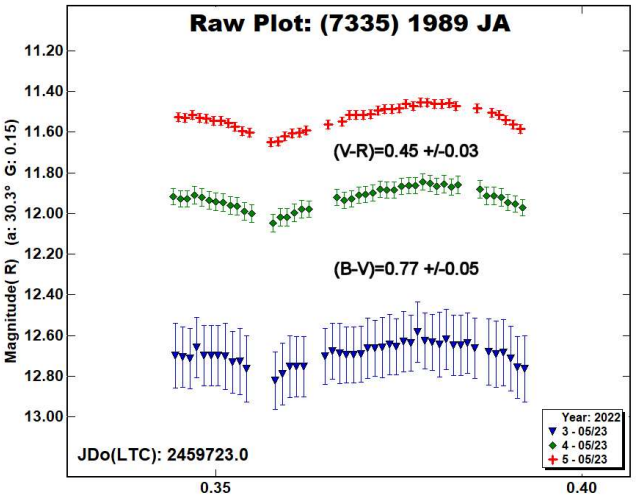

2022 BT is an Apollo Near-Earth asteroid, observed on 2022 January 23 by P. Bacci, M. Maestripieri (104) and L. Buzzi (204) during its close approach to the Earth. We found a synodic period of P = 0.0366 ± 0.0001 h (2.2 minutes) with an amplitude A = 0.76 ± 0.20 mag. There were no previously published results in the LCDB.

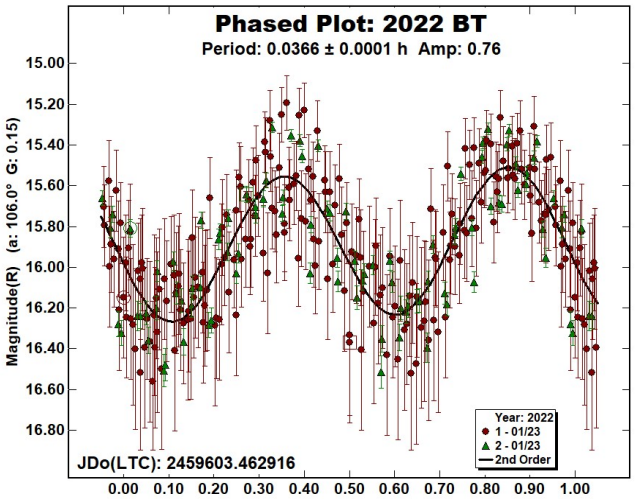

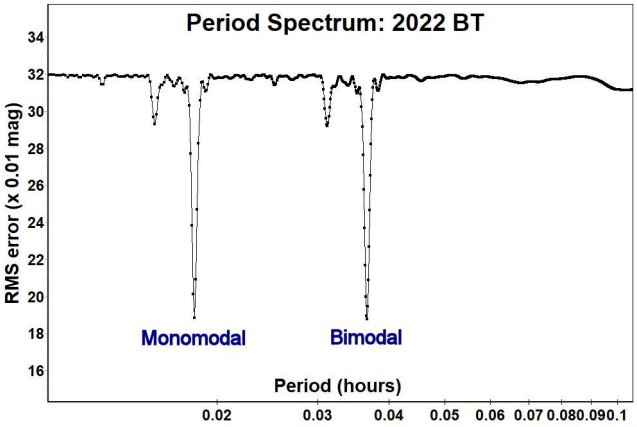

2022 MP is an Aten Near-Earth asteroid, observed on 2022 June 25 and 26 by P. Bacci, M. Maestripieri (104), during its close approach to the Earth. We found an ultra-fast synodic period of P = 0.015678 ± 0.000001 h (56.4 seconds) with an amplitude A = 0.52 ± 0.20 mag. No previously published results were found in the LCDB.

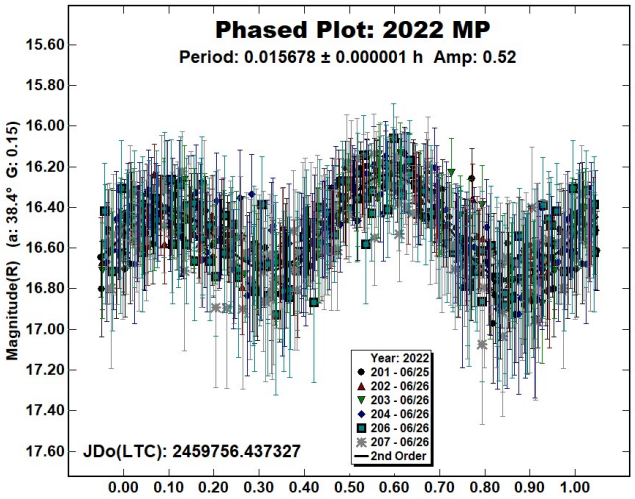

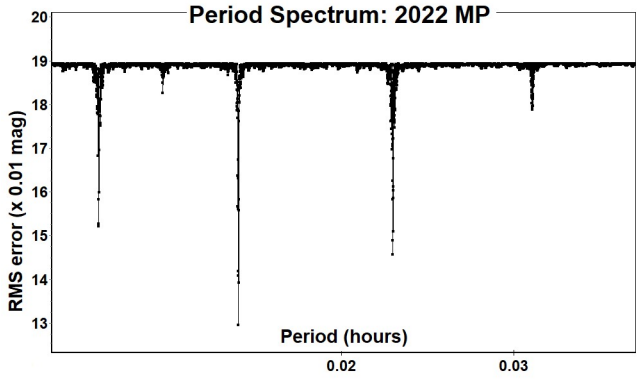

References

Bus, S.J.; Binzel, R.P. (2002). "Phase II of the Small Main-Belt Asteroid Spectroscopic Survey - A Feature-Based Taxonomy." *Icarus* **158**, 146-177.

Clark, M. (2019). "Asteroid Photometry from the Preston Gott Observatory." *Minor Planet Bulletin* **46**, 346-349.

Harris, A.W.; Young, J.W.; Scaltriti, F.; Zappala, V. (1984). "Lightcurves and phase relations of the asteroids 82 Alkmene and 444 Gyptis." *Icarus* **57**, 251-258.

Shevchenko, V.G.; Lupishko, D.F. (1998). "Optical properties of Asteroids from Photometric Data." *Solar System Research* **32**, 220-232.

Tholen, D.J. (1984). "Asteroid taxonomy from cluster analysis of Photometry." Doctoral Thesis. University Arizona, Tucson.

UAI (2022), "Unione Astrofili Italiani" web site. *https://www.uai.it*

Warner, B.D.; Harris, A.W.; Pravec, P. (2009) "The asteroid lightcurve database." *Icarus* **202**, 134-146. Updated 2022 July 02 *https://minplanobs.org/alcdef/index.php*

Warner, B.D.; Stephens, R.; Harris, A.W. (2020). "Binary Asteroids at the Center for Solar System Studies." *Minor Planet Bulletin* **47**, 305-308.

Warner, B.D. (2021). MPO Software, *MPO Canopus* v10.8.5.0. Bdw Publishing. *http://minorplanetobserver.com*

LIGHTCURVES AND ROTATION PERIODS OF 233 ASTEROPE, 240 VANADIS, 275 SAPIENTIA, 282 CLORINDE, 414 LIRIOPE, AND 542 SUSANNA

Frederick Pilcher
Organ Mesa Observatory (G50)
4438 Organ Mesa Loop
Las Cruces, NM 88011 USA
fpilcher35@gmail.com

(Received: 2022 July 5)

Synodic rotation periods and amplitudes are found for 233 Asterope 19.694 ± 0.001 h, 0.41 ± 0.02 mag; 240 Vanadis 10.565 ± 0.002 h, 0.07 ± 0.01 mag; 275 Sapientia 14.933 ± 0.001 h, 0.10 ± 0.01 mag; 282 Clorinde 49.350 ± 0.003 h, 0.19 ± 0.02 mag; 414 Liriope 11.009 ± 0.002 h, 0.14 ± 0.01 mag with 3 unsymmetrical maxima and minima per rotational cycle; 542 Susanna 10.089 ± 0.001 h, 0.09 ± 0.01 mag with 3 unsymmetrical maxima and minima per rotational cycle.

Observations to produce the results reported in this paper were made at the Organ Mesa Observatory with a Meade 35-cm LX200 GPS Schmidt-Cassegrain, SBIG STL-1001E CCD, 60 second exposures, unguided, R filter for 275 Sapientia, clear filter for all other targets. Image measurement and lightcurve construction were with *MPO Canopus* software with all calibration star magnitudes from the CMC15 catalog reduced to the Cousins R band. Zero-point adjustments of a few ×0.01 magnitude were made for best fit. To reduce the number of data points on the lightcurves and make them easier to read, data points have been binned in sets of 3 with maximum time difference 5 minutes.

233 Asterope. Previously published periods are by Harris and Young (1983), 19.7 hours; Behrend (2012web), >10 hours; Piironen et al. (1998), 19.743 hours, all with moderately sparse lightcurves. New observations on six nights 2022 May 10 - June 6 provide an excellent fit to a period of 19.694 ± 0.001 hours, amplitude 0.41 ± 0.02 magnitudes (Fig. 1). This period is consistent with all previously published periods and with improved accuracy due to being based upon a much denser lightcurve.

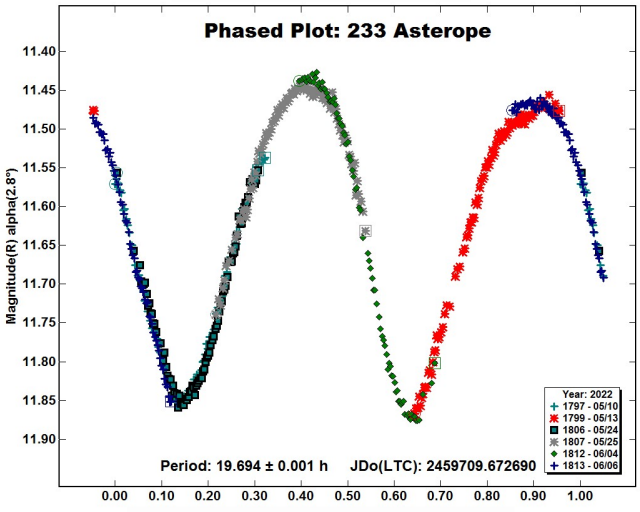

Figure. 1. Lightcurve of 233 Asterope phased to 19.694 hours.

240 Vanadis. Previously published periods and amplitudes are by Denchev (2000), 10.64 hours, 0.34 magnitudes near celestial longitude 132º with an unsymmetric bimodal lightcurve; Behrend (2003web), > 12 hours, > 0.08 magnitudes based on a single 5-hour lightcurve; Alton (2016), 10.57 hours, 0.10 magnitudes near celestial longitude 68º with an irregular monomodal lightcurve.

New observations on 7 nights 2022 May 10 - June 1 near celestial longitude 235º provide an excellent fit to a monomodal lightcurve with period 10.565 ± 0.002 hours, amplitude 0.07 ± 0.01 magnitudes (Fig. 2). The split halves plot of the double period (Fig. 3) shows that the two halves are identical within observational error and rules out the double period. This value is consistent with Denchev (2000) and Alton (2016) and improves the accuracy with a longer interval of observation, 46 rotational cycles as compared with only three cycles in the study by Denchev (2000). The period by Behrend (2003web) is now ruled out.

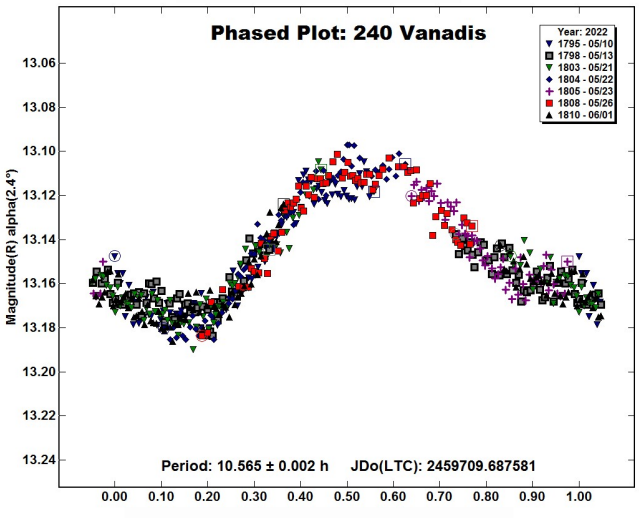

Figure. 2. Lightcurve of 240 Vanadis phased to 10.565 hours.

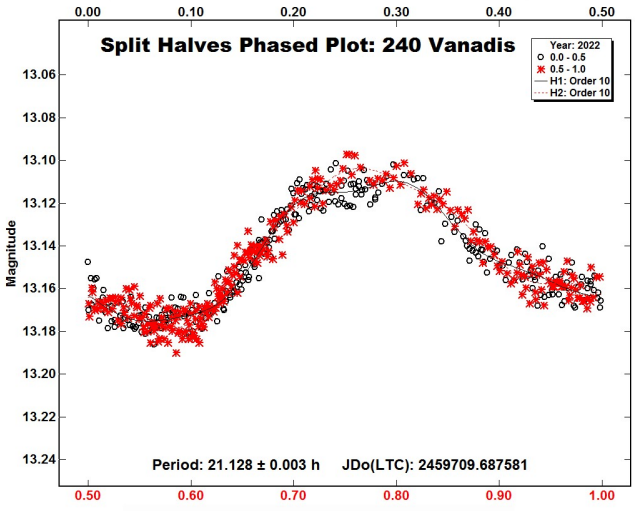

Figure. 3. Split halves phased plot of 240 Vanadis.

The lightcurve published by Denchev (2000) constitutes a second line of evidence to rule out the double period. His lightcurve includes only two nights of data 1999 Jan. 21-22 but covers an entire 10.64-hour rotational cycle with an asymmetric bimodal lightcurve with maximum amplitude 0.34 magnitudes. No object with four maxima and minima per cycle and no albedo variegation can have an amplitude as great as 0.34 magnitude. Hence Denchev's data alone rule out a double period near 21.128 magnitudes.

The amplitude is much smaller at celestial longitudes 235º (this study) and at 68º (Alton, 2016) than at 132º (Denchev, 2000). The rotational pole is much closer to celestial longitude 235º than to celestial longitude 132º. Minor planet 240 Vanadis is another example of the commonly observed phenomenon that a minor planet with a bimodal lightcurve of moderately large amplitude at near equatorial aspect has a monomodal lightcurve of much smaller amplitude at near polar aspect.

275 Sapientia. Previously published periods are by Denchev (2000), >20 hours; Behrend (2005web), 24.07 hours; Kaminski et al. (2010), 9.5 hours; Pilcher (2015), 14.931 hours; Pilcher (2016), 14.932 hours; Warner (2007), 14.766 hours. New observations on 8 nights 2022/04/08 - 2022/05/19 provide an excellent fit to an irregular monomodal lightcurve with period 14.933 ± 0.001 hours, amplitude 0.10 ± 0.01 magnitudes (Fig. 4). A split halves plot of the double period (Fig. 5) shows excellent fit between the two halves of the plot. The double period is ruled out. The new data are compatible with Warner (2007), Pilcher (2015), and Pilcher (2016). All other published periods are now ruled out, and a period near 14.933 hours can be considered secure.

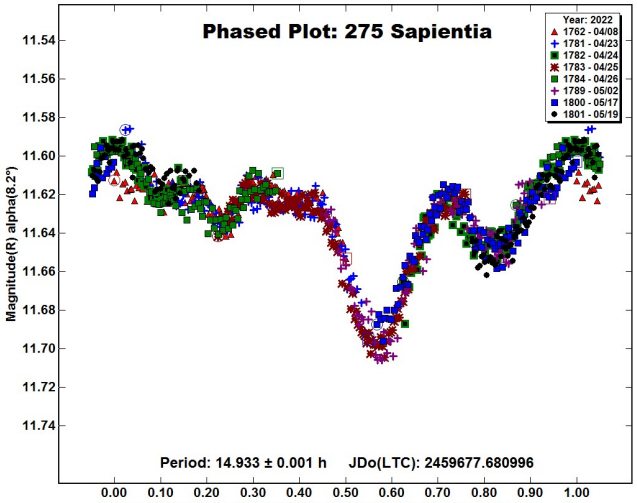

Figure. 4. Lightcurve of 275 Sapientia phased to 14.933 hours.

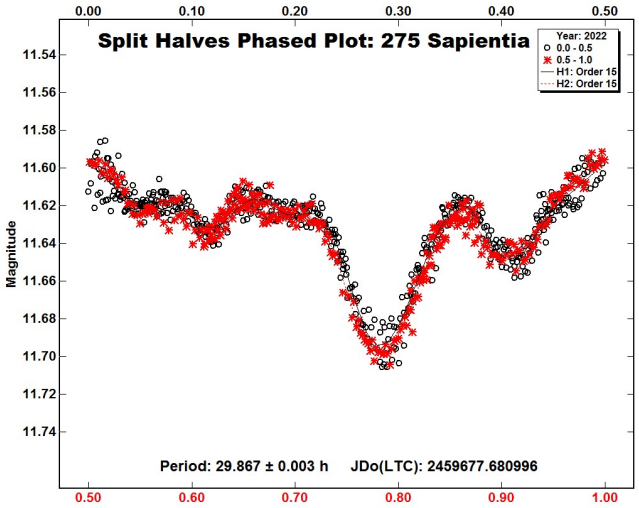

Figure. 5. Split halves phased plot of 275 Sapientia

282 Clorinde. Previously published periods and amplitudes are by Binzel and Mulholland (1983), 6.42 hours, 0.09 magnitudes; Behrend (2018web), 12.142 hours, 0.04 magnitudes; Bonamico and van Belle (2021), 49.352 hours, 0.26 magnitudes with a dense lightcurve obtained in an interval of more than three months 2020/11/26 to 2021/03/04 that looks convincing. New observations on 17 nights 2022/03/27 - 2022/05/20 provide a good fit to a somewhat irregular bimodal lightcurve with period 49.350 ± 0.003 hours, amplitude 0.19 ± 0.02 magnitudes (Fig. 6). This result is in excellent agreement with Bonamico and van Belle (2021). All of the earlier reported short periods are now ruled out.

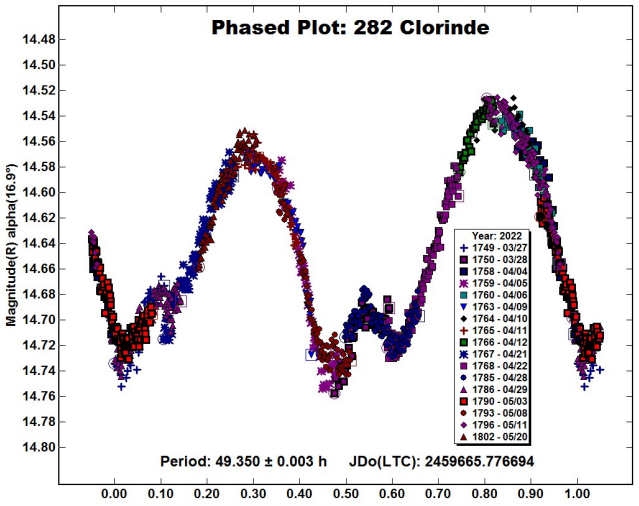

Figure. 6. Lightcurve of 282 Clorinde phaased to 49.350 hours.

414 Liriope. Three early published results all assumed the usual two maxima and minima per rotational cycle: Alvarez (2012), 7.353 hours; Chang et al. (2015), 7.38 hours; and Waszczak et al. (2015), 7.34 hours. Three recent publications all reveal that there are three unsymmetical maxima and minima per rotational cycle with 3/2 of the early and now rejected period: Colazo et al. (2020), 11.005 hours; Pál et al. (2020), 11.0065 hours: Dose (2021), 11.007 hours. New observations on 5 nights 2022/04/30 - 2022/05/09 provide a good fit to a lightcurve with period 11.009 ± 0.002 hours, amplitude 0.14 ± 0.01 magnitudes, and three unsymmetrical maxima and minima per rotational cycle (Fig. 7). The new result is in excellent agreement with Colazo et al. (2020), Pál et al. (2020), and Dose (2021).

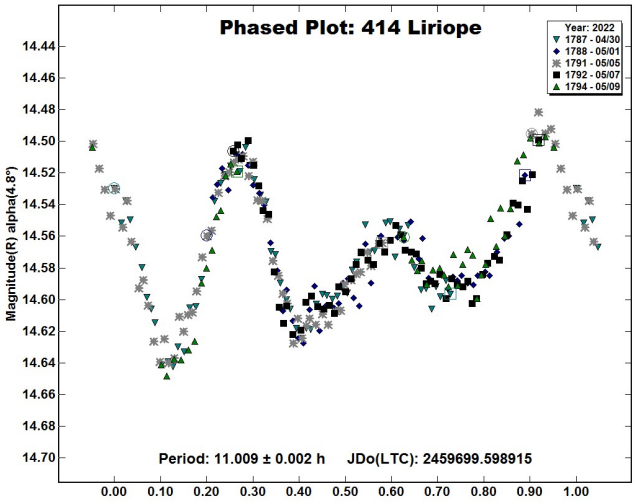

Figure. 7. Lightcurve of 414 Liriope phased to 11.009 hours.

542 Susanna. Previously published periods are by Stephens (2007), 10.069 hours; Behrend (2016web), 10.0869 hours; and Pál et al. (2020), 10.107 hours. New observations on four nights 2022 June 3 - July 1, over an interval of 66 rotational cycles, provide a fit to an irregular lightcurve with three maxima and minima per rotational cycle, period 10.089 ± 0.001 magnitudes, amplitude 0.09 ± 0.01 magnitudes (Fig. 8). This value is consistent with all previously published periods.

Number	Name	2022/mm/dd	Phase	L_{PAB}	B_{PAB}	Period(h)	P.E	Amp	A.E.
233	Asterope	05/10-06/06	* 2.8, 9.0	235	2	19.694	0.001	0.41	0.02
240	Vanadis	05/10-06/01	* 2.4, 5.8	235	2	10.565	0.002	0.07	0.01
275	Sapientia	04/08-05/18	* 8.2, 12.2	213	6	14.933	0.001	0.10	0.01
282	Clorinde	03/27-05/20	* 16.9, 9.5	223	12	49.350	0.003	0.19	0.02
414	Liriope	04/30-05/09	4.8, 6.8	209	11	11.009	0.002	0.14	0.02
542	Susanna	06/03-07/01	* 6.0, 10.3	256	14	10.089	0.001	0.09	0.01

Table I. Observing circumstances and results. The phase angle is given for the first and last date, with a * shown if a minimum value was reached between these dates. L_{PAB} and B_{PAB} are the approximate phase angle bisector longitude and latitude at mid-date range (see Harris et al., 1984).

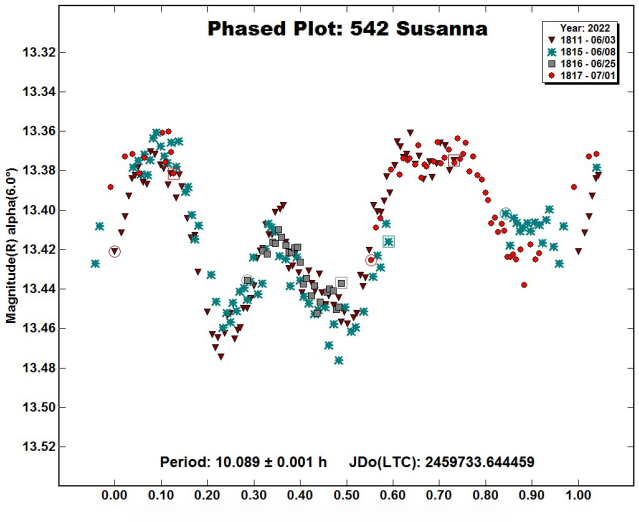

Figute. 8. Lightcurve of 542 Susanna phased to 10.089 hours.

References

Alton, K.B. (2016). "CCD lightcurve for the main-belt asteroid 240 Vanadis." *Minor Planet Bull.* **43**, 217-218.

Alvarez, E.M. (2012). "Period Determination for 414 Liriope." *Minor Planet Bull.* **39**, 21-22.

Behrend, R. (2003web, 2005web, 2012web, 2016web, 2018web). Observatoire de Geneve web site. *http://*obswww.unige.ch/*~behrend/page_cou.html*

Binzel, R.P.; Mulholland, J.D. (1983). "A photoelectric lightcurve survey of small main-belt asteroids." *Icarus* **56**, 519-533.

Bonamico, R.; van Belle, G (2021). "Determining the rotation period of main-belt asteroid 282 Clorinde." *Minor Planet Bull.* **48**, 210.

Chang, C.-K.; Ip, W.-H; Lin, H.-W.; Cheng, Y.-C.; Ngeow, C.-C.; Yang, T.-C.; Waszczak, A.; Kulkarni, S.R.; Levitan, D.; Sesar, B.; Laher, R.; Surace, J.; Prince, T.A. (2015). "Asteroid Spin-State Study Using the Intermediate Palomar Transient Factory." *Astrophys. J. Suppl. Series* **219**, 27.

Colazo, L.M.; Fornari, C.; Santucho, M.; Mottino, A.; Colazo, C.; Melia, R.; Suarez, N.; Vasconi, N.; Arias, D.; Stechina, A.; Scotta, D.; Garcia, J.; Pittari, C.; Ferrero, G. (2020). "Asteroid Photometry and Lightcurve Analysis at Gora's Observatories - Part II." *Minor Planet Bull*. **47**, 337-339.

Denchev, P. (2000). "Photometry of 11 asteroids during their 1998 and 1999 apparitions." *Planet. Space Sci.* **48**, 987-992.

Dose, E.F. (2021). "Lightcurves of fourteen asteroids." *Minor Planet Bull.* **48**, 228-233.

Harris, A.W.; Young, J.W. (1983). "Asteroid Rotation IV. 1979 Observations." *Icarus* **54**, 59-109.

Harris, A.W.; Young, J.W.; Scaltriti, F.; Zappala, V. (1984). "Lightcurves and phase relations of the asteroids 82 Alkmene and 444 Gyptis." *Icarus* **57**, 251-258.

Kaminski, L.I.; Leake, M.A.; Berget, D.J. (2010). "Differential photometry and lightcurve analysis for numbered asteroids 229, 275, 426, 557, 613, 741, 788, 872, 907, and 5010." *J. SE Assoc. for Research in Astron.* **3**, 25-31.

Pál, A.; Szakáts, R.; Kiss, C.; Bódi, A.; Bognár, Z.; Kalup, C.; Kiss, L.L.; Marton, G.; Molnár, L.; Plachy, E.; Sárneczky, K.; Szabó, G.M.; Szabó, R. (2020). "Solar System Objects Observed with TESS - First Data Release: Bright Main-belt and Trojan Asteroids from the Southern Survey." *Astrophys. J. Suppl. Series* **247**, 26.

Piironen, J.; Lagerkvist, C.-I.; Erikson, A.; Oja, T.; Magnusson, P.; Festin, L.; Nathues, A.; Gaul, M.; Velichko, F. (1998). "Physical properties of asteroids XXXII. Rotation periods and UBVRI colours for selected asteroids." *Astron. Astrophys. Suppl. Ser.* **128**, 525-540.

Pilcher, F. (2015). "Rotation period determinations for 275 Sapientia, 309 Fraternitas, and 924 Toni." *Minor Planet Bull.* **42**, 38-39.

Pilcher, F. (2016). "Rotation period determinations for 269 Justitia, 275 Sapientia, 331 Etheridgea, and 609 Fulvia." *Minor Planet Bull.* **43**, 135-136.

Stephens, R.D. (2007). "Photometry from GMARS and Santana Observatories – April to June 2007." *Minor Planet Bull.* **34**, 102-103.

Warner, B.D. (2007). "Asteroid lightcurve analysis at the Palmer Divide Observatory – December 2006 - March 2007." *Minor Planet Bull.* **34**, 72-77.

Warner, B.D., Harris, A.W., Pravec, P. (2009). "The Asteroid Lightcurve Database." *Icarus* **202**, 134-146. Updated 2021 Dec. *https://minplanobs.org/MPInfo/php/lcdb.php*

Waszczak, A.; Chang, C.-K.; Ofek, E.O.; Laher, R.; Masci, F.; Levitan, D.; Surace, J.; Cheng, Y.-C.; Ip, W.-H.; Kinoshita, D.; Helou, G.; Prince, T.A.; Kulkarni, S. (2015). "Asteroid Light Curves from the Palomar Transient Factory Survey: Rotation Periods and Phase Functions from Sparse Photometry." *Astron. J.* **150**, 75.

LIGHTCURVE PHOTOMETRY OPPORTUNITIES: 2022 OCTOBER-DECEMBER

Brian D. Warner
Center for Solar System Studies (CS3)
446 Sycamore Ave.
Eaton, CO 80615 USA
brian@MinorPlanetObserver.com

Alan W. Harris
Center for Solar System Studies (CS3)
La Cañada, CA 91011-3364 USA

Josef Ďurech
Astronomical Institute
Charles University
18000 Prague, CZECH REPUBLIC
durech@sirrah.troja.mff.cuni.cz

Lance A.M. Benner
Jet Propulsion Laboratory
Pasadena, CA 91109-8099 USA
lance.benner@jpl.nasa.gov

We present lists of asteroid photometry opportunities for objects reaching a favorable apparition and have no or poorly-defined lightcurve parameters. Additional data on these objects will help with shape and spin axis modeling using lightcurve inversion. The "Radar-Optical Opportunities" section includes a list of potential radar targets as well as some that might be in critical need of astrometric data.

We present several lists of asteroids that are prime targets for photometry and/or astrometry during the period 2022 October through December. The "Radar-Optical Opportunities" section provides an expanded list of potential NEA targets, many of which are planned or good candidates for radar observations.

In the first three sets of tables, "Dec" is the declination and "U" is the quality code of the lightcurve. See the latest asteroid lightcurve data base (LCDB from here on; Warner et al., 2009) documentation for an explanation of the U code:

http://www.minorplanet.info/lightcurvedatabase.html

The ephemeris generator on the MinorPlanet.info web site allows creating custom lists for objects reaching V ≤ 18.0 during any month in the current year and up to five years in the future, e.g., limiting the results by magnitude and declination, family, and more.

https://www.minorplanet.info/php/callopplcdbquery.php

We refer you to past articles, e.g., Warner et al. (2021a; 2021b) for more detailed discussions about the individual lists and points of advice regarding observations for objects in each list.

Once you've obtained and analyzed your data, it's important to publish your results. Papers appearing in the *Minor Planet Bulletin* are indexed in the Astrophysical Data System (ADS) and so can be referenced by others in subsequent papers. It's also important to make the data available at least on a personal website or upon request. We urge you to consider submitting your raw data to the ALCDEF database. This can be accessed for uploading and downloading data at

http://www.alcdef.org

The database contains more than 10.1 million observations for 23993 objects (as of 2022 July 2), making it one of the more useful sources for raw data of *dense* time-series asteroid photometry.

Lightcurve/Photometry Opportunities

Objects with U = 3- or 3 are excluded from this list since they will likely appear in the list for shape and spin axis modeling. Those asteroids rated U = 1 or have only a lower limit on the period, should be given higher priority over those rated U = 2 or 2+. On the other hand, do not overlook asteroids with U = 2/2+ on the assumption that the period is sufficiently established. Regardless, do not let the existing period influence your analysis since even highly-rated result have been proven wrong at times. Note that the lightcurve amplitude in the tables could be more or less than what's given. Use the listing only as a guide.

		Brightest			LCDB Data		
Number	Name	Date	Mag	Dec	Period	Amp	U
2974	Holden	10 01.4	15.1	+9	856	0.70	2+
5887	Yauza	10 05.1	15.0	+4	54.78	0.30	2
5811	Keck	10 08.4	14.9	+17	>30	0.25	2
1599	Giomus	10 09.6	14.7	+2	9.53	0.06-0.08	2
7194	Susanrose	10 11.5	15.0	+3	4.725	0.24	2
5479	Grahamryder	10 11.7	15.4	+8	7.6	0.08-0.30	2
1438	Wendeline	10 14.9	14.5	+10	41.98	0.23	2-
15790	Keizan	10 17.0	14.8	+9	19.68	0.25	2-
3925	Tret'yakov	10 17.4	14.6	-6	30.962	0.24	2+
2908	Shimoyama	10 19.5	15.3	+19	694.117	0.41	2
1399	Teneriffa	10 21.8	15.1	+1	2.692	0.14	2
35143	1992 UF1	10 22.5	15.5	+10	5.388	0.23-0.26	2
2052	Tamriko	10 22.7	14.3	+12	7.462	0.06-0.15	2
1573	Vaisala	10 26.6	13.9	+2	252	0.76	2
8830	1988 VZ	10 28.4	15.4	+12	7.16		2
21609	Williamcaleb	10 28.8	15.3	+8	112	0.5	2
2757	Crisser	10 30.3	15.1	+14	8.088	0.28	2
3373	Koktebelia	11 02.0	15.2	+10	405.33	0.67	2
9216	Masuzawa	11 02.1	15.3	+15	5.02	0.15	2
7004	Markthiemens	11 03.4	15.5	+14	6.025		2-
18595	1998 BR1	11 07.0	15.0	+16	6.02		2
37306	2001 KW46	11 07.1	14.8	+22	5.621	0.10	2
1690	Mayrhofer	11 10.0	14.7	+18	22.194	0.16-0.45	2
1965	van de Kamp	11 10.1	14.7	+15	>36	0.5	1
5163	Vollmayr-Lee	11 10.8	14.8	+7	4.728	0.15	2
23978	1999 JF21	11 10.8	15.0	+17	34.15	0.09	2
1500	Jyvaskyla	11 13.2	14.0	+26	8.828		2
4649	Sumoto	11 14.2	14.7	+5	26.31	0.15-0.30	2
217628	Lugh	11 14.9	14.7	-7	8.55	0.08	1
2774	Tenojoki	11 15.5	15.3	+29	11.2	0.30	2+
85713	1998 SS49	11 16.3	13.9	+45	5.37	0.06-0.18	2
3153	Lincoln	11 17.6	15.2	+23	4.819	0.08	2
2107	Ilmari	11 18.4	14.6	+16	39.916	0.21	2-
27057	1998 SP33	11 21.6	15.0	+31	7.03	0.23	2+
4943	Lac d'Orient	11 21.9	15.5	+21	11.81	0.42-0.56	2
3454	Lieske	11 22.1	15.1	+12	105	0.73	2-
10260	1972 TC	11 22.2	15.3	+23	3.716	0.54	2
2439	Ulugbek	11 28.8	15.3	+21	4.26		2-
1384	Kniertje	11 29.9	14.5	+1	9.807	0.11-0.33	2
1549	Mikko	12 01.8	14.3	+19	8.74	0.10	2
4817	Gliba	12 02.7	15.1	+17	23.66	0.3	2-
66875	1999 VY52	12 02.9	14.6	+24	2.148	0.25	2
19311	1996 VF3	12 06.2	15.4	+32	13.883	0.35	2
1565	Lemaitre	12 06.4	13.7	+29	11.403	0.03-0.04	2
16872	1998 BZ	12 09.9	15.5	+20	2.81	0.34-0.45	2
11151	Oodaigahara	12 10.8	15.1	+27	15.35	0.20	2
645	Agrippina	12 15.2	13.8	+34	32.6	0.11-0.18	2
3981	Stodola	12 18.1	15.4	+24	102.657	0.08	1
	2014 HK129	12 18.8	14.7	-23	>10	0.5	2
2707	Ueferji	12 25.1	15.5	+24	5.286	0.16	2
6901	Roybishop	12 25.7	15.0	+35	4.766	0.04-0.09	2
1239	Queteleta	12 25.9	14.3	+25	10.278	0.03	1
28017	1997 YV13	12 27.9	14.8	+21	47	0.15	1

Low Phase Angle Opportunities

The Low Phase Angle list includes asteroids that reach very low phase angles ($\alpha < 1°$). The "α" column is the minimum solar phase angle for the asteroid. Getting accurate, calibrated measurements (usually V band) at or very near the day of opposition can provide important information for those studying the "opposition effect."

Use the on-line query form for the LCDB to get more details about a specific asteroid.

https://www.minorplanet.info/php/callopplcdbquery.php

The best chance of success comes with covering at least half a cycle a night, meaning periods generally < 16 h, when working objects with low amplitude. Objects with large amplitudes and/or long periods are much more difficult for phase angle studies since, for proper analysis, the data must be reduced to the average magnitude of the asteroid for each night. Refer to Harris et al. (1989) for the details of the analysis procedure.

As an aside, it is arguably better for physical interpretation (e.g., *G* value versus albedo) to use the maximum light rather than mean level to find the phase slope parameter (*G*), which better models the behavior of a spherical object of the same albedo, but it can produce significantly different values for both *H* and *G* versus using average light, which is the method used for values listed by the Minor Planet Center. Using and reporting the results of both methods can provide additional insights into the physical properties of an asteroid.

The International Astronomical Union (IAU) has adopted a new system, H-G_{12}, introduced by Muinonen et al. (2010). It will be some years before H-G_{12} becomes widely used, and hopefully not until a discontinuity flaw in the G_{12} function has been fixed. This discontinuity results in false "clusters" or "holes" in the solution density and makes it impossible to draw accurate conclusions.

We strongly encourage obtaining data as close to 0° as possible, then every 1-2° out to 7°, below which the curve tends to be non-linear due to the opposition effect. From 7° out to about 30°, observations at 3-6° intervals should be sufficient. Coverage beyond 50° or so is not generally helpful since the H-G system is best defined with data from 0-30°.

It's important to emphasize that all observations should (must) be made using high-quality catalogs to set the comparison star magnitudes. These include ATLAS, Pan-STARRS, SkyMapper, and Gaia2/3. Catalogs such as CMC-15, APASS, or the MPOSC from *MPO Canopus* have too high of significant systematic errors.

Also important is that that there are sufficient data from each observing run such that their location can be found on a combined, phased lightcurve derived from two or more nights obtained *near the same phase angle.* If necessary, the magnitudes for a given run should be adjusted so that they correspond to mid-light of the combined lightcurve. This goes back to the H-G system being based on average, not maximum or minimum light.

The asteroid magnitudes are brighter than in others lists because higher precision is required and the asteroid may be a full magnitude or fainter when it reaches phase angles out to 20-30°.

Num	Name	Date	α	V	Dec	Period	Amp	U
277	Elvira	10 02.5	0.50	13.1	+05	29.69	0.34-0.59	3
1527	Malmquista	10 04.4	0.56	13.3	+03	14.077	0.42-0.54	3
231	Vindobona	10 07.3	0.98	13.7	+08	14.245	0.20-0.29	3
108	Hecuba	10 17.6	0.97	12.8	+12	14.256	0.09-0.12	3
2243	Lonnrot	10 23.9	0.93	14.0	+13			
83	Beatrix	10 29.3	0.43	12.0	+14	10.16	0.18	3
658	Asteria	10 30.3	0.64	13.9	+15	21.034	0.22-0.28	3
124	Alkeste	11 09.0	1.00	11.8	+14	9.906	0.08-0.30	3
384	Burdigala	11 16.0	0.42	12.0	+20	21.1	0.03	2-
419	Aurelia	11 16.8	0.19	12.6	+18	16.784	0.07-0.27	3
478	Tergeste	11 16.8	0.12	11.7	+19	16.101	0.14-0.29	3-
1264	Letaba	11 18.0	0.07	14.0	+19	32.74	0.11-0.28	3
264	Libussa	11 19.4	0.91	11.2	+22	9.2276	0.04-0.59	3
673	Edda	11 25.3	0.45	13.6	+20	22.340	0.12-0.21	3
208	Lacrimosa	11 26.0	0.78	13.0	+23	14.085	0.15-0.33	3
686	Gersuind	11 27.8	0.43	12.4	+20	6.3127	0.33-0.37	3
229	Adelinda	12 06.4	0.61	13.9	+25	6.60	0.04-0.30	3
316	Goberta	12 07.9	0.96	13.7	+20	8.605	0.20-0.27	3
121	Hermione	12 20.0	0.83	11.9	+26	5.5513	0.04-0.62	3
259	Aletheia	12 20.0	0.07	12.6	+24	8.143	0.12	3

Shape/Spin Modeling Opportunities

Those doing work for modeling should contact Josef Ďurech at the email address above. If looking to add lightcurves for objects with existing models, visit the Database of Asteroid Models from Inversion Techniques (DAMIT) web site

https://astro.troja.mff.cuni.cz/projects/damit/

Additional lightcurves could lead to the asteroid being added to or improving one in DAMIT, thus increasing the total number of asteroids with spin axis and shape models.

Included in the list below are objects that:

1. Are rated U = 3- or 3 in the LCDB.
2. Do not have reported pole in the LCDB Summary table.
3. Have at least three entries in the Details table of the LCDB where the lightcurve is rated U ≥ 2.

The caveat for condition #3 is that no check was made to see if the lightcurves are from the same apparition or if the phase angle bisector longitudes differ significantly from the upcoming apparition. The last check is often not possible because the LCDB does not list the approximate date of observations for all details records. Including that information is an on-going project.

Favorable apparitions are in bold text. NEAs are in italics.

		Brightest			LCDB Data		
Num	Name	Date	Mag	Dec	Period	Amp	U
1829	Dawson	10 01.1	14.8	+13	4.254	0.05-0.32	3
479	**Caprera**	**10 03.9**	**12.4**	**-8**	**9.454**	**0.05-0.25**	**3**
2151	Hadwiger	10 07.6	14.4	-1	5.872	0.07-0.38	3
1184	Gaea	10 08.0	14.5	+12	2.871	0.09-0.15	3-
696	**Leonora**	**10 08.2**	**13.0**	**+24**	**26.896**	**0.04-0.31**	**3**
397	**Vienna**	**10 08.6**	**11.5**	**+19**	**15.48**	**0.15-0.20**	**3**
2105	Gudy	10 08.9	14.7	+46	15.795	0.18-0.52	3-
488	Kreusa	10 10.2	13.2	-7	32.645	0.08-0.20	3
1756	**Giacobini**	**10 10.3**	**14.0**	**+16**	**3.853**	**0.21-0.29**	**3**
965	Angelica	10 11.9	14.1	-9	26.752	0.06-0.12	3-
466	Tisiphone	10 12.9	14.0	+31	8.834	0.03-0.18	3
738	Alagasta	10 13.2	14.5	+3	17.89	0.11-0.20	3-
850	Altona	10 24.4	14.6	-9	11.191	0.09-0.17	3
790	Pretoria	10 27.0	13.2	+30	10.37	0.05-0.18	3
1603	**Neva**	**10 27.2**	**14.3**	**+0**	**6.426**	**0.16-0.25**	**3-**
658	**Asteria**	**10 30.3**	**13.9**	**+15**	**21.034**	**0.22-0.28**	**3**
2150	**Nyctimene**	**10 30.6**	**14.9**	**-2**	**6.131**	**0.56-0.90**	**3**
6244	**Okamoto**	**10 31.6**	**15.0**	**+25**	**2.896**	**0.11-0.15**	**3**
1100	Arnica	11 02.3	14.7	+16	14.535	0.09-0.28	3
2227	**Otto Struve**	**11 02.7**	**15.0**	**+8**	**5.397**	**0.15-0.19**	**3**
619	**Triberga**	**11 04.2**	**12.9**	**+3**	**29.311**	**0.25-0.45**	**3**
101	Helena	11 07.5	11.5	+31	23.08	0.09-0.13	3
4363	**Sergej**	**11 10.3**	**15.0**	**+7**	**13.04**	**0.24-0.50**	**3-**
777	Gutemberga	11 13.9	14.9	+32	12.838	0.11-0.28	3
839	Valborg	11 14.3	14.4	+38	10.366	0.14-0.19	3
1304	Arosa	11 14.7	14.5	+3	7.748	0.13-0.38	3
929	Algunde	11 15.9	14.6	+18	3.31	0.11-0.17	3
653	Berenike	11 17.2	13.9	+3	12.489	0.03-0.11	3
1143	**Odysseus**	**11 17.2**	**14.8**	**+18**	**10.114**	**0.15-0.22**	**3**
1264	Letaba	11 18.0	14.0	+19	32.74	0.13-0.43	3
58	Concordia	11 18.5	12.8	+12	9.895	0.01-0.15	3
1132	Hollandia	11 18.7	15.0	+24	5.322	0.15-0.35	3
954	Li	11 21.8	14.5	+18	7.207	0.11-0.25	3
388	Charybdis	11 24.4	12.9	+29	9.516	0.14-0.25	3
57	Mnemosyne	11 27.5	11.1	+4	25.324	0.09-0.24	3-
2034	**Bernoulli**	**11 30.5**	**14.2**	**+35**	**6.249**	**0.19-0.27**	**3**
1052	**Belgica**	**12 01.4**	**13.6**	**+17**	**2.71**	**0.06-0.08**	**3**
1031	Arctica	12 05.1	14.0	+8	24.904	0.16-0.22	3

		Brightest			LCDB Data		
Num	Name	Date	Mag	Dec	Period	Amp	U
917	Lyka	12 06.4	14.5	+32	7.867	0.10-0.26	3
806	Gyldenia	12 10.3	14.8	+35	16.852	0.10-0.27	3
911	Agamemnon	12 10.6	14.8	+49	6.592	0.04-0.29	3
1660	Wood	12 13.9	13.7	-10	6.809	0.14-0.26	3
1509	Esclangona	12 14.2	14.5	+42	3.253	0.11-0.35	3
1589	Fanatica	12 16.7	14.5	+22	2.583	0.10-0.22	3
788	Hohensteina	12 17.0	13.8	+3	37.137	0.10-0.18	3
1046	Edwin	12 18.1	14.7	+35	5.291	0.14-0.27	3
2494	**Inge**	**12 18.2**	**15.0**	**+28**	**6.79**	**0.17-0.92**	**3**
1274	Delportia	12 18.3	14.8	+30	5.56	0.05-0.29	3
259	Aletheia	12 20.0	12.7	+24	8.143	0.09-0.12	3
1967	Menzel	12 24.1	13.9	+28	2.835	0.16-0.39	3
100	Hekate	12 26.4	12.5	+18	27.066	0.11-0.23	3
224	Oceana	12 26.8	12.5	+32	9.401	0.09-0.14	3
1116	Catriona	12 27.4	13.0	+51	8.832	0.09-0.28	3

Radar-Optical Opportunities

Table I below gives a list of near-Earth asteroids reaching maximum brightness for the current quarter-year based on calculations by Warner. We switched to this presentation in lieu of ephemerides for reasons outlined in the 2021 October-December opportunities paper (Warner et al., 2021b), which centered on the potential problems with ephemerides generated several months before publication.

The initial list of targets started using the planning tool at

https://www.minorplanet.info/php/callopplcdbquery.php

where the search was limited to near-Earth asteroids only that were V ≤ 18 for at least part of the quarter.

The list was then filtered to include objects that might be targets for the Goldstone radar facility or, if it were still operational, the Arecibo radar. This was based on the calculated radar SNR using

http://www.naic.edu/~eriverav/scripts/index.php

and assuming a rotation period of 4 hours (2 hours if $D \leq 200$ m) if a period was not given in the asteroid lightcurve database (LCDB; Warner et al., 2009). The SNR values are estimates only and assume that the radar is fully functional.

If an asteroid was on the list but failed the SNR test, we checked if it might be a suitable target for radar and/or photometry sometime through 2050. If so, it was kept on the list to encourage physical and astrometric observations during the current apparition. In most of those cases, the SNR values in the "A" and "G" columns are not for the current quarter but the year given in the Notes column. If a better apparition is forthcoming through 2050, the Notes column in Table I contains SNR values for that time.

The final step was to cross-reference our list with that found on the Goldstone planned targets schedule at

http://echo.jpl.nasa.gov/asteroids/goldstone_asteroid_schedule.html

It's important to note that the final list in Table I is based on *known* targets and orbital elements when it was prepared. It is common for newly discovered objects to move in or out of the list. We recommend that you keep up with the latest discoveries by using the Minor Planet Center observing tools.

In particular, monitor NEAs and be flexible with your observing program. In some cases, you may have only 1-3 days when the asteroid is within reach of your equipment. Be sure to keep in touch with the radar team (through Benner's email or their Facebook or Twitter accounts) if you get data. The team may not always be observing the target but your initial results may change their plans. In all cases, your efforts are greatly appreciated.

For observation planning, use these two sites

MPC: *http://www.minorplanetcenter.net/iau/MPEph/MPEph.html*
JPL: *http://ssd.jpl.nasa.gov/?horizons*

Cross-check the ephemerides from the two sites just in case there is discrepancy that might have you imaging an empty sky.

About YORP Acceleration

Near-Earth asteroids are particularly sensitive to YORP acceleration. YORP (Yarkovsky–O'Keefe–Radzievskii–Paddack; Rubincam, 2000) is the asymmetric thermal re-radiation of sunlight that can cause an asteroid's rotation period to increase or decrease. High precision lightcurves at multiple apparitions can be used to model the asteroid's *sidereal* rotation period and see if it's changing.

It usually takes four apparitions to have sufficient data to determine if the asteroid rotation rate is changing under the influence of YORP. This is why observing an asteroid that already has a well-known period remains a valuable use of telescope time. It is even more so when considering the BYORP (binary-YORP) effect among binary asteroids that has stabilized the spin so that acceleration of the primary body is not the same as if it would be if there were no satellite.

The Quarterly Target List Table

The Table I columns are

Num	Asteroid number, if any.
Name	Name assigned by the MPC.
H	Absolute magnitude from MPCOrb.
Dkm	Diameter (km) assuming $p_V = 0.2$.
Date	Date (mm dd.d) of brightest magnitude.
V	Approximate V magnitude at brightest.
Dec	Approximate declination at brightest.
Period	Synodic rotation period from summary line in the LCDB summary table.
Amp	Amplitude range (or single value) of reported lightcurves.
U	LCDB U (solution quality) from 1 (probably wrong) to 3 (secure).
A	Approximate SNR for Arecibo (if operational and at full power).
G	Approximate SNR for Goldstone radar at full power.
Notes	Comments about the object.

"PHA" is a potentially hazardous asteroid. For good measure, consider that astrometry and photometry have been requested to support Goldstone observations. The sources for the rotation period are given in the Notes column. If none are qualified with a specific period, then the periods from multiple sources were in general agreement. Higher priority should be given to those where the current apparition is the last one V ≤ 18 through 2050 or several years to come.

Num	Name	H	D	Date	V	Dec	Period	Amp	U	A	G	Notes
	2011 TG2	20.3	0.259	10 06.4	16.6	+14				10	–	
177615	2004 HK33	17.73	0.845	10 16.4	14.9	–52				55	15	
422787	**2001 WS1**	**16.84**	**1.27**	**10 23.6**	**14.9**	**+39**				**70**	**20**	**PHA**
523823	2015BG311	18.43	0.612	10 24.0	16.2	+17						Last chance for small telescopes thru 2050.
312942	**1995 EK1**	**17.43**	**0.97**	**10 24.1**	**15.2**	**+76**	**8.444**	**0.45**	**3**	**65**	**20**	**Erikson et al. (2000)**
194268	**2001 UY4**	**18.44**	**0.61**	**10 27.3**	**15.9**	**-15**	**6.8020**	**0.13 0.16**	**2**	**20**	**6**	**Monteiro et al. (2018)**
186822	2004 FE31	17.93	0.771	11 09.5	15.9	-62				165	45	
217628	Lugh	16.62	1.41	11 14.9	14.7	-7	8.55	0.08	1	55	15	Wisniewski et al. (1997)
85713	**1998 SS49**	**15.78**	**2.07**	**11 16.3**	**13.9**	**+45**	**5.370**	**0.06 0.18**	**2**	**65**	**19**	**Warner (2015)**
	2019 OR1	20.8	0.206	11 18.0	16.6	+24				85	25	
99907	1989 VA	18.0	0.746	11 15.1	16.1	-19	2.5246	0.22 0.40	3	3	–	Pravec et al. (2017web) Visual obs. in 2025 10 29.3 V:16.7 +40
143947	2003 YQ117	15.39	2.48	11 21.5	14	-64				260	75	
	2005 LW3	**21.62**	**0.141**	**11 24.3**	**13.3**	**+17**				**?**	**?**	
	2009 HV58	19.6	0.357	11 29.6	16.7	-79				2415	690	
	1979 XB	18.6	0.566	12 01.8	17.3	-5				7		YORP target? 2036 06.4 V:17.1 -12.
	2013 PV2	20.18	0.274	12 05.9	16.4	-14				25	8	Good through end of 2022.
162474	2000 LB16	18.66	0.551	12 11.2	16.0	+39				35	10	
	2015 RN35	**23.1**	**0.071**	**12 16.2**	**13.3**	**-22**						
	2014 HK129	**21.1**	**0.179**	**12 18.8**	**14.7**	**-23**	**>10**	**0.5**	**2**	**8625**	**2475**	**Thirouin et al. (2018)**
	2013 YA14	23.6	0.057	12 24.5	15.3	+52				?	?	Last chance for small telescopes thru 2050.
	2010 XC15	**21.43**	**0.154**	**12 26.8**	**13.3**	**+18**						
199003	2005 WJ56	18.16	0.693	12 31.	16.7	+50	4.3825	0.09 0.15		3	5	Behrend (2007web) Last chance. Brightest on 2023 01 08.5 V:13.7 -16
226554	2003 WR21	19.64	0.351	12 31.	15.7	-13				20	6	Brightest 2023 01 02.3 V:15.6 +55

Table I. A list of near-Earth asteroids reaching brightest in 2022 October-December. PHA: potentially hazardous asteroid. Diameters are based on p_V = 0.20. The Date, V, and Dec columns are the mm/dd.d, approximate magnitude, and declination when at brightest. Amp is the single or range of amplitudes. The A and G columns are the approximate SNRs for an assumed full-power Arecibo (not operational) and Goldstone radars. The references in the Notes column are those for the reported periods and amplitudes. The "?" in the A/G columns are for when the SNR calculator failed for distances less than 0.01 au.

References

Behrend, R. (2007web). Observatoire de Geneve web site. *http://obswww.unige.ch/~behrend/page_cou.html*

Erikson, A.; Mottola, S.; Lagerros, J.S.V.; Lindgren, M.; Piironen, J.; Oja, T.; Hahn, G.; Lagerkvist, C.-I.; Harris, A.W.; Nathues, A.; Neukum, G. (2000). "The Near-Earth Objects Follow-up Program. III. 32 Lightcurves for 12 Objects from 1992 and 1995." *Icarus* **147**, 487-497.

Harris, A.W.; Young, J.W.; Bowell, E.; Martin, L.J.; Millis, R.L.; Poutanen, M.; Scaltriti, F.; Zappala, V.; Schober, H.J.; Debehogne, H.; Zeigler, K.W. (1989). "Photoelectric Observations of Asteroids 3, 24, 60, 261, and 863." *Icarus* **77**, 171-186.

Monteiro, F.; Silva, J.S.; Lazzaro, D.; Arcoverde, P.; Medeiros, H.; Rodrigues, T.; Souza, R. (2018). "Rotational properties of near-earth objects obtained by the IMPACTON project." *Plan. Space Sci*. **164**, 54-74.

Muinonen, K.; Belskaya, I.N.; Cellino, A.; Delbò, M.; Levasseur-Regourd, A.-C.; Penttilä, A.; Tedesco, E.F. (2010). "A three-parameter magnitude phase function for asteroids." *Icarus* **209**, 542-555.

Pravec, P.; Wolf, M.; Sarounova, L. (2017web). *http://www.asu.cas.cz/~ppravec/neo.htm*

Rubincam, D.P. (2000). "Radiative Spin-up and Spin-down of Small Asteroids." *Icarus* **148**, 2-11.

Thirouin, A.; Moskovitz, N.A.; Binzel, R.P.; Christensen, E.J.; DeMeo, F.E.; Person, M.J.; Polishook, D.; Thomas, C.A.; Trilling, D.; Willman, M.C.; Burt, B.; Hinkle, M.L.; Pugh, T. (2018). "The Mission Accessible Near-Earth Objects Survey: Four Years of Photometry." *Astrophys. J. Supp. Series* **2391**, A4.

Warner, B.D.; Harris, A.W.; Pravec, P. (2009). "The asteroid lightcurve database." *Icarus* **202**, 134-146.

Warner, B.D. (2015). "Near-Earth Asteroid Lightcurve Analysis at CS3-Palmer Divide Station: 2014 June - October." *Minor Planet Bull*. **42**, 41-53.

Warner, B.D.; Harris, A.W.; Durech, J.; Benner, L.A.M. (2021a). "Lightcurve Photometry Opportunities" 2021 January - March." *Minor Planet Bull.* **48**, 89-97.

Warner, B.D.; Harris, A.W.; Durech, J.; Benner, L.A.M. (2021b). "Lightcurve Photometry Opportunities" 2021 October - December." *Minor Planet Bull.* **48**, 406-410.

Wisniewski, W.Z.; Michalowski, T.M.; Harris, A.W.; McMillan, R.S. (1997). "Photometric Observations of 125 Asteroids." *Icarus* **126**, 395-449.

INDEX TO VOLUME 49

Colazo, M.; Morales, M.; Fornari, C.; Chapman, A.; García, A.; Santos, F.; Melia, R.; Suárez, N.; Stechina, A.; Scotta, D.; Martini, M.; Santucho, M.; Moreschi, A.; Wilberger, A.; Mottino, A.; Bellocchio, E.; Quiñones, C.; Speranza, T.; Llanos, R.; Altuna L.; Caballero, M.; Romero, F.; Galarza, C.; Colazo, C. "Photometry and Light Curve Analysis of Eight Asteroids by GORA's Observatories" 48-51.

Colazo, M.; Mottino, A.; Scotta, D.; Speranza, T.; Fornari, C.; Stechina, A.; Morales, M.; García, A.; Santos, F.; Santucho, M.; Suárez, N.; Wilberger, A.; Arias, N.; Melia, R.; Bellocchio, E.; Martini, M.; Borello, M.; Galarza, C.; Chapman, A.; Colazo, C. "Photometry and Light Curve Analysis of Six Asteroids by GORA's Observatories" 125-127.

Colazo, M.; Monteleone, B.; Santos, F.; Morales, M.; García, A.; Suárez, N.; Altuna, L.; Caballero, M.; Romero, F.; Speranza, T.; Belllocchio, E.; Santucho, M.; Fornari, C.; Melia, R.; Stechina, A.; Scotta, D.; Arias, N.; Chapman, A.; Ciancia, G.; Wilberger, A.; Anzola, M.; Mottino, A.; Colazo, C. "Asteroid Photometry and Lightcurve Results for Seven Asteroids" 189-192.

Colazo, M.; Scotta, D.; Monteleone, B.; Morales, M.; Ciancia, G.; García, A.; Melia, R.; Suárez, N.; Wilberger, A.; Fornari, C.; Nolte, R.; Bellocchio, E.; Mottino, A.; Colazo, C. "Asteroid Photometry and Lightcurve Analysis for Six Asteroids" 304-306.

Díaz-Vachier, I.; Cotto-Figueroa, D. "Lightcurves of Main-Belt Asteroid 7939 Asphaug and Near-Earth Asteroid 2015 JD1" 30.

Díaz-Vachier, I.; Cotto-Figueroa, D.; Rivas-Díaz, A.; Abreu-Cintrón, J.; Rivera-Rivera, B.; Santana-Rodríguez, P.; Laureno-La Puerta, F. "Lightcurve Analysis of Two Potentially Hazardous Asteroids and Three Near-Earth Asteroids" 14-15.

Dose, E.V. "Lightcurves of Seven Asteroids" 44-47.

Dose, E.V. "Lightcurves of Seventeen Asteroids" 141-148.

Dose, E.V. "Lightcurves of Eight Asteroids" 218-222.

Ergashev, K.E.; Burkhonov, O.A.; Ehgamberdiev, Sh.A.; Abduraimov, S.M. "Rotation Period Determination for Asteroids (19469) 1998 HV45 and (51442) 2001 FZ25" 192-193.

Farfán, R.G.; García, F. "Rotation Period Determination for Asteroid 663 Gerlinde" 5.

Fauerbach, M.; Fauerbach, M. "Photometry and Lightcurve Analysis of 1774 Kulikov, 7145 Linzeux, 11099 Sonodamasaki and (16024) 1999 CT101" 106-107.

Ferrais, M.; Vernazza, P.; Jorda, L.; Jehin, E.; Pozuelos, F.J.; Manfroid, J.; Moulane, Y.; Barkaoui, K.; Benkhaldoun, Z. "Photometry of 25 Large Main-Belt Asteroids with TRAPPIST-North and -South" 307-313.

Fornas, G.; Fornas, A.; Mas, V. "Nine Main Belt Asteroids, One Near Earth, and Two Potentially Hazardous Asteroid Lightcurves" 196-199.

Franco, L.; Marchini, A.; Papini, R.; Scarfi, G.; Bacci, P.; Maestripieri, M.; Aceti, P.; Banfi, M.; Bachini, M.; Succi, G.; Bachini, M.; Galli, G. "Collaborative Asteroid Photometry from UAI: 2021 July – September" 35-37.

Franco, L.; Marchini, A.; Papini, R.; Iozzi, M.; Bacci, P.; Maestripieri, M.; Baj, G.; Galli, G.; Mortari, F.; Gabellini, D.; Ruocco, N.; Tinelli, L.; Montigiani, N.; Mannucci, M.; Scarfi, G.; Salvaggio, F. "Collaborative Asteroid Photometry from UAI: 2021 October – December" 128-130.

Franco, L.; Marchini, A.; Papini, R.; Iozzi, M.; Scarfi, G.; Mortari, F.; Gabellini, D.; Bacci, P.; Maestripieri, M.; Baj, G.; Galli, G.; Coffano, A.; Marinello, W.; Pizzetti, G.; Aceti, P.; Banfi, M.; Tinelli, L.; Montigiani, N.; Mannucci, M.; Noschese, A.; Mollica, M.; Guido, E.; Ruocco, N.; Bachini, M.; Succi, G. "Collaborative Asteroid Photometry from UAI: 2022 January-March" 200-204.

Franco, L.; Marchini, A., Papini, R.; Bacci, P.; Maestripieri, M.; Ruocco, N.; Scarfi, G.; Iozzi, M.; Montigiani, N.; Mannucci, M.; Baj, G.; Valvasori, A.; Guido, E.; Galli, G.; Buzzi, L. "Collaborative Asteroid Photometry from UAI: 2022 April-June" 342-346.

Galdies, C.; Brincat, S.M. "Photometric observations of main-belt asteroids 2229 Mezzarco, 3648 Raffinetti and 3919 Maryanning" 1-2.

Gault, D.; Nosworthy, P.; Nothenius, R.; Bender, K.; Herald, D. "A New Satellite of 4337 Arecibo Detected and Confirmed by Stellar Occultation" 3-5.

González Farfán, R.; García de la Cuesta, F.; Fernández Mañanes, E.; Graciá Ribes, N.; Ruiz Fernández, J.; De Elías Cantalapiedra, J.; Fernández Andújar, J.M.; Delgado Casal, J.; Reina Lorenz, E.; Naves Nogues, R.; Díez Alonso, E. "The Rotation Periods of 3 Juno, 28 Bellona, 129 Antigone, 214 Aschera, 237 Coelestina, 246 Asporina, 382 Dodona, 523 Ada, 670 Ottegebe, 918 Itha, 1242 Zambesia, 1352 Wawel, 1358 Gaika, 4155 Watanabe, and 6097 Koishikawa" 136-140.

González Farfán, R.; García de la Cuesta, F.; Delgado Casal, J.; Reina Lorenz, E.; Ruiz Fernández, J.; De Elías Cantalapiedra, J.; Naves Nogues, R.; Fernández Andújar, J.M.; González Carballo, J.-L.; Fernández Mañanes, E.; Martínez Morales, R. "Periods Determinations for Seventeen Asteroids" 229-233.

Hayes-Gehrke, M.; Ibe-Ekeocha, T.; Ganeshan, A.; Jupiter, J.; Leeson, R.; Ondrusek, C.; Owusu, N.; Patel, D.; Rajpara, J.; Redett, C.; Rodriguez-Velez, G.; Sheth, R.; Vo, A.; Mifsud, M.; Galdies, C.; Marchini, A.; Papini, R. "Lightcurve Analysis and Rotation Period Determination of Asteroid 1455 Mundleria" 248.

Hayes-Gehrke, M.; Bragger, C.; Dang, J.; Houston, J.; Mackay, A.; Mansoor, K.; Lienemann, R.; O'Ferrall, S.; Smelson, A.; Epstein, A.; Patel, J.; Gallagher, N.; Miles, S.; Galdies, C.; Marchini, A.; Papini, R. "Rotation Period Determination and Lightcurve Analysis of Asteroid 3736 Rokoske" 249.

Hubbell, J. "Call for Minor Planet Observers to Join the ALPO Exoplanet Section" 67-68.

Larsen, B.J.; Read, M.T.; Brucker, M.J.; Morgan, C.W.; Larsen, J.A. "Small, Fast Rotator Asteroid 2018 GG" 80.

Loera-González, P.A.; Olguín, L.; Saucedo, J.C.; Contreras, M.E.; Nuñez-López, R.; Domínguez-González, R.; Angulo, O.E.; Chapetti, S.D.; Córdova, D.E.; Cortez, R.A.; Ramírez, M.A.; Vázquez, P.S. "Rotation Periods for Asteroids from Carl Sagan Observatory: 2021 November – 2022 May" 289-290.

Mannucci, M.; Montigiani, N. “Rotational Period Determination and Taxonomic Classification for Asteroid 536 Merapi” 6-7.

Mannucci, M.; Montigiani, N. “Rotational Period Determination for Asteroids 5237 Yoshikawa” 241-242.

Mannucci, M.; Montigiani, N.; Gabellini, D.; Mortari, F. “Rotation Period Determination and Taxonomic Classification for Asteroids 417 Suevia, 554 Peraga, and 47 Winchester” 326-329.

Marchini, A.; Papini, R. “Rotation Period Determination for Asteroid 3616 Glazunov” 252.

Marchini, A.; Papini, R.; Salvaggio, F. “Rotation Period Determination for (9659) 1996 EJ” 167-168.

Marchini, A.; Cavaglioni, L.; Privitera, C.A. “Rotation Period Determination for Asteroids 2232 Altaj, 3699 Milbourn, 4101 Ruikou, (6787) 1991 PF15 and 8416 Okada” 10-13.

Marchini, A.; Cavaglioni, L.; Privitera, C.A.; Papini, R.; Salvaggio, F. “Rotation Period Determination for Asteroids 4988 Chushuho and 7393 Luginbuhl” 120-121.

Michimani, J.; Lazzaro, D.; Rondón, E.; Monteiro, F.; Arcoverde, P.; Evangelista-Santana, M.; Pereira, W.; Mesquita, W., Souza, R.; Rodrigues, T. “Photometry and Lightcurve Analysis of Four Mars-Crossing Asteroids” 272-273.

Montigiani, N.; Mannucci, M. “Rotational Period Determination and Taxonomic Classification for Asteroid 8080 Intel” 77-78.

Nowinski, M.C.; Linder, T.R.; Reichart, D.E.; Haislip, J.B.; Kouprianov, V.V.; Moore, J.P. “Lightcurve Analysis of 10 V-Type Asteroids” 98-101.

Odden, C.; Cahill, C.; Clarke, N.; Clemmons, I.; Gerakaris, E.; Huang, Y.; Javier, F.; Jeong, D.; Kristiansen, S.; Lee, L.; Lin, J.; McCormack, M.; Murtha, E.M.; Quran, M.; Tucci, L.; Yarynich, O.; Zhang, K.; Kemp, J. “Lightcurve Analysis of Asteroid 2999 Dante” 245-246.

Odden, C.; Cahill, C.; Darling, V.; Du, A.; vonEckartsberg, N.; Gerakaris, E.; He, J.; Jin, Y.; Lin, J.; McCormack, M.; Reagan, B.; Shen, X. “Lightcurve Analysis of Asteroid 5889 Mickiewicz” 246-247.

Percy, S.C. “Rotation Period for Asteroid (125072) 2001 UG” 78-79.

Pilcher, F. “Section News: Robert Stephens Named Associate Coordinator of the Minor Planets Section” 67.

Pilcher, F. “Call for Observations” 67.

Pilcher, F. “Minor Planets at Unusually Favorable Elongations in 2022” 57-59.

Pilcher, F. “General Report of Position Observations by the ALPO Minor Planets Section for the Year 2021” 233-235.

Pilcher, F. “Lightcurves and Rotational Periods of 57 Mnemosyne and 58 Concordia” 9-10.

Pilcher, F. “Lightcurves and Rotation Periods of 330 Adalberta, 494 Virtus, 530 Turandot, 784 Pickeringia, and 1009 Sirene” 122-124.

Pilcher, F.; “Lightcurves and Rotation Periods of 233 Asterope, 240 Vanadis, 275 Sapientia, 282 Clorinde, 414 Liriope, and 542 Susanna” 346-349.

Pilcher, F. “Lightcurves and Rotation Periods of 49 Pales, 424 Gratia, 705 Erminia, 736 Harvard, 1261 Legia, 1541 Estonia, and 6371 Heinlein” 185-188.

Pilcher, F. “The Rotation Period of 128 Nemesis is Re-Examined” 162-163.

Pilcher, F.; Dose, E.V. “A Reexamination of the Rotation Period of 1541 Estonia” 250-251.

Pilcher, F.; Franco, L.; Marchini, A.; Papini, R.; Oey, J. “748 Simeisa – An Asteroid with an Earth-Commensurate Rotation Period is Solved” 164-165.

Polakis, T. “1903 Adzhimushkaj: An Extremely Slow Rotator” 160-161.

Polakis, T. “Lightcurves for Thirteen Minor Planets” 131-135.

Polakis, T. “Lightcurves for Fifteen Minor Planets” 179-184.

Polakis, T. “Lightcurves for Sixteen Minor Planets” 298-303.

Polakis, T.; Oey, J.; Colazo, M. “6764 Kirillavrov: A Binary Asteroid” 81-83.

Sani, I.A.; Offor, P.; Njoku-Achu, N.; Nowinski, M.C.; Ofodum, C.; Okere, B. “Lightcurve Photometry of Asteroid 1627 Swings” 159-160.

Sani, I.A.; Nowinski, M.C.; Umahi, A.E.; Okike, O.; Oyibo, M.; Umeh, C.N.; Okolo, O.E.; Okere, B. “Lightcurve Photometry of Asteroid 8693 Matsuki” 242-243.

Scardella, M.; Tomassini, A.; Pierri, F. “Rotation Period Determination of 5987 Liviogratton” 70.

Schmalz, S.; Schmalz, A.; Voropaev, V.; Mokhnatkin, A.; Novichonok, A.; Ivanov, A., Ivanov, V.; Ivanova, N.; Barkov, A.; Lysenko, V.; Yakovenko, N.; Gorbunov, N.; Kurbatov, G.; Shchukin, P.; Reva, I.; Serebryanskiy, A.; Omarov, C.; Celaya Arenas, R.; Kokina, T.; Graziani, F.; diRoberto, R. “Photometric Observations and Rotation Periods of Asteroids 2376 Martynov, (7335) 1989 JA, 12923 Zephyr, and (85184) 1991 JG1” 291-295.

Sioulas, N. “Rotation Period Determination for Asteroid 849 Ara”, 69.

Slivan, S.M.; Colclasure, A.; Escobedo, I.; Henopp, A.; Knight, R.; Mitchell, A.; Wilkin, F.P. “Synodic and Siderial Rotation Periods of Koronis Family Member (1762) Russell” 71-72.

Smith, J. “Rotational Period Determination of 2282 Andrés Bello” 166.

Sonka, A.B.; Nedelcu, A.; Birlan, M. “Rotational Period of Small NEA 2022 KK5” 258-259.

Stephens, R.D.; Warner, B.D. "Main-Belt Asteroids Observed from CS3:"

2021 July – September	31-34.
2021 September – 2022 January	108-110.
2022 January – March	205-218.
2022 April – June	314-326.

Stephens, R.D.; Warner, B.D. "Lightcurve Analysis of L4 Trojan Asteroids at the Center for Solar System Studies:"

2021 July to September	51-55.
2021 October to December	117-119.

Stephens, R.D.; Coley, D.R.; Warner, B.D. "Lightcurve Analysis of L5 Trojan Asteroids at the Center for Solar System Studies: 2022 June" 287-288.

Stephens, R.D.; Coley, D.R.; Warner, B.D. "(29606) 1998 QN94: A Binary Asteroid in a Self-Synchronous Orbit" 260-261.

Warner, B.D. "Asteroid-DeepSky Appulses in 2022" 56.

Warner, B.D.; Stephens, R.D. "Photometric Observations and Data Analysis of NEA Binary Asteroids 5143 Heracles" 73-75.

Warner, B.D.; Stephens, R.D. "On Confirmed and Suspected Binary Asteroids Observed at the Center for Solar System Studies" 22-29.

Warner, B.D.; Stephens, R.D. "On Confirmed and Suspected Binary Asteroids Observed at the Center for Solar System Studies: 2022 February and March" 223-226.

Warner, B.D.; Stephens, D.R.; Coley, D.R. "On Confirmed and Suspected Binary Asteroids Observed at the Center for Solar System Studies: 2022 March-June" 262-267.

Warner, B.D.; Stephens, R.D. "Near-Earth Asteroid Lightcurve Analysis at the Center for Solar System Studies:"

2021 August – October	16-22.
2021 October – December	83-89.
2022 February – March	176-178.
2022 March – June	274-279.

Warner, B.D.; Stephens, R.D. "Lightcurve Analysis of Hilda Asteroids at the Center for Solar System Studies:"

2021 September – December	102-104.
2022 January – March	227-228.
2022 March – May	268-271.

Warner, B.D.; Harris, A.W.; Ďurech, J.; Benner, L.A.M. "Lightcurve Photometry Opportunities:"

2022 January – March	61-65.
2022 April – June	152-156.
2022 July – September	235-239.
2022 October – December	350-354.

Wiley, E.O.; Pilcher, F. "Lightcurve Analysis of Three Main Belt Asteroids: 2265 Verbaandert, 3787 Aivazovskij, and 4258 Berg" 329-332.

Wilkin, F.P.; Schechter, R.Z. "Lightcurve for Koronis Family Member 2498 Tsesevich" 76.

Wilkin, F.P.; Bromberg, J.; AlMassri, Z.; Beauchaine, L.; Nguyen, M. "Lightcurve for Koronis Family Member (1363) Herberta" 253.

Wilkin, F.P.; AlMassri, Z.; Bowels, P.; Pargiello, M.; Sindoni, J. "Lightcurves for Three Koronis Family Asteroids from the Union College Observatory" 267-268.

IN THIS ISSUE

This list gives those asteroids in this issue for which physical observations (excluding astrometric only) were made. This includes lightcurves, color index, and H-G determinations, etc. In some cases, no specific results are reported due to a lack of or poor-quality data. The page number is for the first page of the paper mentioning the asteroid. EP is the "go to page" value in the electronic version.

Number	Name	EP	Page
7	Iris	67	307
13	Egeria	67	307
15	Eunomia	67	307
16	Psyche	67	307
18	Melpomene	67	307
20	Massalia	67	307
21	Lutetia	67	307
22	Kalliope	67	307
24	Themis	67	307
30	Urania	67	307
45	Eugenia	67	307
51	Nemausa	67	307
52	Europa	67	307
87	Sylvia	67	307
87	Sylvia	93	333
88	Thisbe	67	307
105	Artemis	67	307
128	Nemesis	67	307
145	Adeona	67	307
187	Lamberta	67	307
190	Ismene	49	289
216	Kleopatra	67	307
233	Asterope	58	298
233	Asterope	106	346
240	Vanadis	58	298
240	Vanadis	106	346
243	Ida	27	267
275	Sapentia	58	298
275	Sapentia	106	346
282	Clorinde	58	298
282	Clorinde	106	346
321	Florentina	27	267
323	Brucia	58	298
323	Brucia	102	342
324	Bamberta	67	307
342	Endymion	102	342
354	Eleonora	67	307
414	Liriope	106	346
417	Suevia	86	326
476	Hedwig	67	307
513	Centesima	58	298
542	Susanna	102	342
542	Susanna	106	346
554	Peraga	86	326
578	Happelia	102	342
596	Scheila	67	307
704	Interamnia	67	307
705	Erminia	64	304
747	Winchester	86	326
748	Simeisa	64	304
782	Montefiore	17	257
795	Fini	58	298
864	Aase	74	314
914	Palisana	64	304
967	Helionape	93	333
983	Gunila	64	304
1019	Strackea	93	333
1043	Beate	64	304
1055	Tynka	58	298
1156	Kira	93	333
1172	Aneas	47	287
1226	Golia	15	255
1237	Genevieve	58	298
1319	Disa	58	298
1346	Gotha	93	333
1363	Herberta	13	253
1466	Mundleria	8	248
1541	Estonia	10	250
1656	Suomi	102	342
1664	Felix	14	254
1664	Felix	93	333
1783	Albitskij	58	298
1806	Derice	74	314
1816	Liberia	93	333
1878	Hughes	93	333
1884	Skip	93	333
2048	Dwornik	74	314
2067	Aksnes	29	269
2069	Hubble	74	314
2093	Genichesk	74	314
2265	Varbaandert	89	329
2376	Martynov	51	291
2635	Huggins	93	333
2685	Masursky	58	298
2689	Bruxelles	58	298
2713	Luxembourg	27	267
2714	Matti	93	333
2778	Tangshan	22	262
2784	Domeyko	74	314
2858	Carlosporter	74	314
2999	Dante	5	245
3057	Malaren	93	333
3224	Irkutsk	58	298
3263	Bligh	93	333
3306	Byron	58	298
3317	Paris	47	287

3388	Tsanghinchi	93	333	7335	1989 JA	49	289	42701	1998 MD13	93	333
3451	Mentor	47	287	7335	1989 JA	51	291	42811	1999 JN81	74	314
3469	Bulgakov	58	298	7335	1989 JA	102	342	46780	1998 HH52	32	272
3470	Yaronika	74	314	7516	Kranjc	74	314	49699	Hidetakasato	74	314
3477	Kazbegi	93	333	7516	Kranjc	93	333	49937	1999 XO180	56	296
3561	Devine	29	269	7736	Mizhnij Novgorod	93	333	61343	2000 PC5	32	272
3569	Kumon	74	314	7889	1994 LX	22	262	66251	1999 GJ2	34	274
3616	Glazunov	12	252	8551	Daitarabochi	29	269	85184	1991 JG1	51	291
3736	Rokoske	9	249	8566	1996 EN	34	274	85628	1998 KV2	22	262
3787	Aivazovskij	89	329	8693	Matsuki	2	242	100756	1998 FM5	34	274
3894	Williamcooke	74	314	8743	Keneke	29	269	138971	2001 CB21	64	304
3936	Elst	74	314	9509	Amfortas	22	262	163692	2003 CY18	34	274
4055	Magellan	34	274	9698	Idzerda	74	314	170891	2004 TY16	93	333
4221	Picasso	102	342	9992	1997 TG19	74	314	351068	2003 TS13	32	272
4235	Tatishchev	93	333	10302	1989 ML	34	274	377732	2005 XJ8	22	262
4528	Berg	89	329	11001	Andrewulff	93	333	388945	2008 TZ3	34	274
4935	Maslachkova	93	333	11450	Shearer	74	314	464798	2004 JX20	34	274
5009	Sethos	49	289	11512	1991 AB2	49	289	471109	Vladobahyl	4	244
5129	Groom	93	333	11512	1991 AB2	93	333	475665	2006 VY13	22	262
5182	Bray	93	333	12923	Zephyr	51	291		2018 XV5	34	274
5237	Yoshikawa	1	241	13078	1991 WD	56	296		2022 BT	102	342
5456	Merman	56	296	13255	1998 OH14	93	333		2022 GY2	40	280
5693	1993 EA	102	342	16214	Venkatachalam	74	314		2022 HA	40	280
5720	Halweaver	74	314	17170	Vsevustinov	93	333		2022 HC	40	280
5889	Mickiewicz	6	246	21831	1999 TX93	93	333		2022 JL	40	280
6349	Acapulco	15	255	23456	1989 DB	93	333		2022 KK5	18	258
6384	Kervin	74	314	24029	1999 RT198	74	314		2022 KK5	40	280
6455	1992 HE	22	262	24779	Presque Isle	93	333		2022 MN1	40	280
6569	Ondaatje	34	274	25916	2001 CP44	34	274		2022 MP	40	280
6714	Montreal	93	333	27262	1999 XT184	74	314		2022 MP	102	342
6729	Emiko	93	333	27995	1997 WL2	32	272				
6920	Esaki	56	296	29606	1998 QN94	20	260				
6920	Esaki	93	333	29606	1998 QN94	74	314				
7172	Multatuli	93	333	36619	2000 QE151	93	333				

THE MINOR PLANET BULLETIN (ISSN 1052-8091) is the quarterly journal of the Minor Planets Section of the Association of Lunar and Planetary Observers (ALPO, http://www.alpo-astronomy.org). Current and most recent issues of the *MPB* are available on line, free of charge from:

https://mpbulletin.org/

The Minor Planets Section is directed by its Coordinator, Prof. Frederick Pilcher, 4438 Organ Mesa Loop, Las Cruces, NM 88011 USA (fpilcher35@gmail.com). Robert Stephens (rstephens@foxandstephens.com) serves as Associate Coordinator. Dr. Alan W. Harris (MoreData! Inc.; harrisaw@colorado.edu), and Dr. Petr Pravec (Ondrejov Observatory; ppravec@asu.cas.cz) serve as Scientific Advisors. The Asteroid Photometry Coordinator is Brian D. Warner (Center for Solar System Studies), Palmer Divide Observatory, 446 Sycamore Ave., Eaton, CO 80615 USA (brian@MinorPlanetObserver.com).

The Minor Planet Bulletin is edited by Professor Richard P. Binzel, MIT 54-410, 77 Massachusetts Ave, Cambridge, MA 02139 USA (rpb@mit.edu). Brian D. Warner (address above) is Associate Editor, and Dr. David Polishook, Department of Earth and Planetary Sciences, Weizmann Institute of Science (david.polishook@weizmann.ac.il) is Assistant Editor. The *MPB* is produced by Dr. Pedro A. Valdés Sada (psada2@ix.netcom.com). The MPB is distributed by Dr. Melissa Hayes-Gehrke. Direct all subscriptions, contributions, address changes, etc. to:

Dr. Melissa Hayes-Gehrke
UMD Astronomy Department
1113 PSC Bldg 415
College Park, MD 20742 USA
(mhayesge@umd.edu)

Effective with Volume 38, the *Minor Planet Bulletin* is a limited print journal, where print subscriptions are available only to libraries and major institutions for long-term archival purposes. Effective with Volume 50, January 1, 2023 and beyond, printed issues of the *Minor Planet Bulletin* will no longer be distributed. In addition to the free electronic download of the *MPB* noted above, electronic retrieval of all *Minor Planet Bulletin* articles (back to Volume 1, Issue Number 1) is available through the Astrophysical Data System:

http://www.adsabs.harvard.edu/

Authors should submit their manuscripts by electronic mail (rpb@mit.edu). Author instructions and a Microsoft Word template document are available at the web page given above. All materials must arrive by the deadline for each issue. Visual photometry observations, positional observations, any type of observation not covered above, and general information requests should be sent to the Coordinator.

* * * * *

The deadline for the next issue (50-1) is October 15, 2022. The deadline for issue 50-2 is January 15, 2023.